Sperm mitochondria: Species specificity and relationships to sperm morphometric features and sperm function in selected mammalian species

By
Liana Maree

A thesis submitted in partial fulfilment of the requirements for the degree of Doctor of Philosophy in the Department of Medical Bioscience, University of the Western Cape

September 2011

Supervisor: Prof G van der Horst Co-supervisors: Dr SH Kotzé, Prof R Henkel

by

Liana Maree

UNIVERSITY of the
WESTERN CAPE

Sperm mitochondria: Species specificity and relationships to sperm morphometric features and sperm function in selected mammalian species

Liana Maree

KEYWORDS

Sperm mitochondria

Sperm morphometry

Sperm midpiece

Sperm motility

Sperm kinematics

Sperm metabolism

Mammals

Computer-aided sperm/semen analysis

Glycolysis

Oxidative phosphorylation

ABSTRACT

Sperm mitochondria: Species specificity and relationships to sperm morphometric features and sperm function in selected mammalian species

L Maree

PhD, Department of Medical Bioscience, University of the Western Cape

Numerous studies on mammalian spermatozoa have reported large variations in the dimensions of the main sperm structural components, namely the head, midpiece and flagellum. These variations in sperm architecture are believed to be adaptations for functioning of spermatozoa in complex environments outside the male reproductive system. The midpiece of the mammalian spermatozoon contains a varied number of mitochondria, but the reason for the marked difference in the size and structure of this sperm component is not clear. This study confirmed the variations in the sperm morphometry of seven selected mammalian species and revealed unique features of the sperm midpiece and sperm mitochondria of these seven species. Evaluation of several sperm kinematic parameters revealed the unique swimming characteristics of the different spermatozoa. The importance of using standardized motility parameters was highlighted as well as the assessment of different subpopulations of spermatozoa in order to produce more reliable and comparable data. Investigating the role of sperm mitochondria in human sperm metabolism indicated that these organelles are related to sperm function in terms of sperm motility. Furthermore, it was suggested that glycolysis and mitochondrial respiration are linked processes and that both are important for the maintenance of human sperm motility. By optimizing and employing standardized experimental procedures and analysis techniques, this study was able to confirm the species specificity of almost all the sperm parameters evaluated, while also elucidating the phylogenetic relatedness of the non-human primate species. In conclusion, the present study has confirmed that the various midpiece morphometry parameters are related to the remaining sperm morphometry parameters as well as to the sperm kinematic parameters. These proposed associations between the various sperm parameters were used to explain the sperm velocity of two hypothetical and morphologically different sperm structures. Therefore, the results of the current study support the idea of co-evolution between sperm components in mammalian spermatozoa and propose that the midpiece morphometry parameters that are selected for in

these spermatozoa are midpiece volume, total number of mitochondrial gyres, thickness of the mitochondrial sheath and mitochondrial height.

September 2011

DECLARATION

Hereby I, the undersigned, declare that the thesis "*Sperm mitochondria: Species specificity and relationships to sperm morphometric features and sperm function in selected mammalian species*" is my own work, that it has not been submitted previously for any degree or examination at any other university, and that all the sources I have used or quoted have been indicated and acknowledged as complete references.

Liana Maree

Signed: ……………………...   Date: ……………………….

ACKNOWLEDGEMENTS

LIST OF ABBREVIATIONS

# Gyres	number of gyres
A	area
ACH	α-chlorohydrin
ACR	acrosome
ADJ	adjusted
ADP	adenosine diphosphate
AK	adenylate kinase
ALH	amplitude of lateral head displacement
AM	ampulla
ANOVA	one way analysis of variance
ART	assisted reproductive technology
ASMA	automated sperm morphology analysis
ATP	adenosine triphosphate
AVE	average
AX	axoneme
b*	beta coefficient
BCF	beat cross frequency
BPG or bis-P-Gly	bisphosphoglycerate
BSA	bovine serum albumin
BWW	Biggers, Whitten and Whittingham
CA	*Chlorocebus aethiops* (vervet monkey)
cAMP	adenosine 3,5-cyclic monophosphate
CASA	computer-aided sperm/semen analysis
CCCP	carbonyl cyanide *m*-chlorophenylhydrazone
CK	creatine kinase
CoA	coenzyme A
CP	central pair
Cr	creatine
CrP	creatine phosphate
Cyt c	cytochrome c
DA	dynein arms

DEF	default
DMSO	dimethylsulfoxide
DNA	deoxyribonucleic acid
DOG	2-deoxyglucose
Ellipt	ellipticity
Elong	elongation
ETC	electron transfer chain
f/s or f	frames per second
FlowCyt(om)	flow cytometry
FSH	follicle stimulating hormone
G	glucose
G-3-P	glyceraldehyde-3-phosphate
GAPDH(-S)	glyceraldehyde-3-phosphate dehydrogenase(-S)
GPI	glucosephosphate isomerase
H	head
HA	head area
HG	*Heterocephalus glaber* (naked mole-rat)
HK	hexokinase
HL	head length
HS	*Homo sapiens* (human)
HTF	human tubular fluid
IA	iodoacetamide
ICSI	intracytoplasmic sperm injection
IMM	inner mitochondrial membrane
IUI	intrauterine insemination
IVF	*in vitro* fertilization
L	length
LC	longitudinal columns
LDH	lactate dehydrogenase
LH	luteinizing hormone
LIN	linearity
LP	lactate-pyruvate
LPG	lactate-pyruvate-glucose
M	medium

MAD	mean angular displacement
MCT	monocarboxylate transporter
Mitch Ht	mitochondrial height
Mitch	mitochondrial
MM	*Mus musculus* (house mouse)
MMP	mitochondrial membrane potential
MP	midpiece
MPL	midpiece length
MPV	midpiece volume
mRNA	messenger RNA
MS	mitochondrial sheath
mtDNA	mitochondrial DNA
NAD^+	nicotineamide-adenine dinucleotide (oxidized form)
NADH	nicotineamide-adenine dinucleotide (reduced form)
ND	not determined
ODF	outer dense fibers
OMDA	outer microtubule doublets of the axoneme
OMM	outer mitochondrial membrane
OO	*Ovis orientalis* (merino ram)
OXPHOS	oxidative phosphorylation
P or Perim	perimeter
PA	particle area
PBS	phosphate buffered saline
PCA	principal component analysis
PCR	polymerase chain reaction
PDH	pyruvate dehydrogenase
PFK	phosphofructokinase
PGAM	phosphoglycerate mutase
PGK	phosphoglycerate kinase
P-Gly	phosphoglycerate
PK	pyruvate kinase
PN	penis
PM	plasma membrane
PU	*Papio ursinus* (chacma baboon)

Q	ubiquinone
r	correlation coefficient
R	rapid
R^2	R-squared coefficient (regression analysis)
r_a	radius of axonemal-outer dense fiber complex
r_b	radius of midpiece
$r_b - r_a$	thickness of mitochondrial sheath
RLU	relative light units
RM	*Macaca mulatta* (rhesus monkey)
RNA	ribonucleic acid
ROS	reactive oxygen species
Roughn	roughness
RPE	rectal probe electro-ejaculation
rRNA	ribosomal RNA
RS	radial spoke
S	slow
SCA	Sperm Class Analyzer
SCOT-t	succinyl CoA transferase
SD	standard deviation
SLMPL	straight-line midpiece length
SP	sperm
SPL	sperm length
STR	straightness
T	testis
TCA	tricarboxylic acid
TEM	transmission electron microscopy
TEP	tail end piece
TEPL	tail end piece length
TPI	triphosphate isomerase
TPP	tail principal piece
TPPL	tail principal piece length
TR	transverse ribs
tRNA	transfer RNA
TT	total tail

TTL	total tail length
V	volume
VAP	average path velocity
VCL	curvilinear velocity
VD	vas deferens
VSL	straight-line velocity
W	width
WHO	World Health Organization
WOB	wobble

UNIVERSITY *of the*
WESTERN CAPE

CONTENTS

CHAPTER 1: Introduction to study

1.1   General introduction

Sexual reproduction involves the formation of haploid gametes which need to fuse during fertilization to create diploid offspring. Oocytes are typically large, immotile cells which are produced in low numbers and have a large cytoplasmic contribution to embryonic development (optimized for quality). In contrast, spermatozoa are much smaller than oocytes, motile and produced in large numbers. Since spermatozoa only make a small cytoplasmic contribution to the embryo, quality is believed to be compromised for quantity in order to maximize fertilization rates. Moreover, spermatozoa are produced with as little investment as possible and only consist of the minimum number of components or organelles to perform its function (White-Cooper and Bausek, 2010).

Large variations in the dimensions of the main sperm components, namely the head, midpiece and flagellum, have been reported in numerous studies across all animal taxa. These variations in sperm architecture are believed to be adaptations for the functioning of spermatozoa in complex environments outside the male reproductive system (Gage, 1998; Pitnick *et al.*, 2009) and that it is mainly the result of sperm competition and female selection (Gomendio and Roldan, 1993).

In mammalian spermatozoa, most of the variation in sperm size is due to the differences in the length of the midpiece and principal piece of the flagellum (Cummins and Woodall, 1985). The midpiece contains a number of mitochondria which are uniquely wrapped around the flagellum. The primary role of the sperm mitochondria is to produce ATP molecules for different energy-requiring reactions, but mainly for sperm motility (Mann and Lutwak-Mann, 1981). Abnormalities in the structure of the midpiece and the sperm mitochondria have been linked to decreased sperm motility and male fertility (Turner, 2006), indicating the importance of this sperm structural component.

While the variations in the structure of the sperm midpiece and sperm mitochondria have been described in earlier studies (Fawcett, 1970, 1975; Phillips, 1977), possible reasons for these variations have only been proposed in the last two decades (Cardullo and Baltz, 1991; Anderson *et al.*, 2005; Firman and Simmons, 2010).

1.2   Aims and objectives

This study attempted to elucidate the variation that exists in the sperm component dimensions of various mammalian species. Variation in the size and structure of the sperm midpiece and the mitochondria it contains was of particular interest. The main aim of this comparative study was therefore to determine the relationship between the sperm midpiece and mitochondria and the morphometry of the other sperm components as well as its association with sperm function.

In order to achieve this goal, the following objectives were set:

- To optimize and standardize the experimental procedures utilized to evaluate various parameters of the different sperm structural components
- To assess the sperm morphometry of selected mammalian species in order to disclose species diversity and specificity
- To determine the structural features of the midpiece and mitochondria of these mammalian spermatozoa
- To analyze sperm motility parameters of selected mammalian species and determine the degree of variation in these parameters
- To assess the relationship between sperm structure and sperm function by determining the role of sperm mitochondria in sperm metabolism and the maintenance of sperm motility

1.3   Overview of thesis chapters

This thesis is divided into six main chapters, including a literature overview and five research chapters. Each chapter contains its own introduction, materials and methods, results and discussion sections. A general conclusion and a complete reference list are included at the end of the thesis.

Chapter 2: Literature overview

An overview of the literature relating to mammalian spermatozoa and sperm mitochondria is given. The sperm parameters assessed in this study are highlighted and the mammalian species included in the study are introduced.

Chapter 3: *Assessment of sperm morphometry of selected mammalian species using automated and semi-automated image analysis techniques*

The collection of semen/sperm samples and the selection of motile spermatozoa are described. The results include the measurements of numerous sperm morphometry parameters and the discussion highlights the variations found in these sperm parameters.

Chapter 4: *Sperm mitochondria and the sperm midpiece of selected mammalian species*

The quantitative differences in the dimensions and structure of the mitochondrial sheath and individual sperm mitochondria are reported. Additionally, the viability of the sperm mitochondria are confirmed and compared between the mammalian species. Possible relationships between the different midpiece morphometry parameters are discussed.

Chapter 5: *Analysis of sperm motility parameters of selected mammalian species using computer-aided sperm analysis (CASA)*

The percentage motile spermatozoa and the detailed sperm kinematic parameters are compared between seven mammalian species. The importance of using standardized analysis techniques and the selection of reliable motility parameters are highlighted.

Chapter 6: *The role of sperm mitochondria in human sperm metabolism and the maintenance of sperm motility*

The recent contention in the literature on whether glycolysis or oxidative phosphorylation plays the most important role in sperm metabolism is addressed.

Chapter 7: *The relationship of sperm mitochondria and the sperm midpiece to sperm form and function in selected mammalian species*

Data from the previous four chapters are used to determine the relationship between the midpiece morphometry parameters and other sperm morphometry parameters as well as the sperm kinematic parameters. Various statistical exploratory graphs and statistical tests are employed to reveal such relationships between the sperm parameters.

Chapter 8: *Conclusion*

Taking the results of Chapters 3-7 into consideration, a proposal is made regarding the relationship between sperm morphometry and sperm kinematic parameters. General concluding remarks are made and future studies are suggested.

1.4 Research output

The following papers, conference proceedings and conference posters were generated during this study. Copies of the papers are included as part of the Appendices.

1.4.1 Publications

1. van der Horst G, **Maree L**, Kotzé S, Brooks N (2006). Number of sperm mitochondria and sperm velocity: species specificity and relationships in selected mammals. *Proc Microsc Soc S Afr*, 36: 52.

2. van der Horst G, **Maree L** (2009). SpermBlue®: a new universal stain for human and animal sperm which is also amenable to sperm morphology analysis. *Biotechn Histochem*, 84: 299-308.

3. **Maree L**, du Plessis SS, Menkveld R, van der Horst G (2010). Morphometric dimensions of the human sperm head depend on the staining method used. *Hum Reprod*, 25: 1369-1382.

1.4.2 Conference proceedings

1. Oral presentation at a joint seminar (one-day workshop) between Germplasm Conservation & Reproduction Biotechnologies, ARC-Animal Production Institute, Irene, Pretoria and Comparative Sperm Biology Group of Medical Biosciences (21 November 2008, UWC) titled "Sperm mitochondria and relationships to sperm morphometric features, function and sperm quality in Merino rams and selected mammalian species".

2. Oral presentation at the 37th Congress of the Physiology Society of Southern Africa (7-9 September 2009, Stellenbosch) titled "Sperm mitochondria and relationships to sperm morphometry and function in selected primate species".

3. Poster presentation at the Darwin200 Human Evolution Symposium (12 October 2009, UWC) titled "Sperm mitochondria: species specificity and relationships to sperm morphometry and function in selected primate species".

4. Oral presentation at the 11th International Symposium on Spermatology (24-29 June 2010, Japan) titled "Mammalian sperm mitochondria: does the size of the midpiece count?".

4

CHAPTER 2: Literature overview

2.1 Introduction

Mammalian gametes are highly polarized and specialized cells which are adapted for their function, e.g. either transmission of their genetic material to the site of fertilization (spermatozoa) or to support the developing offspring after fertilization (ova). The necessity for the formation of gametes and thus sexual reproduction *per se*, is, however, still debated. Even Darwin (1862) was unable to produce a theory for its existence when he wrote that "We do not even in the least know the final cause of sexuality; why new beings should be produced by the union of two sexual elements… the whole subject is as yet hidden in darkness", as reported by Zimmer (2009).

The unique features of spermatozoa, and sometimes the lack thereof, has been the topic of very interesting research conducted by andrologists and other reproductive biologists across the globe. In order to understand the significance of these sperm features, two complementary research strategies can be applied , namely a) to conduct in-depth studies into the distinctive features of spermatozoa from individual species and b) to follow a comparative approach between the sperm parameters of different species (Martin, 2007). These broad-based comparisons permit identification or recognition of general principles that apply across species (Martin, 2003). In the current study, both these approaches have been applied to gain an understanding of the size and structure of an essential part of spermatozoa, namely the midpiece. Preliminary studies have shown that the size of the sperm midpiece varies among different mammalian species and could be related to sperm functional aspects (van der Horst *et al.*, 2006).

This literature overview will give a broad background to spermatozoa in general and then focus on the formation and functional aspects of sperm mitochondria. A brief discussion on male fertility will highlight the most important sperm parameters to be assessed, as well as its relationship to sperm mitochondria. Lastly, the mammalian species included in the current study will be introduced.

2.2 Sperm as a gamete

2.2.1 Evolution of sexual reproduction and the formation of gametes

The reason why sexual reproduction exists and why it is maintained, has been the research focus of many evolutionary biologists during the past 40 years, but is still not fully understood (Zimmer, 2009). There are many theories in evolutionary biology that attempt to answer these questions (de Visser and Elena, 2007), with the use of both organism-based methods and molecular genetic evidence for supporting these theories (Schurko *et al.*, 2009).

Even though the origin of sexual reproduction is still not known, it is believed that it developed as a subsequent evolutionary event to the existence of meiosis (Wilkins and Holliday, 2009). In sexual reproduction, a new organism is formed by the fusion of two gametes. These gametes, the ova and the spermatozoa, are produced by meiosis, a reduction division, which halves the chromosome number (haploid phase). Another essential step during meiosis is the paring of homologous chromosomes during prophase I and the exchange of genetic material (genetic recombination) between non-sister chromatids. Once the gametes fuse during fertilization, further genetic recombination takes place and the chromosome number is restored (diploid phase). In asexual reproduction, however, no reduction division, genetic recombination or fusion of gametes takes place – the parent's gametes simply develop directly into new offspring through mitotic cell division (Ridley, 1996).

If taking the above into consideration, surely it would be more energy efficient to only have asexual reproduction as the preferred method of reproduction. Yet, the majority of known species (especially eukaryotes) reproduce sexually and obligate asexual reproduction is limited to some prokaryotes (Kondrashov, 1988). The resulting question is: why is sexual reproduction maintained?

Although the cost of sexual reproduction is twofold that of asexual reproduction (due to a 50% chance of producing a male offspring who have half the reproductive potential) (Maynard Smith, 1978), it probably still exists because it has some evolutionary or selective advantage. According to Kondrashov (1988), the hypotheses proposed for the evolution of sexual reproduction can be classified into two groups. Firstly, there might have been some *environmental* changes for which sexually reproducing species were better adapted. In all existing populations, the individuals (with specific genotypes) must be adapted to the demands of their environment. If the environmental conditions subsequently change, only the

6

individuals that have specific adaptations to these new conditions will survive (natural selection). Therefore, this genotype-environment match must be maintained by sex for sexual reproduction to be advantageous. Secondly, there might have been some *mutational (genetical)* changes that caused sexual reproduction to be more advantageous than asexual reproduction. Mutations can either be beneficial or deleterious to an individual under certain circumstances. The advantage of sexual reproduction can thus either be to join beneficial mutations or to eliminate slightly harmful mutations (Zimmer, 2009).

Both the hypotheses mentioned above rely on the occurrence of genetic recombination during meiosis (Barton and Charlesworth, 1998), which allows for an increased variation in the genetic material (crossing over), the accurate exchange of genetic material (homolog pairing) and the creation of new genetic arrangements (fertilization). It is this enhanced variation in the genetic makeup of individuals which could cause them to be selected for when changes occur in the conditions necessary for survival.

Accepting the evolutionary advantages of the process of sexual reproduction, further focus will now be placed on the cells responsible for this process, namely the ova and spermatozoa.

2.2.2   Functional morphology

Ova and spermatozoa are highly specialized since they are the only haploid cells in most diploid organisms and need to "find and fertilize" each other in order to be considered functional. How these functions are accomplished, depends mainly on the environment in which fertilization takes place and is linked to the method of fertilization (internal versus external fertilization). Accordingly, the general morphology and physiology of the gametes have been adapted to be appropriate for this task (Austin, 1976).

Consequently, spermatozoa are very complex cells which have undergone extreme morphological evolution and subsequently have large variations in terms of structure. Comparing spermatozoa from various animal genera, two primary groups have been distinguished, namely 'primitive' and 'modified' spermatozoa (see Fig. 2.1). 'Primitive' spermatozoa are regarded as 'simple' in structure and are apparently only found in species where external fertilization takes place (e.g. shedding of spermatozoa into the surrounding aquatic medium). On the other hand, 'modified' spermatozoa have undergone changes in the head and midpiece and are found in animals that release the spermatozoa near the female

7

within gelatinous coverings or where the spermatozoa are transferred to the female *via* internal fertilization (Austin, 1976). It is assumed that this differentiation in sperm structure happened parallel to the colonization of land during the evolution of animals and plants (Baccetti and Afzelius, 1976).
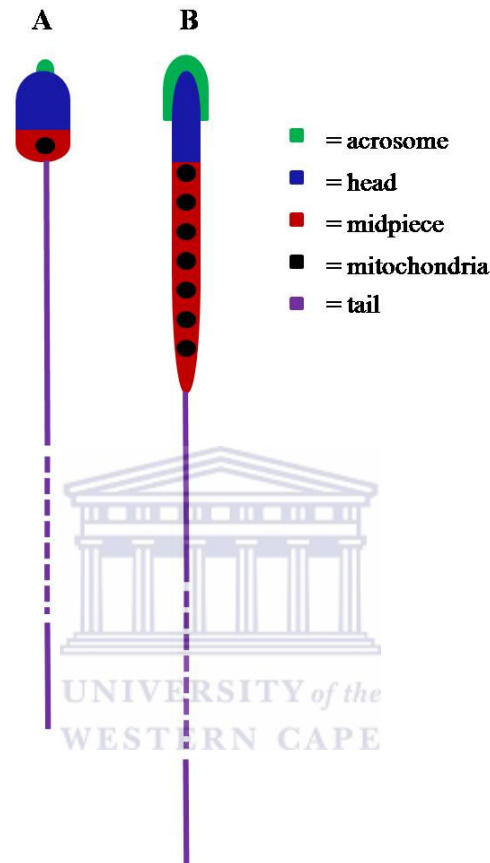
Figure 2.1. Schematic presentation of the two primary groups of spermatozoa. **(A)** The 'primitive' spermatozoon has three distinct components (head, midpiece and tail) and the head contains a round or bullet-shaped nucleus. The acrosome (if present) is mounted on the leading surface of the head. The small midpiece contains only few mitochondria. **(B)** In the 'modified' spermatozoon, the head is a long, tapering cone with the acrosome forming a cap over it. The midpiece extends some distance down the flagellum and contains more or larger mitochondria than in the primitive type. (Modified from Austin, 1976; Baccetti and Afzelius, 1976)

However, not all of the numerous variations in structural features of spermatozoa are related to the conditions of fertilization (Fawcett, 1970). Baccetti and Afzelius (1976) noted that there is much more diversity in the sperm structure of internal fertilizers than in spermatozoa from animals which reproduce by external fertilization in a relative uniform aquatic environment. This fact is highlighted when comparing spermatozoa from a specific animal group, e.g. mammals, which all are internal fertilizers. It is often found that distinct similarities exist between the sperm structure of closely related species, but that there are more profound differences when comparing distant groups. Thus, similarities and differences between

8

spermatozoa reflect "what can be regarded as evolutionary and genetic relationships among mammals" (Austin, 1976). The problem arises when trying to explain similarities between distantly related mammals or variations in sperm structure which seem to have no adaptive significance.

2.3   Mammalian sperm structure

2.3.1   Structural components

The mammalian spermatozoon is derived from the 'primitive' spermatozoon and is an example of a 'modified' spermatozoon, as described in 2.2.2 above (Fig. 2.1). It typically consists of a head partly covered by an acrosome, a neck and a flagellar-like tail which have four components, namely the connecting piece, middle piece (midpiece), principal piece and the end piece (Fig. 2.2).
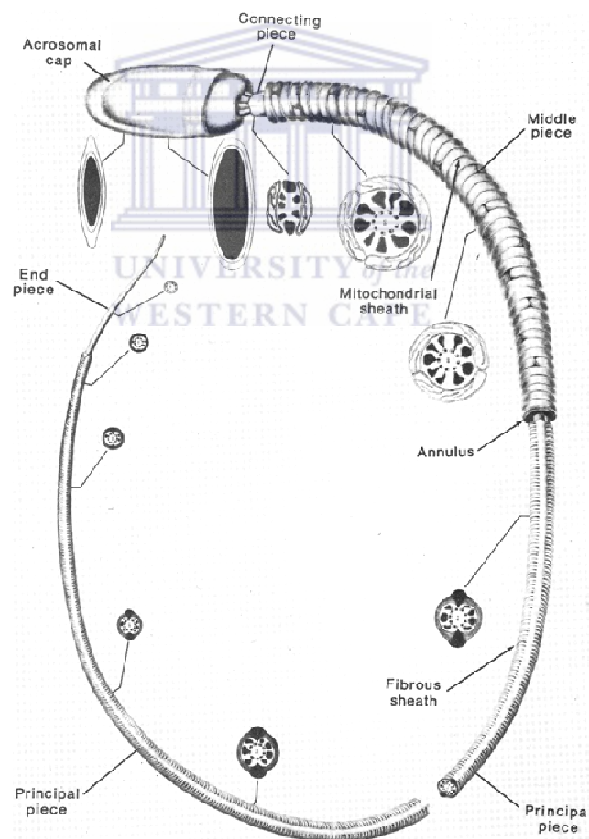
Figure 2.2. Schematic presentation of a typical mammalian spermatozoon indicating the most important components and its cross-sectional view at various levels. (From Fawcett, 1975)

The head of the mammalian spermatozoon is ovate, ensiform or falciform and dorsoventrally flattened. Moreover, the variation in shape and volume of the mammalian sperm head causes it to differ substantially from the smaller, globular or pyriform shape of the 'primitive'

spermatozoon. The acrosome is also not only confined to the tip of the nucleus, but covers a larger portion of the sperm head than in the 'primitive' spermatozoon (Fawcett, 1970). The acrosome contains hyaluronidase enzymes which are released during the acrosome reaction in order to penetrate the corona radiata and zona pellucida surrounding the ovum. The neck typically consists of the connecting piece and the centriole.

The mammalian sperm tail contains an axonemal complex of microtubules, which consists of a central pair (doublet) of single microtubules, surrounded by nine double microtubules (9+2 pattern) (Fig. 2.3). In the proximal part of the sperm tail, peripheral to the axoneme, a further nine dense fibers complete the 9+9+2 pattern (Baccetti and Afzelius, 1976). According to Fawcett (1970), the outer dense fibers can differ among themselves in terms of their shape and cross-sectional area.
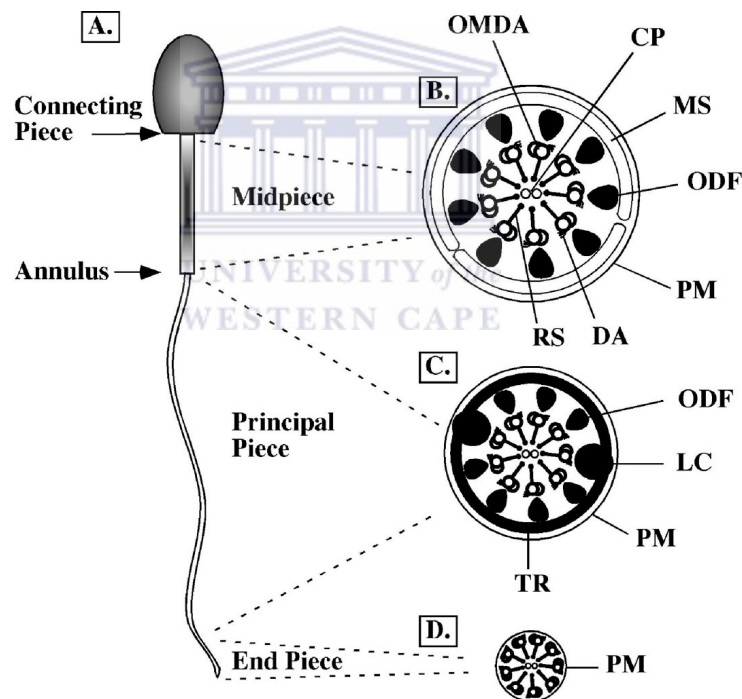
Figure 2.3. Schematic presentation of the ultrastructure of the mammalian sperm flagellum. **(A)** The flagellum is divided into the connecting piece, midpiece, principal piece and end piece. The basic axonemal complex and additional features can be seen in cross-sections through the **(B)** midpiece, **(C)** principal piece and **(D)** end piece. OMDA = outer microtubule doublets of the axoneme, CP = central pair, MS = mitochondrial sheath, ODF = outer dense fibers, PM = plasma membrane, DA = dynein arm, RS = radial spoke, LC = longitudinal columns, TR = transverse ribs (part of fibrous sheath). (From Turner, 2003)

In the midpiece of the mammalian sperm, the axoneme and outer dense fibers are enclosed by a long sheath of mitochondria. The mitochondria itself are elongated and arranged around the core of the sperm tail in a helical fashion. In the principal piece of the flagellum, the

10

axonemal-outer dense fiber complex is surrounded by the fibrous sheath, which is divided in several transverse ribs along the length of the principal piece (Fig. 2.3).

The most pronounced difference between the mammalian and the 'primitive' spermatozoa is the increased structural complexity of the mammalian sperm "motor apparatus", which include the addition of the outer dense fibers to the 9+2 axonemal complex, the enlargement of the midpiece and the presence of the fibrous sheath (Fawcett, 1970). These modifications seem to be adaptations for locomotion through the more viscous fluids (compared to an external aqueous environment) of the female reproductive tract as encountered during internal fertilization. The 'wall effect' caused by the topography of the lining of the female reproductive tract could also contrain the movements of the swimming spermatozoon (Fwacett, 1970; Humphries *et al.*, 2008).

2.3.2 Variations in mammalian sperm morphology and morphometry

The large variations in the size and shape of mammalian spermatozoa are well known. A few examples of these variations are given below.

Two extensive studies on the dimensions of mammalian spermatozoa reported on the differences in measurements of various sperm components (Cummins and Woodall, 1985; Gage, 1998). Compared to many invertebrate spermatozoa, mammalian spermatozoa are characterised as being 'small', but nevertheless, a 12-fold variation was still reported between the 28 μm total sperm length of the porcupine (*Hystrix africaeaustralis*) and the 349 μm of the honey possum (*Tarsipes rostratus*) (Gage, 1998). Although mostly linear measurements were used (head length and width, midpiece length and width, principal piece length) by Cummins and Woodall (1985), their results clearly show the size variation found in 284 mammalian species. Interestingly, they reported that a parameter such as mean head length is relatively constant (5.14-7.85 µm) between different mammalian groups, but that the proportion of head length in terms of total sperm length varies more than twofold (6.0-13.1%).

The acrosomes of different mammalian species themselves have remarkable diversity in their volume and shape, many of which are distinctive of a species or very similar in closely related species (Austin, 1976) (Fig. 2.4). It is typically the apical portion of the acrosome cap which seems to be responsible for the shape characteristic of species and examples include the

11

acrosome of the chinchilla, guinea pig and ground squirrel. In contrast, the acrosomes of monkey, man, bull, boar, rabbit and bat seem to be less elaborate in structure than the aforementioned species and they only have a small apical segment (Fawcett, 1970).
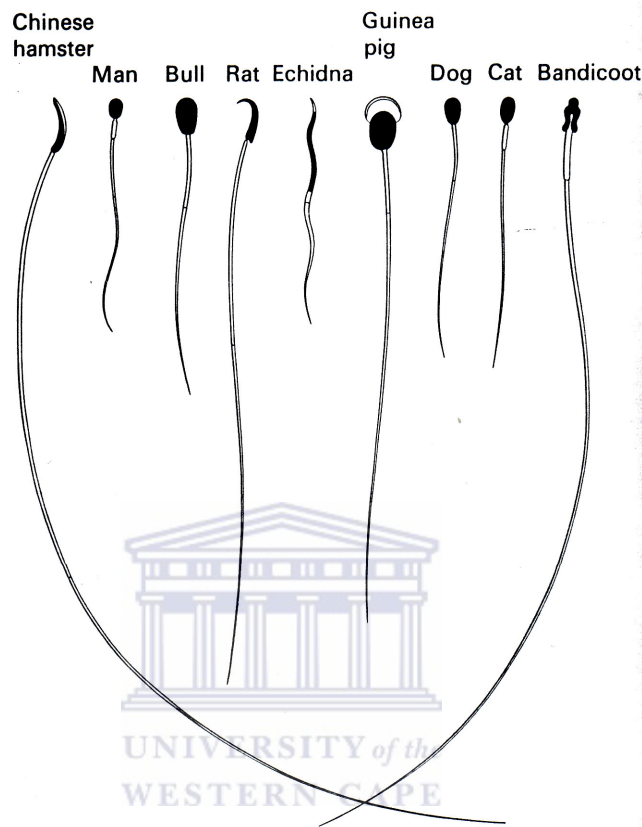
Figure 2.4. Various mammalian spermatozoa, indicating the differences in the size and shape of the head (with acrosome), midpiece and tail. (From Austin, 1976)

Both the sperm head shape and volume also seems to be diverse among mammals. Similar to the acrosomes mentioned above, the sperm head of closely related mammalian species are generally of the same shape, but the head morphology of more distant species could be very different. Downing Meisner *et al.* (2005) found in a comparative study between artiodactylans (hippopotamus, giraffe, deer, antelope), perissodactylans (zebra, white and black rhinoceros) and cetaceans (dolphins and whales) that all the sperm heads were ovate in shape and had a distinct acrosomal apical ridge. However, the sperm head morphology of muroid rodents is falciform in nature and bear apical hook(s) (Breed, 2004).

The sperm tail and its components are no exception when it comes to variation, especially when focusing on the size of the outer dense fibers and the midpiece. In a cross-section of the

12

midpiece and the principal piece, an enormous variation in the initial size and shape of the dense fibers and a decrease in diameter down the length of the tail were found (Fawcett, 1970). Not only does the midpiece differ in terms of its size (length and width) between species, but also the number of gyres in the mitochondrial helix and the dimensions of the individual mitochondria (Austin, 1976).

2.3.3 Adaptive significance

The detailed description of the sperm structure of numerous species has been the focus of many studies, highlighting both the similarities and the variation of the different sperm components between species. The challenge is, however, to understand the adaptive significance of sperm form and function (Gage, 1998). For some sperm characteristics, its relationship to a specific function is quite clear, as expected. On the contrary, many features of sperm morphology and morphometry seem to have no obvious biological advantage or adaptive significance (Austin, 1976), especially when comparative studies are done.

Austin (1976) also stated "…are all the multitudinous minutiae whereby gametes differ between species biologically advantageous in some measure in the particular environment of each species? Or would it be justified in saying rather that many, perhaps most, of the variations in gametes have no adaptive significance, are neutral to selection pressure, and, having arrived by chance mutation, will stay until by chance eliminated?".

Numerous reasons, many only speculative in nature, have been proposed for the evolution of sperm morphology and morphometry in mammals. Most of these proposed reasons are dealing with environmental or genetic factors and a few examples are given below.

The development of the outer dense fibers and the enlargement of the midpiece seem to have developed in relation to the development of internal fertilization (Fawcett, 1970), where spermatozoa have to swim though the mucous secretions in the female tract (Austin, 1976). These adaptations could thus have been to increase the power output and therefore the motility in a more viscous environment. However, no clear-cut relationship between variations in the thickness of the dense fibers, the size of the midpiece and mitochondria and the possible swimming effort exists (Austin, 1976).

Sperm characteristics are highly heritable, whether it is by haploid or diploid gene expression (Immler, 2008). This explains the specific sperm form and function within a species, but why a specific gene has been selected proves to be a bit more complicated. Is it possible that some of the sperm characteristics occur due to 'random genetic drift', which could lead to non-adaptive variation? Or what if a sperm structure progressively changes in the same direction in successive generations, irrespective of selection pressure until it develops into 'ridiculous' proportions, as is seen during the process of orthogenesis? Lastly, it is also possible that the sperm characteristics we can identify in spermatozoa today might be vestigial characters; these might have been advantageous at some stage, but if it is no longer, will gradually be eliminated (Austin, 1976). These three examples provide some theoretical base suggesting that some variation in sperm structures might not have any or very little adaptive value.

Another major driving force behind the variation in sperm design and dimensions is considered to be sperm competition (Cummins, 1990). This process describes the rivalry between the sperm of different males to fertilize a given set of ova (Parker, 1970). It has been shown that spermatozoa with specific size parameters, longevity, and measures of motility can possibly increase its chances for successful fertilization (Firman and Simmons, 2010). A second type of post-copulatory sexual selection of spermatozoa is cryptic female choice, where females select against unfavourable ejaculates (low viability and progeny are less successful) (Ball and Parker, 2003).

Stepping away from variations in sperm morphology and looking at similarities between different species, highlights another fact about adaptive significance. It is expected that similar structures between species developed for similar reasons. One should not forget though that it is also possible for similarities to arise through the chance coincidence that similar solutions might be the answer for different problems, which could be loose standing from genetic or environmental factors (Austin, 1976).

Theredore, trying to understand the significance of all sperm characteristics might not always be evident, but a combination of all these characteristics still makes sperm highly specialized for their function. The difficulty rather lies in identifying those characteristics which play the most important role in improving sperm function.

2.4 Sperm mitochondria

2.4.1 Introduction to mitochondria

Before sperm mitochondria *per se* will be discussed, the following section will briefly introduce mitochondria in general and includes a few recently reported discoveries in terms of its structure and function.

Structural aspects

Mitochondria are double-membrane organelles found in almost all eukaryotic cells, except mature red blood cells and some protozoans (Fawcett, 1981; Cummins, 1998). These energy producing organelles are typically described as being round-shaped, ellipsoid or cylindrical and consist of an outer membrane, an inner membrane, an intermembrane space, lamellar cristae and the central compartment or matrix (Fig. 2.5a). The matrix contains mitochondrial DNA (mtDNA), ribosomes and some small granules (Lodish *et al.*, 1995). The number, size and morphology of mitochondria in a cell depend on the cell type and its functional status (Fawcett, 1981).
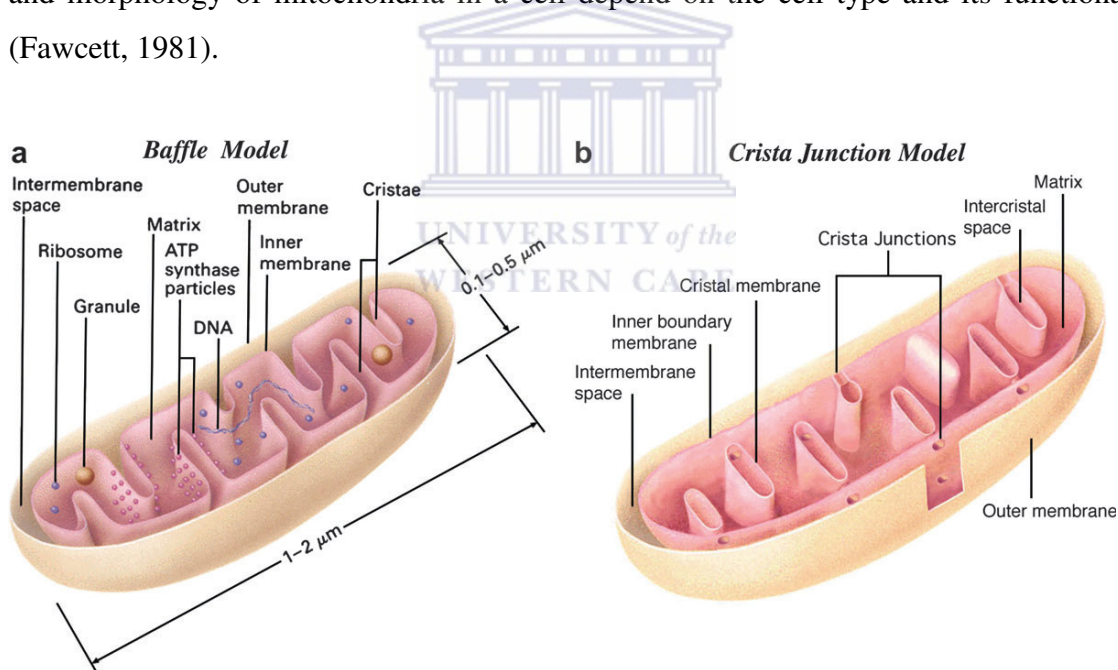
Figure 2.5. Two diagrams of proposed mitochondrial structures. **(a)** The 'baffle' model represents the structure of a 'typical' mitochondrion and its components (as described in the text). **(b)** The 'crista junction' model indicates that the cristae are structurally distinct from the inner mitochondrial membrane and joined to the inner membrane at crista junctions (membrane tubules). The cristal membrane and the intercristal space are thus two additional mitochondrial compartments not recognized in the 'baffle' model. (From Logan, 2006)

According to the serial endosymbiotic theory, mitochondria possibly originated from free-living bacteria, which were capable of metabolizing oxygen and taken into ancestral, nucleus-containing eukaryotic cells (Margulis, 1996). This theory has subsequently been challenged by studies on unicellular eukaryotes which indicated that the nucleus and mitochondrion

originated at more or less the same time in their host cells rather than in two separate events (Gray *et al.*, 1999). Nevertheless, the outer mitochondrial membrane resembles the original host cell plasma membrane and the inner mitochondrial membrane represents the bacterial cell wall and contains the site for ATP production through oxidative phosphorylation (OXPHOS) (Cummins, 1998). The smooth outer membrane is permeable to most small molecules (< 5000 molecular weight) and its lipid:protein ratio is about 50:50. The inner mitochondrial membrane consists of about 76% protein and is relatively impermeable (Lodish *et al.*, 1995). Two types of contact sites have been described between the outer and inner membranes, namely bridge-type sites, that seems to have a structural function in physically keeping the two membranes apart, and closely-apposed type sites, where protein translocation across the membranes can take place (as reviewed by Logan, 2006).

Until recently, it was believed that the inner mitochondrial membrane's surface area is increased by numerous invaginations into the mitochondrial matrix, namely the cristae (Fig. 2.5a). However, when advanced tomographic imaging techniques were employed, Mannella (2006a) reported that the cristae are structurally distinct from the rest of the inner mitochondrial membrane. The cristae are thus connected to the inner mitochondrial membrane by membranous tubules (crista junctions) of various lengths, rather than just being random in-folds of the inner membrane (Fig. 2.5b).

In general, it has been widely accepted that the number of mitochondria per cell and the number of cristae per mitochondrion are related to the energy demands of a specific cell type (Fawcett, 1981). It was shown by Hackenbrock (1968) that the number of crista junctions and the morphology of the intercristal space changes with the metabolic state of the mitochondria, giving rise to two morphology states of these organelles, namely the orthodox state and the condensed state (Fig. 2.6).

Mitochondria in the orthodox state have highly folded but compressed tubular cristae with few junctions with the inner membrane. In the condensed state the intercristal spaces are dilated, there are numerous narrow tubular connections to the intermembrane space and the matrix has condensed (Seitz *et al.*, 1995; Logan, 2006). These two states seem to be interchangeable, with the orthodox state being displayed when intracellular ADP is limiting (higher respiratory rate) and the condensed conformation when ADP is in excess and the respiratory rate has decreased (Mannella, 2006a).

16
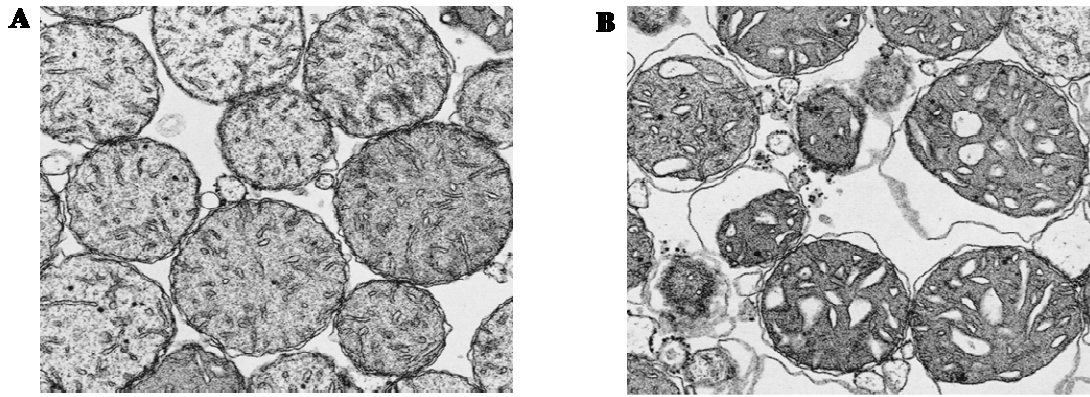
Figure 2.6. The two morphology states of mitochondria, namely **(A)** the orthodox state and **(B)** the condensed state. See text for discussion. (Modified from Hackenbrock, 1968)

mtDNA and its expression

Other unique features of mitochondria compared to other cytoplasmic organelles, are the fact that mitochondria possess their own DNA (mtDNA) and translational system and can divide by cleavage of the existing organelle. The double-stranded mtDNA is circular in nature and 3 to 6 copies are normally present in the mitochondrial matrix at any specific time (Fawcett, 1981). In humans the mtDNA codes for 37 genes that yield 13 mRNAs for translation, two rRNA's (12S and 16S) and 22 tRNA's necessary for mitochondrial protein synthesis. These translated proteins are essential components of enzymes and enzyme complexes of the electron transfer chain (ETC) (Anderson *et al.*, 1981), with the rest of the ETC components being produced from nuclear DNA. Mitochondria are therefore regarded as "semi-autonomous", because the majority of polypeptides needed by the mitochondria to perform all their functions are encoded in the nuclear genome, synthesized in the cytoplasm and imported into the mitochondria (as reviewed by Meinhardt *et al.*, 1999). Anderson *et al.* (1981) also reported that the genetic code directing the translation of mtDNA differs from the universal code and that the mitochondrial tRNA and rRNA molecules have different features to cytosolic RNA's. These differences, as well as the fact that mtDNA has an extremely compact gene organization, seems to be further evidence of the endosymbiotic hypothesis for the origin of mitochondria (Zeviani and Antozzi, 1997).

Although mtDNA only code for a few polypeptides of the ETC, molecular lesions of mtDNA have been associated with an increasing number of defined clinical syndromes, stressing the importance of mitochondria and their role in energy metabolism. Several mutations of mtDNA have been linked to heterogenous clinical manifestations, including myopathies, encephalomyopathies, cardiopathies and complex multisystem syndromes (as reviewed by

Zeviani and Antozzi, 1997). More recently mtDNA mutations have also been implicated in infertility (Jansen and Burton, 2004) and more specifically male infertility (St John *et al.*, 2000; Nakada *et al.*, 2006).

Functional aspects

The role of mitochondria in the production of ATP through oxidative phosphorylation is probably regarded as its primary function. During this process, electrons derived from the oxidation of substrates are directed through the ETC until it is finally accepted by molecular oxygen (Fig. 2.7A).

The ETC is composed of two mobile electron carriers (coenzyme Q/ubiquinone and cytochrome c) and four multimeric enzymatic complexes (complexes I, II, III and IV). The flow of electrons through the ETC is associated with the pumping of protons into the intermembrane space, creating an electrochemical gradient across the inner mitochondrial membrane. This proton gradient is finally used to drive ATP synthesis via enzyme complex V, ATP synthase (the F_0F_1 ATPase complex) (Lodish, 1995) (Fig. 2.7A). The inner mitochondrial membrane has been accepted as the location of the ETC, but more recent studies have shown that most of these enzyme complexes are residing in the membranes of the cristae, rendering these membranes functionally distinct from the inner mitochondrial membrane (Gilkerson *et al.*, 2003).

During the process of oxidative phosphorylation, reactive oxygen species (ROS) are produced when the molecular oxygen is converted into superoxide radicals. Under normal conditions, the ROS produced in the mitochondria are eliminated by antioxidants, but excessive ROS production (due to fever, cancer, stroke or mitochondrial dysfunction) can lead to the oxidation and damage of macromolecules (Ott *et al.*, 2007) (Fig. 2.7B). ROS could typically cause mutations, deletions, insertions and various other lesions in both nuclear DNA and mtDNA (Wiseman and Halliwell, 1996). However, since mtDNA is much more prone to oxidative damage by ROS (due to its location close to ROS production and the lack of protection by histones), the level of modified bases in mtDNA is 10-12-fold higher than in nuclear DNA. Furthermore, ROS could also damage proteins and lipids, many of which could lead to the suppression of mitochondrial metabolism (Ott *et al.*, 2007).
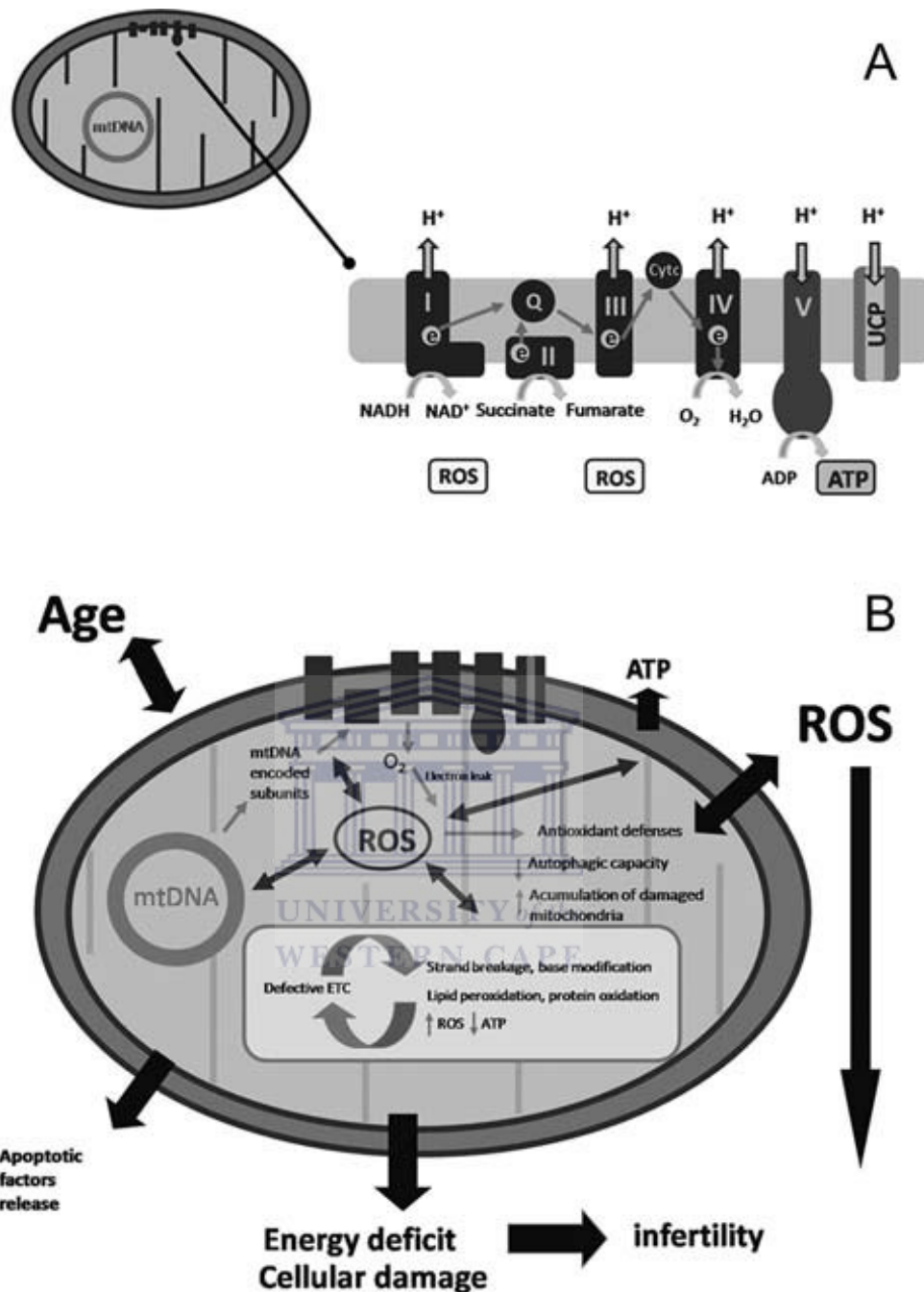
Figure 2.7. Functional aspects of mitochondria. **(A)** The electron transfer chain (ETC) of the inner mitochondrial membrane (and cristal membranes) is composed of five enzyme complexes (I, II, III, IV, V) and two mobile electron carriers (ubiquinone (Q) and cytochrome c (Cytc)) which are involved in the process of oxidative phosphorylation. **(B)** The relationship between various mitochondrial functions, including ATP production, ROS production, apoptosis and oxidative stress. (From Ramalho-Santos *et al.*, 2009)

The consequence of ROS production and damage has linked mitochondria to both the processes of apoptosis (programmed cell death) and ageing. In short, ROS play an important part in the release of cytochrome c and other pro-apoptotic proteins, which can trigger caspase activation and apoptosis (as reviewed by Ott *et al.*, 2007). The "mitochondrial theory of

ageing" is based on the ROS feedback-loop, whereby ROS production by the ETC causes mtDNA damage, which causes the production of insufficient or non-functional ETC enzymes, leading to more ROS production and more ROS-induced damage (Fig. 2.7B). The end-result is that various cell functions can irreversibly be affected and rather than causing cell death, these dysfunctional cells will accumulate in and slowly lead to the death of the organism (Dufour and Larsson, 2004). This dichotomy in the functions of mitochondria was appropriately stated by Logan (2006) in his concluding remarks when he mentioned that "mitochondria are complex semi-autonomous organelles that provide the energy for life and the trigger for death".

Other metabolic functions of mitochondria are mainly related to the cell type in which the mitochondria are located. For example, due to the tricarboxylic acid (TCA) cycle which takes place in the matrix, mitochondria in hepatocytes are involved in ketogenesis, gluconeogenesis, lipogenesis and detoxification of ammonia. In brown adipose tissue, the proton gradient across the inner mitochondrial membrane can be used to produce heat rather than ATP. This process is mediated through the facilitated diffusion of protons into the matrix via thermogenin, a proton channel (Cannon and Nedergaard, 2004). Mitochondria are also very important for the homeostasis of calcium levels inside cells via the storing and releasing of calcium. Thus, the amount of free calcium available for various cellular functions, e.g. signal transduction and cell signalling, are regulated by the mitochondria (Szabadkai and Duchen, 2007).

2.4.2   Structural and functional changes of mitochondria during spermatogenesis and spermiogenesis

Spermatogenesis is initiated by a combination of follicle stimulating hormone (FSH), luteinizing hormone (LH) and testosterone. FSH stimulates the Sertoli cells in the seminiferous tubules of the testis to secrete paracrine factors that regulate spermatogenesis and spermiogenesis. Intricate interactions among Sertoli and Leydig cells also occur involving mainly FSH, LH, testosterone, inhibin and estrogen. During these processes, the dramatic changes in the morphology of the germ cells include: condensation of the nucleus, containing tightly-packed DNA; formation of the acrosome by part of the Golgi apparatus, partly covering the nucleus; development of the tail starts at the opposite end of the nucleus; and most of the cytoplasm, including most of the organelles, is pinched off and removed as part of the residual body (Seitz *et al.*, 1995).

In addition to the germ cells, the mitochondria in the testes also undergo various changes in their morphology, localization and energy metabolism during spermatogenesis and spermiogenesis. According to the classification of mitochondria in terms of the structure of their cristae, three types are recognized during meiosis (Fig. 2.8), namely the orthodox, condensed and intermediate types (see the description of the first two types in section 2.4.1 and Fig. 2.6) (Seitz *et al.*, 1995; Ramalho-Santos *et al.*, 2009).

The orthodox-type mitochondria are found in Sertoli cells, spermatogonia and preleptotene and leptotene primary spermatocytes. The shape of the mitochondria changes from being ovoid in the spermatogonia, to becoming more elongate in the primary spermatocytes. At this stage of the development, the mitochondria are located close to the outer nuclear membrane and their numbers are increasing (De Martino *et al.*, 1979; Seitz *et al.*, 1995). The orthodox form of the mitochondria is an indication of an active functional state of mitochondria. The spermatogonia still have access to all the metabolic substrates originating from the blood and lymph vessels, but as the developing cells are transferred towards the lumen of the seminiferous tubules, they are dependent on the Sertoli cells for metabolites (Meinhardt *et al.*, 1999).
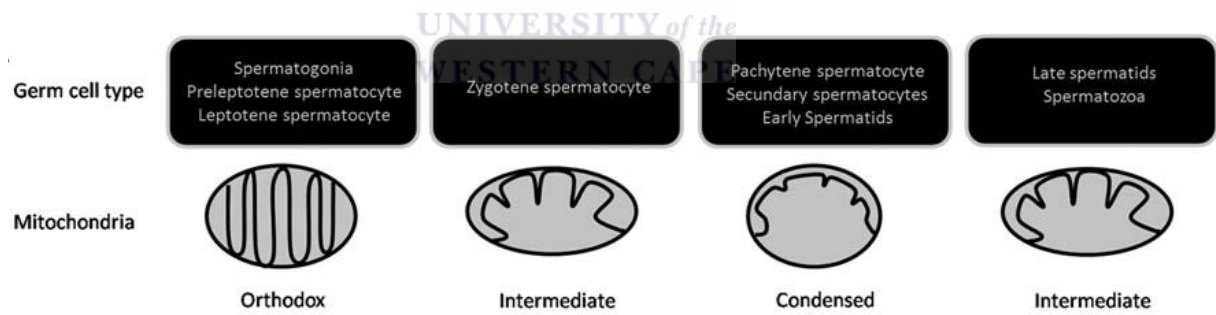
Figure 2.8. Different morphology types of mitochondria in male germ cells during spermatogenesis and spermiogenesis. See text for discussion. (From Ramalho-Santos *et al.*, 2009)

The zygotene spermatocytes have mitochondria of the intermediate form, but this is possibly only a temporary conformation as it changes from the orthodox to the condensed form (Seitz *et al.*, 1995). Condensed-type mitochondria are present in the pachytene primary spermatocytes, secondary spermatocytes and early spermatids. During these phases the mitochondria are small, round-shaped and may appear in clusters during the pachytene stage. Due to their location beyond the blood-testis barrier, these cells only receive lactate and pyruvate as metabolic substrates from the Sertoli cells (Meinhardt *et al.*, 1999). The condensed form of mitochondria is associated with a reduction in the diffusion of ADP into

the cristae, slower transport of ADP across the inner mitochondrial membrane and results in a reduction in ATP synthesis. The relationship between the availability of metabolic substrates, the type of cristae present in the mitochondria and the possible energy advantage associated with a change in the morphology of the cristae still remains to be determined (Mannella, 2006b).

The mitochondria of late spermatids and mature spermatozoa develop crescent-shaped cristae, which is characteristic of the intermediate form. In the spermatids, the mitochondria are located beneath the plasma membrane, which is probably indicative of a high energy demand and extensive exchange of metabolic substrates with the Sertoli cells (Meinhardt *et al.*, 1999). In the late spermatids, some of the mitochondria start migrating towards the developing flagellum and soon thereafter the remaining mitochondria start grouping together (De Martino *et al.*, 1979). The latter mitochondria will eventually leave the developing spermatozoon as part of the residual body.

During spermiogenesis, the mitochondria destined to become part of the motor apparatus of the spermatozoon attach and arrange themselves in the sperm midpiece. The helical fashion in which the spermatozoa coil around the axoneme is common among vertebrates (Fawcett, 1981), but exceptions do occur, e.g. in the bat (Fawcett, 1970) and in cetaceans (Downing Meisner *et al.*, 2005). The exact method by which the mitochondria form a sheath around the axoneme in mouse spermatozoa have been described by Ho and Wey (2007). First, four dextral, longitudinal arrays of spherical mitochondria attach to the axoneme and then pairs of mitochondria from opposing arrays form ring-like structures. These structures allow the mitochondria to be staggered in a specific pattern to forming a double helix. Finally, the mitochondria elongate into rod-shaped organelles that are tightly wrapped around the axoneme and dense fibers (Ho and Wey, 2007). During sperm maturation in the epididymis, the outer mitochondrial membrane becomes extensively cross-linked by disulfide bonds, increasing the stability of this membrane and of the mitochondrial shape (Calvin and Bedford, 1971).

Thus, once the mitochondria are committed to the anterior portion of the flagellum, the number of mitochondria does not seem to change. Interestingly, the length of the midpiece and the number of gyri between sperm from the same species is rather uniform and heritable, but may vary considerably among species (Fawcett, 1970). The location of mitochondria in a

cell is often in close proximity to the site of high energy demand (Fawcett, 1981), which also seems true for the location of mitochondria in the sperm flagellum in terms of supplying ATP for sperm motility. Fawcett (1970) reported on a statement by J Andre in 1969, that the common arrangement of the mitochondria in helical sheaths around the axoneme throughout the animal kingdom might be because it provides the least resistance to bending (e.g. comparing a stiff straight length of wire to a more flexible form if the same wire is coiled). Considering that the spermatozoa will need to be motile to be functional, the location of the mitochondria behind the head and only in the midpiece might also be the most practical position in terms of resulting in the least resistance to the beating of the flagellum and swimming in a liquid medium.

2.4.3 Role of mitochondria in sperm function

Since spermatozoa are such highly differentiated and specialized cells, it leads to the question as to why it removes any superfluous structures during spermiogenesis, but retains some mitochondria. This is probably an indication of the fact that these organelles fulfil a crucial role in sperm function (Ruiz-Pesini *et al.*, 2007; Ramalho-Santos *et al.*, 2009). Their physiological importance is, however, still unclear and much debated in the current literature.

Sperm mitochondria play an important part in most of the functions mentioned for mitochondria in the general section 2.4.1, but other possible roles for sperm mitochondria have recently been implicated. Many studies reporting on the functional aspects of sperm mitochondria have used indirect methods for deducing its importance, e.g. by inhibiting sperm mitochondria in metabolic studies or by investigating sperm mitochondria in cases of male infertility. A few of these examples will be included in the discussion of the function of sperm mitochondria below.

As mentioned before, the primary role of mitochondria is to produce ATP for various purposes. The necessity for the midpiece, and therefore the mitochondria, to be present and to have a normal structure for spermatozoa to be motile, has led to the widely-accepted fact that sperm mitochondria produce the energy needed for sperm motility (as reviewed by Ruiz-Pesini *et al.*, 2007). In asthenozoospermic males (individuals producing sperm with decreased motility), it was found that their sperm had smaller midpieces and a lower number of mitochondrial gyres (Mundy *et al.*, 1995). A reduction in the enzymatic activities of the ETC

has also been linked to a decrease in the motility of asthenozoospermic patients (Folgero *et al.*, 1993; Ruiz-Pesini *et al.*, 1998).

Despite the above reports on the importance of an intact midpiece on sperm motility, the question whether the ATP generated for sperm motility is mainly from the OXPHOS pathway or rather produced via glycolysis have been debated for many decades (Ford, 2006). Recent reports indicating that glycolysis is more important for sperm motility and male fertility in mice (Mukai and Okuno, 2004; Miki *et al.*, 2004) and humans (Nascimento *et al.*, 2008a) have elicited a new interest in this research topic. However, the results still remain controversial, in part due to the difficulty in comparing studies which differed in many aspects, including the mammalian species under investigation, the media and metabolic substrates used, the inhibitors selected for blocking the different pathways and the sperm parameters assessed (as reviewed by Ramalho-Santos *et al.*, 2009). Nevertheless, there is sufficient evidence in the literature to argue in favour of both metabolic pathways.

The fact that glycolytic enzymes have been found to be bound to the fibrous sheath of the principal piece in both mouse and human sperm, could be proof that glycolysis provides a localized source of ATP for sperm motility (Krisfalusi *et al.*, 2006; Kim *et al.*, 2007). In studies where the spermatogenic-cell specific glycolytic enzyme glyceraldehyde 3-phosphate dehydrogenase-S (GAPDH-S) was inhibited or disrupted, both decreased sperm motility and ATP levels where reported despite unchanged mitochondrial activity (Miki *et al.*, 2004; Hung *et al.*, 2008). On the other hand, inhibition of various OXPHOS enzymes or complexes in glucose-containing media caused a decrease in sperm motility (Ruiz-Pesini *et al.*, 2000; St John *et al.*, 2005). Evidence for the support of the importance of mitochondria in sperm motility also comes from proteomic studies of asthenozoospermic sperm samples (Martínez-Heredia *et al.*, 2008). Seventeen proteins have been identified that are expressed at different levels in asthenozoospermic samples relative to the normozoospermic controls and the four of these enzymes which were functionally grouped together for "energy production" are all related to mitochondria (involved in ETC, conversion of pyruvate to acetyl-CoA, TCA-cycle and beta oxidation). Regardless of all the above-mentioned reports, it should always be kept in mind that the processes of glycolysis and OXPHOS are linked and therefore, both are needed for proper sperm functioning. However, the balance between the two processes might be species-specific and depend on the substrates available for energy production (Ford, 2006). Once ejaculated, the spermatozoa are exposed to many different environments and need to be

"versatile" to maximize their chances of reaching the ovum (Ruiz-Pesini *et al.*, 2007), e.g. by interchanging between glycolysis and OXPHOS for production of ATP.

The negative effect of mtDNA rearrangements on sperm motility and morphology have only been realized in the last decade (as reviewed by St John *et al.*, 2005). Both point mutations and large-scale deletions of mtDNA result in reduced production of the ETC subunits and reduced motility (Kao *et al.*, 1998; Spiropoulos *et al.*, 2002). Interestingly, it has been shown that oligoasthenoteratozoospermic males have a higher content of mtDNA, but lower expression of two nuclear-encoded replication factors (polymerase gamma and mitochondrial transcription factor A), that is necessary for mtDNA transcription (Amaral *et al.*, 2007).

Another aspect of ATP generation by mitochondria that has been linked to sperm function is the mitochondrial membrane potential (MMP). This membrane potential is generated across the outer and inner mitochondrial membrane during OXPHOS and is also necessary for import of mitochondrial proteins, calcium homeostasis and metabolite transport (Baumber *et al.*, 2000). By using fluorescent probes to indicate a high MMP, several studies have reported that a decrease in the MMP is associated with decreased sperm motility (Auger *et al.*, 1993; Kasai *et al.*, 2002; Marchetti *et al.*, 2004a). A decrease in MMP was also correlated to an increase in ROS production in human sperm (Wang *et al.*, 2003), but not in equine sperm (Baumber *et al.*, 2000).

Both leukocytes and spermatozoa are responsible for ROS-generation in an ejaculate and as a result spermatozoa and semen possess various substances to protect these gametes from ROS damage (Tremellen, 2008). As discussed before (2.4.1), ROS are normally produced by the mitochondria, but as soon as the balance between ROS production and ROS elimination by anti-oxidants is disrupted or when extrinsic factors increases the amount of ROS produced, this could lead to oxidative stress. Oxidative stress causes damage to the sperm DNA, sperm membrane integrity and it decreases the spermatozoon's ability to bind to the oocyte (Tremellen, 2008). Consequently, increased ROS levels have been associated with male infertility due to decreased sperm motility, DNA fragmentation and increased apoptosis (Agarwal *et al.*, 2008).

Apoptosis has been linked to male infertility in various studies and apoptotic markers have been found in the testis, germ cells and in mature sperm. As mentioned above, one of the

ways in which apoptosis could impair fertility is through DNA damage caused by the mitochondrial generation of ROS and oxidative stress (Aitken and de Iuliis, 2010). The exact mechanisms in sperm apoptosis are not yet characterized, but the presence of activated caspase 3 and 9 is the sperm midpiece has been reported, implicating the role of sperm mitochondria (Weng *et al.*, 2002; Paasch *et al.*, 2004). Furthermore, Marchetti *et al.* (2004b) found that the activity of caspase 3 is negatively correlated with the sperm MMP.

One additional function of sperm mitochondria is its role in Ca^{2+} signalling. Ca^{2+} signalling plays an important part in many key activities of sperm, e.g. chemotaxis, hyperactivation, capacitation and the acrosome reaction. Ca^{2+} signalling pathways are dependent on Ca^{2+} stores, which are usually found in the endoplasmic reticulum of somatic cells. Although spermatozoa do not have an endoplasmic reticulum, Costello *et al.* (2009) reported the existence of two storage organelles for Ca^{2+} in mammalian sperm, namely one in the acrosome and the second in the neck and midpiece region. Although the ability of sperm mitochondria to store and release Ca^{2+} under certain conditions has been documented, it is not clear if this mitochondrial store of Ca^{2+} actually participates in Ca^{2+} signalling of spermatozoa (Publicover *et al.*, 2007).

A more unexpected role of sperm mitochondria is its proposed function in protein synthesis. Although mitochondria are capable of producing several mitochondrial-encoded proteins form mtDNA, the majority of mitochondrial proteins are, however, nuclear-encoded and usually translated into precursor proteins on cytoplasmic ribosomes and then transferred into the mitochondria via specific import channels and chaperones (Meinhardt *et al.*, 1999). Gene expression in mature spermatozoa is, however, progressively shut down during spermiogenesis (Brewer *et al.*, 2003) and these spermatozoa do not contain sufficient cytoplasmic ribosomal complexes to support translation (Miller and Ostermeier, 2006). An interesting study by Gur and Breitbart (2006) has shown that translation of nuclear-encoded proteins does occur in mature spermatozoa and that mitochondrial ribosomes (instead of cytoplasmic ribosomes) are actively involved in this process. They also reported that the new proteins synthesized were to replace degraded proteins and to produce proteins necessary for the process of capacitation. This evidence, as well as the fact that numerous unique RNA transcripts have been found in mature sperm (Zhao *et al.*, 2006), implies that there must be a RNA store in the sperm cell, but the location is not confirmed yet (Miller and Ostermeier, 2006). Other evidence that sperm mitochondria possibly play a role in capacitation was

26

reported by Vorup-Jensen *et al.* (1999), who found that under capacitating conditions, mitochondria became loosely arranged around the axoneme or distended.

Considering the diversity of sperm mitochondrial functions, it would not be surprising if mitochondria also play a role in other sperm functions that may possibly be elucidated in future. Since mitochondria are one of the few structures remaining in the mature sperm, it might be a case of "making the most of what you've got", as the title of Publicover *et al.*'s article (2007) suggests – the mitochondria had to make certain adaptations and take on certain functions to assure the survival of the spermatozoa until it reaches the site of fertilization.

2.4.4   Fate of sperm mitochondria after fertilization

In most mammals, the sperm head as well as the tail (including the midpiece and mitochondria) enter the ovum during the process of fertilization (Sathananthan *et al.*, 1986; Sutovsky *et al.*, 1996). It is, however, only the maternal mitochondria and mtDNA that are detected in the developing embryo, giving rise to the concept of "maternal inheritance" of mtDNA (Ankel-Simons and Cummins, 1996). The intraspecific mechanism of removal of paternal mitochondria has been reported by Sutovsky *et al.* (1999; 2000). In short, sperm mitochondria are selectively destroyed after fertilization by ubiquination in the oocyte cytoplasm, followed by proteolysis and these organelles seem to have disappeared by the eight-cell stage of development. The ubiquination of sperm mitochondria already happens in the testicular spermatids and spermatozoa, but the ubiquinated sites are probably masked by the formation of disulphide bonds during sperm maturation in the epididymis and during transport to the site of fertilization (Sutovsky *et al.*, 1999). Thompson *et al.* (2003) have identified prohibitin, a mitochondrial membrane protein, as one of the ubiquinated substrates that causes the sperm mitochondria to be recognized by the proteasomes in the ovum. Interestingly, the destruction of sperm mitochondria appears to be strain or breed specific, since paternal mtDNA is present in hybrid embryos (Sutovsky *et al.*, 2000).

The reason for the destruction of sperm mitochondria might be linked to the condition of paternal mtDNA. Due to a spermatozoon's high energy demand to sustain motility and various sperm-specific functions, mitochondria need to synthesize ATP through OXPHOS. As mentioned in section 2.4.3, this form of ATP production could give rise to extensive ROS production, oxidative stress and eventually mtDNA damage. Since mitochondria have the capacity to replicate themselves, sperm mitochondria with damaged mtDNA could be

proliferated in the offspring and cause various mitochondrial diseases (Zeviani and Antozzi, 1997). Such inheritance of paternal mtDNA with a mutation in humans has been reported by Schwartz and Vissing (2002). Consideration should also be given to the transmission of paternal mtDNA through nuclear transfer during experimental or therapeutic cloning processes (St John and Schatten, 2004).

Allen (1996) also hypothesized that the elimination of paternal mitochondria is due to the fact that there is a division of labour between the male and female germ-line mitochondria. The male germ-line mitochondria will typically perform oxidative phosphorylation (needed for sperm motility), but at the same time be genetically disabled through mtDNA mutations. The female germ-line mitochondria should, however, not perform oxidative phosphorylation and rather be able to replicate without mtDNA damage. It was also postulated that the solution to the conflict between mitochondrial respiration and mtDNA integrity is to have separate sexes and is possibly another explanation for the prevalence of anisogametic sex.

2.5   The significance of sperm form and function

Considering the main aims of the current study, it would only be possible to compare various sperm features and functions by selecting spermatozoa which could be considered as representative of a 'normal' sperm population. Such spermatozoa should have a good possibility of fertilizing the ovum and would thus be produced by a fertile male.

2.5.1   Determination of male fertility

The question of how fertile a male is (referring to his semen sample), are mostly asked by clinical and agricultural andrologists who are dealing with couples presenting with infertility or who are trying to increase productivity, respectively (Holt and van Look, 2004). A male is generally considered fertile if he has recently sired an offspring and it can thus be assumed that his semen contains a population of fertile spermatozoa. Nevertheless, how fertile a sperm population is cannot be determined precisely and only a probability analysis can be done to assess a male's fertility status. In this regard, it is necessary to a) determine the values for certain semen/sperm parameters of fertile males, b) define the normal ranges of these values and c) statistically compare the observed values of a semen sample of unknown fertility with the normal ranges reported for fertile males (Mortimer, 1994).

Since a male's fertility potential is based on the evaluation and statistical analysis of certain indirect criteria, it is very important that measurements must be accurate and reproducible. At the same time, the techniques used for assessment must be objective, standardized and sensitive to recognize deviations from the normal ranges (Mortimer, 1994).

Normal ranges of selected semen/sperm characteristics for humans have been determined and adjusted by the World Health Organization (WHO) during the last two decades (WHO, 2010). Whereas the WHO criteria represent the lower end of normality (due to its focus on male infertility), a similar set of normal ranges have been proposed by Mortimer (1994), but differs in the fact that it also includes the "borderline" and "pathological" ranges for selected characteristics and might be more useful to predict the probability of conception. On the other hand, the normal ranges for domestic animals are based on the opposite extreme, namely artificial selection for high fertility to increase the success rate of assisted conception. Determination of normal ranges and male fertility in natural populations of animals has *received* much less attention, since it is assumed that natural selection would result in similar semen characteristics among males, but this might not be the case (Gomendio *et al.*, 2007).

2.5.2 Important semen parameters to be assessed

A spermatozoon can only achieve its ultimate goal if multiple sperm functions can occur undisturbed and sequentially prior to, during and after fertilization. Selection of parameters for fertility should therefore be able to measure key features of semen/sperm which will be related to spermatozoa's fertilizing capacity (Holt and van Look, 2004). Numerous studies over the last three decades have reported on the predictive value of certain semen/sperm parameters on *in vitro* fertilization (IVF) and pregnancy outcome (see Agarwal *et al.*, 2003 for detailed list). For discussion purposes, these parameters will be divided into three groups, namely standard semen parameters, sperm functional tests and molecular tests.

Standard semen parameters

The first set of parameters of a semen sample is usually evaluated shortly after collection and liquefaction of the sample. These parameters include the volume, colour, odour, pH, sperm concentration, percentage total motility and percentage normal morphology of the neat semen sample.

In general, the standard semen parameters are used to immediately identify problematic samples or to place a semen sample within a certain threshold (normal range) for specific parameters (Holt, 2005). Measuring parameters such as sperm concentration, total motility and normal morphology should be performed using calibrated equipment and standardized techniques (Gago *et al.*, 1998; Barroso *et al.*, 1999). For instance, care should be taken which type of counting chamber is used, since it was reported that some chambers had a very high coefficient of variation and underestimated the sperm concentration by about 25% (Christensen *et al.*, 2005).

The relationship between the percentage normal sperm in a semen sample and male fertility or fertilization rates has been reported for many mammalian species (Menkveld *et al.*, 1990; Jasko *et al.*, 1990; Coetzee *et al.*, 1998; Hirai *et al.*, 2001). There is also strong clinical evidence that a decrease in activated sperm motility is related to a decrease in male fertility (Turner, 2003) and that there is a correlation between sperm motility and the proportion of morphologically normal spermatozoa (Hirai *et al.*, 2001; Malo *et al.*, 2005).

Although correlations (positive but complex) exist between the above mentioned parameters and *in vitro* fertilization rates or pregnancy outcome, more recent studies have shown that these parameters cannot solely be used to predict male fertility or to identify subfertile males (Gadea *et al.*, 2004, Rijsselaere *et al.,* 2005; Mocé and Graham, 2008). This led to the development of various *in vitro* tests to evaluate the functional aspects of spermatozoa (Henkel *et al.*, 2005; Petrunkina *et al.*, 2007).

Sperm functional tests
Spermatozoa can be regarded as "multi-compartmental cells" and each of these compartments must be intact before it can be considered as a 'functional' spermatozoon (Mocé and Graham, 2008). Not only can a spermatozoon be 'infertile' for a number of different reasons, but semen samples also consist of a heterogeneous population of spermatozoa with many of the cells not being able to reach or to fertilize an oocyte (Holt and van Look, 2004). Sperm functional tests have therefore been developed to address many independent sperm functions and to be sensitive enough to evaluate male fertility. These tests mainly concentrate on evaluating spermatozoa's ability to adapt to a new environment, survive in the female reproductive tract, reach the site of fertilization, respond to fertilizing conditions (capacitation

and acrosome reaction) and to interact with the oocyte (Henkel *et al.*, 2005; Petrunkina *et al.*, 2007).

A few examples of the sperm functions to be considered for research purposes, as well as the related sperm functional tests, include: motility and morphology (CASA systems), plasma membrane integrity (eosin-nigrosin of fluorescent staining, hypo-osmotic swelling test), mitochondrial function (fluorescent probes sensitive to mitochondrial membrane potential), capacitation and the acrosome reaction (peanut agglutinin), oocyte binding and fertilization (zona-free hamster oocyte binding test) and chromatin condensation or DNA integrity (aniline blue staining and Tunel assay) (Henkel *et al.*, 2004; Mocé and Graham, 2008).

Molecular tests

In the last two decades it has been reported that the incidence of male infertility in humans is increasing and could be as high as 40%. While abnormalities in the sperm characteristics of some men are easily identifiable with routine semen analysis or sperm functional tests, there still remain a large proportion of these men which have "unexplained male infertility" (Stouffs *et al.*, 2009). Newly developed and highly sophisticated molecular techniques have recently both shown to be of great value in detecting subtle causes of male infertility based on biochemical aspects (Jeremias and Witkin, 1996; Aitken, 2010).

The introduction of molecular approaches such as polymerase chain reaction (PCR), mass spectrometry and proteomics has given a new dimension to the identification of factors which could cause male infertility. These techniques can be used independently or in combination to identify abnormalities in many sperm functional aspects, e.g. defects in mtDNA or mRNA, presence of abnormal surface molecules, immunological reactions or anomalies in sperm protein expression (Jeremias and Witkin, 1996; Nakada *et al.*, 2006; Oliva and Martínez-Heredia, 2008; Stouffs *et al.*, 2009).

2.5.3 Relationship between sperm mitochondria and selected sperm parameters

Owing to the fact that the size of the sperm midpiece differs markedly between mammalian species (Cummins and Woodall, 1985; Gage, 1998), one method of determining the possible reasons for this variation, is by comparing the sperm characteristics of different mammalian species. The sperm characteristics selected for evaluation in this study included basic

structural and functional aspects of spermatozoa that are related to the sperm midpiece and/or sperm mitochondria.

Standard semen analysis

The standard semen analysis was only used in this study to evaluate if a semen sample meets the basic requirements to be considered an 'acceptable' sample and could be included in the study.

Sperm morphometry

Firstly, it was important to determine the dimensions of the sperm midpiece, since these were used as reference points to the size of the midpiece. Various other sperm dimensions were also measured, as it was reported that the size of the midpiece are related to total sperm length or the size of other sperm components, e.g. head length, head area and flagellum length (Cardullo and Baltz, 1991; Gage, 1998). Since sperm morphology is only important in species which have a large number of 'abnormal' sperm forms (e.g. head morphology in humans), this parameter was not included for comparative purposes – most mammalian species have a low incidence of pleiomorphism (Holt, 2005).

Sperm mitochondrial structure

While the relative size of the midpiece can be determined by the staining of sperm and light microscopic analysis (as above for sperm morphometry), a more detailed study of the structure of the midpiece and individual mitochondria was considered necessary to elucidate species differences. The study of sections through the sperm midpiece using electron micrographs can be used to determine structural aspects, such as the exact location and size of the mitochondria, the internal structure of the mitochondria (e.g. abundance and dimensions of the cristae) and the number of gyres the mitochondrial helix forms (Fawcett, 1970; Bartoov and Messer, 1976). Transmission electron microscopy can often detect subtle structural differences in sperm components, which can reveal major, unexpected abnormalities (Mortimer, 1994; Mundy *et al.*, 1995).

Sperm mitochondrial integrity

Another method of determining the location of the mitochondria in any cell type is by the use of fluorescence probes which selectively stains mitochondria. Several of these fluorescent probes are also sensitive to MMP and can thus be related to the viability/activity and the

metabolic state of the mitochondria (Graham *et al.*, 1990; Windsor and White, 1993; Auger *et al.*, 1993). In the present study, it was important to determine whether the structural aspects of the sperm mitochondria also confirm its functional status.

Sperm motility

Visual evaluation of the percentage motile sperm in a semen sample is an integral part of any semen analysis (Mortimer, 1994). The importance of this sperm feature becomes apparent when taking into consideration that an immotile spermatozoon will probably never reach the site of fertilization in species which depend on internal fertilization (Turner, 2003). Sperm motility will also be affected if other sperm features are compromised, e.g. severe morphological abnormalities, disrupted plasma membrane integrity and even mtDNA mutations (Katz *et al.*, 1982; Kao *et al.* 1998; Rijsselaere *et al.*, 2005).

Therefore, in the current study, sperm motility was used as a prerequisite for selecting a sperm population for further analysis. The direct relationship between sperm mitochondria and motility has also been reported (Gopalkrishnan *et al.*, 1990) and the size of the midpiece was found to be a predictor of sperm kinematics and swimming velocity (Cardullo and Baltz, 1991; Firman and Simmons, 2010).
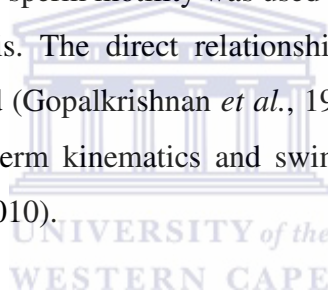
Sperm metabolism

A controversial issue such as which metabolic pathway is more important for certain sperm functions (Miki, 2007; Ruiz-Pesini *et al.*, 2007) and whether sperm mitochondria are necessary for ATP production could not be left unaddressed. By providing evidence for the role of mitochondria in sperm motility and ATP production, it could possibly also provide the answer for the variation in the size or the mitochondrial loading of the midpiece.

Once the relationship between sperm mitochondria and these basic sperm parameters have been elucidated, more detailed studies should be carried out in future. Such studies could then possibly include more in depth molecular techniques which may be applied to the role of sperm mitochondria in infertility, toxicology and contraceptive studies.

2.6 Comparison between mammalian species

2.6.1 Selection of mammalian species

In previous studies, a large number of mammalian species have been included in studies on sperm morphometry and the adaptive significance of sperm form and function (Cummins and Woodall, 1985; Gage, 1998; Anderson *et al.*, 2005). However, most of these studies focused on the difference in size of various sperm components and its relevance to sperm competition. Contradictory reports on the relationship between the size of the midpiece (length and/or volume) and other sperm components in mammalian species have been published in the last decade (Gage and Freckleton, 2003; Anderson *et al.*, 2005; Malo *et al.*, 2006; Firman and Simmons, 2010), but few studies have included a relationship between the midpiece size and sperm functional aspects (Cardullo and Baltz, 1991; Malo *et al.*, 2006; Firman and Simmons, 2010).

In the present study, it was thus decided to include a smaller number of selected mammalian species, but also to evaluate a larger number of both morphometric and functional aspects of the spermatozoa, focussing on the midpiece and sperm mitochondria. The main reason for selecting a smaller number of mammalian species was due to logistical constraints in terms of the number of parameters that was evaluated. The selection of mammalian species for the present study was accordingly based on five criteria: a) the inclusion of a large variation in the morphometry of the entire spermatozoon as well as the midpiece, b) the inclusion of species with different mating strategies, resulting in species with different levels of sperm competition and possible female selection of sperm, c) the inclusion of species which have been used previously for research purposes and of which basic sperm characteristics have been reported, d) the inclusion of various primate species in order to construct a primate model between humans and non-human primates and e) the availability of mammalian species for research purposes for this investigation.

2.6.2 Mammalian species included in the study

Seven mammalian species have been included in the current study, namely human, chacma baboon, rhesus monkey, vervet monkey, merino ram, mouse and naked mole-rat. Each of the species is discussed in more detail below and a rationale for their inclusion is based on some of the above mentioned selection criteria. The use of non-human primates (chacma baboon, rhesus monkey and vervet monkey) as models for human reproductive research provides a further rationale for their inclusion.

Primate models in research

Non-human primates have been identified as key models in human-related studies due to their similarities in most aspects of their anatomy, endocrinology and physiology. Subsequently, these primate species have been appropriately used to examine and extrapolate the effects of experimental manipulations in a broad range of disciplines, e.g. neurobiology, immunology, reproductive biology, cardiology, endocrinology, pathology and psychology (King *et al.*, 1988). While chimpanzees are 98% similar to humans on a genetic basis, the New World monkeys of tropical America share 85% and the Old World monkeys of Asia and Africa 92% of their genetic material with humans (Sibley and Ahlquist, 1987). The most common primates used in research are the Old World monkeys, including the rhesus monkey and the long-tailed macaque, whereas the squirrel monkey is the most popular New World monkey (King *et al.*, 1988).

Since the Old World monkeys generally represent a more relevant human model than New World monkeys, this group of primates should be focussed on for reproductive studies. These primates show close relationships to humans in terms of structural features of the male reproductive tract, hormonal control of reproduction, spermatogenesis and most aspects of fertilization (Harrison and Kubisch, 2005). In this regard, non-human primates are often used in studies on male fertility/infertility, IVF or assisted reproductive technology (ART) procedures, male contraception and reproductive toxicology (van der Horst, 2005).

In the current study, the three non-human primate species are members of the family Cercopithecidae, which are all part of the Old World monkeys (Groves, 2005). Apart from reporting some essential baseline data for many aspects of the spermatozoa of these non-human primate species in the following chapters, this data can also be used to determine which species are to be selected as a primate model for humans for the various sperm parameters.

Human, *Homo sapiens*

Hominids diverged from the African great apes about 7-8 million years ago and have accumulated a variety of novel features in different species during their separate evolutionary trajectory (Martin, 2007; Balter, 2008). *Homo sapiens* itself is currently documented by fossil evidence to have emerged 200 000 years ago. It is postulated that humans adopted a gathering-and-hunting lifestyle for 95% of this period and that during the last 5%, following

the emergence of settlements and domestication worldwide, cultural factors would have had an important influence on lifestyle (Martin, 2007). Comparing human spermatozoa to those of other primates in terms of various aspects of male reproduction have revealed that it falls in the range of primate species with a single male mating system and are thus monogamous (Moller, 1988; Martin, 2003). It also seems that humans are adapted for a mating system with low sperm competition if its relative testis size, size of the sperm midpiece and the absence of a baculum (os penis) is considered (Martin, 2007).

Much of the interest in the evaluation of human semen samples is due to the fact that male factors seem to be the main cause or a co-factor of infertility in 50% of couples having problems to conceive (Stouffs *et al.*, 2009). In order to define and diagnose male infertility, the World Health Organization has gone to great lengths to recommend standardized methods for the evaluation of human semen samples and providing reference values for human semen characteristics (Cooper *et al.*, 2010). In addition, many ART have been developed in the past two decades to overcome problems with fertility and is especially recommended in cases where male infertility is due to an 'unknown' cause (Collins and van Steirteghem, 2004).

This increased focus on male infertility in humans and its causes has warranted the inclusion of *Homo sapiens* as a species. Although the structure of human spermatozoa is very similar to closely-related primates, it displays certain distinctive features (Bedford, 1974) which could be of interest in this comparative study.

Chacma baboon, *Papio ursinus*

The chacma baboon occurs widely in the Southern African sub-region, but in the more arid regions, they only occur where local conditions are suitable. Chacma baboons are gregarious and occur in troops of up to 130 individuals. This species has a multiple partner mating system and the dominant and high-ranking adult males copulate most often. Breeding occurs throughout the year and a single young is born after a gestation period of six months. Adult males weigh on average 31.8 kg (Skinner and Smithers, 1990).

While the olive baboon (*Papio anubis*) is possibly the best studied and reported African baboon species for male reproductive studies (van der Horst, 2005), these baboons do not naturally occur in South Africa. The use of chacma baboons thus seems to be an alternative, especially since these animals are often captured to control their numbers and could

subsequently be made available for research purposes (Bornman *et al.*, 1988). Although the method of semen collection and the basic semen parameters of the chacma baboon have been reported (Bornman *et al.*, 1988), very little alternative information is available on the sperm parameters of this species.

The chacma baboon has therefore been selected to be part of this study in terms of its availability, its relatedness to humans (part of the primate model) and also to report on basic structural and functional aspects of its sperm, which could be useful for future research purposes.

Rhesus monkey, *Macaca mulatta*

Rhesus monkeys have the widest geographic distribution of any species of non-human primate, occurring naturally from the tropical forests of south-eastern Asia to the rugged mountains of north central China. These primates are the most adaptable of all non-human primates, with the broadest range of habitat, and the most cosmopolitan food habits. Rhesus monkeys are intensely social animals and live in groups of 10-60 individuals or more. In Asia, mating occurs throughout the year, but is most prevalent from September to December, and most young are born from March to June, after a gestation period averaging 164 days (Cawthon Lang, 2005). In the Southern hemisphere, the breeding season is from March to August (also autumn and winter months) and most births occur in October to January (Bielert and Vandenbergh, 1981). Males usually reach maturity between four and five years of age and a multiple male mating system is apparent. The males weigh on average 7.7 kg and display a dark reddish scrotum, penis and sex skin folds on the rump (Cawthon Lang, 2005).

Rhesus monkeys have long been used as a model for various reproductive studies, including multiple follicle stimulation, oocyte fertilization by intracytoplasmic sperm injection (ICSI), oocyte/embryo manipulation and cryopreservation of spermatozoa (Hewitson *et al.*, 1998; Wolf, 2004; Nichols and Bavister, 2006). The existence of detailed reports on rhesus monkey reproduction and the possibility of relating the findings of the current study to the available information make it essential to include this species.

Vervet monkey, *Chlorocebus aethiops*

Vervet monkeys (also referred to as African green monkeys) are considered the most widely distributed of all the African monkeys and the most abundant monkeys in the world. These

primates are endemic to Africa and can be found from southern Ethiopia and Somalia to the Western Cape Province in South Africa. Vervet monkeys are also gregarious and occur in multi-male troops of up to 38 (Skinner and Smithers, 1990). In the wild, vervet monkeys are seasonal breeders with a gestation period of 140 days and young may be born throughout the year. However, in captivity, they adapt and breed successfully all year round (Seier, 1986), and are not affected by seasonal variations. The males have a mass of 5.5 kg and the genitals are vividly coloured to signal sexual status, namely a red penis and a blue scrotum (Skinner and Smithers, 1990).

Vervet monkeys are utilized for research in several disciplines including ophthalmology and virology (Kushner *et al.*, 1982) and have proven to be a good model in the areas of nutrition, reproduction and toxicology. Reproductive studies on vervet monkeys have reported on their human-like sperm characteristics (e.g. concentration, motility, pH of seminal fluid, acrosomal integrity) (Seier *et al.*, 1989; van der Horst *et al.*, 1999, Mdhluli *et al.*, 2004). Additionally, this species semen cryopreservation protocols have been determined (Seier *et al.*, 1993) and it could potentially be a valuable research model for studying ART (Sparman *et al.*, 2007).

The vervet monkey has been selected to form part of the study due to its availability as part of a very successful captive breeding program, the existence of successful semen collection protocols for this species, which could be employed for the other non-human primate species, and its reported human-like sperm characteristics.

Merino ram, *Ovis orientalis aries var.* "*merino*" f. "*south african merino*"
The Merino sheep breed was imported to South Africa in the late 1700's from Spain. Although these sheep were the most important wool breed in South Africa for many years, a marked change in the selection objectives of the breed was necessitated when wool became less important as a textile (Cloete and Oliver, 2010). An increase in the price of lamb and mutton meat in recent years has directed some attention to the genetic aspects of meat production from the Merino breed (Cloete *et al.*, 2004).

Most of the published research on Merino ram spermatozoa is focussed on the management of livestock populations and the increase in productivity. Therefore, many studies have been involved in the cryopreservation of ram sperm (Lightfoot and Salamon, 1970; Choudhry *et al.*, 1995), artificial insemination techniques (e.g. determination of the minimum number of

spermatozoa to be deposited and the place of deposition in order to maximize the number of offspring per unit cost of the dose) (Paulenz *et al.*, 2002; de Graaf *et al.*, 2007), selection of fertile sperm populations (Grasa *et al.*, 2004) and abnormalities in the reproductive hormone levels (Auclair *et al.*, 1995).

The Merino ram is the only domesticated species in the current study that has been subjected to strong artificial selection for high fertility and specific improvements in productivity. It will thus be interesting to investigate if this selection history would have had an effect on the current sperm form and function.

House mouse, *Mus musculus*

This species of mouse, as indicated by its common name, normally occurs as a commensal with man and thus explains its cosmopolitan distribution. It is thought that the species of rodent originated in the southeastern steppe of Russia and has subsequently been transported throughout the world due to its close association with humans. The social structure of the house mouse in its natural habitat includes territorial males with several breeding females and therefore a polygamous mating regime exists. These females can give birth to their first litters when they are only 40 days old. The gestation period is 19 days and the average litter size is six (range between one and thirteen) (Skinner and Smithers, 1990).

Due to the fact that the house mouse is highly available, can easily adapt to 'unnatural' conditions and has a short gestation period, it is very successfully used in captive breeding programs worldwide. The house mouse, as for many other rodent species, has been part of innumerable scientific studies as animal models, including studies with male fertility as the main focus. Most recently male infertility has been studied by the use of knockout (transgenic) mice to identify the consequence of gene abnormalities and its influence on, e.g. spermatogenesis (Wang *et al.*, 2009; Ruwanpura *et al.*, 2010), sperm function (Escalier, 2006; Oliva, 2006) and male contraception (Matthiesson and McLachlan, 2006; Page *et al.*, 2008).

The inclusion of the house mouse in the current study was due to its non-relationship with the primates and its different sperm structure. The spermatozoa of the house mouse are very large relative to its body size (in contrast to the primates) and it contains a falciform head with an apical hook. This latter characteristic has recently been investigated as a possible adaptation

for sperm competition (Firman and Simmons, 2009) and is not present in any of the other six species mentioned here.

Naked mole-rat, *Heterocephalus glaber*

The naked mole-rat is also classified as a rodent species and it belongs to the family Bathyergidae and inhabits the arid regions of East Africa, including Kenya, Ethiopia and Somalia (Jarvis, 1985). This subterranean rodent species has, however, an intriguing social structure by exhibiting the classical features of a eusocial society, a feature not known to exist in any other mammalian species (Bennett and Faulkes, 2000). Typical to this type of social system, these animals occur in colonies in which only a single female breeds with a few selected males. Wild colonies contain 40-90 individuals, with most of them classified as "workers" according to a behavioural division of labour and these animals are typically responsible for foraging, nest building and caring for the young (Jarvis, 1981).

Apart from the intriguing social system of the naked mole-rats, these animals also exhibit an extreme example of socially-induced suppression of reproduction (Faulkes *et al.*, 1991). Previous studies have reported that ovulation is blocked in the subordinate, non-breeding females in a colony, but this suppression can be reversed if the responsible social factors are removed (Faulkes *et al.*, 1990). In the subordinate, non-breeding male naked mole-rats, the suppression of reproduction does not seem to be as complete as in the females. Although breeding males had larger reproductive tract masses compared to non-breeders, the non-breeding males still portrayed active spermatogenesis and spermatozoa in the epididymides (Faulkes *et al.*, 1991). In a subsequent study, however, Faulkes *et al.* (1994) reported that the number of spermatozoa was much higher in breeders and that less than 30% of non-breeding males had motile spermatozoa.

Selection of this unique species was based on the fact that it represents the most extreme example of a lack of sperm competition. Since only a few males are selected to be breeders and there is a high occurrence of inbreeding in the naked mole-rat colonies (Bennett and Faulkes, 2000), very little sperm competition is theoretically present and could have an effect on the sperm form and function. It needs to be emphasized, however, that it was extremely difficult to extract spermatozoa from any part of the male reproductive tract of this species. Subsequently, only small volumes of semen could be extruded from the ampulla and as a

result, a few experimental methods, e.g. TEM and fluorescent staining of the sperm midpiece, could not be performed for this species.

2.7   Conclusion

The adaptive significance of many sperm characteristics is still unexplained despite numerous studies focussing on various aspects of these sperm traits. Comparing the spermatozoa of various mammalian species will highlight many similarities and the major differences between their sperm characteristics.

The midpiece of the mammalian spermatozoon contains numerous mitochondria, but the reason for the marked difference in the length or the size of the midpiece (independently or relative to other sperm structures) of different mammalian spermatozoa is not clear. Sperm mitochondria have many different functions which could also be involved in determining the number of mitochondria a spermatozoon needs to contain in order to ultimately fertilize the ovum. The current study will address the relationships between the size of the midpiece and various other structural and functional aspects of mammalian spermatozoa in the research chapters to follow.
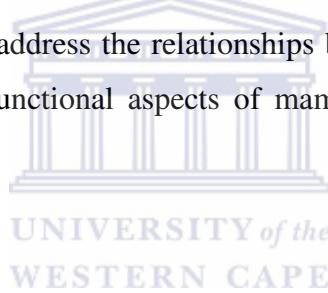
UNIVERSITY *of the*
WESTERN CAPE

CHAPTER 3: Assessment of sperm morphometry of selected mammalian species using automated and semi-automated image analysis techniques

3.1 Introduction

Spermatozoa are highly specialized haploid cells which are adapted for their function of reaching and fertilizing the ovum. In this regard, spermatozoa are typically composed of a sperm head (contains nucleus) which is covered by the acrosome (egg entry apparatus), a motility apparatus (flagellum) and a source of energy production (midpiece containing mitochondria) (White-Cooper and Bausek, 2010). The size and shape of these sperm components are, however, not uniform and the variations of mammalian sperm dimensions are well documented (Cummins and Woodall, 1985; Gage, 1998; Gage and Freckleton, 2003).

The variation in sperm size and shape is not limited to mammalian spermatozoa and occurs across taxa. The adaptive significance of these variations is largely unexplained, but believed to be influenced by three factors, namely phylogeny, mode of fertilization and post-copulatory sperm selection (e.g. sperm competition and cryptic female choice) (Morrow and Gage, 2001; Immler *et al.*, 2007). Since mammals conform to internal fertilization, the sperm component similarities and/or variations are probably due to relatedness between species (phylogeny) and the complex environment the spermatozoa needs to survive in (female reproductive tract).

Although it was originally reported that the size of spermatozoa is inversely related to body mass (Cummins and Woodall, 1985), several subsequent studies have rejected this argument (Gomendio and Roldan, 1991; Gage, 1998). No relationships were also found between body mass and individual sperm components (head length, midpiece length or flagellar length) (Gage, 1998; Anderson *et al.*, 2005). Most of the differences in the size of mammalian sperm are due to the variation in the length of the flagellum, or the length of the midpiece and the principal piece respectively (Cummins and Woodall, 1985). Positive associations between individual sperm components have been reported, e.g. the sperm midpiece and flagellar lengths are related to both the head length and the head area (Gage, 1998). Measurement of absolute sperm components as well as relative sperm components (ratios of individual components) has also been related to sperm swimming speed (Gomendio and Roldan, 1991, 2008; Malo *et al.*, 2006; Humphries *et al.*, 2008).

Several inconsistencies exist in the literature in terms of the variations in sperm dimensions and its possible relationships to sperm function or sperm competition. Many of the earlier studies on this topic have made use of cited sperm measurements in the literature to create large data sets including between 280-450 mammalian species (Cummins and Woodall, 1985; Gomendio and Roldan, 1993; Gage, 1998). Although some of these mentioned studies did not include data of "suspect accuracy" (e.g. sperm measurements from testicular histology specimens), different sample sizes and measurement techniques were employed by the originally published studies (Gomendio and Roldan, 1993; Anderson *et al.*, 2005). By improving the quality and consistency of data sets used to examine evolutionary concepts, it might be possible to eliminate these inconsistencies and provide more informative results (Anderson *et al.*, 2005).

Thus, one of the main aims of the current study was to make use of standardized staining procedures in order to obtain accurate, unbiased measurements of sperm morphometry. Several previous studies have focussed on finding the most suitable staining technique for a specific species (Gravance *et al.*, 1996; Gago *et al.*, 1998; Rijsselaere *et al.*, 2005; Soler *et al.*, 2005), while other studies reported that staining techniques can affect sperm head shape and dimensions (Davis and Gravance, 1994; Meschede *et al.*, 1993). In the current study, it was first of all important to select a universal staining technique which a) could be utilized for all seven mammalian species, b) would cause as few changes as possible to the sperm morphology and morphometry and c) would be able to stain spermatozoa differentially and indicate the boundaries of each sperm component. A recently developed stain, SpermBlue®, has been able to satisfy all three criteria mentioned above for the evaluation and measurement of sperm morphology and morphometry of numerous species (van der Horst and Maree, 2009; Maree *et al.*, 2010). Secondly, the accuracy and reproducibility of morphometry measurements can be improved by utilizing image analysis (WHO, 2010). Although computer aided sperm analysis (CASA) systems have only been developed and utilized during the last two decades, these systems can increase the precision and reproducibility of morphometric measurements (Garrett and Baker, 1995). Another advantage of SpermBlue® is that this staining technique is also amenable to automated sperm morphometry analysis (ASMA) (van der Horst and Maree, 2009).

Other equally important aims of this chapter were to indicate the variations in sperm morphometry of selected mammalian species and to highlight the species specificity of these measurements, especially the sperm midpiece.

3.2   Materials and methods

3.2.1   Standardization of materials and methods

The comparative nature of this study necessitated the use of standardized experimental procedures to ensure that the possible relationships reported among sperm parameters will not be due to or influenced by biased, subjective or inaccurate measurements and evaluations (Comhaire *et al.*, 1992; Barratt, 1995). The planning and execution of all these experimental procedures also entailed measures to reduce random and systematic errors in semen/sperm analysis and to minimize statistical sampling errors (WHO, 2010).

Where possible, previously reported semen/sperm analysis techniques were implemented in the current study. Occasionally, these techniques were modified to allow the exact same procedure to be used for all the species included in this study. Thus, the description of the materials and methods in this and the following chapters comprises all seven species, unless stated otherwise.
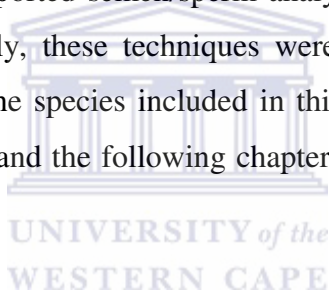
3.2.2   Access to different mammalian species

Ethical clearance for this study was obtained from the Ethics Committee of the University of the Western Cape (Project number: ScRIRC2007/3/30). Access to the naked mole-rats was grated via the Department of Zoology at the University of Cape Town (Ethical Clearance number: 2005/V7/JOR).

3.2.2.1   Human donor program

Human semen samples were obtained from nine healthy volunteers taking part in a semen donor program at the Reproductive Research Laboratory, Division of Medical Physiology, Department of Biomedical Sciences, Stellenbosch University (South Africa). A total of 19 semen samples were collected over a period of six weeks, but only ten samples were selected for comparative analysis. Selection of these samples was based on the quality of the samples and the prerequisite that all experimental procedures should have been performed on each and accordingly all samples in order for them to be considered.

All procedures for sample collection were in accordance with ethical guidelines of the University of the Western Cape as well as the research unit where semen was collected (Division of Medical Physiology, Department of Biomedical Sciences, Stellenbosch University). The Helsinki Declaration governing research on humans has also been adhered to (Christie, 2000). A consent form (see Appendix 1) was signed by each human donor and these donors were assured of their anonymity, that their semen sample was used for research purposes only, that it will not be used for any cloning research, and that the semen sample was destroyed after experimentation.

3.2.2.2 Chacma baboons

The chacma baboon males included in the present study were caught in the wild and belonged to a colony of 90 individuals housed at the Delft Animal Centre, Medical Research Council (Cape Town, South Africa). All the animals were housed and maintained in accordance with the revised South African National Standard for the Care and Use of Animals for Scientific Purposes (South African Bureau of Standards, SANS 10386).

The males were housed outdoors in single cages, but with full visual, olfactory and auditory contact with conspecifics. Tactile contact was made possible through grooming panels of wired mesh, which allowed grooming between adjacent individuals. The animals were maintained on a standard diet of pelleted feed (Aquafeeds, Cape Town, South Africa) and fresh fruit or vegetables. The diet was supplemented once a week with bread slices covered with vitamin C syrup (Portfolio Pharmaceuticals, Johannesburg, South Africa). Fresh drinking water was supplied twice a day (de Villiers and Seier, 2010). The body weight of the animals ranged between 26.2 kg and 36.5 kg (average 29.6 kg). All males were stimulated on a regular basis for sample collection and eventually ten semen samples were selected for inclusion in the study based on the same criteria as for the human semen samples.

3.2.2.3 Rhesus monkeys

Seven male rhesus monkeys, between the ages of 8 and 14 years, were selected from an outdoor breeding colony at the Delft Animal Centre, Medical Research Council (Cape Town, South Africa). The original breeding stock are from Chinese origin and the colony has a ten-year history of successful first generation reproductive performances. One wild caught, prime adult male has been specifically selected and maintained for his fertility. The remaining six

males were captive breed, sub-adult males, of which five were breeding males with known fertility and the sixth male had unknown fertility.

All the animals were housed and maintained in accordance with the revised South African National Standard for the Care and Use of Animals for Scientific Purposes (South African Bureau of Standards, SANS 10386). Males were housed indoors in double galvanized steel cages in rooms with temperature between 25–27 °C and 12-hour light/dark controls. Five of the males were paired with a compatible breeding female, while the remaining two were singly caged but were allowed social interaction *via* a grooming panel with an adjacent female. The animals were maintained on a standard diet of special monkey cubes (Equifeeds, Cape Town, South Africa) and bread slices with added Multivitamin Syrup (Portfolio Pharmaceuticals, Johannesburg, South Africa). The diet was supplemented with seasonal fruit or vegetables and the animals were provided with foraging logs and various other enrichment devices on a daily basis. Drinking water was available *ad libitum.* The body weight of the animals ranged between 7.20 kg and 9.85 kg (average 8.38 kg).

Due to the fact that these animals are seasonal breeders, samples were collected over a period of three months (June to August) when the males consistently produced reliable semen samples (high in sperm concentration, motility and normal morphology). During these three months all males were stimulated on a regular basis for sample collection and eventually ten semen samples were selected for inclusion in the study based on the same criteria as for the human semen samples.

3.2.2.4   Vervet monkeys

Ten adult vervet monkey males (two wild caught and eight captive bred), between the ages of four to twelve years, were selected from an indoor breeding colony at the Primate Unit, Medical Research Council (Cape Town, South Africa). The colony has a history of successful reproductive performances for three generations. Eight of the selected males were breeding males of known fertility who had continuous contact with breeding partners throughout the study. The two males with unknown fertility were housed in single galvanized steel cages, with access to an exercise cage and a female companion twice a week.

All the animals were housed and maintained in accordance with the revised South African National Standard for the Care and Use of Animals for Scientific Purposes (South African

Bureau of Standards, SANS 10386). The conditions in the closed indoor environment were maintained at 25-27 °C, a humidity of 45%, about 15-air changes/hour and a photoperiod of 12 hours (Seier, 1986). Their diet consisted of a stiff porridge of pre-cooked maize meal, enriched with vitamin and mineral mixes as well as trace elements and a protein supplement. The diet was supplemented with seasonal fruit at noon. Seier (1986) reported that this diet supported good reproductive performance and breeding at this facility. Additionally, monkeys were provided with foraging logs and various other enrichment devices on a daily basis. Drinking water was available *ad libitum* via an automated water system. The body weight of the animals ranged between 4.23 kg to 6.10 kg (average 5.15 kg). All males were stimulated on a regular basis for sample collection and eventually ten semen samples were selected for inclusion in the study based on the same criteria as for the human semen samples.

3.2.2.5   Merino rams

The merino rams included in the present study were part of an experimental breeding flock which were divergently selected for maternal multiple rearing ability from a common base population since 1986 (Cloete *et al.*, 2004). The animals were kept at the Elsenburg Experimental Farm (Elsenburg Agricultural Centre, South Africa) on kikuyu pastures and had free access to water. Ten fertile rams between the ages of 2-4 years were selected from the breeding flock and their body weight ranged between 54.0 kg and 78.5 kg (average 64.4 kg). These rams were separated from the other sheep and housed together for about one month before the sampling started. During this time, none of the rams came into contact with any ewes and therefore no ejaculation took place for a few weeks *prior* to sampling.

3.2.2.6   House mice

Male mice (C57 strain) were obtained from the Animal Unit of the University of Cape Town (South Africa). The animals were housed and maintained in an animal room at the Department of Medical Biosciences, University of the Western Cape (South Africa). The mice were kept in standard cages (3-4 per cage), at temperatures between 20 °C and 23 °C and exposed to a 12:12 hour day-night cycle. The animals were fed standardized pelleted food and water was available *ad libitum*. Ten male mice aged four to eight months were sacrificed for the current study and had body weights ranging between 30.39 g and 35.85 g (average 32.17 g).

3.2.2.7 Naked mole-rats

Male naked mole-rats were obtained from a captive breeding colony at the University of Cape Town (South Africa). The animals were housed in artificial burrow systems, at temperatures between 28 °C and 30 °C and relative humidity of 40-60%. The burrow systems consisted of interconnecting Perspex tubes which joined the nest chambers, toilet chambers and food chambers. Electric lamps (40 W) were placed outside the nest chamber and at several points along the tubes to increase the temperature to 32-34 °C (Faulkes *et al.*, 1990; 1991). The animals had access to fresh food and water *ad libitum* and a cereal supplement containing vitamins and minerals was also provided on a daily basis.

The ten males selected for the current study included five breeders and five subordinates (non-breeders). The breeders were either taken from a colony (consisting of a queen, a breeder and several subordinates) or they were males which were individually housed with a female for several months. The breeders and subordinates were distinguished from each other by observations of mating. The animals had a body weight range between 39.5 g and 56.2 g (average 46.9 g).

3.2.3 Collection and evaluation of semen/sperm samples

3.2.3.1 Masturbation

Human semen samples were obtained by masturbation after 2-3 days of sexual abstinence. Donor semen selection was based on the evaluation of sample size ($\geq$ 2 ml), sperm concentration ($\geq$ 20 x 10^6/ml) and percentage sperm motility ($\geq$ 50 % forward progression) (WHO, 1999) for this particular study. The sperm concentration and motility were assessed by pipetting 5 µl semen into a 20 µm deep chamber of a Leja slide (SC 20-01-04 B) (Leja Products B.V., Nieuw-Vennep, The Netherlands), and automated analysis with the Motility/Concentration module of the Sperm Class Analyzer$^®$ (SCA) CASA system version 4.0.0.5 (Microptic S.L., Barcelona, Spain). Additionally a Basler A602fc digital camera (Microptic S.L., Barcelona, Spain) was mounted (C-mount) onto a Nikon Eclipse 50i microscope (IMP, Cape Town, South Africa) or a Olympus CH2 microscope (Wirsam, Cape Town, South Africa), both equipped with phase contrast optics and a heated stage (Fig. 3.1).

There was no specific selection for or against the percentage normal spermatozoa in a semen sample and accordingly any bias was excluded in favour of morphological normal or abnormal spermatozoa. The semen was allowed to undergo liquefaction for 30-60 minutes at

37 °C in a CO_2 incubator before further analysis. The average human semen parameters are displayed in Table 3.1.
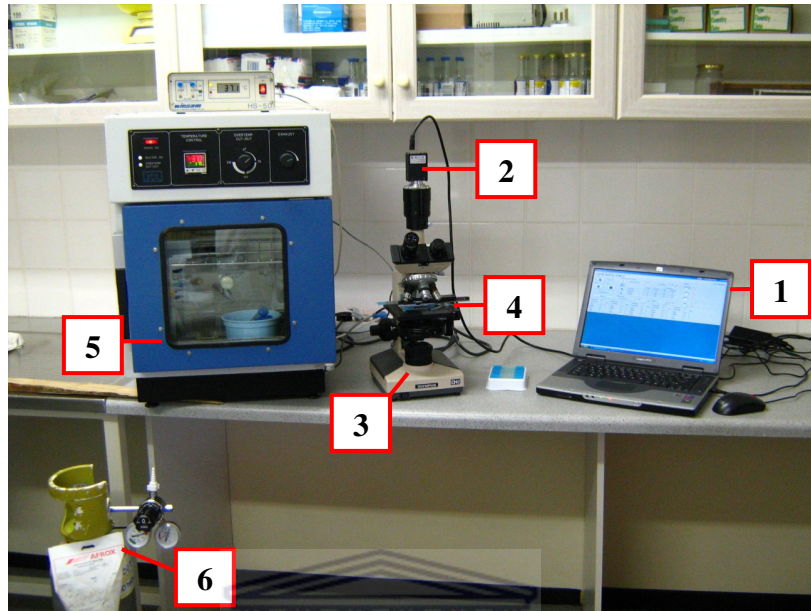
Figure 3.1. Equipment used for incubation and assessment of semen parameters as well as CASA analysis of sperm morphometry and motility. 1) Laptop with SCA® software for CASA analysis, 2) Basler A602fc digital camera, 3) Olympus CH2 microscope, 4) Heated stage, 5) Oven with sealed Perspex box for incubation, 6) 5% CO_2 mixture used for incubation.

Table 3.1. Semen characteristics (mean ± SD) of selected mammalian species (n=10 individuals for each species)

	HS	PU	RM	CA	OO
Volume (ml)	3.5 ± 0.8	0.9 ± 0.5	0.4 ± 0.2	0.7 ± 0.3	1.0 ± 0.4
Sperm concentration ($x10^6$/ml)	63.9 ± 18.6	212.5 ± 252.6	193.6 ±122.9	72.35 ± 18.0	3846.1 ± 2772.9
Motility (%)	72.8 ± 15.9	73.4 ± 16.7	69.2 ± 10.2	57.4 ± 15.5	74.1 ± 10.7
Osmolality (mOsm/kg)	356.8 ± 19.8	332.3 ± 9.6	352.5 ± 15.8	340.1 ± 17.6	ND

HS = *Homo sapiens* (human), PU = *Papio ursinus* (chacma baboon), RM = *Macaca mulatta* (rhesus monkey), CA = *Chlorocebus aethiops* (vervet monkey), OO = *Ovis orientalis* (merino ram), ND = not determined

3.2.3.2 Electro-ejaculation

Semen samples were obtained from the non-human primate species (chacma baboon, rhesus monkey and vervet monkey) as well as the Merino rams by rectal probe electro-ejaculation (RPE). Although it has been reported that semen/spermatozoa obtained through RPE has lower quality (decreased viability and fertilizing capability) than when an artificial vagina has been used (Mattner and Voglmayr, 1962; Denil *et al.*, 1992), Marco-Jimènez *et al.* (2005) found that the quality of fresh ram semen was not significantly different between these two

semen collection methods and that RPE resulted in a higher number of stable and functional frozen-thawed spermatozoa.

Non-human primates

Before each RPE procedure, the bottom of the animals' home cages was visually checked for the presence of white coagulum, which would be evidence of recent masturbation and elimination of the individual for RPE on a specific day. The animals were immobilized with an intramuscular injection of ketamine hydrochloride (Anaket V, Cape Medical Supplies, Cape Town) at 10 mg/kg and, depending on the primate, was placed in either dorsal or lateral recumbence (dorsal recumbence for the vervet monkey and lateral recumbence for the chacma baboon and rhesus monkey). The penis was cleaned with a mild detergent, then rinsed thoroughly with water and dried with a sterile gauze cloth.

The electro-ejaculation equipment consisted of a transformer (Eloff Transformers, Montague Gardens, Cape Town, South Africa) connected to a rectal probe. The latter was 15.4 mm in diameter with two brass bands (4.2 mm x 4.0 mm) embedded in the tip and 10 mm apart (Fig. 3.2). The transformer allowed various current settings (2.5 V, 3.5 V, 4.5 V, 5.5 V and 8 V), of which the position was manually controlled by one operator whilst another operated the placement of the rectal probe. The same RPE equipment and operators were used throughout the study to ensure consistency.
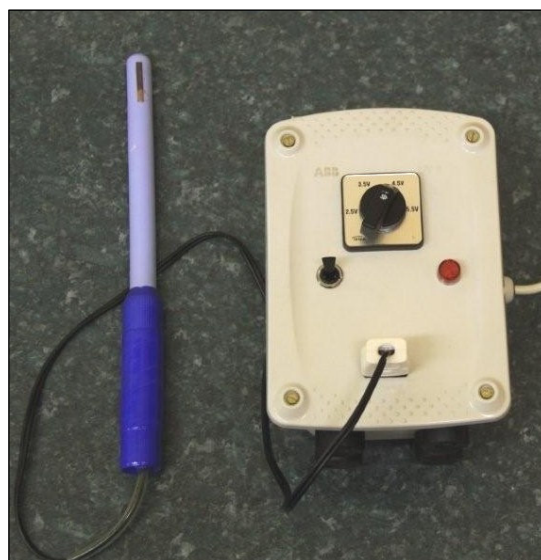
Figure 3.2. The rectal probe and transformer used for electro-ejaculation in the three non-human primate species.

The rectal probe was coated with a lubricating gel (Kyrogel, Kyron Laboratories, Benrose, South Africa) and gently inserted into the rectum of the animal, with the brass bands positioned at the level of the prostate gland. Stimulation started at 2.5 V, while the probe was adjusted inside the rectum to obtain an erection. The erection would cease after 15-30 seconds and the probe had to be gently withdrawn a short distance and then re-positioned to re-establish the erection. The same current was applied for 1-2 minutes, followed by a 15-20 second rest period (no stimulation) and an increase in the voltage thereafter. The same procedure and higher voltages were applied until ejaculation was achieved (Seier *et al.*, 1989; Cseh *et al.*, 2000). During the procedure, the penis was milked to get the maximal emission of semen from the urethra.

Ejaculates were collected directly into pre-warmed 15 ml (vervet and rhesus monkeys) or 50 ml (baboons) wide-mouthed graded plastic tubes. The ejaculates of all three non-human primate species were typically composed of two fractions, a liquid and a coagulated fraction. After collection, the semen samples were placed in an incubator for 30 minutes at 37 °C to allow liquefaction to occur. Only the liquid part of the semen sample was used for further analysis and the coagulum was discarded after its volume was recorded. The quality of the semen samples were also evaluated by utilizing the same method and equipment as described for the human samples, but the cut-off values were different. Although the semen volume, sperm concentration and sperm motility varied markedly between samples (see large variations in these values in Table 3.1), the following values were used as a guideline for the evaluation of a semen sample: a) the percentage total motile sperm in semen should be higher than 40 % for all three non-human primate species; b) the concentration of motile sperm in a semen samples should be higher than 25×10^6/ml for chacma baboons and vervet monkeys and 30×10^6/ml for rhesus monkeys. Similar large variations in the semen volume and sperm concentration have been reported for the baboon (*Papio ursinus* and *Papio anubis*) (Bornman *et al.*, 1988; Schaffer *et al.*, 1992).

Merino rams

Before the RPE procedure, each ram's testes were first palpated and evaluated by an animal health technician for any lumps or other abnormalities. The RPE equipment used for the rams was basically the same as for the primates, including a rectal probe connected to a transformer. A standard RPE procedure was followed as recommended by the state veterinarian.

Ejaculates were collected into pre-warmed 60 ml clean, wide-mouthed plastic specimen jars and placed in an incubator for 5 minutes at 37 °C. Thereafter, the semen was transferred to a pre-warmed 15 ml graded plastic tube to record the volume of the ejaculate and to prepare the sample for further analysis. The quality of the semen samples were also evaluated by utilizing the same method and equipment as described for the human samples and average values of selected ram semen parameters are presented in Table 3.1.

3.2.3.3   Extraction of spermatozoa from the reproductive tract

Sperm collection from both the mouse and the naked mole-rat was done by removal of the reproductive tract and careful dissection of the cauda epididymis (mouse) or ampulla (naked mole-rat.

Mouse

Male mice were sacrificed by cervical dislocation and immediately thereafter the right and left testis, epididymis and vas deferens were removed. Before the dissection, the testes were pushed caudally and then an incision was made into the abdominopelvic cavity, cutting through the tunica vaginalis until the testis and reproductive tract were exposed. After removal, the mentioned tissues were placed into a small plastic petri dish in pre-warmed Ham's F10 solution (Invitrogen, Cape Town, South Africa). Further dissections took place under a Zeiss SV8 stereo-microscope (Zeiss, Cape Town, South Africa), fitted with a removable Schott KL1500 cold light source (Zeiss, Cape Town, South Africa) and a heated (37 °C) warm plate.

Firstly, the dissected male reproductive tract was cleaned by carefully trimming off all unnecessary blood vessels and fat tissue using microscissors (Advanced Laboratory Solutions, Johannesburg, South Africa). When all parts of the reproductive tract could be clearly differentiated (Fig. 3.3), the vas deferens and/or the cauda epididymis were removed and placed into a second pre-warmed petri dish containing ± 200 µl Ham's F10.

If the cauda epididymis was used, only the part closest to the vas deferens, comprising of larger convoluted tubes, was removed (see Fig. 3.3). This part of the cauda epididymis was considered to contain a population of spermatozoa that would be moving into the vas deferens after ejaculation and therefore have similar morphological and swimming characteristics. Subsequently, a small piece of the vas deferens or cauda epididymis was cut off and placed

into a third pre-warmed petri dish containing ± 100 µl Ham's F10. Sperm extraction from these ducts is described in section 3.2.4.3.
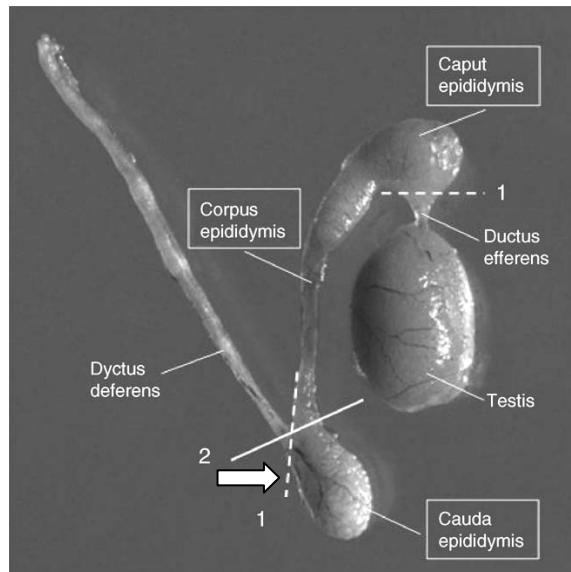
Figure 3.3. Photograph of the dissected male reproductive system of the mouse indicating the cauda epididymis and vas deferens (dyctus deferens). The part of the cauda epididymis used for sperm extraction is indicated with the white arrow. (From Tayama *et al.*, 2006)

Naked mole-rat

Male naked mole-rats were sacrificed by inhalation of halothane (Norpharm, Cape Town, South Africa) and immediately thereafter the testis, epididymis, vas deferens and ampulla (sperm storage sac) were removed from both sides (similar to procedure described by Faulkes *et al.*, 1994). Since the testes of the naked mole-rats are located intra-abdominally, dissection was done by making an incision in the abdominal cavity and exposing the reproductive tract (Fig. 3.4A).

The reproductive tract was tied off at the junction between the ampulla and the penis (see Fig. 3.4B) to avoid losing any of the contents of the tubes during dissection. After removal, the mentioned tissues were placed into a small plastic petri dish in pre-warmed Ham's F10 solution (only 30 °C due to the lower body temperature of this species). Further dissections took place under the Zeiss stereo-microscope, fitted with the removable cold light source and a heated (also only 30 °C) warm plate.

Similar to the mouse, the reproductive tract was cleaned and then the ampulla, vas deferens cauda epididymis were removed and individually placed into alternative pre-warmed petri dishes containing ± 100 µl Ham's F10. Since the ampulla, a widening of the distal part of the
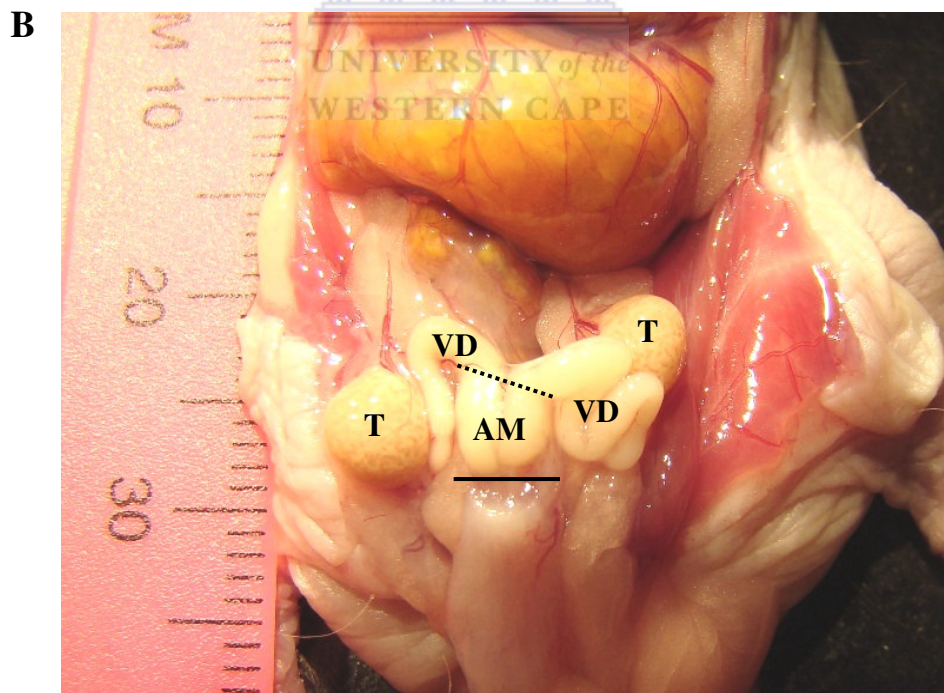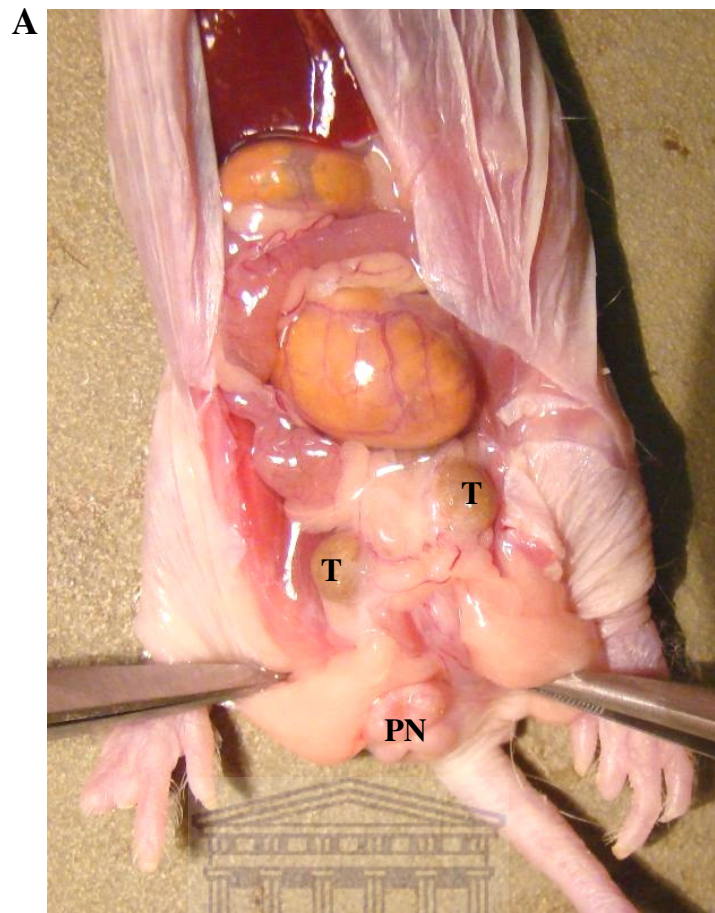
Figure 3.4. Photographs of the intact male reproductive system of the naked mole-rat. **A)** The intra-abdominal location of the testis (T) relative to the penis (PN) and other abdominal organs. **B)** The different parts of the intact reproductive system, including the testis (T), vas deferens (VD) and ampulla (AM). The solid line indicates the position where the reproductive tract was bound off before removal and the dashed line indicates the position where the ampulla was clamped off before separating it from the rest of the reproductive tract. The distance between two short lines on the ruler next to the specimen represents 1 mm.

vas deferens, contains the stored spermatozoa to be ejaculated, this part of the tract was carefully clamped off at the junction with the urethra and cut off first (see Fig. 4B) to avoid losing any of the contents. Subsequently, a small piece of the vas deferens and cauda epididymis were cut off and placed into separate pre-warmed petri dishes containing 50 µl Ham's F10. Sperm extraction from these ducts is described in section 3.2.4.3.

3.2.4 Selection of motile spermatozoa

3.2.4.1 Culture media used

Various culture media have been used in numerous studies for sperm extraction and selection procedures, including human tubular fluid (HTF), Ham's F10, Tyrode's medium, Dulbecco's phosphate buffered saline, Earle's medium, Biggers, Whitten and Whittingham (BWW) medium, M2 and M16 media. Depending on the purpose of sperm selection or sperm function to be tested, many of these media have been modified, for instance by increasing the concentration of sodium bicarbonate ($NaHCO_3$) and omitting HEPES to induce capacitation or increasing the calcium and bicarbonate concentrations to initiate hyperactivation (Mortimer, 1994; Mortimer, 1997).

Only one of these media was selected as culture medium for all the species investigated in the current study. Since motile spermatozoa needed to be obtained *via* the same selection protocol and because culture media vary in their chemical composition, it was important to be consistent in the culture medium used. Ham's F10 (Invitrogen, Cape Town, South Africa) was the preferred medium for the current study as it has been proven to sustain sperm functions for a long period of time (Mahadevan *et al.*, 1997; Brinders, 1994) and has been used in similar studies on spermatozoa from various species (Bornman *et al.*, 1988; Spinks *et al.*, 1997; van der Horst *et al.*, 1999; Lambrechts *et al.*, 2000; Younglai *et al.*, 2001). The chemical composition of Ham's F10 is included as Appendix 1. In all the procedures that included Ham's F10 in the current study, this medium was supplemented with 3% bovine serum albumin (BSA) (Sigma, Cape Town, South Africa).

3.2.4.2 Swim-up technique

The swim-up technique selects motile spermatozoa by their ability to swim out of the seminal plasma of a semen sample and into the culture medium. The technique used in the current study is a modification of the "direct swim-up" sperm preparation technique recommended by the WHO (WHO, 2010) and is described below. This technique was used for the selection of

motile sperm from human, the three non-human primate species and the merino ram semen samples.

After a semen sample was collected and allowed to liquefy for a few minutes (if necessary), the sample was mixed well to allow spermatozoa to be equally distributed throughout the sample. A volume of pre-warmed Ham's F10 medium was placed in a clean 2 ml microcentrifuge tube or 15 ml plastic tube and then a volume of semen was slowly pipetted underneath the Ham's F10. Care was taken not to mix the two liquid fractions and a clear interface between the semen (bottom) and Ham's F10 (top) was evident afterwards. The ratio of Ham's to semen used for this technique varied among species and depended on the concentration of spermatozoa in the semen sample. In general, however, the volume of Ham's F10 was 2-3 times the volume of semen used. A summary of these volumes is displayed in Table 3.2.

Table 3.2. The volume of semen and medium used for swim-up preparations and the sperm concentration and total sperm motility (mean ± SD) of swim-up and swim-out preparations (n=10 individuals for each species)

	HS	PU	RM	CA	OO	MM	HG
Semen (µl)	200-300	50-100	50	50-100	10-40	–	–
Ham's F10 (µl)	500-600	150	100-150	150	1000	–	–
Sperm concentration (x10^6/ml)	3.2 ± 1.1	2.4 ± 1.4	6.4 ± 2.7	5.9 ± 5.7	6.6 ± 4.2	1.7 ± 0.8	43.0 ± 45.2
Motility (%)	94.5 ± 3.2	93.9 ± 2.9	94.0 ± 5.5	94.7 ± 4.7	84.6 ± 5.6	89.7 ± 6.2	7.25 ± 6.7

HS = *Homo sapiens* (human), PU = *Papio ursinus* (chacma baboon), RM = *Macaca mulatta* (rhesus monkey), CA = *Chlorocebus aethiops* (vervet monkey), OO = *Ovis orientalis* (merino ram), MM = *Mus musculus* (house mouse), HG = *Heterocephalus glaber* (naked mole-rat)

The tubes were placed into a sealed Perspex container (flushed with 5 % CO_2) in a pre-warmed oven, with the microcentrifuge tubes in an upright position and the 15 ml tubes at an angle of about 45 ° (to increase the surface area of the semen and medium interface). Swim-up samples were incubated for 5-10 minutes before the first sampling started. In order to verify that motile sperm are being selected and to measure the swimming parameters of the spermatozoa, a small sample (≤ 5 µl) was taken from the middle of the Ham's F10 fraction of the swim-up preparation. The final concentration and percentage total motility of the spermatozoa in the selected samples are also displayed in Table 3.2. Subsequent sampling of motile sperm for the other experimental procedures also took place from the Ham's F10 fraction, without disturbing the interface between the semen and the Ham's F10.

56

3.2.4.3 Swim-out technique

The swim-out technique was used to select motile sperm from the species (mouse and naked mole-rat) in which the spermatozoa were collected after removal of a part of the reproductive tract (as described in section 3.2.3.3 above).

After the ampulla or a small piece of the vas deferens or cauda epididymis were cut off and placed in a separate pre-warmed petri dish with a small volume of Ham's F10, motile spermatozoa were allowed to swim out of the duct and into the surrounding medium. If the spermatozoa did not immediately swim out of the duct or if the concentration of spermatozoa swimming out were too low, the piece of duct was gently pressed with a forceps to force more spermatozoa out of the duct. The spermatozoa were allowed to freely swim out into the medium for a few seconds before the first sampling started. A "cloud" of spermatozoa, increasing in size with time, could clearly be identified under the stereo-microscope as motile spermatozoa which were swimming away from the duct (Fig. 3.5).
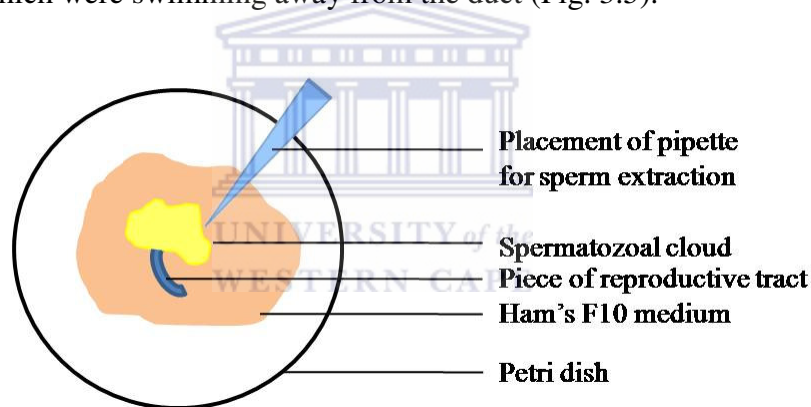
Figure 3.5. Schematic presentation of the swim-out technique. The motile spermatozoa are extracted from the edge of the spermatozoal cloud. The piece of reproductive tract indicated was either part of the cauda epididymis (mouse) or the ampulla (naked mole-rat).

A small sample (≤ 5 µl) was taken from the edge of the spermatozoal cloud (see Fig. 3.5) within 5 minutes for verification of sperm motility and to measure the swimming parameters of the spermatozoa. Subsequent sampling of motile sperm also took place from either the edge of the spermatozoal cloud or from the motile sperm dispersed into the Ham's F10. If sampling was done at later time intervals (e.g. 30 minutes), the swim-out sample was placed into a sealed Perspex container (flushed with 5 % CO_2) in a pre-warmed oven (Fig. 3.1). The final concentration and percentage total motility of the spermatozoa in the selected samples is also displayed in Table 3.2.

3.2.5   Sperm morphometry measurements

3.2.5.1   Preparation of sperm smears

All sperm smears were made and processed for staining after the swim-up and swim-out sperm preparations were incubated for 30 minutes and the motility of the selected spermatozoa was verified (see section 3.2.4.2 and 3.2.4.3). For all morphometry slides, 10 μl of the sperm preparation was used to make duplicate sperm smears, resulting in two to ten spermatozoa per field viewed at a 1000 x magnification. The sperm smears were allowed to air dry before the staining procedure commenced.

3.2.5.2   Staining procedure

SpermBlue® was selected for the staining of spermatozoa since it was proven that this staining technique differentially stain the different parts of spermatozoa and can be used for a wide variety of species (van der Horst and Maree, 2009). SpermBlue® fixative and stain were supplied by Microptic SL, Barcelona, Spain. The staining procedure described by van der Horst and Maree (2009) was followed.

In short, the dried smears were placed vertically into a Coplin jar containing SpermBlue® fixative. Alternatively, dried smears were placed horizontally down onto filter paper and 0.5-1.0 ml of fixative solution was dispersed onto the smear with a plastic disposable pipette. Smears were fixed for 10-13 minutes at 20-25 °C. After fixation, the slides were removed from the staining tray and held at an angle of 60-80° to drain off excess fixative. Fixed smears were subsequently placed vertically into a staining tray containing SpermBlue® stain. Alternatively, fixed slides were placed horizontally down onto filter paper and 0.45-0.50 ml of stain was dispersed onto the smear with a plastic disposable pipette. Smears were stained for 12-15 minutes at 20-25 °C. After staining, the excess stain was drained onto filter paper and then washed off by gently dipping the slides into distilled water (one dip for 3 seconds). Fluid was drained from slides by putting it an upright position (at about 70° angle) and then allowed to air dry. When stained smears were dry, a cover slip was mounted onto the slide with DPX mounting medium.

3.2.5.3 CASA equipment and capturing of morphometry data (automated)

Sperm morphometry was measured with the Morphology module of the SCA® system version 4.0.0.5 (Microptic S.L., Barcelona, Spain). Capturing of the data involved a Basler A312fc digital camera (Microptic S.L., Barcelona, Spain) that was mounted (C-mount) onto a Nikon

Eclipse 50i microscope (IMP, Cape Town, South Africa). The stained spermatozoa were analyzed with bright field optics, using a blue filter and a 40 x objective, 60 x objective or a 100 x oil immersion objective. The brightness was set at 314 and the contrast at 100 on the SCA® system, while the light setting of the microscope was optimized for each objective used. All spermatozoa which did not overlap with each other were considered for analysis.

The SCA® system automatically detects the acrosome, head and midpiece of spermatozoa and makes rapid and accurate measurements of various parameters. For the purpose of this study, only the acrosome and head parameters were automatically evaluated (see section 3.2.5.4 for the measurement of the other sperm components). A total of nine morphometric parameters were assessed, including the sperm head length, width, perimeter, surface area, ellipticity, elongation, roughness, regularity and the percentage acrosome coverage of the head. Table 3.3 summarizes the various morphometric measurements and the formulas used by the SCA® system for the derived parameters.

Table 3.3. Morphometric parameters of the sperm head automatically measured by the SCA® system (from Maree *et al.*, 2010)

Parameter	Formula
Length (μm)	L
Width (μm)	W
Perimeter (μm)	P
Area (μm^2)	A
Ellipticity	L/W
Elongation	(L-W)/(L+W)
Roughness	$4\pi\,(A/P^2)$
Regularity	$\pi\,(L*W/4*A)$
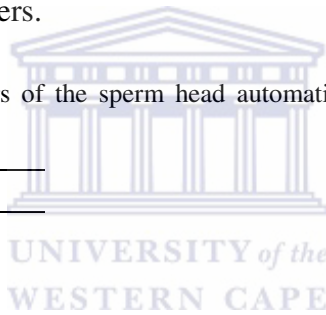
The ellipticity parameter measures whether the sperm head is thin or tapered and thus, the higher the value, the thinner the head. Elongation measures whether the sperm head is round or not and thus, if this value is more or less 0, it means that the head is spherical. The roughness indicates whether the sperm head is amorphous or irregular and thus, the smaller the value, the more irregular the head is due to a large perimeter. Regularity measures whether the sperm head is pyriform and thus if the top and bottom half of the sperm head are symmetric or not. In the current study the sperm head and acrosome of human, baboon, rhesus- and vervet monkeys were assessed by ASMA, while only the sperm head of the ram was automatically assessed. The 40 x objective was used for the analysis of the ram

spermatozoa, the 60 x objective for the baboon, rhesus- and vervet monkey spermatozoa and the 100 x oil immersion objective for the human spermatozoa. A total of 100 spermatozoa was analysed per sample, as this number was found to be representative of the whole sperm population (Maree *et al.*, 2010).

3.2.5.4 Alternative image analysis (semi-automated)

Semi-automated analysis of sperm morphometry involved a Olympus Astra 20 digital camera (Wirsam, Cape Town, South Africa) that was mounted onto a Zeiss Photomicroscope III (Zeiss, Cape Town, South Africa), equipped with bright field optics, including a 40 x objective, a 100 x oil immersion objective and a Optivar (intermediate lens providing a 1.25 x, 1.6 x or 2.0 x initial objective magnification). Morphometry parameters were measured with the analySIS® FIVE soft imaging system (Wirsam, Cape Town, South Africa).

The morphometry parameters assessed with this procedure included all the parameters mentioned above (section 3.2.5.3) for the sperm head of the mouse and naked mole-rat, as well as the acrosome of the ram spermatozoa. The acrosome of the mouse and naked mole-rat were not determined. Additionally, the following sperm parameters were assessed or calculated (using the formulas in Table 3.3) for all seven species included in the study: the length, width, perimeter, surface area, ellipticity, elongation, roughness and regularity of the midpiece and the lengths of the principal piece and end piece, The 40 x objective was used for the measurement of the principal piece of the spermatozoa, while the 100 x oil immersion objective was used for all the other measurements. Only 50 spermatozoa were analyzed per sample, but this number should still be representative of the whole sperm population (Maree *et al.*, 2010).

3.2.5.5   Calculation of sperm parameters and ratios

Apart from the sperm parameters mentioned in 3.2.5.3 and 3.2.5.4 above, additional sperm parameters and ratios were calculated from the measurements obtained and were also used in the statistical analysis. A tenth head parameter, the width/length ratio were calculated as recommended by Davis and Gravance (1994). The total sperm tail length was determined by adding the measurements of the midpiece, principal piece and end piece lengths together. Similarly, the length of the total spermatozoon was determined by adding the measurements of the total tail length and the head length together. Thirteen sperm component ratios were

determined from the length and area of the head and the lengths of the midpiece, tail principal piece, tail end piece, total tail and total spermatozoon.

3.2.6 Statistical analysis

The MedCalc® programme version 10.4.0.0 (Mariakerke, Belgium) was used for basic statistical analyses. Tests were performed for normality of distribution and most data sets represented normal distributions. Levene's test for equality of variances was applied and when P > 0.05, one way analysis of variance (ANOVA) analysis was performed for parametric data distributions. Any significant differences (P < 0.05) as indicated in the ANOVA table between groups were furthermore analyzed using the Student-Newman-Keuls test for pairwise comparisons. If Levene's test showed P < 0.05, independent T-tests with equal or unequal variances (depending on F-test result) were employed for individual differences. In subsets of data that appeared to have non-parametric data distributions, the Kruskal-Wallis test was employed and further elaborated for individual differences using the Mann-Whitney test for independent samples.

Data is represented as the mean ± standard deviation (SD) in the tables and *P* < 0.05 was considered significant using the analyses above. In the figures where data are represented as box-and-whisker plots, each box plot displays the following parameters for a given distribution: a) median (center line of box), b) second and third quartile values representing the middle 50% of the values (central box), c) range of data excluding data points lying outside the one and a half times interquartile range (T-bars) and d) data points lying outside the one and a half time (plotted with a square marker) or three times the interquartile range (plotted with a round marker).

Cluster analysis have been used as an exploratory data analysis tool to separate the seven mammalian species included in the study into different groups using different data sets of selected sperm parameters. This analysis method makes use of different algorithms to group objects of a similar kind together in order to have a maximal degree of association between objects in the same group and a minimal association otherwise. Horizontal Hierarchical Tree Plots have been constructed using the STATISTICA data analysis software system, version 10 (StatSoft Inc.), with each individual of a specific species indicated on the vertical axis and the linkage distance between these individuals on the horizontal axis. Euclidean distances (the geometric distance between objects in the multidimensional space) and complete linkage (the

greatest distance between any two objects in different clusters) have been used to separate the clusters.

3.3. Results

Sperm morphology

The SpermBlue® staining technique was suitable for staining the spermatozoa of all seven mammalian species (Fig. 3.6A-G). Not only are all the sperm components visible, but each sperm component is stained differentially to identify the boundaries of the head, acrosome, midpiece, principal piece and end piece. Thus, all these individual components could be measured by automated or semi-automated image analysis. Most of the species had ovate-shaped sperm heads, except for the two rodent species. The house mouse typically had a falciform head shape (Fig. 3.6F), whereas the naked mole-rat spermatozoa portrayed various head shapes, including elongated, lobed and amorphous heads (Fig. 3.6G). No major differences were apparent among the midpiece and tail morphology of the seven species, except for the naked mole-rat spermatozoa which did not have a thin, elongated midpiece as was evident in the other six species, but rather a small, almost round midpiece that closely adheres to the head (Fig. 3.6G).
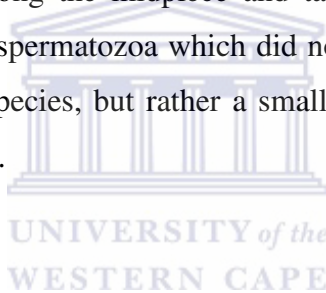
Sperm morphometry

Figure 3.7 and Figure 3.8 show examples of the morphometric analysis by utilizing the SCA® system (automated) or the analySIS® FIVE system (semi-automated), respectively. In Figure 3.7, each analyzed spermatozoon is shown on the left and to its immediate right the automated analysis of the acrosome (yellow), head (blue) and midpiece (green) of the same spermatozoon can be seen. However, only the morphometric dimensions of the head and acrosome determined by this technique have been used for further analysis. Figure 3.8 clearly shows the detail and accuracy of the semi-automated measurements of the different sperm components.

The morphometric values of 23 sperm parameters as measured by either automated or semi-automated image analysis are presented in Table 3.4. Considering all the parameters, it was evident that the head length, head area, head perimeter, midpiece length, midpiece area,midpiece perimeter, midpiece ellipticity and the lengths of the principal piece, end piece, total flagellum and total sperm were significantly different (P < 0.05) between almost all

62
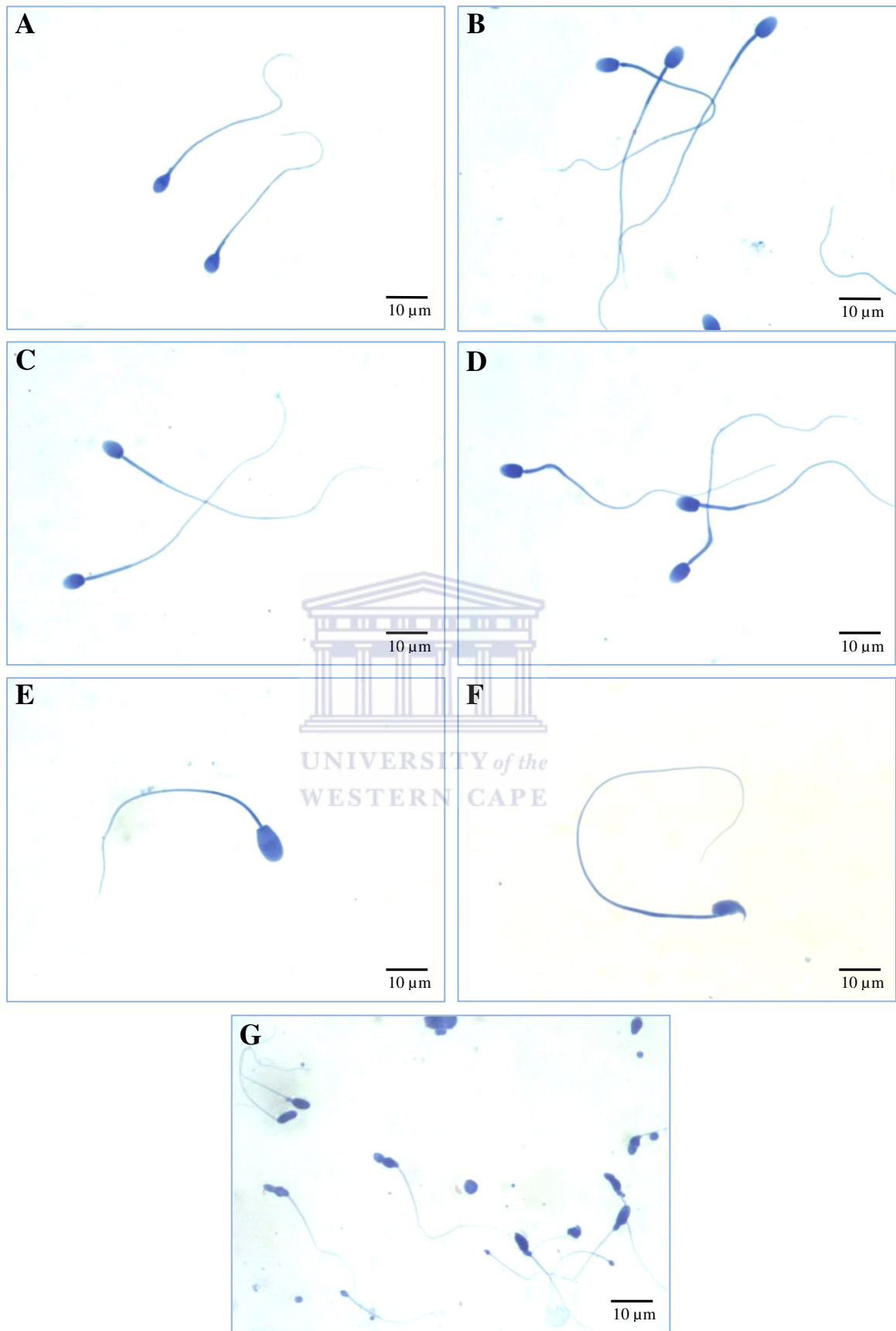
Figure 3.6. SpermBlue® stained spermatozoa from seven mammalian species illustrating the differences in sperm morphology and morphometry. **A**) *Homo sapiens* (human), **B**) *Papio ursinus* (chacma baboon), **C**) *Macaca mulatta* (rhesus monkey), **D**) *Chlorocebus aethiops* (vervet monkey), **E**) *Ovis orientalis* (merino ram), **F**) *Mus musculus* (house mouse), **G**) *Heterocephalus glaber* (naked mole-rat).
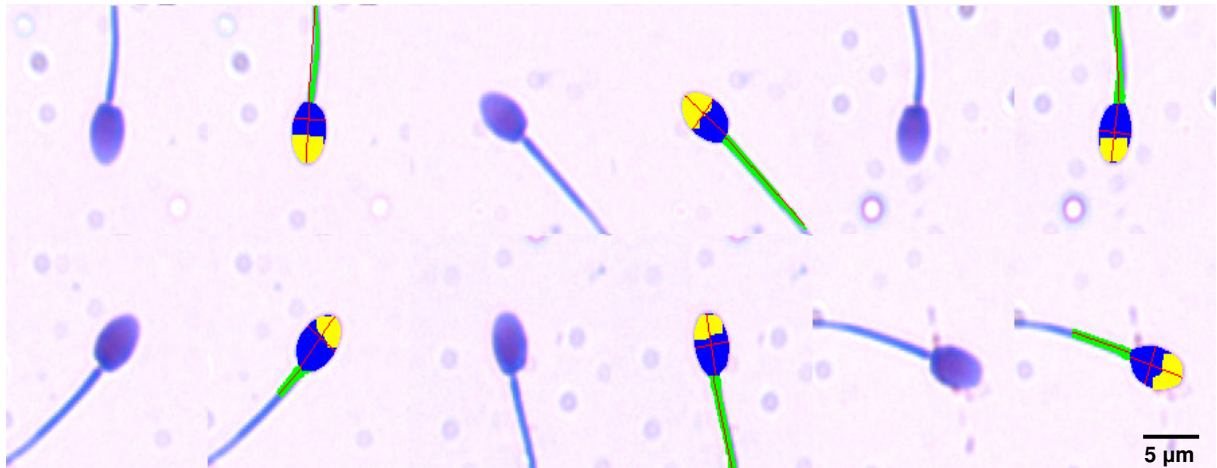
Figure 3.7. SCA® analysis of baboon spermatozoa stained with SpermBlue®. Six pairs of spermatozoa are shown - on the left side of the pair is the image of the spermatozoon as detected by the camera and to its immediate right the analyses of the acrosome (yellow), head (blue) and midpiece (green) of the same spermatozoon are superimposed on it. Actual head and acrosome measurements are presented in Table 3.4 (midpiece parameters were measured as illustrated in Figure 3.8).

seven species (no difference, however, between the baboon and rhesus monkey for some of the parameters). On the other hand, many of the parameters that had similar values ($P > 0.05$), e.g. the head and midpiece parameters, were among the four primate species, especially between the baboon and rhesus monkey.

If the data in Table 3.4 were viewed in terms of the three major sperm components (head, midpiece and tail) or the whole spermatozoon, differences were found in the relative sizes of these components when the seven species were arranged in order from smallest to largest absolute measurement for selected parameters. For instance, when the first four head parameters were evaluated, the species could be arranged as follow: HG < HS < CA < PU < RM < MM < OO. However, this arrangement changed to HG < HS < PU < CA < RM < OO< MM for five of the midpiece parameters, to HG < HS < CA < PU < RM < OO < MM for the principal piece or in combination with the end piece and to HG < HS < OO < CA < PU < RM < MM for the total tail and sperm lengths. Thus, whereas the naked mole-rat and human sperm always had the lowest values and the mouse the largest value in most cases, the non-human primate and ram values did not result in a consistent trend. For example, the ram spermatozoa had the largest sperm head relative to the other species, a reasonably large midpiece length but an intermediate tail length. These 'inconsistencies' are further explored as part of the sperm morphometry ratios below.

64
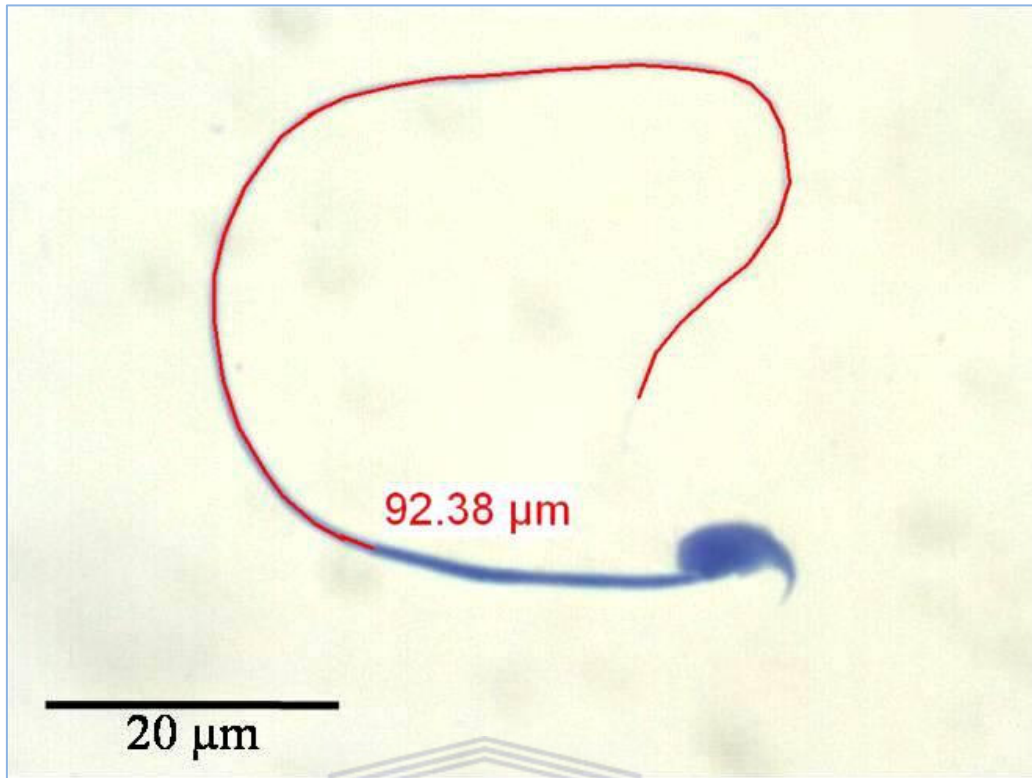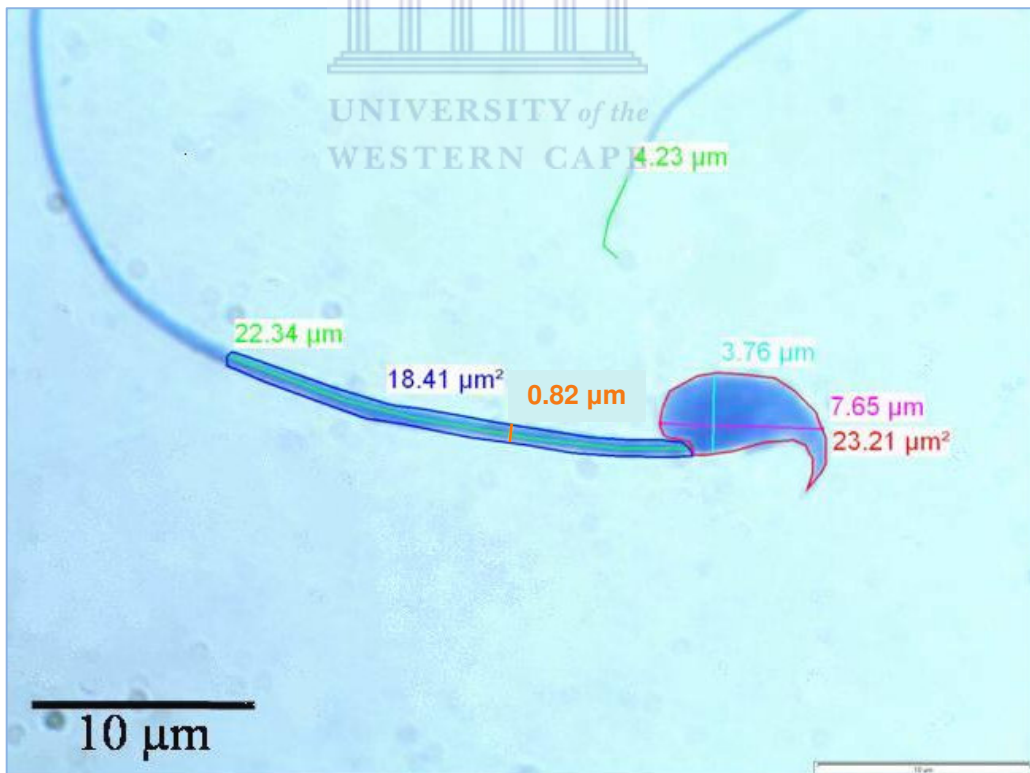
Figure 3.8. Semi-automated analysis of a mouse sperm with analySIS® FIVE image analysis software. **A**) The tail principal piece was measured by accurately tracing the part of the tail between the midpiece and the end piece. **B**) Various sperm parameters were measured by accurately tracing the boundaries of the following components: green (top) = tail end piece, green (left) = midpiece length, blue = midpiece area (midpiece perimeter was traced, but value is not shown), orange = midpiece width, turquoise = head width, pink = head length, red = head area (head perimeter was traced, but value is not shown).

65

Table 3.4. Sperm morphometry measurements (mean ± SD) of various sperm components for seven mammalian species (n=10 individuals for each species)

	HS	PU	RM	CA	OO	MM	HG
HLength (µm)	4.85 ± 0.34[a]	5.56 ± 0.34[b]	5.81 ± 0.17[c]	5.10 ± 0.18[d]	8.81 ± 0.15[e]	7.52 ± 0.24[f]	4.04 ± 0.33[g]
HWidth (µm)	2.91 ± 0.14[a]	3.48 ± 0.18[b]	3.59 ± 0.04[b]	3.03 ± 0.19[a]	5.17 ± 0.07[c]	3.57 ± 0.15[b]	2.24 ± 0.14[d]
HArea (µm^2)	11.41 ± 0.84[a]	16.33 ± 1.49[b]	17.12 ± 0.51[b]	13.34 ± 1.09[c]	38.12 ± 0.85[d]	21.95 ± 1.48[e]	7.61 ± 0.91[f]
HPerimeter (µm)	13.37 ± 0.82[a]	15.42 ± 0.78[b]	15.94 ± 0.34[b]	13.98 ± 0.51[c]	23.88 ± 0.34[d]	25.23 ± 0.65[e]	11.69 ± 0.75[f]
HEllipticity	1.68 ± 0.13[a]	1.60 ± 0.08[b]	1.62 ± 0.05[a]	1.69 ± 0.10[a]	1.71 ± 0.03[a]	2.11 ± 0.08[c]	1.84 ± 0.09[d]
HElongation	0.25 ± 0.04[abc]	0.23 ± 0.03[a]	0.24 ± 0.02[ab]	0.25 ± 0.03[bc]	0.26 ± 0.01[ce]	0.36 ± 0.02[d]	0.28 ± 0.02[e]
HW/HL ratio	0.60 ± 0.05[abc]	0.63 ± 0.03[a]	0.62 ± 0.02[ab]	0.60 ± 0.03[bc]	0.59 ± 0.01[c]	0.48 ± 0.02[d]	0.56 ± 0.03[e]
HRoughness	0.80 ± 0.04[a]	0.86 ± 0.02[b]	0.85 ± 0.01[bc]	0.86 ± 0.02[b]	0.84 ± 0.01[c]	0.43 ± 0.02[d]	0.70 ± 0.03[e]
HRegularity	0.97 ± 0.01[a]	0.93 ± 0.01[b]	0.96 ± 0.01[ae]	0.91 ± 0.01[c]	0.94 ± 0.01[be]	0.96 ± 0.03[ae]	0.95 ± 0.02[e]
HACRCoverage (%)	48.32 ± 7.31[a]	52.59 ± 6.39[a]	58.75 ± 8.09[b]	51.13 ± 6.48[a]	58.21 ± 2.20[b]	ND	ND
MPLength (µm)	4.64 ± 0.26[a]	9.97 ± 0.15[b]	10.95 ± 0.19[c]	10.46 ± 0.34[d]	15.06 ± 0.14[e]	22.19 ± 0.17[f]	1.11 ± 0.10[g]
MPWidth (µm)	0.78 ± 0.04[a]	0.84 ± 0.04[b]	0.86 ± 0.02[b]	0.86 ± 0.05[b]	0.75 ± 0.01[a]	0.85 ± 0.03[b]	1.12 ± 0.08[c]
MPArea (µm^2)	3.70 ± 0.32[a]	8.29 ± 0.25[b]	9.31 ± 0.31[c]	8.74 ± 0.52[d]	11.14 ± 0.32[e]	18.73 ± 0.73[f]	1.15 ± 0.16[g]
MPPerimeter (µm)	11.43 ± 0.63[a]	22.37 ± 0.34[b]	24.40 ± 0.38[c]	23.43 ± 0.72[d]	33.28 ± 0.30[e]	48.35 ± 0.46[f]	4.37 ± 0.29[g]
MPEllipticity	5.97 ± 0.45[a]	11.89 ± 0.60[bd]	12.73 ± 0.44[c]	12.19 ± 0.33[cd]	20.21 ± 0.46[e]	26.23 ± 0.96[f]	1.02 ± 0.05[g]
MPElongation	0.71 ± 0.02[a]	0.84 ± 0.01[b]	0.85 ± 0.00[b]	0.85 ± 0.01[b]	0.91 ± 0.00[c]	0.93 ± 0.00[d]	0.01 ± 0.03[e]
MPRoughness	0.36 ± 0.02[a]	0.21 ± 0.01[b]	0.20 ± 0.01[b]	0.20 ± 0.02[b]	0.13 ± 0.00[c]	0.10 ± 0.00[d]	0.75 ± 0.02[e]
MPRegularity	0.77 ± 0.02[a]	0.79 ± 0.01[b]	0.80 ± 0.01[b]	0.81 ± 0.01[b]	0.79 ± 0.02[b]	0.79 ± 0.01[b]	0.88 ± 0.06[c]
TPPLength (µm)	39.37 ± 3.35[a]	58.02 ± 0.91[b]	58.02 ± 0.82[b]	52.64 ± 0.87[c]	41.68 ± 0.48[d]	93.11 ± 1.69[e]	26.78 ± 4.13[f]
TEPLength (µm)	5.62 ± 0.59[a]	3.37 ± 0.27[b]	2.97 ± 0.15[c]	2.87 ± 0.21[c]	2.04 ± 0.16[d]	4.15 ± 0.28[e]	ND
TPP+TEP (µm)	44.99 ± 3.57[a]	60.95 ± 1.23[b]	60.99 ± 0.88[b]	55.51 ± 0.98[c]	43.74 ± 0.51[a]	97.26 ± 1.63[d]	26.78 ± 4.13[e]
TTLength (µm)	49.63 ± 3.71[a]	70.92 ± 1.17[b]	71.94 ± 0.98[b]	65.47 ± 1.66[c]	58.81 ± 0.58[d]	119.45 ± 1.64[e]	28.56 ± 2.89[f]
SPLength (µm)	54.48 ± 3.96[a]	76.49 ± 1.26[b]	77.75 ± 1.06[b]	70.56 ± 1.73[c]	67.61 ± 0.64[d]	126.97 ± 1.79[e]	32.61 ± 2.83[f]

HS = *Homo sapiens* (human), PU = *Papio ursinus* (chacma baboon), RM = *Macaca mulatta* (rhesus monkey), CA = *Chlorocebus aethiops* (vervet monkey),
OO = *Ovis orientalis* (merino ram), MM = *Mus musculus* (house mouse), HG = *Heterocephalus glaber* (naked mole-rat)
H = head, W = width, L = length, ARC = acrosome, MP = midpiece, TPP = tail principal piece, TEP = tail end piece, TT = total tail, SP = sperm
a, b, c, d, e, f, g = values labelled with different superscript letters in the same row were significantly different (P < 0.05), ND = not determined

The cluster analysis presented in Figure 3.9 was constructed by including all the sperm morphometry values presented in Table 3.4. The arrangement of the individuals of each species on the vertical axis indicated that the sperm morphometry values were species specific. Almost all the individuals of a specific species were grouped together in its own cluster (small linkage distances) before it was linked to another species, except for the baboon and rhesus monkey where a small degree of overlap occurred between the individuals. The linkage distance between the different species clusters indicated that the three non-human primate species were closely related in terms of sperm morphometry. The human and naked mole-rat also formed an additional cluster, as well as the non-human primates and the ram. There did not appear to be a close relationship between the mouse and all six afore mentioned species.

Sperm morphometry ratios

The different sperm parameters are also presented as ratios in Table 3.5, where one sperm parameter was expressed as a ratio of another parameter. Once again, significant differences ($P < 0.05$) were found among the seven mammalian species, but the trend of ratios relative to one another was not consistent with the absolute sperm morphometry data reported above. When the midpiece to head ratios were evaluated, the species could be arranged as HG < HS < OO < PU < RM < CA < MM. Both the tail to head and total sperm to head ratios revealed the arrangement OO < HG < HS < RM < PU < CA < MM. A third arrangement were found for the tail to midpiece, with and without head, or the total sperm to midpiece, with or without head, ratios, namely OO < MM < CA < RM < PU < HS < HG. Most similarities ($P > 0.05$) found in the sperm parameter ratios were among the three non-human primate species.

A second cluster analysis is presented in Figure 3.10 for the sperm parameter ratios included in Table 3.5. Although there was still a close relationship between the three non-human primate species, these species were much closer associated to the mouse as in Figure 3.9 when the absolute sperm morphometry measurements were taken into account. Additional clusters were formed between the afore-mentioned four species and the human and more distantly between these species and the ram. The naked mole-rat did not associate with any of the other six mammalian species in terms of sperm morphometry ratios. Once again there was a clear grouping of species on the vertical axis, except for the slight overlapping of individuals of the non-human primate species.

67
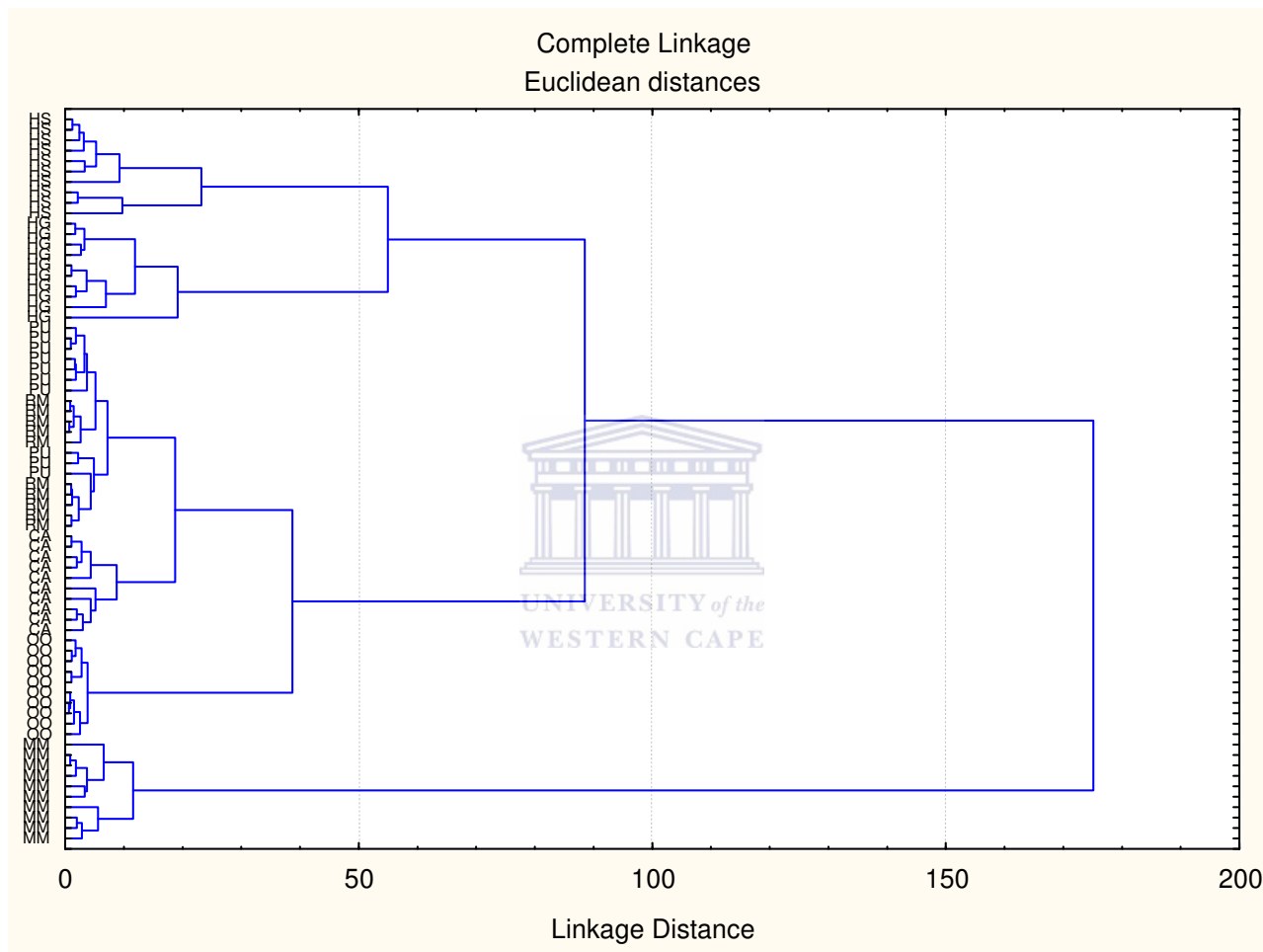
Figure 3.9. Cluster analysis of 23 sperm morphometry parameters illustrating the clustering of species on the vertical axis and indicating the relatedness among the seven mammalian species on the horizontal axis (linkage distance). The actual values of the sperm morphometry parameters are presented in Table 3.4. HS = *Homo sapiens* (human), PU = *Papio ursinus* (chacma baboon), RM = *Macaca mulatta* (rhesus monkey), CA = *Chlorocebus aethiops* (vervet monkey), OO = *Ovis orientalis* (merino ram), MM = *Mus musculus* (house mouse), HG = *Heterocephalus glaber* (naked mole-rat).

Table 3.5. Sperm morphometry ratios (mean ± SD) of various sperm components for seven mammalian species (n=10 individuals for each species)

	HS	PU	RM	CA	OO	MM	HG
MPL/HL	0.96 ± 0.06 [a]	1.80 ± 0.11[b]	1.89 ± 0.07[c]	2.06 ± 0.09[d]	1.71 ± 0.02[e]	2.96 ± 0.10[f]	0.28 ± 0.04[g]
MPL/HA	0.41 ± 0.02[a]	0.62 ± 0.06[b]	0.64 ± 0.03[b]	0.79 ± 0.06[c]	0.40 ± 0.01[a]	1.02 ± 0.07[d]	0.15 ± 0.03[e]
TTL/HL	10.25 ± 0.38[a]	12.79 ± 0.79[b]	12.40 ±0.35[b]	12.86 ± 0.44[b]	6.68 ± 0.11[c]	15.90 ± 0.44[d]	7.12 ± 0.97[c]
TTL/HA	4.36 ± 0.31[a]	4.37 ± 0.38[a]	4.21 ± 0.12[a]	4.93 ± 0.41[b]	1.54 ± 0.03[c]	5.46 ± 0.36[d]	3.81 ± 0.64[e]
TTL/MPL	10.70 ± 0.68[a]	7.11 ± 0.18[b]	6.57 ± 0.09[b]	6.26 ± 0.22[bd]	3.90 ± 0.03[c]	5.38 ± 0.08[d]	25.91 ± 3.34[e]
TTL/HL+MPL	5.23 ± 0.27[a]	4.57 ± 0.14[b]	4.29 ± 0.03[c]	4.21 ± 0.12[ce]	2.46 ± 0.03[d]	4.02 ± 0.05[e]	5.57 ± 0.69[f]
TTL/TPPL+TEPL	1.11 ± 0.01[a]	1.16 ± 0.00[b]	1.18 ± 0.00[c]	1.18 ± 0.03[c]	1.34 ± 0.01[d]	1.23 ± 0.00[e]	1.04 ± 0.01[f]
SPL/HL	11.25 ± 0.58[a]	13.79 ± 0.79[b]	13.40 ± 0.35[b]	13.86 ± 0.44[b]	7.68 ± 0.11[c]	16.90 ± 0.44[d]	8.12 ± 0.97[c]
SPL/HA	4.79 ± 0.32[a]	4.72 ± 0.39[a]	4.54 ± 0.12[ae]	5.32 ± 0.43[b]	1.77 ± 0.03[c]	5.81 ± 0.37[d]	4.35 ± 0.66[e]
SPL/MPL	11.75 ± 0.73[a]	7.68 ± 0.19[b]	7.10 ± 0.11[b]	6.75 ± 0.24[bd]	4.49 ± 0.04[c]	5.72 ± 0.09[d]	29.57 ± 3.53[e]
SPL/HL+MPL	5.74 ± 0.27[a]	4.93 ± 0.13[b]	4.64 ± 0.03[c]	4.54 ± 0.13[c]	2.83 ± 0.02[d]	4.27 ± 0.05[e]	6.36 ± 0.68[f]
SPL/TTL	1.10 ± 0.01[a]	1.08 ± 0.01[b]	1.08 ± 0.00[b]	1.08 ± 0.00[b]	1.15 ± 0.00[c]	1.06 ± 0.00[d]	1.14 ± 0.02[c]
SPL/TPPL+TEPL	1.21 ± 0.01[a]	1.26 ± 0.01[b]	1.27 ± 0.00[c]	1.27 ± 0.03[c]	1.55 ± 0.01[d]	1.31 ± 0.01[e]	1.19 ± 0.03[f]

HS = *Homo sapiens* (human), PU = *Papio ursinus* (chacma baboon), RM = *Macaca mulatta* (rhesus monkey), CA = *Chlorocebus aethiops* (vervet monkey),
OO = *Ovis orientalis* (merino ram), MM = *Mus musculus* (house mouse), HG = *Heterocephalus glaber* (naked mole-rat)
MP = midpiece, L = length, H = head, A = area, TT = total tail, TPP = tail principal piece, TEP = tail end piece, SP = sperm
a, b, c, d, e, f, g = values labelled with different superscript letters in the same row were significantly different (P < 0.05)
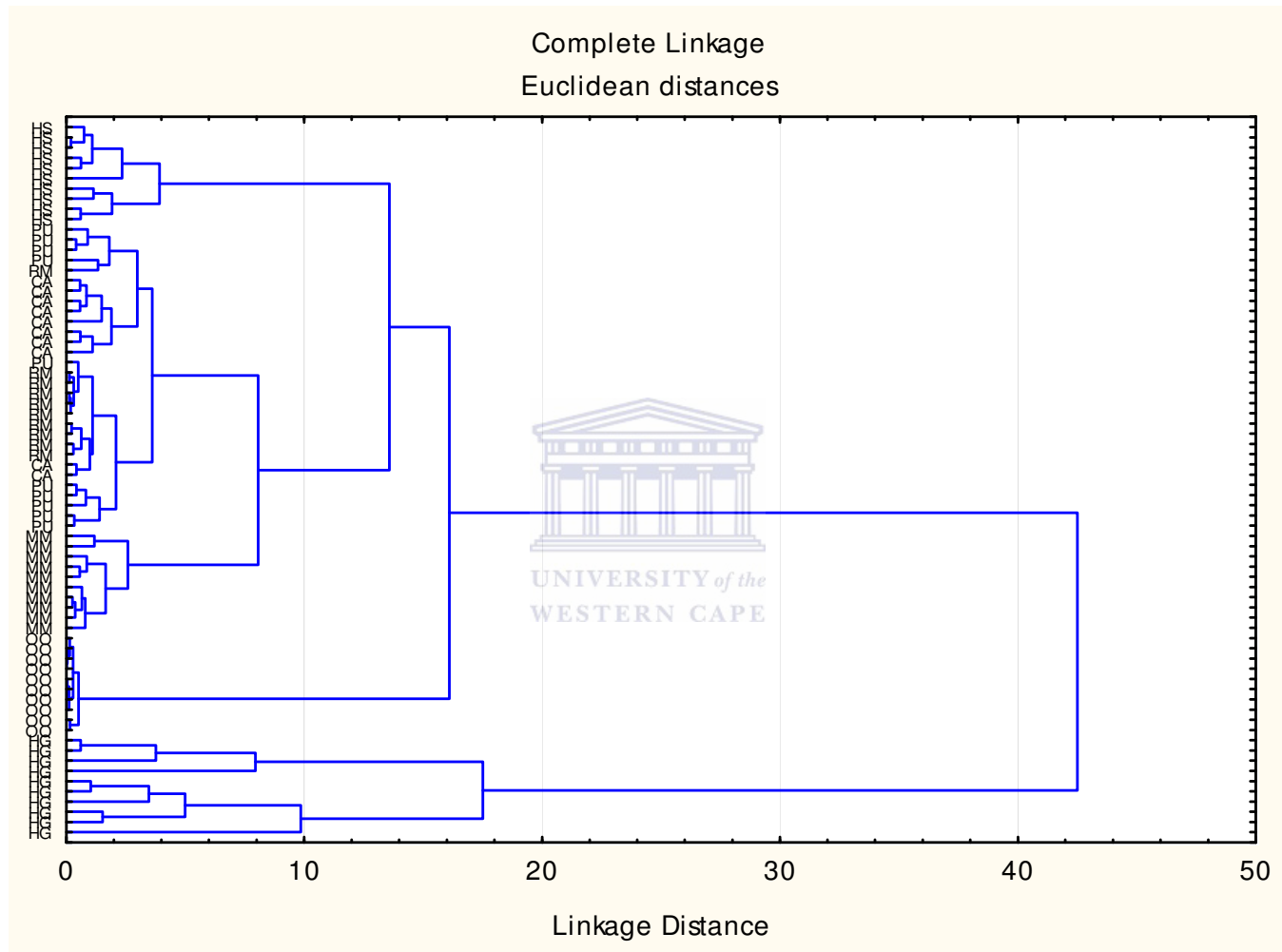
Figure 3.10. Cluster analysis of 13 sperm morphometry ratios illustrating the clustering of species on the vertical axis and indicating the relatedness among the seven mammalian species on the horizontal axis (linkage distance). The actual values of the sperm morphometry ratios are presented in Table 3.5. HS = *Homo sapiens* (human), PU = *Papio ursinus* (chacma baboon), RM = *Macaca mulatta* (rhesus monkey), CA = *Chlorocebus aethiops* (vervet monkey), OO = *Ovis orientalis* (merino ram), MM = *Mus musculus* (house mouse), HG = *Heterocephalus glaber* (naked mole-rat).

70

Sperm midpiece

Considering only the midpiece data, the six midpiece parameters are presented as box-and-whisker plots in Figure 3.11 and species differences for these parameters are indicated. As mentioned above, a similar trend was found for the midpiece length, area, perimeter, ellipticity and elongation among the seven species if they were arranged from the lowest to the highest values for these five parameters, namely HG < HS < PU < CA < RM < OO < MM. The midpiece width and regularity also had similar trends, while the naked mole-rat was the major exception by having the largest values for these two measurements. Due to the fact that the naked mole-rat's midpiece length and width were almost equal, it also resulted in an elongation of almost 0. The roughness values followed the opposite trend than the elongation values, e.g. due to the mouse sperm having the largest midpiece perimeter, it resulted in having the lowest roughness value. The opposite was true for the naked mole-rat elongation and roughness. The regularity of the naked mole-rat sperm midpiece was the highest due to its circular morphology and symmetry. Human spermatozoa had the lowest value for midpiece regularity which could be due to the fact that these midpieces often had a pyriform shape by being wider closest to the head and thinner at the distal end of the midpiece (data not shown).
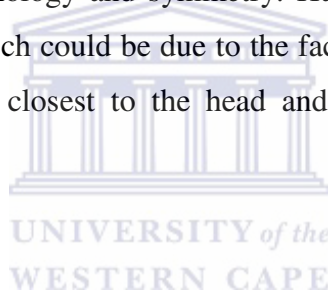
3.4   Discussion

The first step in relating the variation in selected sperm structures to sperm form and function (see Chapter 7) was to indicate the variations present in the sperm morphology and morphometry of the seven mammalian species included in this study. The standardization of the methods used to select motile spermatozoa and the subsequent techniques employed to measure the sperm components were necessary to accurately determine any species diversity.

Sperm morphology assessment is generally used as a parameter to evaluate the semen quality and fertility potential of a male, by classifying spermatozoa according to the normality of their different components (head, midpiece and tail) (Coetzee *et al.*, 1998). Since spermatozoa were selected for their motility rather than their normal morphology in the present study, the percentage normal spermatozoa were not determined. However, the sperm morphology of the seven species as revealed by SpermBlue® staining clearly indicated the similarities and differences among the seven species and allowed for the assessment of the two dimensional size of the various sperm components. Although mammalian spermatozoa have many similar characteristics, species-specific variations are found in nearly all sperm

71
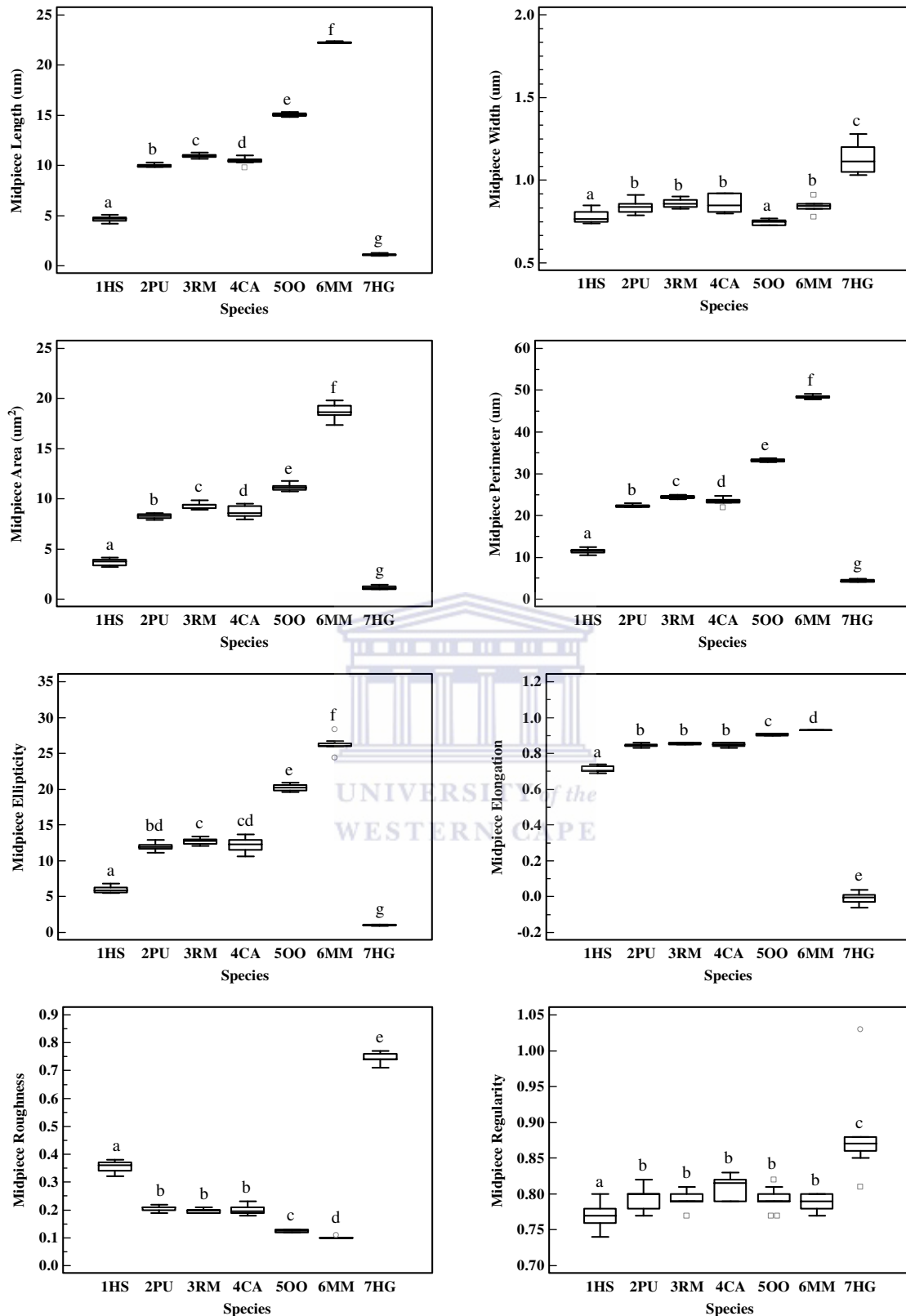
Figure 3.11. Box-and-whisker plots illustrating the variations found within the midpiece parameters of the seven mammalian species (n = 10 individuals per species). The actual values of these variables are shown in Table 3.4. HS = *Homo sapiens* (human), PU = *Papio ursinus* (chacma baboon), RM = *Macaca mulatta* (rhesus monkey), CA = *Chlorocebus aethiops* (vervet monkey), OO = *Ovis orientalis* (merino ram), MM = *Mus musculus* (house mouse), HG = *Heterocephalus glaber* (naked mole-rat). a, b, c, d, e, f, g = boxes labelled with different letters were significantly different (P < 0.05).

72

components (Fawcett, 1975).

More importantly was the assessment of sperm morphometry in order to quantify species variation of the different sperm components. Measurements of the sperm morphometry parameters determined in the present study fall within the ranges previously reported for spermatozoa of human and other primates, ram, mouse and naked mole-rat (Cummins and Woodall, 1985; Morrow and Gage, 2001, van der Horst *et al.*, 2011). Sperm morphometry measurements were found to be species specific for various head, midpiece and tail parameters. Similarities in several sperm parameters among the non-human primate spermatozoa, especially between the baboon and rhesus monkey, are probably due to their close phylogenetic relationship as deducted from the mammalian phylogenetic tree (Liu *et al.*, 2001; Gage and Freckleton, 2003). Most of the variation among the species was due to significant differences in the lengths of the sperm head, midpiece and tail, whereas the head and midpiece widths had less variation. Since a combination of the length and the width were used to determine the area, perimeter, ellipticity and elongation parameters, the species specificity for the latter parameters can also be explained.

Previous studies on sperm morphometry have reported relationships between the lengths of the head, midpiece and flagellum. Gage (1998) found significant relationships between the head length and area and the lengths of the midpiece and flagellum when comparing 445 mammalian species. It was therefore suggested that these three sperm components probably co-evolved. It is however not clear which factors determine the size of the mammalian sperm head and no relationship was found between the head size and the chromosome number or genome mass (Gage, 1998). Considering the metabolic requirements of mammalian sperm, Cardullo and Baltz (1991) reported the existence of an allometric relationship between the midpiece length and the flagellum length. Since the current study mainly focussed on the size of the midpiece, only relationships between the midpiece and other sperm components were considered and are discussed in Chapter 7.

Subsequent studies on sperm morphometry suggested that not only the absolute sperm measurements but also relative measurements should be taken into account, especially when aiming to find associations between sperm form and function, e.g. sperm morphology and swimming speed (Humphries *et al.*, 2008). The shape of the sperm head seems to influence sperm motility as head elongation (HL/HW) was positively correlated to the sperm

swimming speed (Malo *et al.*, 2006). The same study also reported that length of the principal piece plus end piece relative to flagellum length was positively associated with sperm velocity (Malo *et al.*, 2006). As sperm motility is a fundamental characteristic of spermatozoa, it was argued that the relationship between the size of the sperm component which needs to be driven forward (head) and the size of the sperm component which generates the force for movement (flagellum) should also be considered, e.g. a ratio of head length to tail length (Humphries *et al.*, 2008). Several of these sperm component ratios have therefore also been reported in the current study to determine if there is a specific ratio between the various sperm components for all species. The ratio between the midpiece and the other sperm components was particularly of interest. Since the midpiece contains the mitochondria which are necessary for energy production and probably motility, it would also be interesting to see whether the absolute or relative midpiece size is related to sperm function (Chapter 7).

The contribution of each sperm component to the total size of the sperm was not consistent among the seven species. Independent arrangements of the absolute measurements of the sperm head, midpiece and tail from smallest to largest, revealed differences in the arrangement of the species relative to each other. These inconsistent contributions were confirmed by the relative measurements of selected sperm components. In the midpiece length to head length ratio (MPL/HL), the naked mole-rat had the lowest value due to the fact that its midpiece only contributes 3.4% to the total length of the sperm and its head 12.4%. On the other hand, mouse had the largest ratio since its midpiece contributes 17.5% to the total sperm length and its head only 5.9%. In both the tail length to head length ratio (TTL/HL) and the tail length to midpiece length ratio (TTL/MPL), the ram sperm had the lowest value since its head contributed 13.0% (highest of all seven species) to the total length of the sperm and its midpiece 22.3% (highest of all seven species) and principal piece 61.6% (lowest of all seven species). Similar differences in the proportions of sperm components to the overall size of the sperm were also reported by Cummins and Woodall (1985).

The two cluster analyses confirmed that the sperm component measurements were species specific for both the absolute and the relative sperm morphometry parameters. However, the same association among the seven species were not found when the absolute sperm morphometry parameters were compared to the sperm morphometry ratios. The close association between the three non-human primates in both cluster analyses is due to their

74

similarities in many of the sperm components and thus the sperm component ratios, which once again is probably due to their close phylogeny. Cluster analyses will also be included in the chapters to follow to determine if perhaps the midpiece morphometry (Chapter 4) or the swimming parameters (Chapter 5) reveal similar associations among the seven mammalian species.

The midpiece of the mammalian spermatozoon is generally described as elongated, but enormous variation has been reported in the actual length of the midpiece for various mammalian species (Fawcett, 1975). This species specificity in the sperm midpiece dimensions was also found in the current study. Since the length, area, perimeter, ellipticity and elongation all presented a similar trend in size among the seven species, only one of these parameters, midpiece length, was is most cases selected for comparative purposes in the following chapters. Apart from the naked mole-rat, the midpiece width revealed fewer differences among the other six species compared to their midpiece length. Interestingly though, ram spermatozoa had the smallest midpiece width, but their midpiece length was second largest compared to the other species. Moreover, mouse spermatozoa had the longest midpiece but its width was not significantly different from that of the non-human primate species. Taking this into account, it would probably be more accurate to determine the three dimensional shape of the midpiece (a combination of midpiece length and width) to obtain a more accurate size of the midpiece for comparative purposes. The midpiece roughness and regularity as determined in the present study are not commonly used to describe the midpiece morphometry of spermatozoa, but was merely included to further indicate the species specificity of the midpiece morphometry (roughness) or the consistency in the shape of the mammalian midpiece (regularity). The low regularity and pyriform shape of the human sperm midpiece are likely due to the fact that the neck and proximal part of the midpiece is often surrounded by a fusiform mass of residual cytoplasm (Fawcett, 1975).

The reason for the variation in sperm size, especially in mammals, has not been resolved and seems to be multi-factorial. Since Gage (1998) found that there is no inverse relationship between sperm length and body weight in mammals, several other factors have been considered to influence sperm size, e.g. sperm competition and female reproductive tract design (Pitnick *et al.*, 2009).

Sperm competition occurs in multiple partner mating systems and the intensity of sperm competition is measured in terms of the relative size of the testes, where higher levels of sperm competition is positively correlated with relatively larger testes (as reviewed by Gage and Freckleton, 2003). In general, it has been reported that there exists a positive relationship between sperm competition and sperm size, with polyandrous species having longer sperm across various taxa (Pitnick *et al.*, 2009). However, the results for mammalian species from different comparative studies are not consistent. Although positive correlations for sperm competition and sperm length have been reported for primates and rodents (Gomendio and Roldan, 1991), the opposite was found by several other studies and after statistically controlling for phylogeny (Hosken, 1997; Anderson and Dixson, 2002; Anderson *et al.*, 2005; Gage and Freckleton, 2003). A possible reason for these inconsistencies was given by Pitnick *et al.* (2009) who warned that too large comparative studies might mask lineage-specific relationships, as was found by Immler and Birkhead (2007) in passerine bird species. Gomendio and Roldan (2008) also alluded to the fact that care should be taken not to use unresolved phylogenies when correcting for the influence of relatedness of species in comparative studies, as this could obscure meaningful relationships. Surprisingly, a positive correlation was found between the relative testis size and the midpiece volume, but not with any other sperm component, in primates (Anderson and Dixson, 2002) and in a study of 123 mammalian species (Anderson *et al.*, 2005). Although sperm competition as such does not form part of the current study, the possible relationship between sperm size and multiple partner mating systems seems to hold true. In the naked mole-rat where sperm competition is essentially absent (van der Horst *et al.*, 2011) and in humans where single partner systems prevail (Martin, 2003), these species had the smallest sperm dimensions in all the absolute sperm measurements, as well as when only the midpiece dimensions were considered.

The relationship between the structural aspects of the female reproductive tract and sperm morphometry has also been reported for various taxa (Pitnick *et al.*, 2009). In mammals, the relative oviduct length differs among species and a positive association was found between this female trait and sperm midpiece volume (Anderson *et al.*, 2006). In the same study a positive relationship was also found between the relative oviduct length and the relative testis size. These results suggest a co-evolution of oviduct length, testis size and sperm morphometry due to sexual selection (sperm competition and cryptic female choice) (Anderson *et al.*, 2006).

In conclusion, variations in sperm morphometry of the seven mammalian species were found. Moreover, these sperm morphometry parameters were species specific for both absolute and relative sperm measurements. The importance of considering ratios of sperm components in a comparative study was highlighted, since the species did not reveal a consistent trend when comparing the absolute sperm measurements with the sperm component ratios. Most of the midpiece dimensions were also species specific, but the midpiece volume should be a more accurate measurement of the size of the midpiece. Thus, the midpiece volume and several other midpiece dimensions, as well as the sperm mitochondria and their arrangement within the midpiece, will be evaluated in Chapter 4.

CHAPTER 4: Sperm mitochondria and the sperm midpiece of selected mammalian species

4.1 Introduction

The midpiece of the mammalian spermatozoon comprises that part of the sperm flagellum located closest to the head and consists of the 'motor apparatus' enclosed by the mitochondrial sheath (Fawcett, 1970). Large variations in the dimensions of the midpiece have been reported for mammalian species (Austin, 1976; Cummins and Woodall, 1985) and were also found in the current study (Chapter 3). Even though most of the midpiece parameters were species specific, these light microscopic measurements did not result in a consistent trend among the seven mammalian species. Thus, a more detailed study of the volume of the midpiece and the ultrastructure of the mitochondria contained in it was necessary to possibly reveal more variations in the structure of the midpiece and to clarify the putative differences in the midpiece parameters.

Mammalian sperm mitochondria are generally elongated and arranged in a tight helix around the axoneme complex and outer dense fibers of the sperm flagellum (Fawcett, 1970). A few exceptions include the crescentic mitochondria of the bat (*Myotis lucifugus*) (Fawcett, 1970) and the spherical, randomly arranged mitochondria of several cetaceans, such as the humpback dolphin (*Sousa plumbea*) and the long-beaked common dolphin (*Delphinus capensis*) (Downing Meisner *et al.*, 2005). The nature of the helix itself seems to vary between species, either presenting as a single or double helix (rhesus monkey), double or triple helix (mouse), triple or quadruple helix (bull) or a quintuple helix (rabbit) (Phillips, 1977). Inside the mitochondrial sheath, each mitochondrion is arranged in an end-to-end fashion with adjacent mitochondria. It also associates with other mitochondria (above or below) along its lateral surfaces. This organized arrangement of the sperm mitochondria is due to three structural specializations of the outer mitochondrial membrane, namely a network of studs between adjacent mitochondria, a paracrystalline structural domain where it faces the outer dense fiber-axoneme complex and its close association with the plasma membrane (Olson and Winfrey, 1990; 1992).

Despite this typical structural arrangement of sperm mitochondria in the midpiece, several variations occur in the size, shape and number of the individual mitochondria in different

mammalian species. Due to its helical arrangement, it is difficult to determine the exact number of mitochondria in the midpiece of any species, but the number of gyres in longitudinal sections of the midpiece can be counted using electron micrographs (Fawcett, 1970). The relatively short midpiece of the human consists of about 15 gyres, whereas the exceptionally long midpieces of several rodent species contain as many as 300 gyres (Fawcett, 1975). Cross-sections of the midpiece also revealed considerable differences in both the width of the mitochondrial sheath and the size of the outer dense fibers (Fawcett, 1970). In some mammalian species (e.g. bats, marsupials and the Chinese hamster) all the mitochondria seem to be of identical size and shape and results in very regular arrangements of the mitochondria along the entire length of the midpiece. In other species, however, the mitochondria seem to be of unequal length, arranged less regularly along the midpiece and the arrangement of those mitochondria closest to the neck region differs from that in the rest of the midpiece (Phillips, 1977).

During spermatogenesis three different types of mitochondria can be identified according to the number and shape of the mitochondrial cristae, namely the orthodox, intermediate and condensed form of mitochondria (Seitz *et al.*, 1995). Spermatozoa typically contain intermediate type mitochondria with a less condensed matrix and a few cristae (Ramalho-Santos *et al.*, 2009). Earlier assessment of the internal structure of sperm mitochondria, however, revealed variations in the abundance and orientation of the cristae, including circumferential and spiral arrangements and well as cristae orientated parallel to the surface of the mitochondria (Fawcett, 1970). Recently it was reported that the mitochondrial cristae are not merely in-folds of the inner mitochondrial membrane, but rather are structurally distinct from this membrane and attached to it by membranous tubules (Mannella, 2006b).

Additional methods of evaluating sperm mitochondria and the difference between various species involve sperm functional tests which assess the vitality or activity of the mitochondria. Numerous studies have recommended the use of these tests rather than just relying upon conventional semen analysis and sperm morphology evaluations for the prediction of a male's fertility potential (Gopalkrishnan *et al.*, 1995; Troiano *et al.*, 1998; Marchetti *et al.*, 2004b). One such functional test, namely flow cytometry, has been used to assess the viability of spermatozoa, to locate specific sperm components or to detect the presence of certain cellular metabolites in spermatozoa (Kasai *et al.*, 2002; Marchetti *et al.*, 2002; Bussalleu *et al.*, 2005). This extremely sensitive and accurate analysis technique also

has the advantages of assessing thousands of cells in a short period of time and the possibility of simultaneously staining different sperm components (multiple staining) followed by independent evaluation of each fluorescent probe (Graham *et al.*, 1990; Bussalleu *et al.* 2005; Gallon *et al.*, 2006). Various fluorochromes, e.g. Rhodamine 123, JC1, $DiOC_6(3)$ and CMX-Ros, have been used in previous studies to determine the mitochondrial membrane potential, which is an indicator of the energetic state of the mitochondria and the activity of the mitochondrial respiratory chain (Marchetti *et al.*, 2004a). The disadvantage of these fluorescent dyes are, however, that they are unstable upon illumination, are not entirely specific for mitochondria nor do they allow for fixation or multiple labelling. Care should therefore be taken as to which fluorescent probe is selected for a specific study (Poot *et al.*, 1996).

The main aims of this chapter were to investigate the unique features of the midpiece and sperm mitochondria of selected mammalian species by assessing and comparing various ultrastructural parameters and mitochondrial viability among the seven species.

4.2   Materials and methods

4.2.1 Mammalian species included, collection of samples and selection of motile spermatozoa

All seven mammalian species introduced in Chapter 3 were also investigated in terms of their midpiece morphometry measurements. Only five individuals per species were used for these measurements. Unfortunately, sperm mitochondrial viability assessment could not be done on the naked mole-rat spermatozoa, since the volume of the ampulla and vas deferens contents were too small. The collection of the semen or spermatozoa as well as the selection of motile spermatozoa was described in Chapter 3.

4.2.2   Staining of spermatozoa for morphology and morphometry assessment

The preparation of sperm smears and the SpermBlue® staining procedure were identical to that reported in Chapter 3. Digital photographs were taken with an Olympus Astra 20 digital camera (Wirsam, Cape Town, South Africa) that was mounted onto a Zeiss Photomicroscope III (Zeiss, Cape Town, South Africa), equipped with bright field optics, a 100 x oil immersion objective and an Optivar (lens providing a 1.25 x, 1.6 x or 2.0 x intermediate objective magnification). The length of the midpiece was determined with the analySIS® FIVE soft imaging system (Wirsam, Cape Town, South Africa).

4.2.3 Transmission electron microscopy (TEM)

4.2.3.1 Fixation of material and preparation of grids

Motile sperm samples were prepared as previously described (Chapter 3) and from this motile sperm population a sub-sample from five animals per species was subsequently used for transmission electron microscopy using standard preparation techniques (Chemes *et al.*, 1998). This involved pipetting 200-400 µl motile sperm preparation into a microcentrifuge tube and centrifugation for 10 minutes at 300 *g* and room temperature. After the supernatant was discarded, the motile sperm were re-suspended and fixed in 500 µl of 2.5% phosphate buffered glutaraldehyde and postfixed in 1% osmium tetroxide in the same buffer. The fixed samples were subsequently processed for TEM including contrasting with lead citrate and uranyl acetate. A Reichert ultramicrotome (SMM Instruments, Johannesburg, South Africa) with a diamond knife (Agar Scientific, Randburg, South Africa) was used to make silver to gold sections.

4.2.3.2 Production of electron micrographs

Thin sections on copper grids were examined using a Jeol JEM 1011 transmission electron microscope at 80 kV (Advanced Laboratory Solutions, Johannesburg, South Africa). Electron micrographs were produced with a Megaview III digital camera fitted onto the microscope and by means of the ITEM software package (Advanced Laboratory Solutions, Johannesburg, South Africa). Various magnifications (ranging from 5 000 x to 80 000 x) have been employed to produce electron micrographs of whole spermatozoa or different components of spermatozoa, especially the midpiece and mitochondria.

4.2.3.3 Use of electron micrographs for midpiece measurements

The electron micrographs were used to evaluate various parameters of the sperm midpiece and mitochondria. Sperm midpieces (at least ten spermatozoa per individual of each species) sectioned in both sagittal or coronal planes (longitudinal sections) and transverse planes (cross-sections) were analyzed. The midpiece measurements were determined with the analySIS® FIVE soft imaging system (Wirsam, Cape Town, South Africa). The longitudinal sections were used to verify the total length of the midpiece (MPL) (as determined with bright field microscopy and SpermBlue® staining in section 4.2.2) and the number of mitochondrial gyres in the midpiece (y). A third parameter, the height of the mitochondria in each gyre (h), was calculated from these two measurements and thus h = MPL/y. The cross-sections of the sperm midpieces were used to determine the radius of the axonemal-outer

dense fiber complex (r_a) and the radius of the midpiece (r_b). The midpiece volume (MPV) was determined with a modified formula for the measurement of the volume of a cylinder, as reported by Cardullo and Baltz (1991). The formula used to calculate this parameter was MPV = $\pi(r_b^2 - r_a^2)$MPL, where the volume of the axoneme is subtracted from the volume of the mitochondrial sheath. Another calculated parameter included in the current study was the straight-line midpiece length (SLMPL), a measurement of the length of the mitochondrial helix. This parameter was employed by Birkhead *et al.* (2005) to measure the straight-line helix of the midpiece in bird species where the degree of coiling of the midpiece varied between males. The formula used to calculate this parameter was SLMPL = (MPL/h)c, where $c = \sqrt{h^2 + (2\pi r)^2}$ and r = $r_b - r_a$.

4.2.4   Assessment of mitochondrial viability

4.2.4.1   MitoTracker® and staining method

The location and viability of sperm mitochondria were assessed by staining the mitochondria with a fluorescent probe, MitoTracker® Red CM-H_2XRos (Invitrogen, Cape Town, South Africa). This specific fluorescent stain was selected for the current study due to the fact that it is part of a series of mitochondrion-selective dyes that are only concentrated by active mitochondria and retained after cell fixation (Poot *et al.*, 1996). The cell-permeant MitoTracker® probes contain a mildly thiol-reactive chloromethyl moiety that can react with accessible thiol groups on peptides and proteins to form aldehyde-fixable conjugates once the probe accumulates in the mitochondria. MitoTracker® Red CM-H_2XRos (a derivative of dihydro-X-rosamine) and MitoTracker® Orange CM-H_2TMRos (a derivative of dihydro-tertramethylrosamine) are both reduced probes that do not fluoresce until they enter an actively respiring cell, are oxidized to the corresponding fluorescent probe and are sequestered in the mitochondria (see Fig. 4.1 for an example of these reactions for MitoTracker® Orange CM-H_2TMRos) (Molecular Probes, 2006).

Sperm mitochondria were stained with MitoTracker® Red CM-H_2XRos according to the manufacturer's recommended protocol, but with some modifications as described below.

Preparation of stock solution and staining solution

A vial of 50 µg lyophilized MitoTracker® product (stored at -20 °C) was allowed to warm to room temperature before opening it. The lyophilized solid was dissolved in 100 µl dimethylsulfoxide (DMSO) to a final concentration of 1mM. This stock solution was stored

in 10 µl aliquots at -20 ^{o}C in the dark. The staining solution was prepared by diluting the 1mM stock solution (thawed) to a final working concentration of 25 nM in pre-warmed Ham's F10 medium (37 ^{o}C).
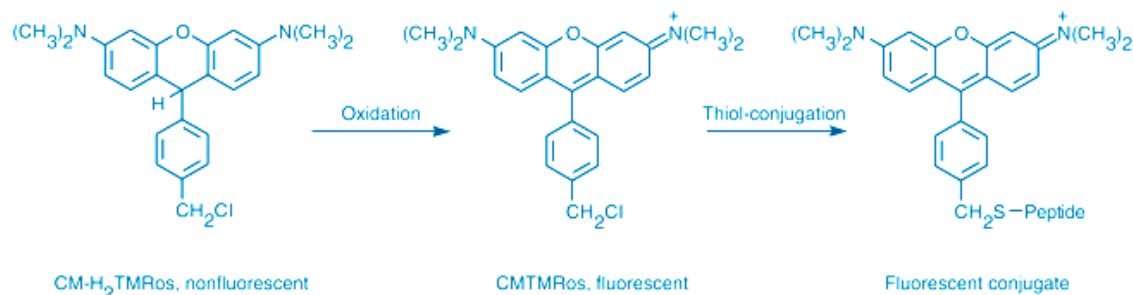
Figure 4.1. The intracellular reactions of MitoTracker[®] Orange CM-H$_2$TMRos. After entry into an actively respiring cell, the probe is sequestered in the mitochondria where it is oxidized to MitoTracker[®] Orange CMTMRos and it reacts with thiols on proteins and peptides to form fixable thiol-conjugates. (From Molecular Probes, 2006)

Sperm preparation and staining

A sample of motile spermatozoa was prepared by either the swim-up or swim-out technique (as described in section 3.2.4). After 30 minutes of incubation, 200-500 µl of the selected motile sperm suspension was placed into a microcentrifuge tube and centrifuged at 300 *g* for 10 minutes (the same protocol was followed in all the subsequent centrifugation steps). The supernatant was removed without disturbing the pellet. Spermatozoa were re-suspended in 50 µl pre-warmed staining solution and incubated for 45 minutes at 37 ^{o}C. Hereafter, spermatozoa were re-pelleted by centrifugation, the supernatant was carefully removed and spermatozoa were re-suspended in 50 µl fresh, pre-warmed Ham's F10. Spermatozoa were washed to remove any stain left in the suspension by centrifugation, removal of supernatant and re-suspension in 50 µl fresh, pre-warmed Ham's F10. Spermatozoa can either be observed under the fluorescence microscope after the washing step or it can be fixed for later observation. In the current study, all samples were fixed after staining with MitoTracker[®] for consistency in the protocol.

Sperm fixation

If spermatozoa were fixed, the sample was not re-suspended in fresh Ham's F10 after the washing step (described above), but it was rather re-suspended in 50 µl pre-warmed Ham's F10 containing 3.7% formaldehyde. Thereafter, spermatozoa were incubated for 15 minutes at 37 ^{o}C and then rinsed twice with phosphate buffered saline (PBS) (room temperature). Rinsing involved centrifugation of the sample after fixation, removal of supernatant and re-

suspension in 100 µl PBS. This centrifugation step was repeated and finally spermatozoa were re-suspended in 100 µl PBS. Stained samples were kept in the dark at 4 ^{o}C until further analysis with fluorescence microscopy and flow cytometry.

For each motile sperm sample, a negative control (no MitoTracker® staining) and duplicated stained samples were prepared. A sample representing disruption in the mitochondrial activity (positive control) was also prepared for each species by adding a freeze-thaw-cycle step before spermatozoa were stained with MitoTracker®. After the first centrifugation step and discarding of the supernatant, the sample was frozen for 15-20 minutes, then thawed at room temperature and these two steps were repeated twice. Afterwards, the same staining and fixation steps were followed for these positive controls, as described above.

4.2.4.2 Fluorescence microscopy

The MitoTracker® stained spermatozoa were observed with a fluorescent microscope within 4-5 days of preparation to avoid changes in fluorescence intensity over time. Observation and capturing of data involved an Olympus Cell^{R} system attached to an IX-81 inverted microscope (Olympus Life and Material Sciences, Europe) fitted with an F-view-II cooled CCD camera (Soft Imaging System, Germany). Since the MitoTracker® Red CM-H$_2$XRos has an excitation wavelength of 579 nm and an emission wavelength of 599 nm, a TexasRed filter was used for observations. In order to orientate spermatozoa under the fluorescence microscope and to confirm location of mitochondria, the sperm nuclear material was also stained with Hoechst 33342 (Sigma, South Africa) and observed with a DAPI filter. For verification of mitochondrial staining, 5 µl of MitoTracker® stained, fixed spermatozoa was mixed with 5 µl of Hoechst stain on a microscope slide and covered with a cover slip. A 10 x objective was used for observation of mouse and ram spermatozoa and a 20 x objective for human, baboon, rhesus monkey and vervet monkey spermatozoa. More detailed examples of staining were captured with a 60 x/1.4 oil immersion objective.

4.2.4.3 Flow cytometry

After fluorescence microscopic observation and verification of the stained mitochondria, 400 µl of PBS (room temperature) was added to the remaining MitoTracker® stained sample as preparation for flow cytometry. Analysis of the MitoTracker® stained and fixed spermatozoa involved a FACSCalibur flow cytometer (Becton Dickinson, San Jose, CA, USA) and the red fluorescence was detected in the FL3 channel. The forward scatter and side scatter values

were recorded on a linear scale, while the fluorescent values were recorded on a logarithmic scale. The forward scatter voltage were set at either E00 or E01 and the AmpGain for forward and side scatter were adjusted for each species until a clear cluster (representing the spermatozoa) could be detected. Ten thousand events were acquired for each sample and saved for later analysis. These listmode data files were analyzed by means of the WinMDI software package, version 2.9 (Purdue University Cytometry Laboratories, IN, USA).

4.2.5 Statistical analysis

The statistical software and statistical tests utilized were identical to those described in Chapter 3.

4.3 Results

Midpiece morphology

The margins of the midpiece can clearly be identified on the SpermBlue® stained spermatozoa (Fig. 4.2). Only one spermatozoon is depicted for most species due to the uniformity of the sperm morphometry of these species. Since these photographs were all taken at the same magnification, the difference in the size (length and width) of the midpiece can be seen among the seven species (actual values of the midpiece parameters were presented in Table 3.4). In Figures 4.2A-F, the midpiece was typically elongated in these six species. In contrast, the small size of the naked mole-rat spermatozoon and its spherical midpiece is depicted in Figure 4.2G.

TEM of the midpiece

Longitudinal sections through the midpiece of the seven species are presented in Figure 4.3 and these examples are representative of each species. In all the species except for the naked mole-rat, the mitochondria were tightly wrapped around the axonemal complex, with some of the mitochondrial helix visible in Figure 4.3D and F. The mitochondrial gyres are clearly visible in all these electron micrographs and have been used to count the number of gyres in the total midpiece of each species (see Midpiece morphometry below). In the naked mole-rat, however, the mitochondria were loosely arranged around the axonemal complex and the size of the mitochondria varied (Fig. 4.3G). In the human, there was often not a close association between the plasma membrane and the mitochondrial helix in the proximal part of the midpiece due to residual cytoplasm accumulating in this region (Fig. 4.3A).
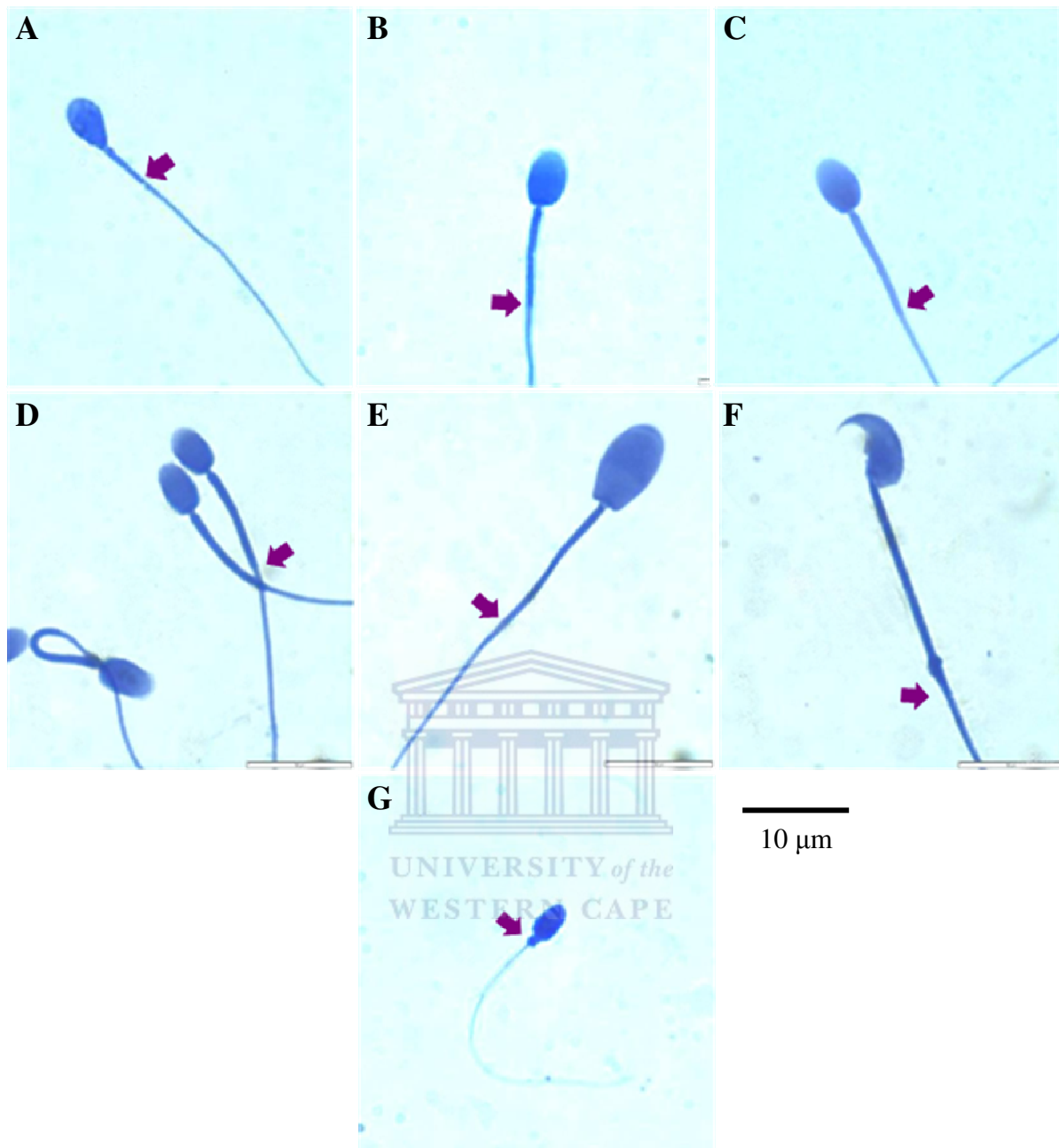
Figure 4.2. SpermBlue® stained spermatozoa illustrating the midpiece morphology. The distal end of the midpiece is indicated with an arrow for each of the spermatozoa. **A**) *Homo sapiens* (human), **B**) *Papio ursinus* (chacma baboon), **C**) *Macaca mulatta* (rhesus monkey), **D**) *Chlorocebus aethiops* (vervet monkey), **E**) *Ovis orientalis* (merino ram), **F**) *Mus musculus* (house mouse), **G**) *Heterocephalus glaber* (naked mole-rat).

Figure 4.3 furthermore indicates the average number of gyres per 2 μm section of the length of the midpiece for six of the seven species (value not determined for the naked mole-rat). Comparing this number of gyres for the six species revealed that the gyres of the different spermatozoa are not the same size. The baboon, rhesus monkey, vervet monkey and mouse had a comparable number of gyres in a 2 μm section of the midpiece, but the human sperm midpiece had less and the ram sperm midpiece had more gyres. The mitochondria of the human were therefore larger in terms of its height, while the ram had a significantly smaller
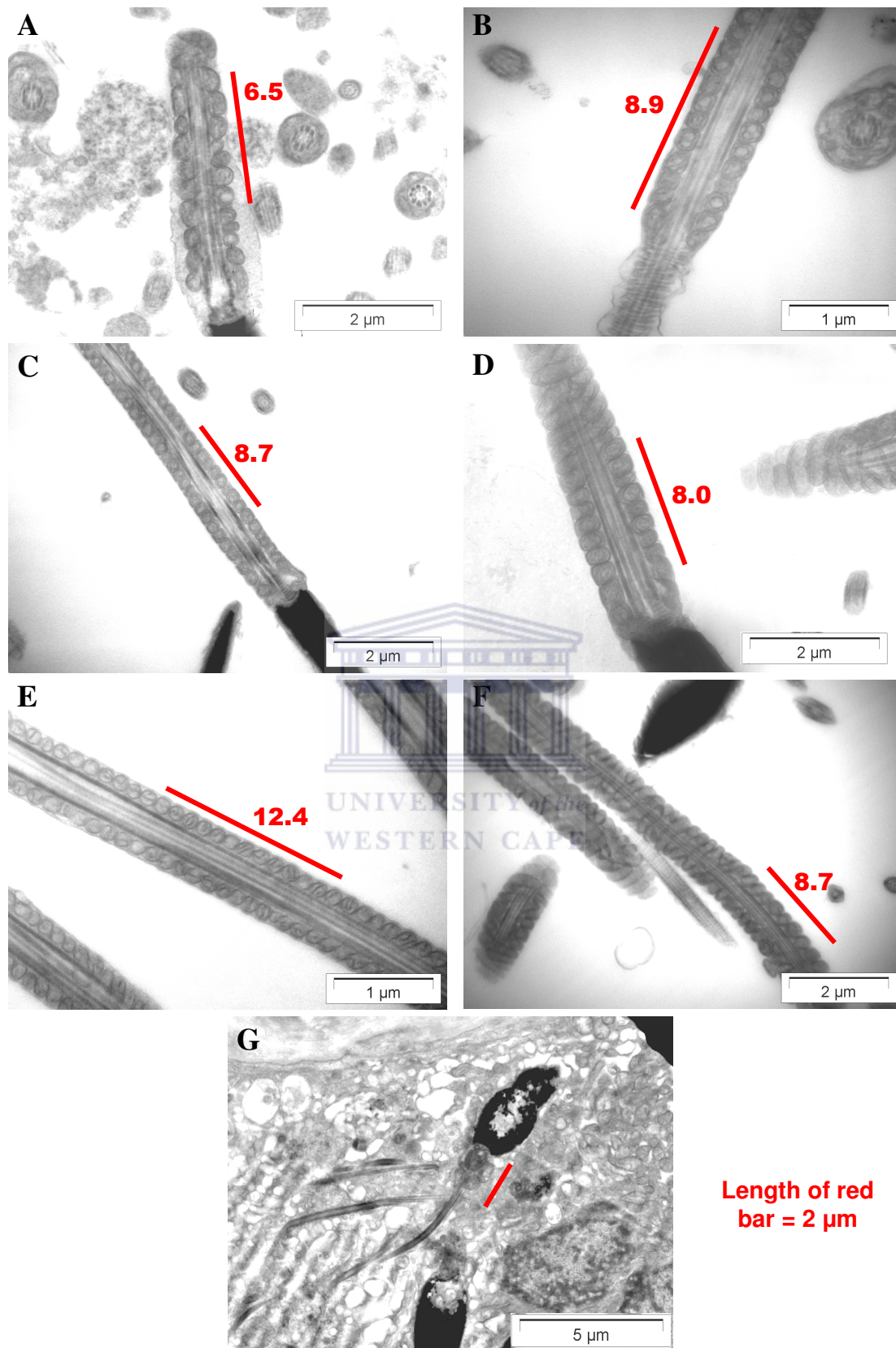
Figure 4.3. Longitudinal sections through the midpiece of the sperm flagellum illustrating the location and size of the mitochondrial gyres and individual mitochondria. **A**) *Homo sapiens* (human), **B**) *Papio ursinus* (chacma baboon), **C**) *Macaca mulatta* (rhesus monkey), **D**) *Chlorocebus aethiops* (vervet monkey), **E**) *Ovis orientalis* (merino ram), **F**) *Mus musculus* (house mouse), **G**) *Heterocephalus glaber* (naked mole-rat). The structures surrounding the naked mole-rat spermatozoon (G) is the ampulla tissue from which the spermatozoa were extracted. The number next to the red bar indicates the average number of mitochondrial gyres in each 2 µm section of the midpiece length for each species (not determined for naked mole-rat).

mitochondrial height (also see Table 4.1).

Cross-sections through the midpiece of the seven species are presented in Figure 4.4. As seen in Figure 4.3, the mitochondria were closely associated with the outer dense fiber-axonemal complex. The 9+9+2 arrangement of the outer dense fibers and axoneme were present in all species. The size and shape of the outer dense fibers was similar among the seven species, with the ram, mouse and naked mole-rat spermatozoa having slightly larger outer dense fibers. The mitochondrial sheath was clearly visible and therefore these and other similar electron micrographs were used to determine the thickness of the mitochondrial sheath (see Midpiece morphometry below). The smaller cross-sections of the principal piece of the sperm flagellum (without the mitochondrial sheath) can also be seen in Figure 4.4B and D.

Higher magnifications of midpiece longitudinal sections are presented in Figure 4.5 for six of the species included in the study. Only one spermatozoon is depicted per species due to the uniformity of the midpiece morphometry. Apart from displaying the size and the shape of the mitochondria in the gyres, these electron micrographs also reveal the structure and abundance of the mitochondrial cristae. Using the terminology of Fawcett (1970), the orientation of the cristae of all six species were long and orientated parallel to the surface of the mitochondria. This structure of the cristae conformed to the intermediate type of mitochondria. In the baboon, vervet monkey and ram, the cristae also appeared to be dispersed into the mitochondrial matrix, whereas the cristae of the other three species seemed to be located closer to the outer mitochondrial membrane. Although no quantitative value was determined for the abundance of the cristae, the mitochondria of the baboon and vervet monkey seemed to have a higher concentration of cristae and slightly larger intercristal spaces.

Midpiece morphometry

The radius of the axonemal-outer dense fiber complex (r_a) and the radius of the midpiece (r_b) were determined as illustrated in Figure 4.6. The morphometric parameters derived from these and other midpiece measurements are presented in Table 4.1. The midpiece length reported here differ slightly from the values presented in Table 3.4 since the length measurements of only five individuals per species were included in the current midpiece parameters instead of the ten individuals in Chapter 3. Due to many irregularities in the midpiece of the naked mole-rat spermatozoa, measurements for this species were not included.
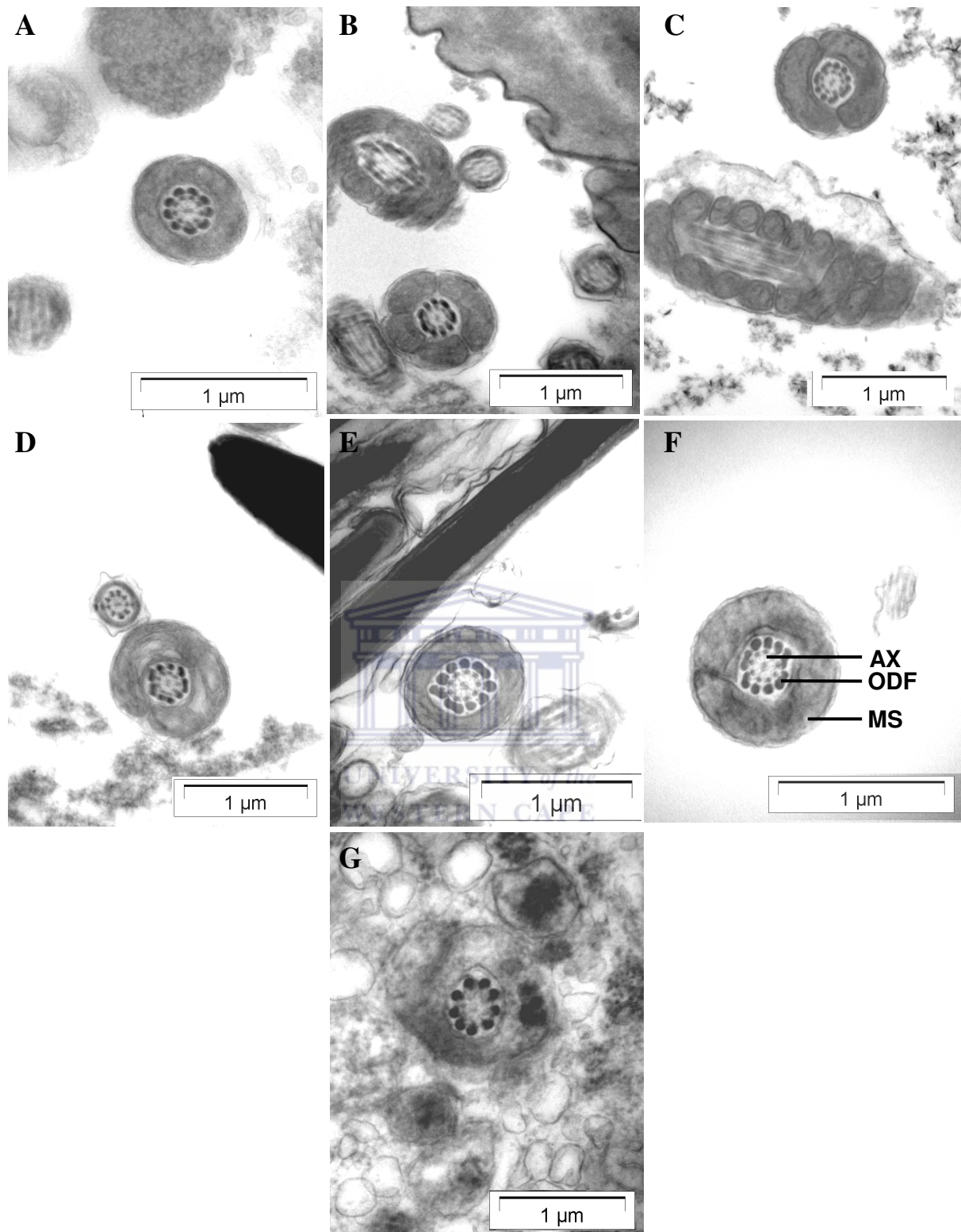
Figure 4.4. Cross-sections through the midpiece of the sperm flagellum illustrating the thickness of the mitochondrial sheath surrounding the axoneme. The 9+9+2 arrangement of the axoneme and outer dense fibers is clearly visible in all seven species (also see Fig. 4.6). **A**) *Homo sapiens* (human), **B**) *Papio ursinus* (chacma baboon), **C**) *Macaca mulatta* (rhesus monkey), **D**) *Chlorocebus aethiops* (vervet monkey), **E**) *Ovis orientalis* (merino ram), **F**) *Mus musculus* (house mouse), **G**) *Heterocephalus glaber* (naked mole-rat). The structures surrounding the naked mole-rat sperm midpiece (G) is the ampulla tissue from which the spermatozoa were extracted. AX = axoneme, ODF = outer dense fibers, MS = mitochondrial sheath.
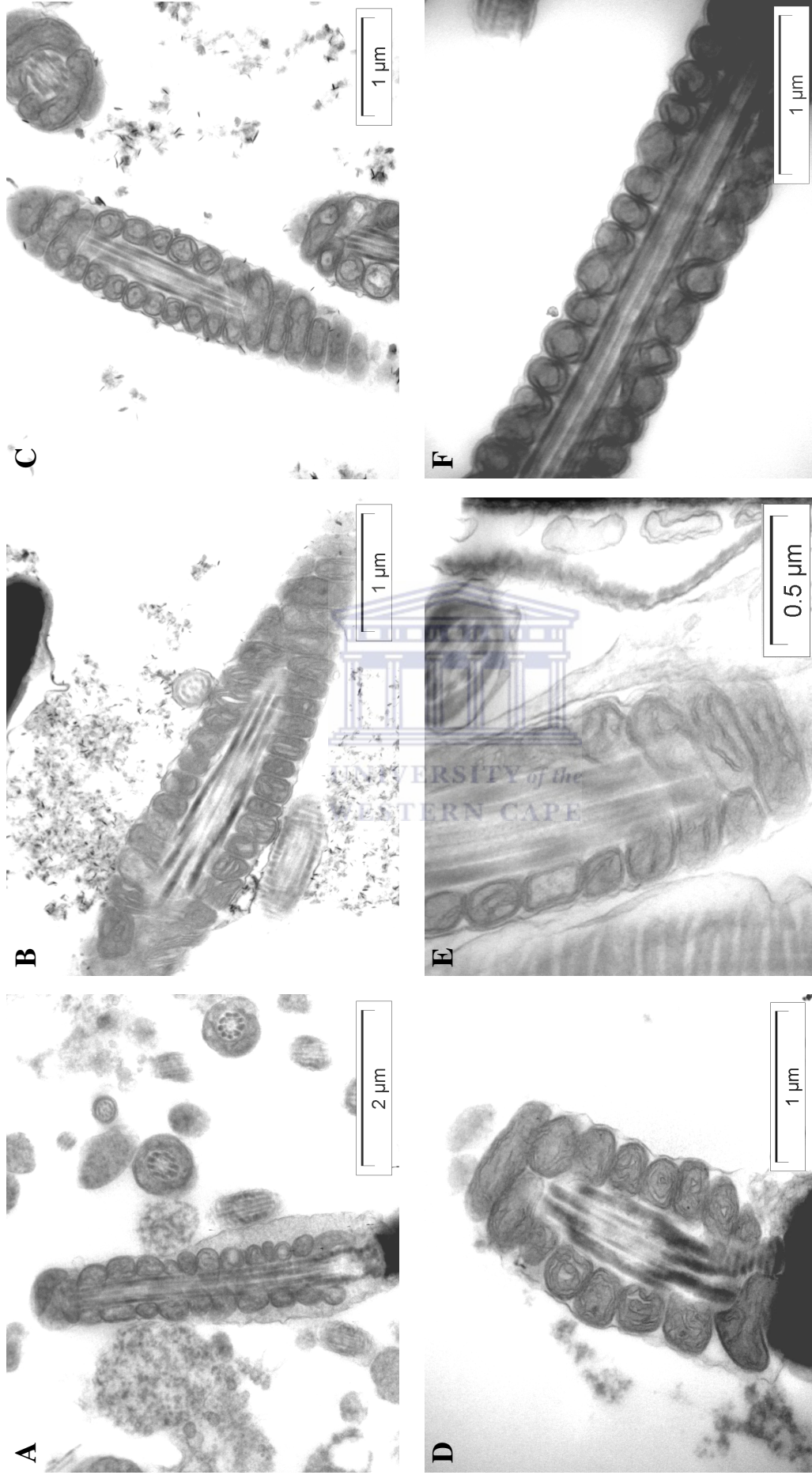
Figure 4.5. Longitudinal sections through parts of the sperm midpiece illustrating the structure and abundance of the mitochondrial cristae for each species. **A)** *Homo sapiens* (human), **B)** *Papio ursinus* (chacma baboon), **C)** *Macaca mulatta* (rhesus monkey), **D)** *Chlorocebus aethiops* (vervet monkey), **E)** *Ovis orientalis* (merino ram), **F)** *Mus musculus* (house mouse).
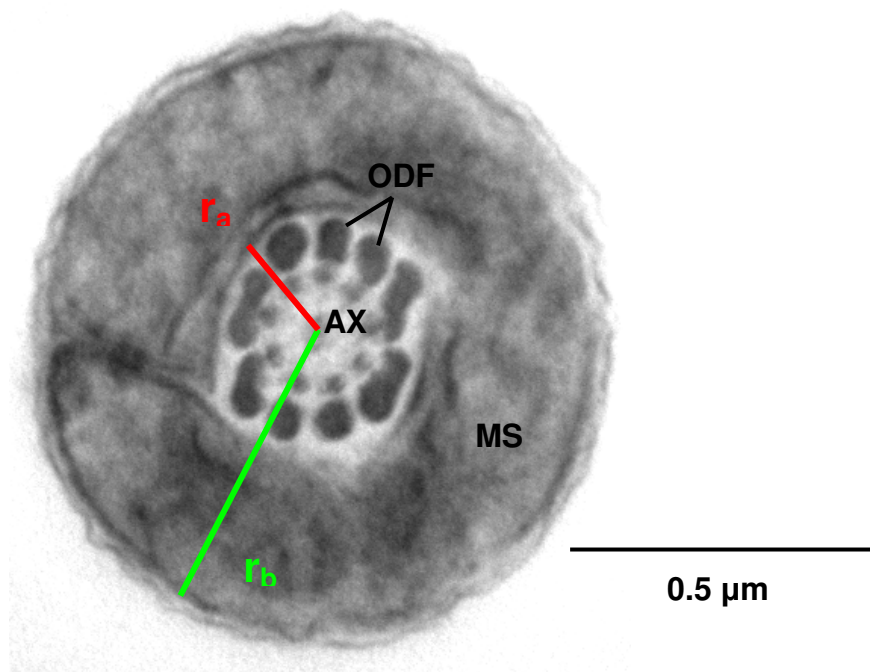
Figure 4.6. Cross-section through the flagellum of a mouse spermatozoon to illustrate the measurement of the radius of the axonemal-outer dense fiber complex (r_a) and the radius of the midpiece (r_b). The actual measurements of these midpiece parameters are presented in Table 4.1 and were used in the calculation of the thickness of the mitochondrial sheath ($r_b - r_a$), midpiece volume (MPV) and the straight-line midpiece length (SLMPL). AX = axoneme, ODF = outer dense fibers, MS = mitochondrial sheath.

Most of the similarities in the midpiece measurements ($P > 0.05$) were found among the non-human primates. If these three species are treated as a group, there were significant differences ($P < 0.05$) between the species for almost all of the midpiece parameters. The only parameter that did not differ among the six species was the radius of the axoneme (r_a). Interestingly, there was once again not a consistent trend among the midpiece measurements for the six species. For instance, human spermatozoa did not always have the lowest values, nor did mouse spermatozoa always have the highest values. The ram midpiece parameters portrayed the most variation in terms of its size relative to the other five species. These variations in the midpiece measurements are further explored in Figure 4.12 below.

The midpiece volume is also presented as ratios to other sperm components in Table 4.2. The values used for the head length, head area, total tail length and sperm length were taken from Table 3.4 in Chapter 3. Evaluation of the midpiece volume to head ratios revealed variations among the six species that resulted in the following arrangement of the species: HS/OO < OO/HS < RM < PU < CA < MM, with only the human and merino ram measurements differing between the head length and head area ratios. The total tail and sperm length ratios revealed another arrangement, namely CA < MM < PU < RM < OO < HS.

Table 4.1. Midpiece morphometry and flow cytometry measurements (average ± SD) of various midpiece parameters for six mammalian species (n=5 individuals for each species)

	HS	PU	RM	CA	OO	MM
Number of gyres	14.98 ± 2.14[a]	44.42 ± 2.77[b]	47.70 ± 1.12[b]	42.86 ± 4.37[b]	93.04 ± 2.37[c]	96.53 ± 1.92[d]
Mitochondrial height (µm)	0.32 ± 0.04[a]	0.23 ± 0.01[b]	0.23 ± 0.00[bc]	0.25 ± 0.02[c]	0.17 ± 0.01[d]	0.23 ± 0.00[bc]
r_b **(µm)**	0.41 ± 0.02[a]	0.48 ± 0.02[bd]	0.47 ± 0.05[bd]	0.50 ± 0.02[b]	0.38 ± 0.03[c]	0.46 ± 0.01[d]
r_a **(µm)**	0.20 ± 0.01	0.22 ± 0.02	0.21 ± 0.02	0.20 ± 0.01	0.21 ± 0.03	0.22 ± 0.00
$r_b - r_a$ **(µm)**	0.21 ± 0.01[a]	0.26 ± 0.01[b]	0.25 ± 0.03[b]	0.30 ± 0.02[c]	0.17 ± 0.01[d]	0.24 ± 0.01[b]
MPLength (µm)	4.59 ± 0.27[a]	9.95 ± 0.16[b]	10.97 ± 0.12[c]	10.67 ± 0.26[d]	15.02 ± 0.14[e]	22.14 ± 0.22[f]
MPVolume (µm³)	1.97 ± 0.22[a]	5.78 ± 0.36[b]	5.98 ± 1.23[b]	6.98 ± 0.77[c]	4.71 ± 0.71[d]	11.50 ± 0.82[e]
SLMPL (µm)	20.72 ± 3.22[a]	73.29 ± 5.81[b]	76.24 ± 7.63[b]	80.43 ± 9.51[b]	100.75 ± 4.04[c]	149.28 ± 7.71[d]
Flow cytometry	10.03 ± 1.93[a]	16.09 ± 4.87[b]	18.07 ± 5.01[b]	35.47 ± 4.67[c]	71.27 ± 11.96[d]	80.41 ± 11.07[e]

HS = *Homo sapiens* (human), PU = *Papio ursinus* (chacma baboon), RM = *Macaca mulatta* (rhesus monkey), CA = *Chlorocebus aethiops* (vervet monkey), OO = *Ovis orientalis* (merino ram), MM = *Mus musculus* (house mouse)

r_b = radius of the midpiece, r_a = radius of the axonemal-outer dense fiber complex, $r_b - r_a$ = thickness of the mitochondrial sheath, MP = midpiece, SLMPL = straight-line midpiece length

a, b, c, d, e, f = values labelled with different superscript letters in the same row were significantly different (P < 0.05)

Table 4.2. Midpiece volume ratios (average ± SD) of various sperm components for six mammalian species (n=5 individuals for each species)

	HS	PU	RM	CA	OO	MM
MPV/HL	0.40 ± 0.04[a]	1.05 ± 0.10[b]	1.02 ± 0.21[b]	1.37 ± 0.21[c]	0.54 ± 0.07[d]	1.51 ± 0.11[c]
MPV/HA	0.17 ± 0.02[a]	0.35 ± 0.04[b]	0.35 ± 0.08[b]	0.50 ± 0.08[c]	0.12 ± 0.02[d]	0.52 ± 0.05[c]
TTL/MPV	25.86 ± 2.26[a]	12.22 ± 0.86[b]	12.44 ± 2.62[bc]	9.49 ± 1.14[cd]	12.66 ± 1.61[b]	10.45 ± 0.76[bcd]
SPL/MPV	28.37 ± 2.50[a]	13.18 ± 0.92[b]	13.45 ± 2.84[b]	10.24 ± 1.24[c]	14.55 ± 1.83[b]	11.12 ± 0.80[c]

HS = *Homo sapiens* (human), PU = *Papio ursinus* (chacma baboon), RM = *Macaca mulatta* (rhesus monkey), CA = *Chlorocebus aethiops* (vervet monkey), OO = *Ovis orientalis* (merino ram), MM = *Mus musculus* (house mouse)

MPV = midpiece volume, HL = head length, HA = head area, TTL = total tail length, SPL = sperm length

a, b, c, d = values labelled with different superscript letters in the same row were significantly different (P < 0.05)

Mitochondrial viability/activity

The staining of the sperm mitochondria with a fluorescent probe was verified by comparing light microscopy and two fluorescent filter overlays, as presented in Figure 4.7. The MitoTracker® stain was only present in the midpiece (Fig. 4.7B) and was therefore regarded as a suitable fluorescent probe for assessing the sperm mitochondrial viability/activity. This fluorescent probe as well as the method of staining was suitable for all six species evaluated (Fig. 4.8).
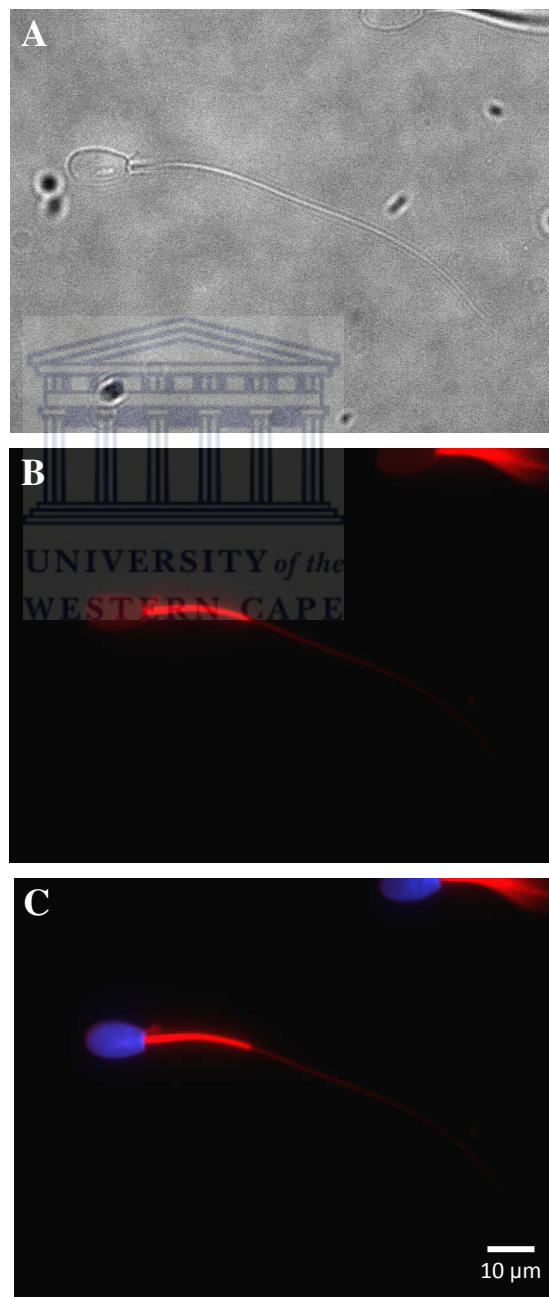
Figure 4.7. Series of photographs to illustrate the use of fluorescent microscopy to verify the staining of sperm mitochondria. **A**) Bright field microscopy indicating the location of a ram spermatozoon. **B**) The same spermatozoon with the overlay as observed with the TexasRed filter. **C**) A duplicate of 'B' with the addition of the DAPI filter overlay.

93
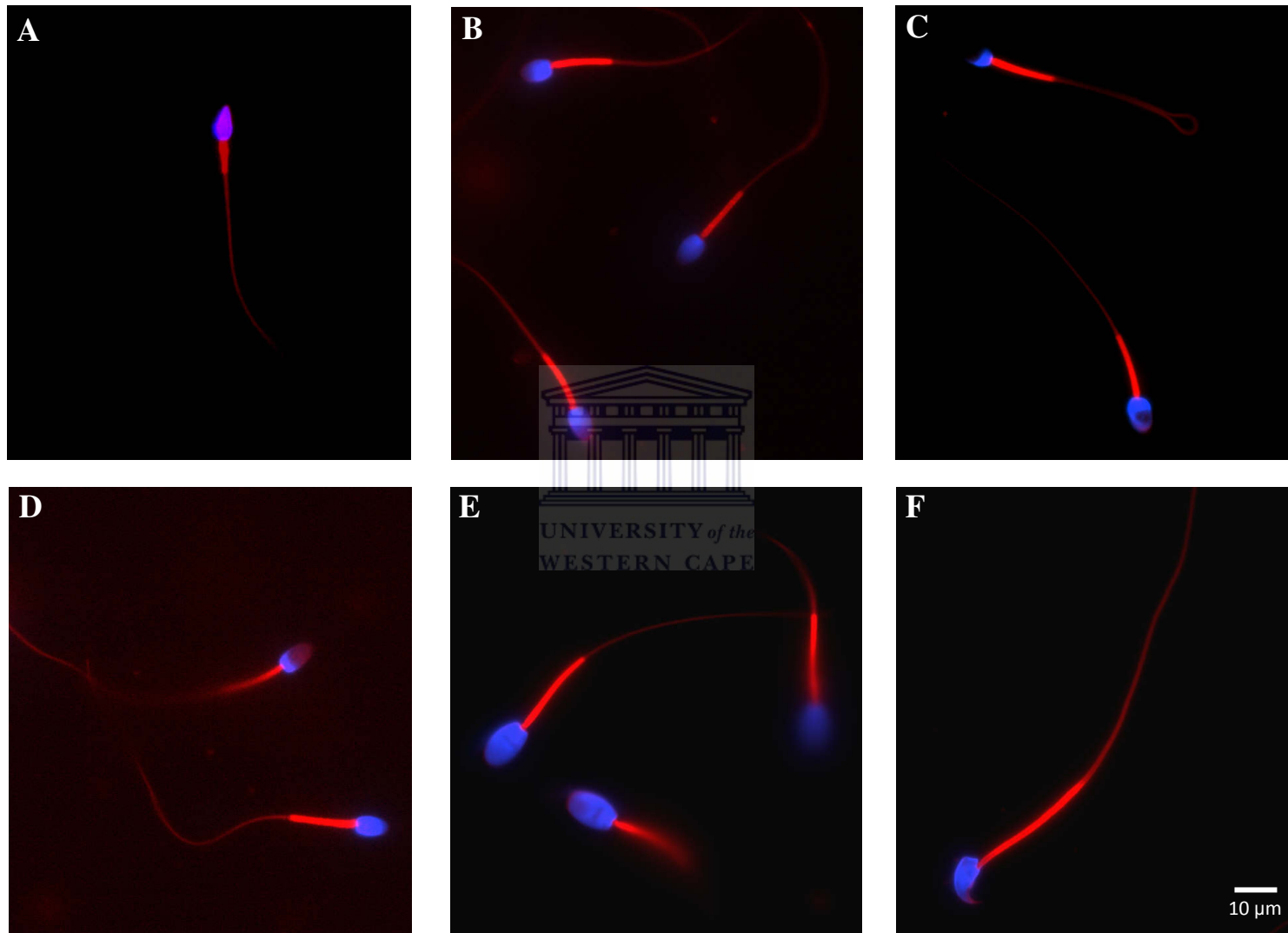
Figure 4.8. Spermatozoa stained with MitoTracker® Red CM-H₂XRos to illustrate the location and viability of sperm mitochondria for the individual species. Sperm nuclear material was stained with Hoechst (blue heads). **A**) *Homo sapiens* (human), **B**) *Papio ursinus* (chacma baboon), **C**) *Macaca mulatta* (rhesus monkey), **D**) *Chlorocebus aethiops* (vervet monkey), **E**) *Ovis orientalis* (merino ram), **F**) *Mus musculus* (house mouse).

At least 100 spermatozoa per individual for all six species were evaluated and almost all spermatozoa had similar staining patterns. This was expected since only motile spermatozoa were selected for all the experimental procedures undertaken for species comparative purposes. Further verification that the MitoTracker® fluorescent probe only stained actively respiring mitochondria is presented in Figure 4.9 when the flow cytometric analysis of the negative control (no staining) was compared to the positive control (freeze-thaw-cycle) and the motile spermatozoa.

Comparisons of the flow cytometric analyses of all six species are presented in Figure 4.10. The actual measurements of these analyses are presented in Table 4.1. It is evident from both the graph in Figure 4.10 and from the statistically compared fluorescence staining intensities in Table 4.1 that most of the species (not the baboon and the rhesus monkey) were significantly different ($P < 0.05$) from each other with regards to these measurements.
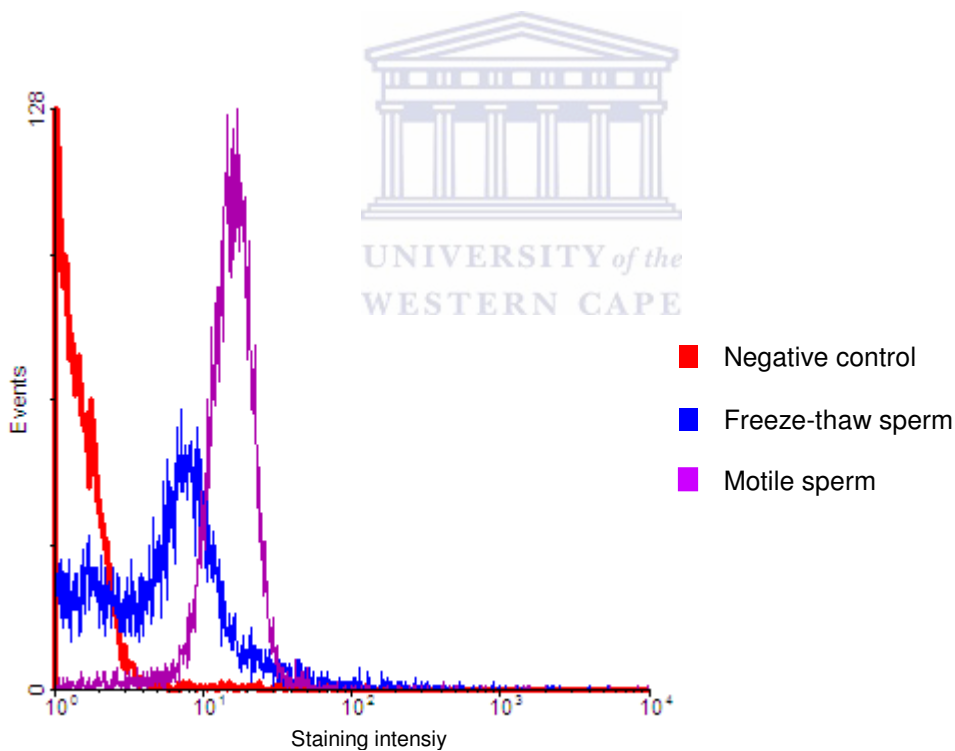
Figure 4.9. Flow cytometric analysis of rhesus monkey spermatozoa illustrating the difference in staining intensity (log scale) of the negative control (no staining), freeze-thaw spermatozoa (positive control) and motile spermatozoa. Notice the shift to the left when the sperm mitochondria were disrupted by the freeze-thaw-cycle.
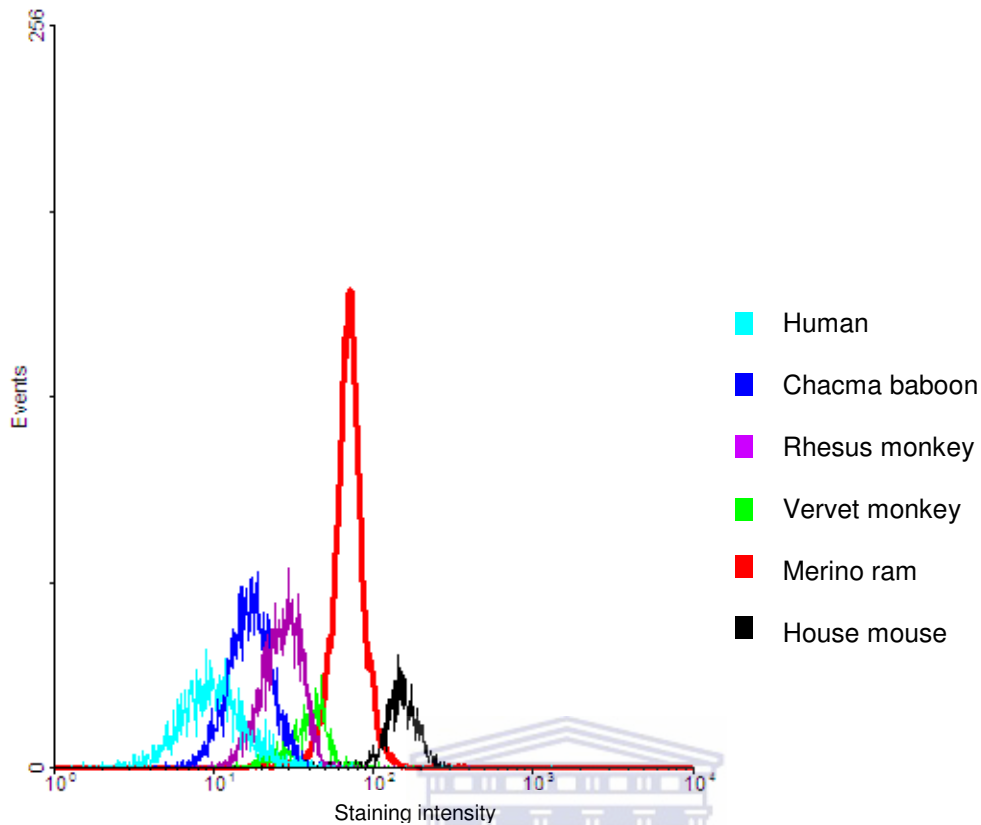
Figure 4.10. Flow cytometric analysis of sperm mitochondria stained with MitoTracker® Red CM-H$_2$XRos illustrating the difference in staining intensity (log scale) of the six different species (only one individual per species were used to create the graph). The average staining intensity values are presented in Table 4.1.

Species specificity and variation of midpiece parameters

The cluster analysis presented in Figure 4.11 was constructed by including all the midpiece parameters presented in Table 4.1. The close distribution of the individuals of the same species on the vertical axis revealed the species specificity of the midpiece parameters for most of the species. No pertinent difference was found between the baboon and rhesus monkey due to the overlapping of the individuals of these two species on the vertical axis and the small linkage distance between the individuals. This confirms the similarities in midpiece measurements for these two species reported above (Table 4.1). The linkage distance between the other species indicated that the three non-human primate species were more closely related in terms of the midpiece parameters. More distantly related clusters were formed between the ram and mouse as well as between the human and non-human primate species.

In order to visualize the variation in midpiece measurements among six of the mammalian species, the relative difference between the midpiece parameters for the individual species are illustrated in Figure 4.12.

96
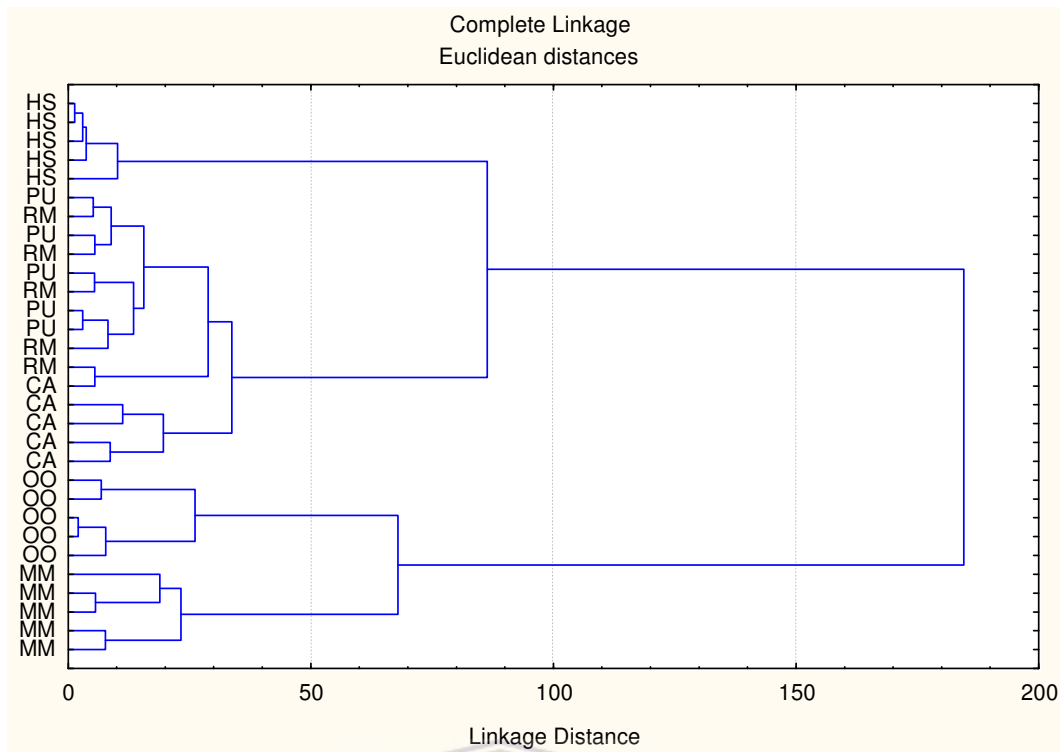
Figure 4.11. Cluster analysis of nine midpiece morphometry parameters illustrating the clustering of species on the vertical axis and indicating the relatedness among the six mammalian species on the horizontal axis (linkage distance). The actual values of the midpiece morphometry parameters are presented in Table 4.1. HS = *Homo sapiens* (human), PU = *Papio ursinus* (chacma baboon), RM = *Macaca mulatta* (rhesus monkey), CA = *Chlorocebus aethiops* (vervet monkey), OO = *Ovis orientalis* (merino ram), MM = *Mus musculus* (house mouse).

Comparing these measurements among the species revealed that, in general, the longer the sperm midpiece of a species, the more mitochondrial gyres were present, the larger was the midpiece volume and straight-line midpiece length and the higher was the fluorescent staining intensity. Although the human spermatozoa had the smallest value for most of the midpiece parameters, it did not have the thinnest mitochondrial sheath and it had the largest mitochondrial height. The vervet monkey had very similar values to the other two non-human primates, but its mitochondrial sheath was the thickest among the six species, resulting in a larger midpiece volume than the baboon and rhesus monkey ($P < 0.05$). The fluorescent staining intensity of the vervet monkey was also significantly higher compared to the other two non-human primates ($P < 0.05$). The merino ram spermatozoa had the second largest number of gyres, midpiece length, SLMPL and fluorescent intensity but the thinnest mitochondrial sheath and the smallest mitochondrial height, resulting in the second smallest midpiece volume. The mouse spermatozoa had the largest value for most midpiece parameters, except for its mitochondrial height and mitochondrial sheath thickness that were comparable to the non-human primates.

97
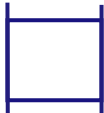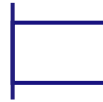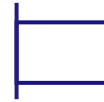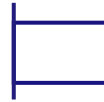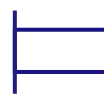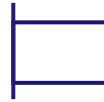
Species	HS	PU	RM	CA	OO	MM
Number of gyres	15.0	44.4	47.7	42.9	93.0	96.5
Mitochondrial height	0.32	0.23	0.23	0.25	0.16	0.23
r_a & r_b / $r_b - r_a$	0.21	0.26	0.25	0.30	0.17	0.24
MPL	4.6	10.0	11.0	10.7	15.0	22.1
MPV	2.0	5.8	6.0	7.0	4.7	11.5
SLMPL	20.7	73.3	76.2	80.4	100.8	149.3
Flow cytometry	10.0	16.1	18.1	35.5	71.3	80.4

Figure 4.12. Schematic presentation of nine midpiece morphometry parameters to illustrate the variation present among the six species included. The size of the shapes for each parameter represents the relative difference in the actual values (rounded off) as indicated. The statistically compared midpiece morphometry measurements are presented in Table 4.1. HS = *Homo sapiens* (human), PU = *Papio ursinus* (chacma baboon), RM = *Macaca mulatta* (rhesus monkey), CA = *Chlorocebus aethiops* (vervet monkey), OO = *Ovis orientalis* (merino ram), MM = *Mus musculus* (house mouse), r_a = radius of axonemal-outer dense fiber complex, r_b = radius of midpiece, $r_b - r_a$ = thickness of the mitochondrial sheath, MPL = midpiece length, MPV = midpiece volume, SLMPL = straight-line midpiece length.

98

4.4   Discussion

The variations found in the sperm midpiece morphometry of the seven mammalian species (Chapter 3) were confirmed in this chapter and further investigated by assessing additional midpiece parameters and several structural aspects of the sperm mitochondria. Both the midpiece measurements and the cluster analysis confirmed the species specificity for the midpiece parameters in most species included in this study (with the baboon and rhesus monkey being the exception). The general trend found among these parameters was that a longer midpiece translated into more mitochondrial gyres, a larger midpiece volume, a longer straight-line midpiece length and an increased fluorescent staining intensity. The implications of this trend in the midpiece parameters, as well as the individual species' deviations from it, and the possible applications of specific parameters are discussed in more detail below.

The large difference between the midpiece morphology of the naked mole-rat and that of the other six species was highlighted by the evaluation of the electron micrographs. The midpiece of the naked mole-rat was not as organized as the other species investigated and the size and shape of the mitochondria also seemed to be inconsistent. Van der Horst *et al.* (2011) reported that naked mole-rat spermatozoa only had between five and seven mitochondria, which were elongated, oval or spherical in shape. This large variation in naked mole-rat midpiece morphometry made it difficult to measure the midpiece parameters accurately. As mentioned before, the low volume of the ampulla contents also made it impossible to stain the midpiece of the naked mole-rat spermatozoa with a fluorescent probe to determine its fluorescent staining intensity. However, according to the midpiece morphometry measurements reported in Chapter 3 and the trend in midpiece parameters reported above, the naked mole-rat would probably have the smallest number of mitochondrial gyres, midpiece volume, straight-line midpiece length and the lowest fluorescent staining intensity of all seven species. Therefore, most of the discussions to follow only included comparisons of the other six mammalian species investigated.

The arrangement and number of mitochondrial gyres in the midpiece of the six mammalian species were consistent for each species, but varied among the different species. The number of gyres for each species determined in the current study falls within the range of the numbers reported in previous studies (Fawcett, 1970; Phillips, 1977; Mundy *et al.*, 1995). The reason for the difference in the size (mitochondrial height) and the number of mitochondrial gyres is not clear but could be an adaptation for structural and/or functional aspects of sperm motility.

Phillips (1977) stated that the helical arrangement of sperm mitochondria might be the most efficient means of fitting mitochondria of unequal length into a cylinder (mitochondrial sheath) and that this arrangement is probably most favourable for strength and flexibility during motility. Furthermore, this helical arrangement might also allow a degree of sliding of the mitochondria when the flagellum bends during activated motility (Phillips, 1977). Since the mitochondria are regarded as one of the major sources of energy production for sperm motility, the size and number of mitochondrial gyres could be a trade-off between including enough mitochondria for the required energy production and arranging the mitochondria for optimal structural support, ultimately resulting in efficient sperm motility.

Austin (1976) suggested the existence of a direct relationship between the magnitude of the mitochondria (thickness of the mitochondrial sheath and size of the mitochondria) and the diameter of the coarse fibers, as more energy would be required to bend the thicker outer dense fibers. However, both Austin (1976) and Fawcett (1970) reported many exceptions to this relationship in various mammalian species. Moreover, Fawcett (1970) pointed out that the overall diameter of the sperm flagellum is not only related to the thickness of the outer dense fibers but also to the distance between these fibers and the axoneme (increasing the radius of the axonemal-outer dense fiber complex). In the current study, no apparent differences were found in the size of the outer dense fibers among the species. These fibers were closely associated with the outer nine axonemal doublets in all seven species. Thus, none of the relationships suggested by Fawcett (1970) or Austin (1976) seem to explain the differences found in the thickness of the mitochondrial sheath for the mammalian species included in this study. This might be due to the fact that these earlier studies referred to more extreme variations in the diameter of the midpiece and mitochondrial sheath.

Since large variations and no consistent trend in the midpiece length or midpiece width among the seven species were reported in Chapter 3, it was decided to also determine the midpiece volume for a more accurate assessment of the size of the midpiece. The differences found among the six species in terms of the thickness of the mitochondrial sheath are further support that the mitochondrial volume, which takes this parameter into consideration, might be a better measure of the functional midpiece size. The value of also including volumetric measurements for comparative studies was confirmed by Anderson *et al.* (2005). The latter found a positive correlation between sperm competition and sperm midpiece volume, while this relationship was not found for linear sperm morphometry parameters, e.g. head, midpiece

or tail length for the same study (Anderson *et al.*, 2005) or previous investigations (Gage, 1998; Gage and Freckleton, 2003). The midpiece volume measurements reported in the current study followed an almost similar trend when compared to the number of mitochondrial gyres, the thickness of the mitochondrial sheath or the midpiece length among the six species (see further discussion below). However, the ratios of the midpiece volume to head length and head area revealed a species arrangement similar to that reported in Chapter 3 for the midpiece length to head length and head area ratios. Thus, it is possible that the actual value of the midpiece length and midpiece volume is not as important as the ratio between these two midpiece parameters and other sperm components, e.g. the sperm head.

The measurement of the straight-line midpiece length revealed the same arrangement among the six species as for midpiece length and number of gyres. These similarities are not surprising, as these two parameters were used to calculate the straight-line midpiece length. Since the straight-line midpiece length measures the length of the mitochondrial helix, an application of this parameter could be to calculate the number of mitochondria present in the sperm midpiece, provided the length of the sperm mitochondria is known. In a study by Bartoov and Messer (1976), the mitochondrial fraction was isolated from ejaculated ram spermatozoa through dithiothreitol treatment. This fraction contained residual mitochondrial helices and individual elongated mitochondria of which the length and width could be determined. The average width of the ram sperm mitochondria was reported as 0.165 μm (SD, ± 0.024 μm), which is identical to that found in the present study (merino ram mitochondrial sheath thickness = 0.17 μm). The average length reported for the ram sperm mitochondria reported by Bartoov and Messer (1976) was 1.256 μm (SD, ± 0.133 μm). If this value is divided into the straight-line midpiece length for merino ram (100.75 μm) (Table 4.1), the number of mitochondria in the ram sperm midpiece would be about 80. Using this method to determine the length of the sperm mitochondria of other mammalian species, which is expected to differ among species, it will be possible to compare the exact number of sperm mitochondria among species. Another method to determine the exact number of mitochondria in the sperm midpiece could be by using the procedure of Ho and Wey (2007) to determine the three dimensional formation of the mitochondrial sheath during spermiogenesis. This method involves the following steps: 1) making serial TEM sections through the midpiece, 2) digitally tracing the boundaries of the mitochondria in midpiece cross-sections on electron micrographs and then 3) three dimensionally reconstruct parts of the midpiece to count the number of mitochondria per unit length of the midpiece (Ho and Wey, 2007).

The flow cytometric analyses using the MitoTracker[®] fluorescent probe revealed species specific values for most species, except for the baboon and rhesus monkey which had similar fluorescent staining intensities ($P > 0.05$). These fluorescence measurements revealed a similar arrangement among the six species as for the number of gyres, midpiece length and straight-line midpiece length. The only exception was the vervet monkey which had a significantly higher fluorescent intensity than the other two non-human primates, but for the other three parameters mentioned, no difference was found among these non-human primates. It is not evident what caused the higher fluorescence in the vervet monkey sperm midpieces, but it might be due to the fact that the vervet monkey had a thicker mitochondrial sheath as well as a larger midpiece volume ($P < 0.05$) than the other two non-human primates. However, this assumption does not seem to be valid when comparing the merino ram and vervet monkey midpiece parameters. In terms of the thickness of the mitochondrial sheath and the volume of the midpiece, the ram had lower values than the vervet monkey, but the ram still had an average fluorescence value twice that of the vervet monkey.

Another explanation for the higher fluorescence value of the vervet monkey compared to the other non-human primates might be due to the fact that the vervet monkey sperm mitochondria had a higher concentration of cristae (as seen in the electron micrographs). The increase in the quantity of the cristae possibly resulted in the higher fluorescence intensity due to the fact that more cristae relates to more electron transport chain proteins and thus more enzymatic activity (Gilkerson *et al.*, 2003). In this case, the higher concentration of cristae reported for the baboon sperm mitochondria should also have increased their fluorescence intensity, which was not the case. However, the larger midpiece volume of the vervet monkey might be the compensatory factor for their higher fluorescence value. It can furthermore be speculated that the higher fluorescent intensity of the ram midpiece could be due to their larger number of mitochondrial gyres. The ram spermatozoa probably compensate for their low midpiece volume by including more, smaller mitochondria in the midpiece, which could increase the total surface area of the cristae and thus the enzymatic activity. However, no direct measurements of the number of cristae or enzymatic activity in the sperm mitochondria and its relationship to the fluorescent intensity were made in this study.

The general trend among the six species in terms of the number of mitochondrial gyres, the size of the midpiece length, the size of the straight-line midpiece length and the intensity of the flow cytometric analysis suggests that the fluorescence value of the sperm midpiece is not

only a measurement of the mitochondrial activity, but also reflects the size of the midpiece in all the species investigated. A possible application of the flow cytometric analysis could therefore be to investigate the differences in midpiece measurements often encountered between fertile and infertile patients or animals (Gopalkrishnan *et al.*, 1991; Piasecka *et al.*, 2007; Schneider *et al.*, 2009). For example, in humans it has been shown that asthenozoospermic patients not only had spermatozoa with lower mitochondrial enzymatic activities (determined with methods other than flow cytometric analysis) (Gopalkrishnan *et al.*, 1995; Ruiz-Pesini *et al.*, 1998), but also shorter midpieces with fewer mitochondrial gyres (Mundy *et al.*, 1995; Lhuillier *et al.*, 2009). A study using flow cytometry by Piasecka and Kawiak (2003) confirmed this structural and functional relationship in the sperm midpiece of asthenozoospermic patients. They reported lower fluorescent values for the sperm midpiece and spermatozoa with shorter midpieces in asthenozoospermic patients. This study also highlighted the fact that the sperm mitochondria were often fully functional but reduced in number due to midpiece malformations (Piasecka and Kawiak, 2003). Similar studies could be undertaken in other mammalian species to validate the use of such a basic flow cytometric analysis for sperm midpiece abnormalities. Additionally, the use of flow cytometry should be employed on a more regular basis since it was shown that determination of the sperm mitochondrial activity index and the sperm mitochondrial membrane potential provided more reliable measurements of midpiece abnormalities than with standard semen analysis methods (Gopalkrishnan *et al.* 1995; Troiano *et al.*, 1998).

In conclusion, this detailed study of the sperm midpiece and the sperm mitochondria revealed and confirmed the species specificity of these midpiece parameters as well as the variations in these parameters among the species investigated. Although a general trend was reported for the number of mitochondrial gyres, midpiece volume, midpiece length, straight-line midpiece length and fluorescent staining intensity, the reason for the individual species variation in some of these midpiece parameters could only be speculated upon. Since none of these midpiece measurements was identical among all seven species, the variation found in the midpiece parameters might be a compensatory mechanism to include the optimal amount or size of sperm mitochondria to still be functionally efficient. Other possible explanations for these midpiece variations might only be found by investigating the relationship between these different midpiece morphometry measurements and the sperm components evaluated in Chapter 3 (see Chapter 7) and sperm functional parameters, e.g. sperm motility (Chapter 5).

CHAPTER 5: Analysis of sperm motility parameters of selected mammalian species using computer-aided sperm analysis (CASA)

5.1 Introduction

Motility is a common feature of spermatozoa, especially for flagellate spermatozoa, and is an important sperm characteristic for both internal and external fertilizing species (Holt and van Look, 2004). After spermatozoa are produced in the testis, they are still non-motile and only acquire functional competence during sperm maturation in the epididymis due to several morphological and physiological changes. Spermatozoa become motile once they come into contact with seminal plasma or other physiological media (Mortimer, 1997).

The sperm flagellum is the 'motor apparatus' of the spermatozoon and contains the microtubule-based machinery for generation of the flagellar beat, namely the axoneme (Cummins, 2009). The structure of the axoneme is highly conserved in almost all eukaryotic cilia and flagella and the structure of the mammalian sperm flagellum was described in Chapter 2 (see Fig. 2.3). Flagellar bending that occurs in motile spermatozoa is a result of the asymmetric sliding of the dynein arms against the microtubule doublets in the axoneme. The flagellum of mammalian spermatozoa contains three additional structures, including the mitochondrial sheath, the outer dense fibers and the fibrous sheath (Fig. 2.3) (Turner, 2003). Abnormalities in any one or more of these mentioned flagellar structures could result in decreased or absence of sperm motility (Chemes *et al.*, 1998). The molecular mechanisms involved in the generation of sperm motility have only been described in the last two decades with increased reports on testis and sperm specific genes and gene products necessary for sperm motility (Ren *et al.*, 2001; Turner, 2003; Harris *et al.*, 2007; Suarez, 2008).

The ultimate goal of a spermatozoon is to fertilize the ovum, but to accomplish this, it must travel relatively long distances (internal fertilizers) and become primed for fertilization through capacitation and other related processes (Ren *et al.*, 2001). During its transport through the female reproductive tract, most mammalian spermatozoa display two types of physiological motility, namely activated motility and hyperactivated motility (Turner, 2003). Activated motility is seen in freshly ejaculated spermatozoa, where the flagellum generates a symmetrical and low amplitude waveform that results in the spermatozoon swimming in a relatively straight line. Hyperactivated motility, on the other hand, is mostly seen in

spermatozoa recovered from the site of fertilization. Characteristics of hyperactivation include the generation of asymmetrical waveforms and increased amplitude of flagellar bending, which results in vigorous movement patterns previously described as figure-eight, whiplash, star-spin or circling swimming trajectories (Katz and Yanagimachi, 1980; Suarez, 1996). The role of activated motility is currently proposed as necessary in propelling the spermatozoa from the site of semen deposition to the oviduct. The role of hyperactivated motility, however, seems to be multi-factorial, including detachment from the oviductal epithelium, aiding the sperm in reaching the site of fertilization (ampulla) and penetration of the cumulus and zona pellucida of the oocyte (Ho and Suarez, 2001; Suarez and Pacey, 2006).

The importance of sperm motility is highlighted by the fact that the measurement of this parameter forms an essential part of most semen or sperm evaluation criteria (Mocé and Graham, 2008). One of the frequently encountered problems in subfertile or infertile males is the presence of low numbers of motile spermatozoa (asthenozoospermia). Subsequently, a great number of studies have reported a correlation between a decrease in sperm motility (both activated and hyperactivated motility) and a decrease in the fertilization rate, which may call for the use of assisted reproductive techniques to achieve fertilization (see review by Turner, 2003). Higher sperm motility has also been related to increased *in vitro* fertilization rates and pregnancy rates (Zinaman *et al.*, 2000; Sifer *et al.*, 2005). In terms of sperm morphology and morphometry, the percentage normal sperm morphology and the size of various sperm components (e.g. head length and total sperm length) have been positively correlated with the percentage motile spermatozoa and the sperm swimming speed (Malo *et al.*, 2005; Gomendio *et al.*, 2007; Humphries *et al.*, 2008).

The standard method for the evaluation of sperm motility in most laboratories has been and still is the use of light microscopy and the visual estimation of the percentage motile spermatozoa in a semen sample. Sperm motility characteristics could only be evaluated subjectively before the 1980's, but the introduction of computer-aided semen/sperm analysis (CASA) systems has led to more objective and less variable motility assessments (Agarwal *et al.*, 2003; Mocé and Graham, 2008). Other advantages of using CASA include an increase in the accuracy and reproducibility of the sperm concentration and percentage motility measurements (see review by Rijsselaere *et al.*, 2005). Furthermore, CASA allows the determination of various sperm movement characteristics (kinematics) and the detection of subtle changes in sperm motion that cannot be identified by conventional sperm motility

analysis (Agarwal *et al.*, 2003; Rijsselaere *et al.*, 2005). Objective measurements of sperm movement characteristics of individual spermatozoa have also been found to be more predictive of the spermatozoa's functional ability than just measuring the total percentage motile spermatozoa in a semen sample (Mortimer, 1994). In clinical studies, individual sperm kinematic parameters have shown close correlations with IVF, intrauterine insemination (IUI) and pregnancy results (Garrett *et al.*, 2003; Shibahara *et al.*, 2004). Fewer data are available on the comparison of these kinematic parameters among different species and their relationship with sperm structural aspects.

The use of CASA requires the standardization of all capturing techniques and analysis methods in order to allow comparison of the data among research laboratories and to previously published studies. Factors to consider when CASA is used, include temperature dependency of the spermatozoa, effect of preparation depth, duration of the observations, number of trajectories needed for reliable analysis and kinematic thresholds of progressive spermatozoa (Mortimer, 1994; Kraemer *et al.*, 1998). Additional factors that could also have an effect on sperm kinematic measurements have been noted in a few studies, e.g. the effect of time of capturing, image sampling frequency (frame rate) and assessment of different motility parameters (Mortimer *et al.*, 1998; Holt and van Look, 2004).

The main aim of the current chapter was to determine the variation in sperm kinematic parameters of selected mammalian species. These measurements will allow the calculation of correlations with the sperm and midpiece morphometric data reported in the previous chapters. Secondly, this chapter aimed to indicate the importance of using standardized analysis techniques and selecting the relevant motility parameters for analysis.

5.2   Materials and methods

5.2.1 Mammalian species included, collection of samples and selection of motile spermatozoa

All seven mammalian species introduced in Chapter 3 were also investigated in terms of sperm motility characteristics and individual sperm kinematic parameters. The collection of the semen or spermatozoa as well as the preparation of motile sperm populations was described in Chapter 3.

5.2.2 CASA equipment, capturing properties and analysis properties

Sperm motility was measured with the Motility/Concentration module of the Sperm Class Analyzer® (SCA) version 4.0.0.5 or 4.1.0.1 (Microptic S.L., Barcelona, Spain). Capturing of the data involved a Basler A602fc digital camera (Microptic S.L., Barcelona, Spain) that was mounted (C-mount) on either a Nikon Eclipse 50i microscope (IMP, Cape Town, South Africa) or an Olympus CH2 microscope (Wirsam, Cape Town, South Africa), both equipped with phase contrast optics and a heated stage. The use of two different microscopes was only for logistical reasons, the Olympus microscope being compact enough to transport to more remote localities for sperm collection. A comparison was done between the two microscopes and no significant difference was found between them for sperm motility measurements (results not shown).

The capturing properties of the SCA® system were set as follows: number of images = 50; images per second = 50 or 75 (see section 5.2.3); optics = Ph- (negative phase contrast); chamber = Leja 20; automatic analysis. The analysis properties for the various mammalian species are presented in Table 5.1. The particle area setting was determined by visual evaluation of the captured fields and selecting those ranges of particle area size which resulted in only detecting the sperm head for the motility analysis and thus excluding any other cells or debris. The curvilinear velocity (VCL) intervals of the three classes of sperm swimming speed were arbitrarily selected as the default values for the initial motility analysis (see 5.2.5 for changes in motility analysis) and differed from the much lower default values of the SCA® system. The SCA® default values were however used for the progressivity and circularity of sperm tracks. The connectivity setting was determined by visual evaluation of the captured fields and selecting the setting where individual sperm tracks were captured as continuous tracks. The number of average path velocity (VAP) points was determined by visual interpolation of what the average path would look like if it was manually drawn onto the curvilinear path of individual spermatozoa. This method is regarded as the 'gold standard' for derivation of the average path and avoids selecting a too high or too low number of points to be used for the smoothing of the average path (Mortimer, 1997).

5.2.3 Capturing of data – standardized procedure, time of analysis and frame rate

Motility parameters were assessed by pipetting 5 μl of a motile sperm preparation from either a swim-up or a swim-out preparation into a 20 μm deep chamber of a Leja slide. The slide was pre-warmed on the heated stage (37 °C, except for the naked mole-rat setting of 30 °C) of

Table 5.1. SCA® motility analysis properties for the different mammalian species

	HS	PU	RM	CA	OO	MM	HG
Species*	Human	Human	Human	Human	Ram	Rodent	Rodent
Particle area (µm²)	20<PA<80	20<PA<80	20<PA<80	10<PA<90	15<PA<70	20<PA<70	10<PA<70
VCL Slow (µm/s)	20<S<30	50<S<80	50<S<80	50<S<80	50<S<80	50<S<80	15<S<30
VCL Medium (µm/s)	30<M<50	80<M<120	80<M<120	80<M<120	80<M<120	80<M<120	30<M<50
VCL Rapid (µm/s)	R>50	R>120	R>120	R>120	R>120	R>120	R>50
Progressivity (% of STR)	>80	>80	>80	>80	>80	>80	>80
Circular (% of LIN)	<50	<50	<50	<50	<50	<50	<50
Connectivity	12	20	20	12	20-25	40	8
VAP points 50f/s	7	7	7	7	7	11	3
VAP points 75f/s	9	11	9	11	11	15	ND

HS = *Homo sapiens* (human), PU = *Papio ursinus* (chacma baboon), RM = *Macaca mulatta* (rhesus monkey), CA = *Chlorocebus aethiops* (vervet monkey), OO = *Ovis orientalis* (merino ram), MM = *Mus musculus* (house mouse), HG = *Heterocephalus glaber* (naked mole-rat)

* = species name selected from list of options from SCA® system

VCL = curvilinear velocity, STR = straightness, LIN = linearity, VAP = average path velocity, f/s = frames per second, PA = particle area, S = slow, M = medium, R = rapid, ND = not determined

the microscope.

Depending on the sperm concentration, between two and ten fields were captured, until a total number of 200 motile spermatozoa were analyzed (as recommended by Mortimer 1994; WHO, 1999). Since sperm motility is sensitive to changes in temperature, the slide was removed from the slide holder after a field was captured and allowed to re-heat on the microscope stage for ± 20 seconds before it was returned to the centre of the stage. Fields were captured randomly to eliminate any bias towards higher sperm concentration or motility, but fields that included debris or clumps of sperm were avoided to decrease incorrect analysis. All captured sperm tracks were visually verified to delete any incorrectly recorded tracks, e.g. due to colliding spermatozoa.

The effect of time of data capturing on sperm motility was evaluated in order to determine if there was a difference between the selected mammalian species in this study and to recommend standardized procedures for future studies. Sperm motility was therefore evaluated at two different time points, at 5-10 minutes after the swim-up or swim-out preparation was made and 30 minutes after the preparations were made. These sperm preparations were incubated until after the 30 minute evaluation of sperm motility. Since the motility of the naked mole-rat spermatozoa decreased within a few minutes after the swim-out sample was taken, sperm motility was only measured at the 5-10 minute time point for this species.

The effect of frame rate on sperm motility parameters was evaluated by capturing sperm tracks at both 50 frames/second and 75 frames/second for both time intervals. The 50 frames/second setting was used as the standard frame rate throughout the study. It was intended to also capture the sperm tracks at 100 frames/second in order to compare the sperm kinematic parameters captured at the different frame rates. The 4.0.0.5 and 4.1.0.1 versions of the SCA® system, however, only allowed a maximum frame rate setting of 75 frames/second, which was subsequently selected as the higher frame rate setting to be compared with the standard frame rate (50 frames/second). After capturing sperm tracks at one of these frame rates, the frame rate setting of the SCA® system was quickly changed and a subsequent set of tracks was captured at the higher or lower frame rate. Since the motility and swimming speed of the naked mole-rat spermatozoa were much lower than the other species, this species' motility was only measured at 50 frames/second.

5.2.4 Motility parameters assessed

The SCA® system automatically detects the sperm head (visualized as a white dot with phase contrast optics) and makes rapid and accurate measurements of various sperm motility parameters. A total of eight parameters were assessed, including the curvilinear velocity (VCL), straight line velocity (VSL), average path velocity (VAP), linearity (LIN), straightness (STR), wobble (WOB), amplitude of lateral head displacement (ALH) and beat cross frequency (BCF). Table 5.2 summarizes the various sperm motility parameters and their derivatives and Figure 5.1 is a diagrammatic presentation of these parameters. The ALH parameter was measured as indicated in Figure 5.1 and not as the full width (wave) of the VCL track or doubling of the riser values (risers method) as described by Mortimer (1994; 1997).

Table 5.2. Different sperm kinematic parameters measured by the SCA® system

Parameter	Description	Measurement
VCL (µm/s)	Curvilinear velocity	Time-averaged velocity of a sperm head along its actual curvilinear path
VSL (µm/s)	Straight-line velocity	Time-averaged velocity of a sperm head along the straight line between its first detected position and its last
VAP (µm/s)	Average path velocity	Time-averaged velocity of a sperm head along its average path
LIN (%)	Linearity	Linearity of the curvilinear path = VSL/VCL
STR (%)	Straightness	Linearity of the average path = VSL/VAP
WOB (%)	Wobble	Measure of oscillation of the actual path about the average path = VAP/VCL
ALH (µm)	Amplitude of lateral head displacement	Magnitude of lateral displacement of a sperm head about its average path
BCF (Hz)	Beat cross frequency	Average rate at which the curvilinear path crosses the average path

5.2.5 Selection of the correct SCA® properties for sperm motility analysis

The SCA® system provides various options of sperm motility measurements to be used for the evaluation of a semen/sperm sample, e.g. individual kinematic parameters, the percentage total motility, progressive motility, rapid, medium and slow swimming spermatozoa and the Type a-d classification recommended by the WHO (WHO, 1999). All these measurements are presented as an average of all the captured fields in the SCA® system's motility reports.

110
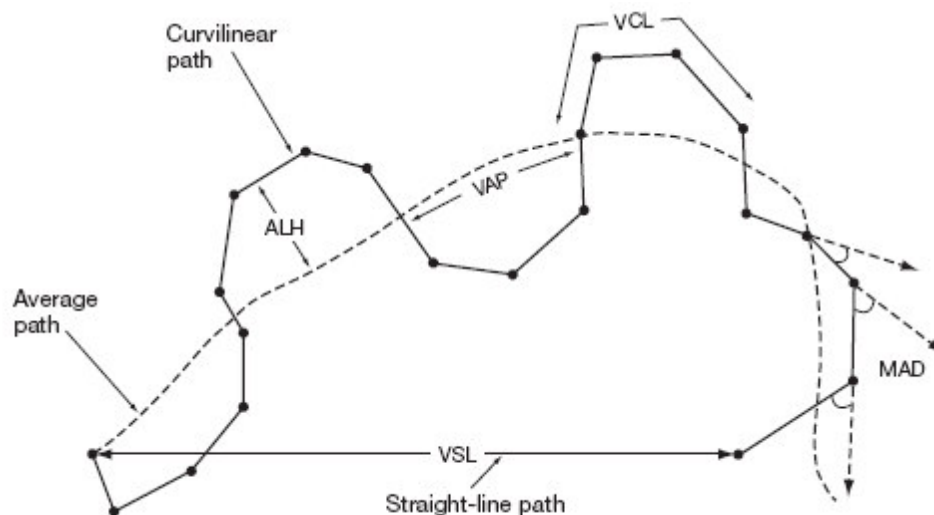
Figure 5.1. Schematic presentation of various sperm motility parameters as determined by the SCA® system. A description of the motility parameters is given in Table 5.2. ALH = amplitude of lateral head displacement, VAP = average path velocity, VCL = curvilinear velocity, VSL = straight-line velocity, MAD = mean angular displacement (this parameter was not determined in the current study). (From WHO, 2010)

One of these options, namely the measurement of rapid, medium and slow swimming spermatozoa, was investigated in order to determine a) the difference between the kinematic parameters of these three classes and that of the total motile sperm population and b) the default VCL interval values that should be selected for each species for future studies, especially for studies involving the evaluation of male fertility or the treatment of spermatozoa. It is also expected that the evaluation of the percentage rapid, medium and slow swimming spermatozoa and their kinematic parameters will be more efficient in showing an effect on sperm motility than only taking the percentage total motility into consideration.

The percentage total motile spermatozoa and the rapid, medium and slow swimming spermatozoa were first evaluated by selecting the same default values for the VCL intervals for most species (see Table 5.1 for the values used). These default values were initially selected in our laboratory as preliminary cut-off values and used as a standard method for sperm motility analysis. The selection of these default values were mainly for two reasons: a) the default values of the SCA® system were set for the evaluation of human spermatozoa at 25 frames/second and thus not entirely applicable to other species and b) to be able to compare the motility characteristics of various species' spermatozoa. Only human spermatozoa were analyzed with lower default values for the VCL intervals of the three swimming speed classes, since the swimming speed for this species is much lower than the other species (the naked mole-rat was not included in this evaluation).

111

Hereafter, the VCL intervals for these three swimming speed classes were manually adapted to finally include more or less 80% rapid swimming spermatozoa, 15% medium swimming spermatozoa and 5% slow swimming spermatozoa. These percentages were calculated from the percentage total motility, e.g. if a sample had 90% total motility, the VCL intervals were adapted to eventually have 72% rapid swimming spermatozoa, 13.5% medium swimming spermatozoa and 4.5% slow swimming spermatozoa. The cut-off values of the percentage spermatozoa in each swimming speed class (80%, 15% and 5%) for each species were arbitrarily selected as being representative of a good quality sperm sample. The employment of these cut-off values will result in the generation of baseline data on various sperm motility parameters for future studies.

5.2.6   Statistical analysis

The statistical software and statistical tests utilized were identical to those described in Chapter 3.

5.3   Results

Effect of time of data capturing on sperm kinematic parameters

The percentage total motility and the sperm kinematic parameters of six of the mammalian species are presented in Table 5.3. For each species, a statistical comparison was done between the motility parameters at 5-10 minutes and at 30 minutes after the sperm sample was prepared. No differences (P > 0.05) were found in the total percentage motile spermatozoa between the two capturing times. Although the general trend among all six species and for all the parameters assessed was a decrease in the values at the 30 minute measurement, the only significant decreases were found for LIN, STR and WOB in human spermatozoa and for the VSL and VAP in mouse spermatozoa. Only the data captured at 50 frames/second is presented in Table 5.3 – similar differences were found at 75 frames/second (see Appendix 3).

Effect of capturing frame rate on sperm kinematic parameters

The percentage total motility and the sperm kinematic parameters of six of the mammalian species captured at two different frame rates are presented in Table 5.4. All the data presented in Table 5.4 were captured at 5-10 minutes after the sperm preparations were made. Similar differences were found when the sperm tracks were captured at the 30 minute time point (see Appendix 4). For each species, a statistical comparison was done between these motility parameters at 50 frames/second and 75 frames/second. A significant increase (P < 0.05) was

Table 5.3. Sperm motility and kinematic parameter measurements (mean ± SD) captured at 50 frames/second for six mammalian species (n = 10 individuals per species) to indicate the effect of the time of capture on these parameters

	Homo sapiens		*Papio ursinus*		*Macaca mulatta*	
	5-10 min	**30 min**	**5-10 min**	**30 min**	**5-10 min**	**30 min**
Motility (%)	94.5 ± 3.2	93.7 ± 2.5	93.9 ± 2.9	91.9 ± 5.1	94.0 ± 5.5	91.4 ± 5.4
VCL (µm/s)	118.8 ± 17.3	115.4 ± 14.2	367.7 ± 45.5	345.7 ± 36.7	292.3 ± 19.2	289.9 ± 30.4
VSL (µm/s)	85.8 ± 13.7	75.4 ± 9.1	337.8 ± 40.2	313.3 ± 36.6	217.6 ± 34.3	236.6 ± 44.1
VAP (µm/s)	92.8 ± 13.7	83.9 ± 8.9	357.2 ± 44.2	333.3 ±38.3	251.6 ± 27.9	261.3 ± 37.8
LIN (%)	72.3 ± 5.6[a]	65.6 ± 6.6[b]	92.0 ± 3.6	90.6 ± 4.3	74.2 ± 9.3	81.1 ± 9.2
STR (%)	92.2 ± 2.6[a]	89.8 ± 2.5[b]	94.7 ± 3.0	94.0 ± 3.6	86.1 ± 5.4	90.0 ± 5.1
WOB (%)	78.3 ± 4.3[a]	73.0 ± 5.5[b]	97.2 ± 1.2	96.3 ± 1.6	85.9 ± 5.8	89.9 ± 5.9
ALH (µm)	2.4 ± 0.2	2.6 ± 0.3	3.4 ± 0.4	3.2 ± 0.3	4.0 ± 0.4	3.6 ± 0.4
BCF (Hz)	18.7 ± 1.7	18.0 ± 2.0	15.4 ± 1.4	15.1 ± 1.1	17.3 ± 1.3	17.5 ± 1.8

	Chlorocebus aethiops		*Ovis orientalis*		*Mus musculus*	
	5-10 min	**30 min**	**5-10 min**	**30 min**	**5-10 min**	**30 min**
Motility (%)	94.7 ± 4.7	92.1 ± 2.7	84.6 ± 5.6	82.2 ± 6.6	89.7 ± 6.2	87.4 ± 6.6
VCL (µm/s)	328.8 ± 18.6	322.5 ± 20.6	246.6 ± 38.4	226.9 ± 20.1	293.3 ± 30.3	256.8 ± 26.3
VSL (µm/s)	293.0 ± 24.4	287.4 ± 26.5	182.3 ± 38.6	159.9 ± 31.0	119.7 ± 12.0[a]	91.0 ± 16.5[b]
VAP (µm/s)	315.4 ± 20.6	309.0 ± 24.1	208.3 ± 39.1	187.6 ± 31.6	147.4 ± 13.4[a]	115.9 ± 15.9[b]
LIN (%)	89.0 ± 4.4	89.0 ± 3.4	74.4 ± 12.0	70.5 ± 12.5	41.3 ± 6.2	35.3 ± 3.6
STR (%)	92.8 ± 3.0	92.9 ± 1.8	87.2 ± 5.1	84.9 ± 4.5	81.3 ± 4.1	78.2 ± 4.1
WOB (%)	95.9 ± 1.8	95.7 ± 1.9	84.8 ± 10.3	82.7 ± 12.2	50.6 ± 5.6	45.0 ± 2.5
ALH (µm)	3.0 ± 0.2	3.2 ± 0.2	3.6 ± 0.8	3.6 ± 0.6	9.1 ± 1.2	8.7 ± 0.9
BCF (Hz)	13.9 ± 1.2	13.4 ± 1.4	17.4 ± 2.9	17.4 ± 3.6	10.5 ± 1.4	8.4 ± 1.6

VCL = curvilinear velocity, VSL = straight-line velocity, VAP = average path velocity, LIN = linearity, STR = straightness, WOB = wobble, ALH = amplitude of lateral head displacement, BCF = beat cross frequency

a, b = values labelled with different superscript letters in the same row for each individual species were significantly different (P < 0.05)

Table 5.4. Sperm motility and kinematic parameter measurements (mean ± SD) captured at 5-10 minutes after the sperm preparation was made for six mammalian species (n = 10 individuals per species) to indicate the effect of the capturing frame rate on these parameters

	Homo sapiens		*Papio ursinus*		*Macaca mulatta*	
	50 f/s	**75 f/s**	**50 f/s**	**75 f/s**	**50 f/s**	**75 f/s**
Motility (%)	94.5 ± 3.2	94.2 ± 3.0	93.9 ± 2.9[a]	96.8 ± 3.8[b]	94.0 ± 5.5	95.5 ± 4.6
VCL (μm/s)	118.8 ± 17.3	134.1 ± 23.9	367.7 ± 45.5	369.4 ± 34.9	292.3 ± 19.2[a]	325.5 ± 19.0[b]
VSL (μm/s)	85.8 ± 13.7	85.2 ± 15.2	337.8 ± 40.2	343.7 ± 35.4	217.6 ± 34.3	239.3 ± 31.7
VAP (μm/s)	92.8 ± 13.7	96.7 ± 15.3	357.2 ± 44.2	355.7 ± 36.1	251.6 ± 27.9	262.9 ± 25.6
LIN (%)	72.3 ± 5.6[a]	63.6 ± 4.6[b]	92.0 ± 3.6	93.0 ± 2.0	74.2 ± 9.3	73.5 ± 8.7
STR (%)	92.2 ± 2.6[a]	87.9 ± 2.4[b]	94.7 ± 3.0	96.6 ± 0.9	86.1 ± 5.4	90.7 ± 4.1
WOB (%)	78.3 ± 4.3[a]	72.4 ± 4.0[b]	97.2 ± 1.2	96.3 ± 1.3	85.9 ± 5.8	80.7 ± 6.3
ALH (μm)	2.4 ± 0.2	2.2 ± 0.3	3.4 ± 0.4[a]	2.4 ± 0.5[b]	4.0 ± 0.4[a]	3.2 ± 0.5[b]
BCF (Hz)	18.7 ± 1.7[a]	24.7 ± 2.9[b]	15.4 ± 1.4[a]	21.9 ± 2.1[b]	17.3 ± 1.3[a]	31.5 ± 4.8[b]

	Chlorocebus aethiops		*Ovis orientalis*		*Mus musculus*	
	50 f/s	**75 f/s**	**50 f/s**	**75 f/s**	**50 f/s**	**75 f/s**
Motility (%)	94.7 ± 4.7	95.3 ± 5.4	84.6 ± 5.6	87.9 ± 4.7	89.7 ± 6.2	91.3 ± 6.2
VCL (μm/s)	328.8 ± 18.6	333.2 ± 17.8	246.6 ± 38.4	258.3 ± 40.1	293.3 ± 30.3[a]	342.0 ± 40.7[b]
VSL (μm/s)	293.0 ± 24.4	303.4 ± 20.0	182.3 ± 38.6	185.1 ± 46.6	119.7 ± 12.0	125.2 ± 16.5
VAP (μm/s)	315.4 ± 20.6	317.7 ± 18.6	208.3 ± 39.1	207.4 ± 44.8	147.4 ± 13.4	157.3 ± 15.9
LIN (%)	89.0 ± 4.4	91.0 ± 2.5	74.4 ± 12.0	72.2 ± 15.7	41.3 ± 6.2	36.9 ± 4.8
STR (%)	92.8 ± 3.0[a]	95.5 ± 1.2[b]	87.2 ± 5.1	88.4 ± 5.5	81.3 ± 4.1	79.5 ± 4.9
WOB (%)	95.9 ± 1.8	95.3 ± 1.6	84.8 ± 10.3	80.9 ± 14.8	50.6 ± 5.6	46.2 ± 3.5
ALH (μm)	3.0 ± 0.2[a]	2.1 ± 0.3[b]	3.6 ± 0.8	3.0 ± 1.0	9.1 ± 1.2	8.2 ± 1.0
BCF (Hz)	13.9 ± 1.2[a]	18.9 ± 1.0[b]	17.4 ± 2.9[a]	26.1 ± 4.2[b]	10.5 ± 1.4[a]	11.9 ± 2.1[b]

VCL = curvilinear velocity, VSL = straight-line velocity, VAP = average path velocity, LIN = linearity, STR = straightness, WOB = wobble, ALH = amplitude of lateral head displacement, BCF = beat cross frequency, f/s = frames per second

a, b = values labelled with different superscript letters in the same row for each individual species were significantly different (P < 0.05)

found in the total percentage of motile spermatozoa of the baboon samples, which may have been due to a sampling effect. For all five other species, a similar percentage motile spermatozoa was evaluated at each frame rate.

The only significant increases found in the VCL values between the two frame rates were for rhesus monkey and mouse spermatozoa ($P < 0.05$). The LIN, STR and WOB values for human spermatozoa significantly decreased at the higher frame rate ($P < 0.05$) despite the fact that none of the velocity parameters had significantly increased measurements. The only other significant different value for the velocity derivatives was an increase in the STR for the vervet monkey. In general, the ALH values decreased at the higher frame rate, but were only significant in three of the six species. The BCF values had increased values at the higher frame rate for all six species.

Visual assessment of the difference in the sperm motility tracks often revealed more detail at 75 frames/second compared to 50 frames/second, especially in those species where the VCL measurements significantly increased at 75 frames/second. An example of this difference in the sperm motility tracks captured at the two frame rates are presented in Figure 5.2 for rhesus monkey spermatozoa. It is evident from the differences in the tracks in Figure 5.2A compared to Figure 5.2B that the lower curvilinear velocity (50 frames/second) (Table 5.4) resulted in a shorter (i.e. slower VCL) and smoother actual path.

Selection of the correct properties for sperm motility analysis
The average, default and adjusted sperm motility and kinematic parameters of six mammalian species, captured at 50 frames/second and 5-10 minutes after the sperm preparation was made, are presented in Table 5.5. The total percentage motile spermatozoa (Total AVE) is the sum of the percentage motile spermatozoa in the rapid, medium and slow swimming speed classes (Rapid DEF + Medium DEF + Slow DEF or Rapid ADJ + Medium ADJ + Slow ADJ). The percentage motile spermatozoa in the 'default' swimming speed classes (Rapid DEF, Medium DEF, Slow DEF) was a result of the selected default values for VCL intervals (see Table 5.1) according to the standard method of sperm motility comparisons in our laboratory. Among the six species evaluated, only the baboon and ram had a significantly lower percentage motile spermatozoa in Rapid DEF compared to Total AVE ($P < 0.05$), but Rapid DEF still included more than 90% of the total motile spermatozoa in these two species.

115
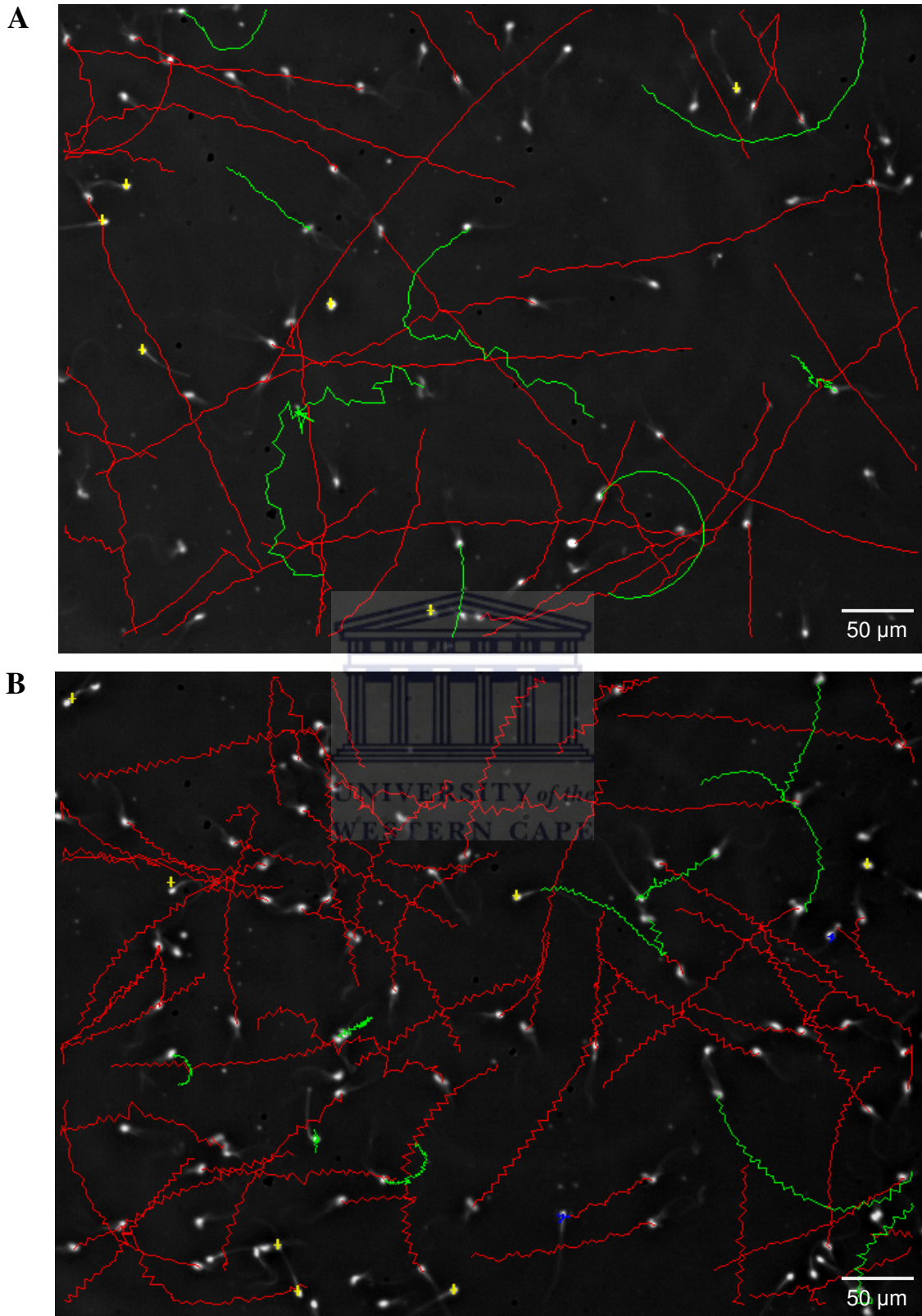
Figure 5.2. Sperm motility tracks of the same sample of rhesus monkey spermatozoa to illustrate the difference in the kinematic parameters captured at different frame rates by the SCA® system. **A**) 50 frames/second, **B**) 75 frames/second. The actual kinematic parameters are presented in Table 5.4. Red tracks = rapid progressive swimming spermatozoa, green tracks = rapid swimming spermatozoa, blue tracks = medium progressive swimming spermatozoa, yellow crosses = static spermatozoa.

Table 5.5. Sperm motility and kinematic parameter measurements (mean ± SD) captured at 50 frames/second for six mammalian species (n = 10 individuals per species) to indicate the effect of selecting different VCL intervals for the three sperm swimming speed classes

Homo sapiens	Total AVE	Rapid DEF	Medium DEF	Slow DEF	Rapid ADJ	Medium ADJ	Slow ADJ
Motility (%)	94.5 ± 3.2^a	90.4 ± 4.5^a	2.8 ± 1.7	1.4 ± 0.8	75.7 ± 2.7	14.2 ± 0.7	4.6 ± 0.2
VCL (µm/s)	118.8 ± 17.3^a	122.4 ± 16.8^a	25.5 ± 14.0	9.4 ± 5.7	131.4 ± 18.2^a	76.4 ± 18.6^b	33.4 ± 9.9^c
VSL (µm/s)	85.8 ± 13.7^a	88.9 ± 13.6^a	11.0 ± 7.8	2.7 ± 2.2	96.6 ± 15.4^a	49.6 ± 13.1^b	15.7 ± 5.3^c
VAP (µm/s)	92.9 ± 13.7^a	96.0 ± 13.4^a	15.9 ± 9.5	5.4 ± 3.7	103.6 ± 15.1^a	56.9 ± 13.5^b	21.9 ± 6.4^c
LIN (%)	72.3 ± 5.6^a	72.7 ± 5.8^a	37.6 ± 18.3	26.4 ± 14.2	73.6 ± 6.2^a	64.7 ± 4.3^a	47.1 ± 7.7^c
STR (%)	92.2 ± 2.6^a	92.5 ± 2.6^a	59.4 ± 23.8	46.3 ± 22.5	93.1 ± 2.7^a	87.0 ± 3.0^b	71.2 ± 5.5^c
WOB (%)	78.3 ± 4.3^a	78.5 ± 4.4^a	55.8 ± 22.1	50.5 ± 19.4	78.9 ± 4.7^a	74.6 ± 3.1^b	65.8 ± 6.9^c
ALH (µm)	2.4 ± 0.2^a	2.4 ± 0.2^a	0.4 ± 0.4		2.5 ± 0.2^a	1.9 ± 0.3^b	
BCF (Hz)	18.7 ± 1.7^a	18.8 ± 1.7^a	1.5 ± 1.8		19.5 ± 1.8^a	13.7 ± 3.2^b	
VCL interval (µm/s)		50.0	30.0	20.0	89.2 ± 19.2	59.8 ± 16.3	22.8 ± 3.0

Papio ursinus	Total AVE	Rapid DEF	Medium DEF	Slow DEF	Rapid ADJ	Medium ADJ	Slow ADJ
Motility (%)	93.9 ± 2.9^a	91.6 ± 2.5^b	1.5 ± 0.9	0.9 ± 0.7	75.3 ± 2.1	14.1 ± 1.0	4.5 ± 0.3
VCL (µm/s)	367.7 ± 45.5^a	374.4 ± 45.9^a	34.8 ± 23.3	16.2 ± 15.7	403.2 ± 52.0^a	241.6 ± 52.0^b	86.8 ± 34.9^c
VSL (µm/s)	337.8 ± 40.2^a	344.4 ± 39.8^a	24.5 ± 16.6	9.0 ± 7.7	374.7 ± 42.7^a	200.0 ± 55.2^b	69.9 ± 34.6^c
VAP (µm/s)	357.2 ± 44.2^a	363.9 ± 44.3^a	29.9 ± 20.7	11.6 ± 10.2	393.5 ± 49.6^a	227.2 ± 51.7^b	77.9 ± 34.2^c
LIN (%)	92.0 ± 3.6^a	92.1 ± 3.6^a	71.4 ± 11.7	52.7 ± 34.1	93.1 ± 3.6^a	82.1 ± 7.7^b	78.5 ± 11.6^{bc}
STR (%)	94.7 ± 3.0^a	94.7 ± 2.9^a	83.2 ± 11.7	65.6 ± 38.4	95.4 ± 2.8^a	87.4 ± 7.1^b	88.0 ± 9.4^b
WOB (%)	97.2 ± 1.2^a	97.2 ± 1.2^a	85.6 ± 5.7	62.4 ± 35.5	97.6 ± 1.2^a	93.9 ± 2.6^b	88.9 ± 6.4^c
ALH (µm)	3.4 ± 0.4^a	3.4 ± 0.4^a	0.5 ± 0.5		3.5 ± 0.5^a	2.7 ± 0.5^b	
BCF (Hz)	15.4 ± 1.4^a	15.5 ± 1.4^a	3.3 ± 3.3		15.5 ± 1.5^a	14.3 ± 2.5^a	
VCL interval (µm/s)		120.0	80.0	50.0	296.3 ± 50.0	185.6 ± 46.5	64.5 ± 11.7

VCL = curvilinear velocity, VSL = straight-line velocity, VAP = average path velocity, LIN = linearity, STR = straightness, WOB = wobble, ALH = amplitude of lateral head displacement, BCF = beat cross frequency, AVE = average, DEF = default, ADJ = adjusted

a, b, c = values labelled with different superscript letters as well as different colours in the same row for each individual species were significantly different ($P < 0.05$)

Table 5.5. Continued

Macaca mulatta	Total AVE	Rapid DEF	Medium DEF	Slow DEF	Rapid ADJ	Medium ADJ	Slow ADJ
Motility (%)	94.0 ± 5.5[a]	92.7 ± 6.2[a]	1.0 ± 1.0	0.3 ± 0.3	75.5 ± 4.4	13.9 ± 1.0	4.6 ± 0.3
VCL (µm/s)	292.3 ± 19.2[a]	295.0 ± 18.3[a]	56.6 ± 43.1	20.5 ± 26.3	315.3 ± 20.4[b]	215.6 ± 26.3[c]	133.7 ± 28.4[d]
VSL (µm/s)	217.6 ± 34.3[a]	219.9 ± 34.2[a]	32.5 ± 27.1	8.6 ± 9.7	233.5 ± 37.6[a]	170.6 ± 32.9[b]	92.4 ± 32.3[c]
VAP (µm/s)	251.6 ± 27.9[a]	254.1 ± 27.5[a]	42.7 ± 33.1	13.1 ± 14.9	270.2 ± 30.1[a]	191.9 ± 30.8[b]	111.4 ± 30.4[c]
LIN (%)	74.2 ± 9.3[a]	74.3 ± 9.3[a]	44.0 ± 28.9	29.9 ± 29.4	73.9 ± 10.0[a]	78.4 ± 7.7[a]	68.3 ± 15.4[a]
STR (%)	86.1 ± 5.4[a]	86.2 ± 5.5[a]	57.6 ± 33.1	41.9 ± 38.9	86.0 ± 5.7[a]	88.4 ± 4.8[a]	82.1 ± 12.3[a]
WOB (%)	85.9 ± 5.8[a]	86.0 ± 5.7[a]	59.7 ± 34.1	42.0 ± 37.5	85.6 ± 6.3[a]	88.6 ± 4.8[a]	82.6 ± 10.0[a]
ALH (µm)	4.0 ± 0.4[a]	4.0 ± 0.5[a]	0.8 ± 0.9		4.2 ± 0.6[a]	2.9 ± 0.2[b]	
BCF (Hz)	17.3 ± 1.3[a]	17.4 ± 1.3[a]	3.8 ± 4.4		17.7 ± 1.5[a]	17.0 ± 1.6[a]	
VCL interval (µm/s)		120.0	80.0	50.0	239.9 ± 28.4	169.8 ± 26.0	81.0 ± 25.5

Chlorocebus aethiops	Total AVE	Rapid DEF	Medium DEF	Slow DEF	Rapid ADJ	Medium ADJ	Slow ADJ
Motility (%)	94.7 ± 4.7[a]	91.2 ± 6.4[a]	2.0 ± 1.6	1.5 ± 1.3	75.8 ± 3.7	14.3 ± 0.9	4.6 ± 0.3
VCL (µm/s)	328.8 ± 18.6[a]	337.9 ± 13.9[a]	55.6 ± 31.6	36.2 ± 25.9	362.1 ± 17.0[b]	219.8 ± 48.8[c]	105.2 ± 45.6[d]
VSL (µm/s)	293.0 ± 24.4[a]	301.8 ± 19.2[a]	32.7 ± 19.6	15.1 ± 10.0	327.9 ± 23.9[b]	176.6 ± 51.7[c]	69.2 ± 45.2[d]
VAP (µm/s)	315.4 ± 20.6[a]	324.7 ± 15.3[a]	43.6 ± 23.8	23.2 ± 16.4	350.0 ± 19.3[b]	202.2 ± 49.7[c]	85.9 ± 46.6[d]
LIN (%)	89.0 ± 4.4[a]	89.3 ± 4.3[a]	54.1 ± 27.9	34.8 ± 20.1	90.5 ± 4.2[a]	79.3 ± 9.9[b]	61.7 ± 17.8[c]
STR (%)	92.8 ± 3.0[a]	93.0 ± 3.0[a]	65.9 ± 29.5	54.2 ± 30.0	93.6 ± 2.9[a]	86.3 ± 7.6[b]	77.0 ± 14.0[b]
WOB (%)	95.9 ± 1.8[a]	96.1 ± 1.7[a]	71.9 ± 27.2	51.3 ± 28.3	96.6 ± 1.7[a]	91.6 ± 4.1[b]	78.6 ± 10.8[c]
ALH (µm)	3.0 ± 0.2[a]	3.0 ± 0.2[a]	0.8 ± 0.7		3.1 ± 0.2[a]	2.7 ± 0.5[b]	
BCF (Hz)	13.9 ± 1.2[a]	13.9 ± 1.2[a]	4.2 ± 4.4		14.1 ± 1.1[a]	13.3 ± 3.1[a]	
VCL interval (µm/s)		120.0	80.0	50.0	279.7 ± 35.2	163.8 ± 48.0	64.0 ± 24.1

VCL = curvilinear velocity, VSL = straight-line velocity, VAP = average path velocity, LIN = linearity, STR = straightness, WOB = wobble, ALH = amplitude of lateral head displacement, BCF = beat cross frequency, AVE = average, DEF = default, ADJ = adjusted
a, b, c, d = values labelled with different superscript letters as well as different colours in the same row for each individual species were significantly different ($P < 0.05$)

Table 5.5. Continued

Ovis orientalis	Total AVE	Rapid DEF	Medium DEF	Slow DEF	Rapid ADJ	Medium ADJ	Slow ADJ
Motility (%)	84.6 ± 5.6[a]	75.1 ± 7.7[b]	7.0 ± 6.2	2.6 ± 1.3	67.9 ± 4.6	12.5 ± 1.0	4.2 ± 0.6
VCL (µm/s)	246.6 ± 38.4[a]	262.6 ± 34.4[a]	79.0 ± 27.5	44.8 ± 16.3	231.3 ± 48.4[a]	134.0 ± 40.5[b]	66.9 ± 19.3[c]
VSL (µm/s)	182.3 ± 38.6[a]	195.2 ± 38.8[a]	54.8 ± 26.8	20.0 ± 9.2	188.9 ± 28.4[a]	93.7 ± 25.3[b]	35.9 ± 16.7[c]
VAP (µm/s)	208.3 ± 39.1[a]	222.6 ± 38.5[a]	64.1 ± 28.3	29.6 ± 10.0	211.9 ± 34.8[a]	109.9 ± 30.1[b]	47.5 ± 17.0[c]
LIN (%)	74.4 ± 12.0[a]	74.6 ± 12.1[a]	66.2 ± 20.8	46.0 ± 16.2	82.5 ± 5.1[a]	71.6 ± 11.3[b]	52.2 ± 15.3[c]
STR (%)	87.2 ± 5.1[a]	87.3 ± 5.1[a]	81.4 ± 13.7	66.9 ± 14.1	89.3 ± 1.3[a]	85.4 ± 2.7[b]	73.1 ± 10.7[c]
WOB (%)	84.8 ± 10.3[a]	85.0 ± 10.3[a]	78.7 ± 18.8	67.5 ± 12.3	92.4 ± 5.1[a]	83.6 ± 11.8[a]	70.4 ± 12.0[b]
ALH (µm)	3.6 ± 0.8[a]	3.7 ± 0.8[a]	1.4 ± 0.6		3.8 ± 0.9[a]	2.4 ± 0.8[b]	
BCF (Hz)	17.4 ± 2.9[a]	17.8 ± 2.9[a]	7.5 ± 4.7		18.1 ± 3.2[a]	20.2 ± 3.5[a]	
VCL interval (µm/s)		120.0	80.0	50.0	174.8 ± 42.8	104.7 ± 24.6	54.0 ± 5.2

Mus musculus	Total AVE	Rapid DEF	Medium DEF	Slow DEF	Rapid ADJ	Medium ADJ	Slow ADJ
Motility (%)	89.7 ± 6.2[a]	86.3 ± 7.0[a]	2.2 ± 1.5	1.2 ± 0.8	71.9 ± 5.1	13.6 ± 1.2	4.2 ± 0.4
VCL (µm/s)	293.3 ± 30.3[a]	301.4 ± 30.2[a]	39.2 ± 23.0	20.0 ± 15.9	320.7 ± 32.4[a]	193.4 ± 41.1[b]	80.1 ± 41.6[c]
VSL (µm/s)	119.7 ± 12.0[a]	123.5 ± 13.3[a]	12.4 ± 10.0	6.7 ± 5.6	128.8 ± 14.0[a]	90.2 ± 19.4[b]	28.6 ± 17.7[c]
VAP (µm/s)	147.4 ± 13.4[a]	151.6 ± 14.5[a]	20.6 ± 16.7	10.0 ± 8.0	158.1 ± 15.5[a]	113.1 ± 21.6[b]	41.7 ± 21.8[c]
LIN (%)	41.3 ± 6.2[a]	41.4 ± 6.3[a]	26.1 ± 15.9	26.8 ± 17.5	40.5 ± 6.0[a]	47.5 ± 10.5[a]	34.7 ± 12.1[b]
STR (%)	81.3 ± 4.1[a]	81.5 ± 4.2[a]	51.2 ± 24.9	52.1 ± 29.4	81.5 ± 4.1[a]	79.7 ± 8.5[a]	66.7 ± 12.5[b]
WOB (%)	50.6 ± 5.6[a]	50.6 ± 5.6[a]	44.0 ± 21.3	40.2 ± 23.5	49.6 ± 5.4[a]	59.4 ± 10.1[b]	51.5 ± 11.8[ab]
ALH (µm)	9.1 ± 1.2[a]	9.2 ± 1.3[a]	0.7 ± 0.7		9.8 ± 1.3[a]	5.4 ± 1.3[b]	
BCF (Hz)	10.5 ± 1.4[a]	10.5 ± 1.4[a]	2.2 ± 2.1		10.3 ± 1.4[a]	10.9 ± 2.1[a]	
VCL interval (µm/s)		120.0	80.0	50.0	241.8 ± 33.4	146.0 ± 39.5	70.0 ± 27.8

VCL = curvilinear velocity, VSL = straight-line velocity, VAP = average path velocity, LIN = linearity, STR = straightness, WOB = wobble, ALH = amplitude of lateral head displacement, BCF = beat cross frequency, AVE = average, DEF = default, ADJ = adjusted
a, b, c = values labelled with different superscript letters as well as different colours in the same row for each individual species were significantly different ($P < 0.05$)

The change in the percentage motile spermatozoa in the 'adjusted' swimming speed classes (Rapid ADJ, Medium ADJ, Slow ADJ) was due to adapting the VCL intervals to include 80% rapid swimming spermatozoa, 15% medium swimming spermatozoa and 5% slow swimming spermatozoa. A clear difference was found between the percentage motile sperm of the three default and adjusted swimming speed classes. As can be seen from the VCL intervals for the adjusted swimming speed classes, these intervals were unique for each species (no statistical comparison was done). An example of how the adaptation in the VCL intervals influenced the percentage motile spermatozoa across the three classes is presented in Figure 5.3 for vervet monkey spermatozoa.

No significant differences were found among the sperm kinematic parameters of the total motile, default rapid and adjusted rapid swimming speed spermatozoa for most of the species. The only two exceptions were the rhesus monkey and the vervet monkey where the swimming speed parameters were significantly higher in the adjusted rapid swimming spermatozoa compared to the other two motility groups. The small percentage spermatozoa included in the default medium and slow swimming speed classes of all six species seemed to be an 'artefact' when the extremely slow swimming speeds of spermatozoa in these two classes were considered. If only the adjusted swimming speed classes were considered, the sperm kinematic parameters were significantly different among the three classes for most parameters (P < 0.05). Examples of the sperm motility tracks and kinematic parameters of human spermatozoa grouped into the three adjusted swimming speed classes by the adapted VCL intervals are presented in Figure 5.4. Please note the difference in scale of the three diagrams – if the same scale was used in all three diagrams, it was not possible to see the detail of the motility tracks in the medium and slow swimming spermatozoa.

Similar adaptations were made to the VCL intervals of the sperm motility data of all six species captured at 75 frames/second and 5-10 minutes after the preparation was made, as well as at 50 and 75 frames/second and 30 minutes after the preparation was made (data not shown). A summary of the VCL intervals for the default and adjusted sperm swimming speed classes at the two different frame rates and time intervals are presented in Table 5.6.

Variation and species specificity of sperm motility parameters
The average sperm kinematic parameter measurements of different mammalian species, captured at 50 frames/second or 75 frames/second and at 5-10 minutes after the sperm
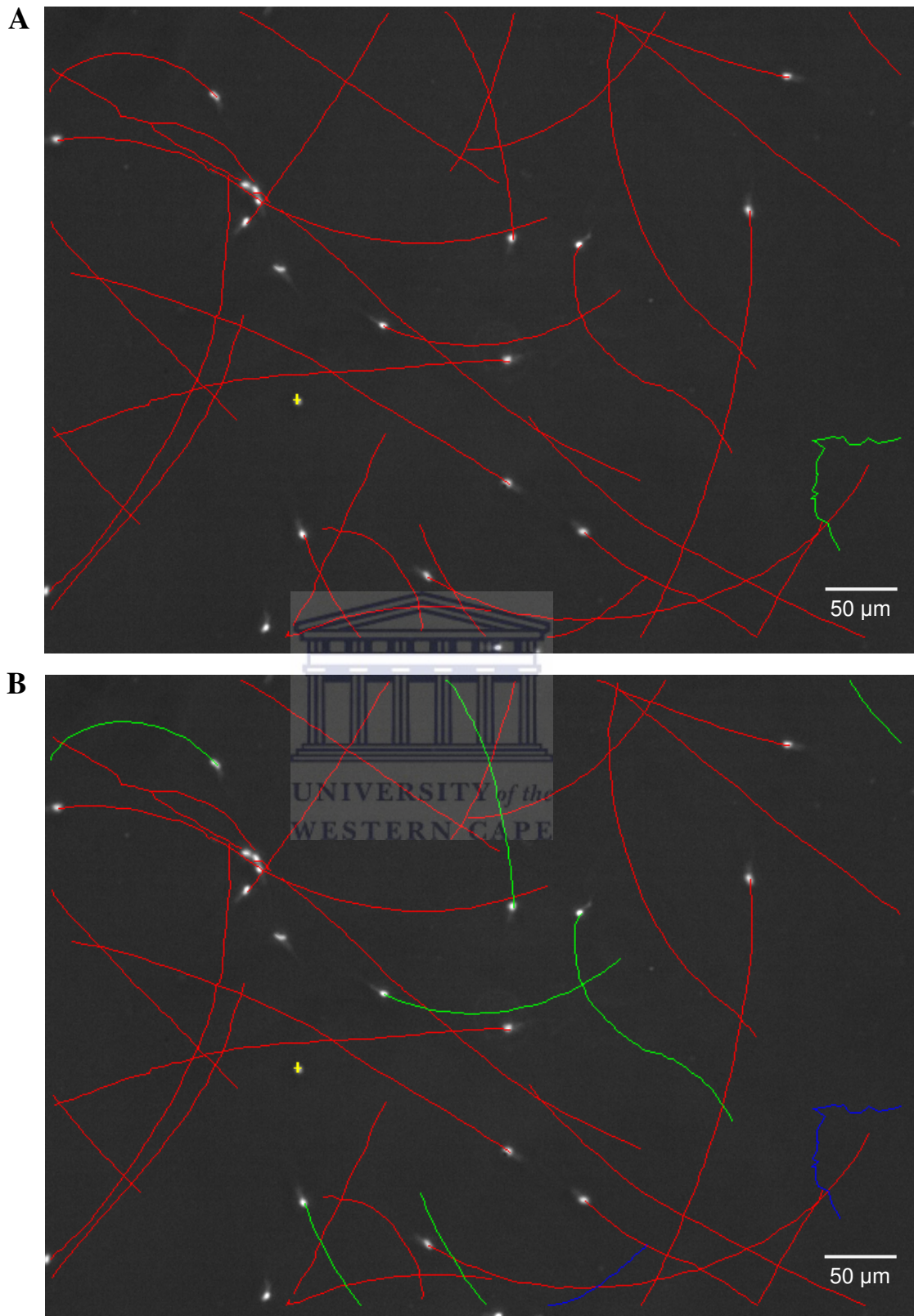
Figure 5.3. Identical sperm motility tracks of vervet monkey spermatozoa to illustrate how the adaptations in the VCL intervals for rapid, medium and slow swimming spermatozoa resulted in the adjusted percentages of the three classes captured at 50 frames/second by the SCA® system. **A**) Rapid > 120 < Medium > 80 < Slow > 50, **B**) Rapid > 280 < Medium > 164 < Slow > 64. The actual kinematic parameters of the spermatozoa included in these three swimming speed classes are presented in Table 5.5. Red tracks = rapid progressive swimming spermatozoa, green tracks = rapid swimming spermatozoa, blue tracks = medium progressive swimming spermatozoa, yellow crosses = static spermatozoa.

A Scale = 1 : 69.5 μm *

Classification	Rapid
VCL (μm/s)	130.1
VSL (μm/s)	98.3
VAP (μm/s)	102.9
LIN (%)	75.5
STR (%)	95.5
WOB (%)	79.1
ALH (μm)	2.2
BCF (Hz)	27.0

B Scale = 1 : 33.7 μm *

Classification	Medium
VCL (μm/s)	75.7
VSL (μm/s)	46.9
VAP (μm/s)	66.3
LIN (%)	62.0
STR (%)	70.8
WOB (%)	87.5
ALH (μm)	1.7
BCF (Hz)	15.3

C Scale = 1 : 13.3 μm *

Classification	Slow
VCL (μm/s)	50.1
VSL (μm/s)	20.5
VAP (μm/s)	34.4
LIN (%)	40.9
STR (%)	59.5
WOB (%)	68.6
ALH (μm)	1.0
BCF (Hz)	7.7

* Please note difference in scale for A, B and C
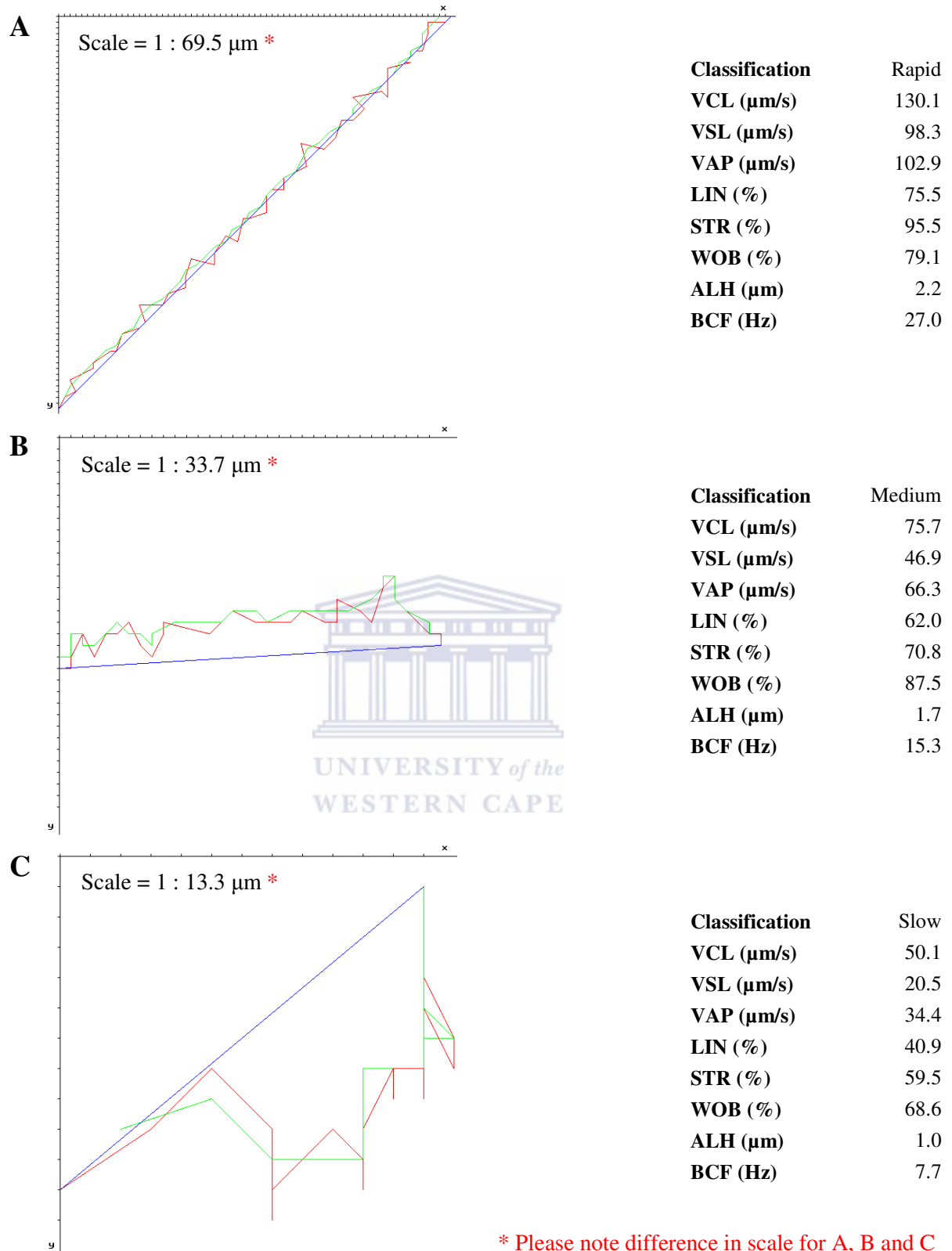
Figure 5.4. Representative sperm motility tracks of the same sample of human spermatozoa to illustrate the differences in the kinematic parameters of the three swimming speed classes captured at 50 frames/second by the SCA® system and after adjusting the VCL intervals. **A**) Rapid swimming sperm, **B**) Medium swimming sperm, **C**) Slow swimming sperm. Red line = VCL, green line = VAP, blue line = VSL. The average kinematic parameters of the spermatozoa included in these three swimming speed classes are presented in Table 5.5. VCL = curvilinear velocity, VSL = straight-line velocity, VAP = average path velocity, LIN = linearity, STR = straightness, WOB = wobble, ALH = amplitude of lateral head displacement, BCF = beat cross frequency.

Table 5.6. The average default and adjusted VCL intervals for the two different frame rates and two different time intervals of six mammalian species

Swimming speed class	Capturing properties	HS	PU	RM	CA	OO	MM
Rapid DEF		50.0	120.0	120.0	120.0	120.0	120.0
Rapid ADJ	10 min, 50f/s	89.2	296.3	239.9	279.7	174.8	241.8
	30 min, 50f/s	82.9	275.5	242.5	254.0	158.3	211.3
	10 min, 75f/s	101.8	315.2	265.4	295.5	183.8	283.4
	30 min, 75f/s	89.1	281.4	258.6	287.5	154.2	237.2
Medium DEF		30.0	80.0	80.0	80.0	80.0	80.0
Medium ADJ	10 min, 50f/s	59.8	185.6	169.8	163.8	104.7	146.0
	30 min, 50f/s	48.3	157.7	160.3	128.0	88.7	143.5
	10 min, 75f/s	69.3	202.1	191.0	185.7	78.6	169.1
	30 min, 75f/s	56.0	176.6	163.3	163.7	78.8	120.0
Slow DEF		20.0	50.0	50.0	50.0	50.0	50.0
Slow ADJ	10 min, 50f/s	22.8	64.5	81.0	64.0	54.0	70.0
	30 min, 50f/s	22.4	59.5	69.5	56.5	51.0	62.5
	10 min, 75f/s	24.7	48.0	70.5	75.0	39.6	52.9
	30 min, 75f/s	26.0	69.8	68.6	50.6	46.5	51.6

HS = *Homo sapiens* (human), PU = *Papio ursinus* (chacma baboon), RM = *Macaca mulatta* (rhesus monkey), CA = *Chlorocebus aethiops* (vervet monkey), OO = *Ovis orientalis* (merino ram), MM = *Mus musculus* (house mouse)
VCL = curvilinear velocity, DEF = default, ADJ = adjusted, f/s = frames/second

Table 5.7. Sperm kinematic parameter measurements (mean ± SD) for different mammalian species (n = 10 individuals per species) captured at 5-10 minutes after the sperm preparation was made and at 50 frames/second (top) or 75 frames/second (bottom)

50f/s	HS	PU	RM	CA	OO	MM	HG
VCL (μm/s)	118.8 ± 17.3[a]	367.7 ± 45.5[b]	292.3 ± 19.2[c]	328.8 ± 18.6[d]	246.6 ± 38.4[e]	293.3 ± 30.3[c]	35.6 ± 6.7[f]
VSL (μm/s)	85.8 ± 13.7[a]	337.8 ± 40.2[b]	217.6 ± 34.3[c]	293.0 ± 24.4[d]	182.3 ± 38.6[e]	119.7 ± 12.0[f]	16.4 ± 5.8[g]
VAP (μm/s)	92.8 ± 13.7[a]	357.2 ± 44.2[b]	251.6 ± 27.9[c]	315.4 ± 20.6[d]	208.3 ± 39.1[e]	147.4 ± 13.4[f]	25.9 ± 5.8[g]
LIN (%)	72.3 ± 5.6[a]	92.0 ± 3.6[b]	74.2 ± 9.3[a]	89.0 ± 4.4[b]	74.4 ± 12.0[a]	41.3 ± 6.2[c]	44.8 ± 8.4[c]
STR (%)	92.2 ± 2.6[a]	94.7 ± 3.0[b]	86.1 ± 5.4[c]	92.8 ± 3.0[ab]	87.2 ± 5.1[c]	81.3 ± 4.1[d]	61.7 ± 9.0[e]
WOB (%)	78.3 ± 4.3[a]	97.2 ± 1.2[b]	85.9 ± 5.8[c]	95.9 ± 1.8[b]	84.8 ± 10.3[c]	50.6 ± 5.6[d]	72.3 ± 4.1[e]
ALH (μm)	2.4 ± 0.2[a]	3.4 ± 0.4[bcd]	4.0 ± 0.4[bc]	3.0 ± 0.2[d]	3.6 ± 0.8[c]	9.1 ± 1.2[e]	0.6 ± 0.4[f]
BCF (Hz)	18.7 ± 1.7[a]	15.4 ± 1.4[b]	17.3 ± 1.3[a]	13.9 ± 1.2[b]	17.4 ± 2.9[a]	10.5 ± 1.4[c]	6.6 ± 5.8[c]

75f/s	HS	PU	RM	CA	OO	MM
VCL (μm/s)	134.1 ± 23.9[a]	369.4 ± 34.9[b]	325.5 ± 19.0[c]	333.2 ± 17.8[c]	258.3 ± 40.1[d]	342.0 ± 40.7[b]
VSL (μm/s)	85.2 ± 15.2[a]	343.7 ± 35.4[b]	239.3 ± 31.7[c]	303.4 ± 20.0[d]	185.1 ± 46.6[e]	125.2 ± 16.5[f]
VAP (μm/s)	96.7 ± 15.3[a]	355.7 ± 36.1[b]	262.9 ± 25.6[c]	317.7 ± 18.6[d]	207.4 ± 44.8[e]	157.3 ± 15.9[f]
LIN (%)	63.6 ± 4.6[a]	93.0 ± 2.0[b]	73.5 ± 8.7[c]	91.0 ± 2.5[b]	72.2 ± 15.7[c]	36.9 ± 4.8[d]
STR (%)	87.9 ± 2.4[a]	96.6 ± 0.9[b]	90.7 ± 4.1[c]	95.5 ± 1.2[b]	88.4 ± 5.5[ac]	79.5 ± 4.9[d]
WOB (%)	72.4 ± 4.0[a]	96.3 ± 1.3[b]	80.7 ± 6.3[c]	95.3 ± 1.6[b]	80.9 ± 14.8[c]	46.2 ± 3.5[d]
ALH (μm)	2.2 ± 0.3[a]	2.4 ± 0.5[a]	3.2 ± 0.5[b]	2.1 ± 0.3[a]	3.0 ± 1.0[b]	8.2 ± 1.0[c]
BCF (Hz)	24.7 ± 2.9[ad]	21.9 ± 2.1[a]	31.5 ± 4.8[b]	18.9 ± 1.0[c]	26.1 ± 4.2[d]	11.9 ± 2.1[e]

HS = *Homo sapiens* (human), PU = *Papio ursinus* (chacma baboon), RM = *Macaca mulatta* (rhesus monkey), CA = *Chlorocebus aethiops* (vervet monkey), OO = *Ovis orientalis* (merino ram), MM = *Mus musculus* (house mouse), HG = *Heterocephalus glaber* (naked mole-rat)

f/s = frames/second, VCL = curvilinear velocity, VSL = straight-line velocity, VAP = average path velocity, LIN = linearity, STR = straightness, WOB = wobble, ALH = amplitude of lateral head displacement, BCF = beat cross frequency

a, b, c, d, e, f, g = values labelled with different superscript letters in the same row for each individual species were significantly different (P < 0.05)

preparations were made, are presented in Table 5.7. Significant differences (P < 0.05) were found in all the kinematic parameters and among most of the seven species.

At the 50 frames/second frame rate, the baboon and vervet monkey spermatozoa produced the fastest (VCL, VSL and VAP) and highly linear swimming tracks (no difference between these two species for LIN, STR and WOB). The LIN of the human, rhesus monkey and ram spermatozoa was lower but similar among each other (P > 0.05), whereas the mouse and naked mole-rat had the lowest LIN values. The ALH values of the three non-human primates and the ram spermatozoa were very similar (P > 0.05), but human and naked mole-rat had lower ALH values and the mouse had a much higher ALH value (P < 0.05). While the BCF values of the human, rhesus monkey and ram spermatozoa were the highest (P < 0.05), baboon and vervet monkey had similar (to each other) but lower BCF values and the mouse and naked mole-rat spermatozoa had the lowest BCF values (P < 0.05). Overall, the naked mole-rat spermatozoa had the lowest sperm kinematic parameter measurements, except for the WOB parameter. Examples of the differences in the sperm kinematic parameters among the seven species are presented in Figure 5.5 (captured at 50 frames/second and 5-10 minutes after the sperm preparations were made).

At the higher frame rate, it was mostly the changes in the VCL parameters of the rhesus monkey and mouse (also see Table 5.4) that were causing these two species to have similar values to different species as for the 50 frames/second measurements. For example, the VCL of the rhesus monkey and mouse were similar at 50 frames/second, but at 75 frames/second the mouse and baboon had similar VCL values. The same change in results was found between the rhesus monkey (due to increased VCL) and the vervet monkey (due to similar VCL). The decrease in ALH and the increase in BCF were not linear between the 50 and 75 frames/second and again this resulted in changes in the similarities of these two parameters among the six species.

The cluster analyses presented in Figure 5.6 and 5.7 were constructed by including all the sperm kinematic parameters presented in Table 5.7. In Figure 5.6, the close distribution of the individuals of the same species on the vertical axis revealed the species specificity of the kinematic parameters for most of the species. The displacement of individuals of the rhesus monkey and ram and those of the baboon and vervet monkey outside their own clusters confirmed the similarities in the kinematic measurements for these species as reported in
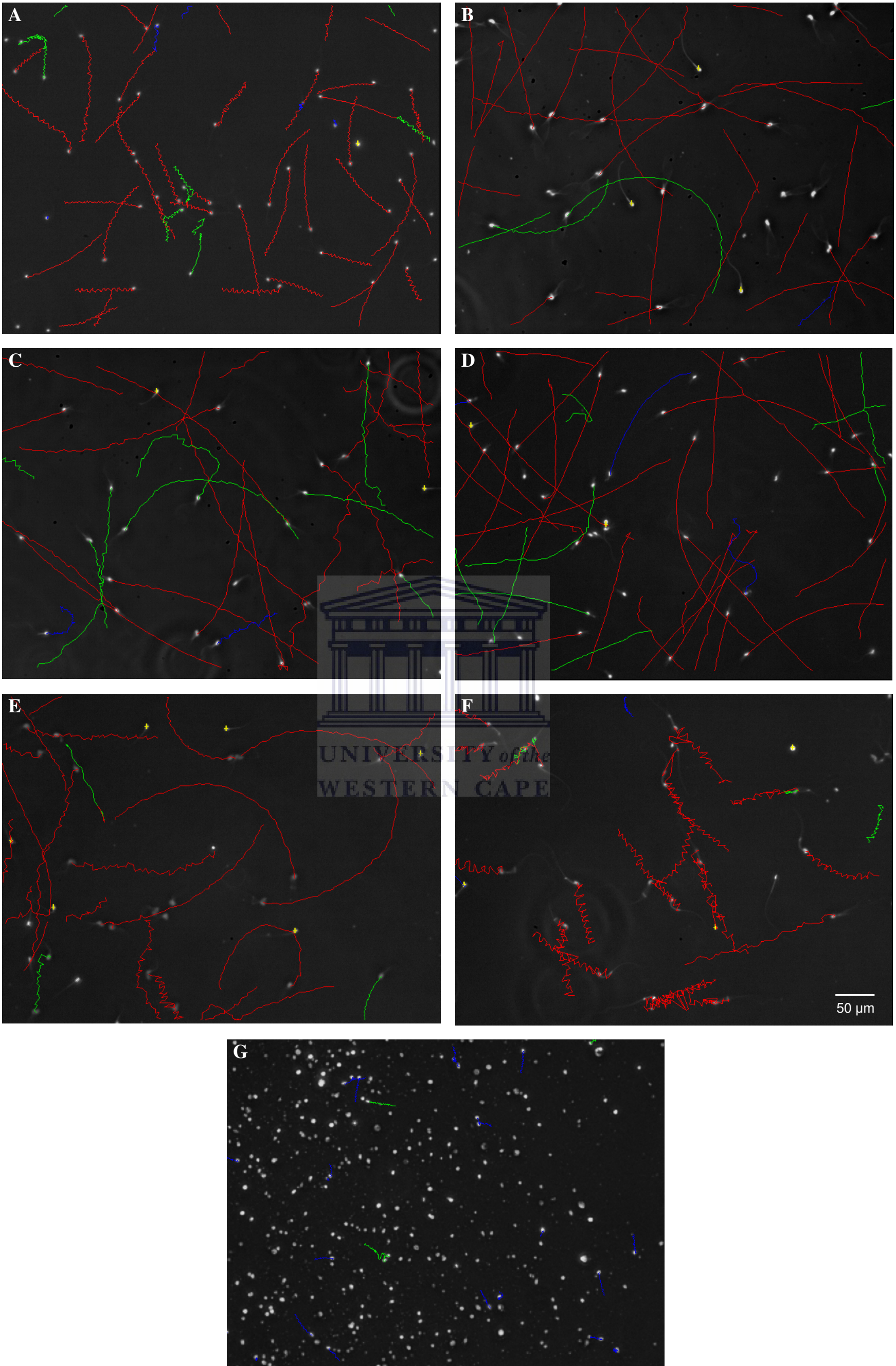
Figure 5.5. Sperm motility tracks of the seven mammalian species to illustrate the differences in the kinematic parameters captured at 50 frames per second by the SCA® system. **A)** *Homo sapiens* (human), **B)** *Papio ursinus* (chacma baboon), **C)** *Macaca mulatta* (rhesus monkey), **D)** *Chlorocebus aethiops* (vervet monkey), **E)** *Ovis orientalis* (merino ram), **F)** *Mus musculus* (house mouse), **G)** *Heterocephalus glaber* (naked mole-rat).

126
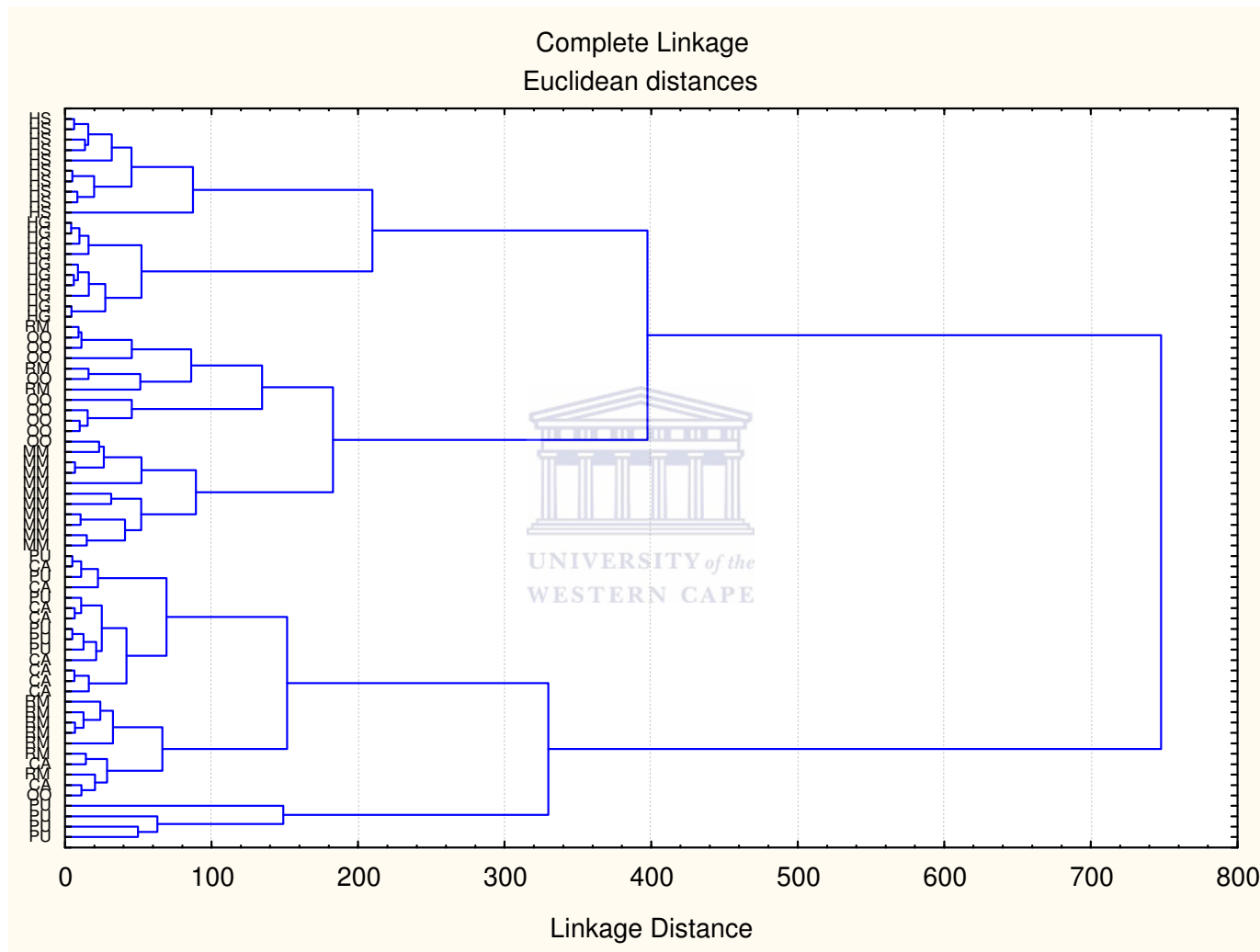
Figure 5.6. Cluster analysis of eight sperm motility parameters captured at 50 frames/second illustrating the clustering of species on the vertical axis and indicating the relatedness among the mammalian species on the horizontal axis (linkage distance). The actual values of the sperm motility parameters are presented in Table 5.7. HS = *Homo sapiens* (human), PU = *Papio ursinus* (chacma baboon), RM = *Macaca mulatta* (rhesus monkey), CA = *Chlorocebus aethiops* (vervet monkey), OO = *Ovis orientalis* (merino ram), MM = *Mus musculus* (house mouse), HG = *Heterocephalus glaber* (naked mole-rat).

127
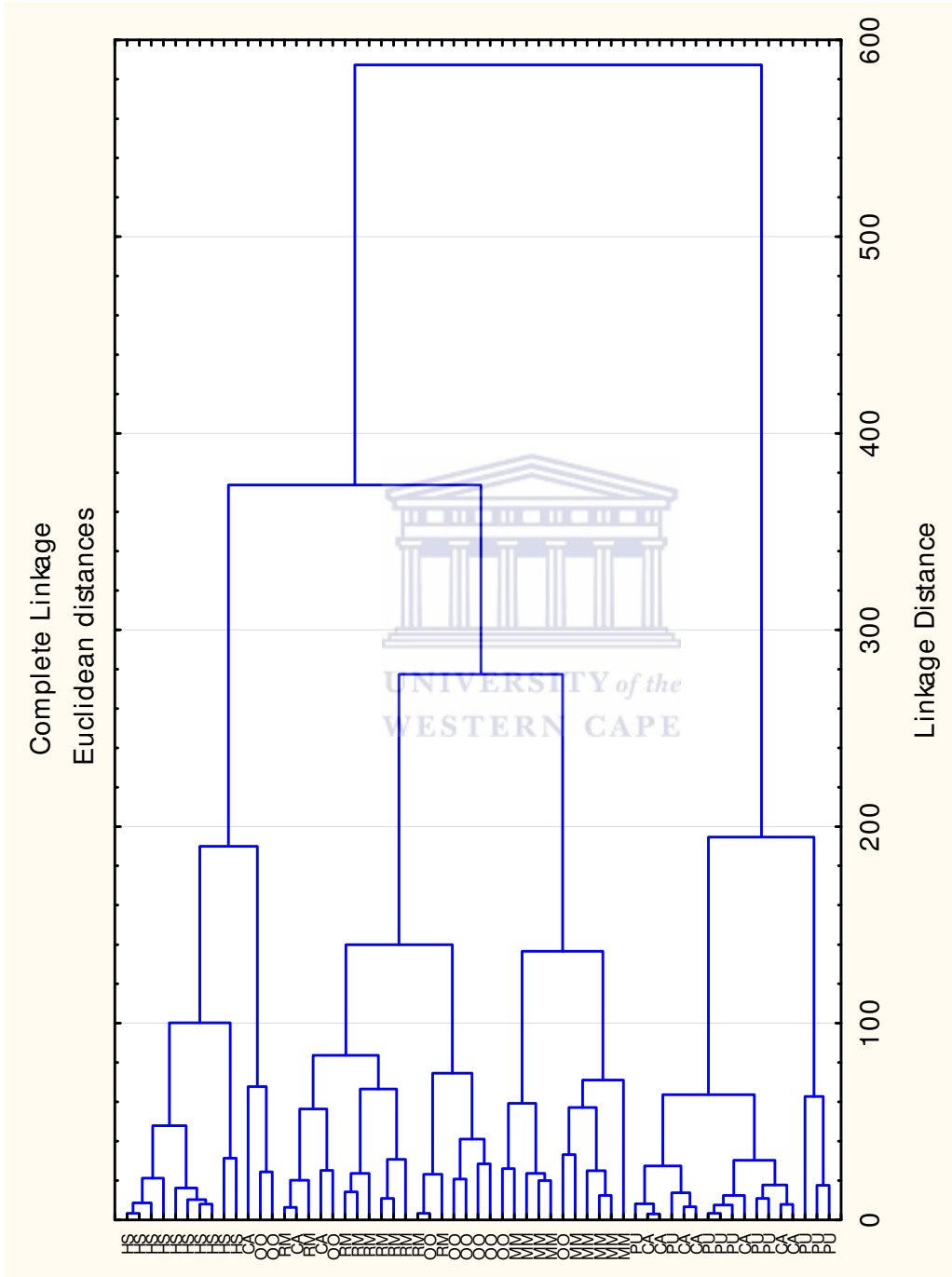
Figure 5.7. Cluster analysis of eight sperm motility parameters captured at 75 frames/second illustrating the clustering of species on the vertical axis and indicating the relatedness among the mammalian species on the horizontal axis (linkage distance). The actual values of the sperm motility parameters are presented in Table 5.7. HS = *Homo sapiens* (human), PU = *Papio ursinus* (chacma baboon), RM = *Macaca mulatta* (rhesus monkey), CA = *Chlorocebus aethiops* (vervet monkey), OO = *Ovis orientalis* (merino ram), MM = *Mus musculus* (house mouse).

128

Table 5.7 for the 50 frames/second frame rate. The linkage distance between the species indicated that the human and naked mole-rat was more closely related in terms of the kinematic parameters, as well as the ram and mouse spermatozoa and lastly the three non-human primate species. A more distantly related cluster was also formed between the human, naked mole-rat, ram and mouse kinematic parameters. In Figure 5.7, it can be seen that the changes in certain kinematic parameters for specific species due to the higher frame rate (see Table 5.7) did not result in any major changes in the cluster analysis. The only visible change was the placement of the rhesus monkey individuals relative to those of the other five species. Although there were still overlapping of individuals found between the rhesus monkey and the ram, there was less association between the rhesus monkey and the other two non-human primate species.

5.4 Discussion

Sperm functionality was assessed in this chapter by the evaluation of sperm motility and the sperm swimming characteristics of seven mammalian species. To achieve this, only highly motile spermatozoa were selected, since these spermatozoa probably also had a high fertility potential (Windsor, 1997; Kasai *et al.*, 2002; Marchetti *et al.*, 2002). The sperm population selected therefore only included spermatozoa which portrayed activated motility and as a result, the discussion below will mostly focus on this type of sperm motility.

The results for the effect of time of data capturing on sperm motility revealed no major differences between the sperm kinematic parameters captured at 5-10 minutes and 30 minutes. The only exceptions were some parameters of the human and mouse spermatozoa that had significantly decreased values at the 30 minute capturing time point for both frame rates and thus resulted in changed motility kinematics. For example, the trend of decreased values in the VCL, VSL and VAP parameters of human spermatozoa at 30 minutes was probably the reason for the significantly lower LIN, STR and WOB values reported (50 frames/second measurements). Since the motility measurements have generally decreased at the 30 minute compared to 10 minute evaluation in all six species, more significant differences will possibly be detected at later time intervals, e.g. one hour after the sperm preparation was made.

According to the above results, it is recommended to assess the sperm kinematics of the activated motility of spermatozoa as soon as possible after a motile sperm population has been

prepared, but it must be noted that species differences do occur. Another factor to consider with regards to the time of data capturing, is the time between semen collection, sperm preparation and the onset of hyperactivated motility, especially if only activated motility needs to be assessed. Mortimer and Mortimer (1990) have reported a transition phase in the motility of human spermatozoa in the time between activated and hyperactivated motility. Spermatozoa in this transition phase had significantly different motility characteristics from forward progressive swimming spermatozoa (activated motility) and hyperactivated motility. Care should thus be taken not to assess spermatozoa in the transition phase, since the onset of this phase could be soon after spermatozoa are separated from the seminal plasma (Mortimer and Mortimer, 1990). Since the time of onset of hyperactivated motility also differ among species (Cooper, 1984; Mortimer and Mortimer, 1990; Kinukawa *et al.*, 2003) and to avoid the changes in sperm motility found at 30 minutes, only the kinematic parameters captured at the 5-10 minute time point were used for species comparisons in the current chapter and in Chapter 7 to follow.

Capturing of sperm tracks at a higher frame rate results in more data points being captured in the same time interval (e.g. one second) and therefore more precise information is obtained about the actual path that was followed by a spermatozoon. However, it was reported that not all sperm kinematic parameters were frame rate dependent and that VCL and BCF were the two parameters mostly affected by frame rate (Mortimer *et al.*, 1988). In the current study it was also found that only certain kinematic parameters were influenced by the higher frame rate, but that the same effects were not seen in all six species evaluated.

The increased VCL values in the rhesus monkey and mouse spermatozoa at 75 frames/second clearly indicated that some detail of the sperm tracks were missed if a lower frame rate was selected. This would clearly be the case if a species' sperm tracks have a low LIN and high ALH values (e.g. mouse) or a combination of a lower LIN, high ALH and high BCF (e.g. rhesus monkey) at 50 frames/second. If these three parameters are considered for all six species included in this comparison, one would expect the human and ram spermatozoa to also have significantly higher VCL values at a higher frame rate. Although these two species' VCL values have shown an increase at 75 frames/second, it was not significant, but if an even higher frame rate could be selected, e.g. 100 frames/second, the increases in the VCL parameter might become significant. The fact that the three sperm velocity derivatives (LIN, STR, and WOB) were significantly different between the two frame rates for human

spermatozoa was evidence of the changes that were portrayed in the VCL and VAP parameters, but none of these changes were significant. On the contrary, the species with highly linear swimming spermatozoa (LIN ≥ 90%), e.g. the baboon and vervet monkey, showed no frame rate dependency for the VCL values. Since changes in three of the kinematic parameters mentioned above (VCL, LIN and ALH) are used to define hyperactivated sperm motility (Mortimer, 1997), CASA evaluation of this type of sperm motility might also require evaluation at a higher frame rate.

The lower ALH and higher BCF values reported for most species at the higher frame rate were consistent with previous findings (Mortimer *et al.*, 1988). According to these authors, the more detailed sperm tracks created at higher frame rates caused the detection of small deviations of the sperm head, especially at the apices of the lateral head displacements. However, these displacements were probably not real head displacements, but false head movements due to the initiation of the flagellar wave (Serres *et al.*, 1984; Mortimer *et al.*, 1988). These minor deviations in the curvilinear path not only results in an increased amount of smaller ALH values being recorded, but also in an increased number of times that the average path crosses the curvilinear path (BCF) (Mortimer *et al.*, 1988).

According to Holt and van Look (2004), most spermatozoa in a semen sample are incapable of fertilizing an oocyte. This is due to the fact that only a low percentage of spermatozoa possess all the necessary mechanisms to enable multiple cell functions to occur flawlessly and synchronously during events such as sperm transport, capacitation, hyperactivation, acrosome reaction and egg penetration. This means that any sperm population consists of a heterogeneous combination of individual spermatozoa which will respond differently to changes in its environment or when exposed to unnatural conditions. Thus, if possible, one should assess these heterogeneous sperm 'subpopulations' in order to predict a male's fertility potential more effectively. Moreover, if only the average response of the whole sperm population is measured, much less significant information might be generated (Holt and van Look, 2004).

Applying the above findings to sperm motility measurements, it might not be sufficient to only consider the total percentage motile spermatozoa in a sperm population, but rather the motility of sperm subpopulations and their kinematic parameters. CASA systems have the advantage of providing both detailed measurements of several parameters for both the whole

131

sperm population and individual spermatozoa (Holt and van Look, 2004). The question remains as to which alternative motility parameter(s) to employ in order to measure the unique motility characteristics of such sperm subpopulations. One option that was previously recommended by the WHO, is the Type a-d classification of spermatozoa according to the progressivity of their motility (WHO, 1999). This classification is, however, only based on human spermatozoa and could not be used for the comparison of different mammalian species. Thus, the need for a different method of evaluating sperm subpopulations was identified and addressed in the present study.

The SCA$^®$ CASA system provides a further quantitative option for the classification of different subpopulation of spermatozoa by identifying three motility classes (rapid, medium, slow) according to the swimming speed of individual spermatozoa. This sperm motility analysis method not only provides objective measurements of the sperm characteristics of each swimming speed class, but it could also possibly be more sensitive to detect changes in the motility of a sperm population. Since the grouping of spermatozoa into one of these three classes is based on certain cut-off values for swimming speed (VCL), it is necessary to select the correct VCL intervals to make meaningful deductions from the data.

It was evident from the results that the selected default VCL intervals for the three swimming speed classes were too low and too generalized for all six species evaluated. The high percentage (> 90%) of spermatozoa in the default rapid swimming speed class was expected, since the techniques employed for sperm selection resulted in mostly motile spermatozoa included in the sperm population evaluated. The very low percentage spermatozoa in the default medium and slow swimming speed classes and their significantly lower sperm velocities, however, created a "false" picture of the motility characteristics of the spermatozoa belonging to each swimming speed class. By adjusting the VCL intervals to include 80%, 15% and 5% spermatozoa in each of the three swimming speed classes respectively, created reliable and comparable sperm subpopulations. This was confirmed by the fact that the kinematic measurements of the adjusted rapid swimming speed class was still similar to those in the default rapid class, but that the medium and slow swimming speed classes had more convincing kinematic characteristics. Moreover, these adjusted VCL intervals resulted in the determination of the unique kinematic characteristics of each swimming speed class and these characteristics and the VCL intervals were specific for each of the mammalian species evaluated. The value of this method, namely to identify different sperm subpopulations, will

only become known when it is used in sperm treatment studies where the effect of the treatment can be assessed by evaluation of the effect on the percentage spermatozoa included in each swimming speed class (see Chapter 6).

The sperm motility characteristics reported in this study fall within the ranges reported in earlier studies on the same species (Mortimer and Mortimer, 1990; Mortimer and Maxwell, 1999; Harris *et al.*, 2007). However, since sperm kinematics were captured at 60 Hz in most of these earlier studies, a comparison of absolute values was not possible. The sperm kinematic measurements of all seven mammalian species included in this study were mostly species specific, but not for all parameters assessed. Some degree of similarity also existed in the motility characteristics of the baboon and vervet monkey as well as between the rhesus monkey and the ram.

A comparison of the arrangement of species using cluster analyses in this chapter with those of Chapter 3 and Chapter 4 did not always reveal the same association between the seven species. Although the baboon and vervet monkey had very similar motility characteristics, the three non-human primate species seemed less closely associated as reported for sperm morphometry, sperm morphometry ratios or midpiece morphometry, where there was a very close association between baboon and rhesus monkey. The sperm motility characteristics of the human and naked mole-rat revealed a similar association as for sperm morphometry, but this association was not found in the sperm morphometry ratios. A similar association found between the ram and mouse motility characteristics were reported for the midpiece morphometry of these two species. Furthermore, when the seven species were arranged from highest to lowest absolute values for five of the midpiece morphometric parameters in Chapter 3, the following trend was reported: HG < HS < PU < CA < RM < OO < MM. Although the same arrangement was not found for the absolute kinematic parameters at 50 frames/second (HG < HS < OO < RM < MM < CA < PU), there seems to be a similar association among the species as for some of their midpiece parameters. Thus, a more detailed analysis of all these sperm components, midpiece components and sperm motility measurements is necessary to reveal the association between the sperm parameters investigated (see Chapter 7).

In this study the main aim was to determine the relationship between midpiece morphometry and other sperm parameters and will be further explored in Chapter 7. However, a number of

previous studies have reported correlations between sperm motility characteristics and other sperm parameters and can also be applied to this study. For instance, Gomendio and Roldan (1991, 2008) have reported that sperm length is positively correlated with maximum swimming speed in eutherian mammals. If the trend in the total sperm length measurements in Chapter 3 is compared to that of the 75 frames/second VCL measurements in this chapter, this relationship seems to be true for the seven species included in this study. Two other studies reported on the positive relationship between sperm swimming speed and head elongation as well as the relative length of the principal plus end piece to the total tail length (TPPL+TEPL/TTL) in natural populations (Malo *et al.* 2006; Gomendio *et al.*, 2007). Similar relationships were not evident from this study when comparing the trend in the VCL measurements to that of the head elongation and the inverse of the TTL/TPPL+TEPL measurements for all seven species.

In conclusion, this detailed analysis of sperm motility parameters has confirmed the importance of the standardization of capturing techniques and analysis methods, especially when CASA systems are employed. For future studies that include the measurement of activated sperm motility, it is recommended that capturing of the data takes place as soon as possible after spermatozoa have been separated from the seminal plasma. The frame rate at which motility data are captured should be determined for each species, since all the species included in the current study did not show the same effect for all kinematic parameters when the frame rate was increased. When comparisons of sperm kinematics are made among species or with previous studies, care should also be taken as to which frame rate is/was used since it was confirmed that certain kinematic parameters are frame rate dependant. The CASA system employed in the current study allowed the identification of sperm subpopulations according to the swimming speed of individual spermatozoa, but only if the VCL intervals were adjusted to species specific cut-off values. Finally, it was also determined that there was a high degree of species specificity for the kinematic measurements of activated motility among the seven mammalian species investigated. Whether or not sperm mitochondria contribute to the maintenance of activated sperm motility (Chapter 6) and if the sperm midpiece can predict the swimming characteristics of spermatozoa for the seven mammalian species (Chapter 7), still needs to be determined.

CHAPTER 6: The role of sperm mitochondria in human sperm metabolism and the maintenance of sperm motility

6.1 Introduction

Energy metabolism is essential for maintenance of normal sperm functions. Intracellular ATP is required for various important cellular reactions and spermatozoal activities such as ion transport, protein phosphorylation and motility. Comparing these mentioned events, it was postulated by Mann and Lutwak-Mann (1981) that flagellar motion is the major energy-demanding chain of events in viable spermatozoa. Although the detailed molecular reactions involved in the generation of the flagellar beat (cAMP/protein kinase A and calcium signalling pathways) have been described in the last two decades (see Turner, 2003; 2006 for reviews), the source of energy to support sperm motility has been debated for more than 60 years (Storey, 2008).

It is generally accepted that the two main pathways for energy production in spermatozoa are the catabolism of glucose and fructose through glycolysis in the cytoplasm and the utilization of pyruvate and lactate during oxidative phosphorylation (OXPHOS) in the mitochondria. Numerous studies have reported on the importance of both these pathways and the substrates they utilize during the different stages of spermatogenesis. Spermatogonia and mature spermatozoa exhibit high glycolytic activity, whereas pachytene spermatocytes and spermatids seem to prefer pyruvate and lactate as their energy source (Voglmayr, 1975; Grootegoed *et al.*, 1984; Nakamura *et al.*, 1984). In ejaculated spermatozoa glycolysis seems to be essential for the processes of capacitation and hyperactivation, while the acrosome reaction mainly uses ATP generated by OXPHOS (Miki, 2007; Hung *et al.*, 2008). Many species differences have, however, been reported in terms of the metabolic substrates utilized by spermatozoa for specific sperm functions (Mann and Lutwak-Mann, 1981; Williams and Ford, 2001). Examples of these species differences include the requirement of glucose for hyperactivation and fertilization in the mouse (Urner and Sakkas, 1996), the inhibition of sperm capacitation in bull spermatozoa by glucose (Galantino-Homer *et al.*, 2004) and the fact that lactate is the preferred substrate of boar sperm metabolism (Jones, 1997).

The importance of both glycolysis and OXPHOS for the maintenance of sperm motility has been investigated and confirmed for many mammalian species (Storey, 2008). Since

OXPHOS can generate about eighteen times more ATP-molecules than glycolysis and can utilize a variety of substrates for respiration (Ford and Rees, 1990), it has been widely accepted that the energy required for sperm motility is produced by mitochondrial respiration under normal conditions (Ruiz-Pesini *et al.*, 2007). Recent reports have, however, presented evidence that glycolysis is the essential or primary pathway for sperm motility in mice and humans (Mukai and Okuno, 2004; Miki *et al.*, 2004; Nascimento *et al.*, 2008a). These reports opened a whole new debate on the subject of sperm metabolism. Various reasons have been put forward as to why glycolysis, OXPHOS or the combination of these two pathways are necessary for sperm energy production (Ford, 2006; Ruiz-Pesini *et al.*, 2007; Miki, 2007).

There are two major reasons for stating that the ATP needed for sperm motility have a purely glycolytic origin. Firstly, it was shown in several studies that the inhibition of specific enzymes in the glycolytic pathway caused a dramatic decrease in sperm motility. At the same time sperm motility was maintained in the presence of glucose when the electron transfer chain (ETC) of mitochondria was inhibited (Mukai and Okuno, 2004; Miki *et al.*, 2004; Nascimento *et al.*, 2008a). Secondly, recent studies have reported that various glycolytic enzymes (some shown to be sperm-specific) are attached to the fibrous sheath and thus confined to the principal piece of the sperm flagellum. This supports the proposal that these enzymes provide a localized source of ATP for sperm motility through glycolysis (Krisfalusi *et al.*, 2006; Kim *et al.*, 2007; Nakamura *et al.*, 2008). Another aspect which favours the importance of this localized production of ATP in the principal piece, is whether or not diffusion alone would be sufficient to deliver the ATP required for flagellar bending to the tip of the sperm tail. This might especially be a problem in rodent spermatozoa, which have long sperm flagella, resulting in a large distance between the mitochondria in the midpiece (site of ATP production) and the end piece (Turner, 2003; Ford, 2006).

On the other hand, various reasons can also be put forward as proof of the important role mitochondrial respiration plays in sperm motility. Earlier studies on sperm metabolism have shown that oxygen consumption, mitochondrial activity and a high mitochondrial membrane potential, which are all directly linked to OXPHOS, correlate with sperm motility (Ford and Harrison, 1981; Gopalkrishnan *et al.*, 1995; Marchetti *et al.*, 2002). Similar to the inhibition of glycolytic enzymes, it was also reported that substances which specifically inhibit the individual enzymatic complexes of the ETC caused a significant decrease in sperm motility in the presence or absence of glucose and the presence of pyruvate or lactate (Mukai and Okuno,

136

2004; St John *et al.*, 2005). Many of these ETC enzymatic complexes are partially encoded by mitochondrial DNA (mtDNA). Therefore studies focussing on male infertility due to mtDNA deletions and an associated decrease in human sperm motility, have confirmed the necessity of an intact ETC for OXPHOS and sperm motility (Ruiz-Pesini *et al.*, 2000; Spiropoulos *et al.*, 2002). Furthermore, a number of testis-specific enzymes for metabolic reactions taking place in the mitochondria have been identified, e.g. lactate dehydrogenase C4 (LDH C_4), pyruvate dehydrogenase (PDH) and succinyl CoA transferase (SCOT-t). The existence of these testis-specific enzymes indirectly indicates that these mitochondrial reactions are important for normal sperm metabolism (Clausen, 1969; Gerez de Burgos *et al.*, 1994; Burgos *et al.*, 1995; Tanaka *et al.*, 2001).

In view of several recent studies on the role of glycolysis and OXPHOS in sperm motility (Mukai and Okuno, 2004; Miki *et al.*, 2004; Pasupuleti, 2007; Hung *et al.*, 2008; Nascimento *et al.*, 2008a) and since the main focus of the current study was mammalian sperm mitochondria, a related question arose. Are the variations in the size of the sperm midpiece and mitochondria and sperm motility parameters reported for the different mammalian species (Chapters 3, 4 and 5) related to mitochondrial respiration? Initially the aim was to determine and compare the efficiency of OXPHOS in maintaining the sperm motility of at least three of the mammalian species studied here. However, due to the many variations in the media, metabolic substrates, inhibitors and protocols used in previous studies on different mammalian species' spermatozoa, it was difficult to compare the results of these studies. This lead to the decision to only perform detailed sperm metabolic experiments on one of the species included in the present study at first, namely human spermatozoa, in order to create a standardized protocol for future studies.

Human spermatozoa were selected for the metabolic experiments of the current study for several reasons. In the context of the current study, human spermatozoa had the smallest midpiece, the lowest midpiece parameters and the slowest swimming spermatozoa apart from the naked mole-rat. It was also postulated that human spermatozoa are exposed to low levels of sperm competition (Martin, 2007) and therefore might not be exposed to strong selection pressures for a high percentage of normal spermatozoa. Additionally, a large number of studies have reported on the association between abnormalities in the human sperm midpiece and mitochondria on male infertility (Gopalkrishnan *et al.*, 1991, 1995; Mundy *et al.*, 1995; Martínez-Heredia *et al.*, 2008). Taking all these factors into consideration, it was assumed that

human spermatozoa have the most compromised mitochondria of all the mammalian species included in this study (except for the naked mole-rat). Moreover, if it can be proven in this study that sperm mitochondria and OXPHOS are important to maintain sperm motility in human spermatozoa, it could be hypothesized that it would be equally or even more important in the other mammalian species.

The main aim of this chapter was therefore to determine if OXPHOS and/or glycolysis can maintain human sperm motility and ATP production in the presence of various metabolic substrates and in combination with inhibitors of both these metabolic pathways.

6.2 Materials and methods

6.2.1 Preparation of media

A basic culture medium was prepared for sperm suspension and incubation similar to the modified HTF medium reported by Nascimento *et al.* (2008a), who also investigated the role of glycolysis and OXPHOS in human sperm metabolism. The modified medium used in the current study contained 5.72 g/L NaCl (98 mM), 0.35 g/L KCl (4.7 mM), 0.3 g/L CaCl$_2$·2H$_2$O (2 mM), 0.05 g/L MgSO$_4$·7H$_2$O (0.2 mM), 0.34 g/L NaHCO$_3$ (4 mM), 0.05 g/L KH$_2$PO$_4$ (0.4 mM) and 5.0 g/L HEPES (21 mM). Since this medium contained no metabolic substrates, it will be referred to as "free medium" hereafter. Three additional media were prepared by adding either 0.5 g/L D-glucose (2.8 mM), 2.4 g/L Na-lactate (21 mM) and 0.05 g/L Na-pyruvate (0.5 mM), or a combination of these to the free medium (see Table 6.1 for details of the four different media). The pH of all four media was set at 7.4 and the osmolality of the media was measured (Table 6.1).

6.2.2 Selection of metabolic inhibitors

Initially four metabolic inhibitors were selected for the study, including two glycolytic inhibitors and two inhibitors of the ETC, to test their efficacy in inhibiting human sperm motility. Both 2-deoxyglucose (DOG) and iodoacetamide (IA) are inhibitors of a specific step in the glycolytic pathway as indicated in Figure 6.1. DOG competes with glucose for the enzyme hexokinase and thus inhibits the first step of glycolysis. IA inhibits the enzyme glyceraldehyde-3-phosphate dehydrogenase (GAPDH) and thus the remaining steps of the glycolytic pathway cannot occur.

138

Table 6.1 Composition and osmolatility of the four different media prepared for sperm metabolism studies (exact concentrations of chemicals are given in the text)

	Free medium	G medium*	LP medium*	LPG medium*
NaCl	✓	✓	✓	✓
CaCl$_2$·2H$_2$O	✓	✓	✓	✓
MgSO$_4$·7HO	✓	✓	✓	✓
NaHCO$_3$	✓	✓	✓	✓
KH$_2$PO$_4$	✓	✓	✓	✓
HEPES	✓	✓	✓	✓
D-Glucose	X	✓	X	✓
Na-lactate	X	X	✓	✓
Na-pyruvate	X	X	✓	✓
Osmolality (mOsm/kg)	293	323	311	319

✓ = included, X = not included

* = glucose (G) medium, lactate-pyruvate (LP) medium, lactate-pyruvate-glucose (LPG) medium
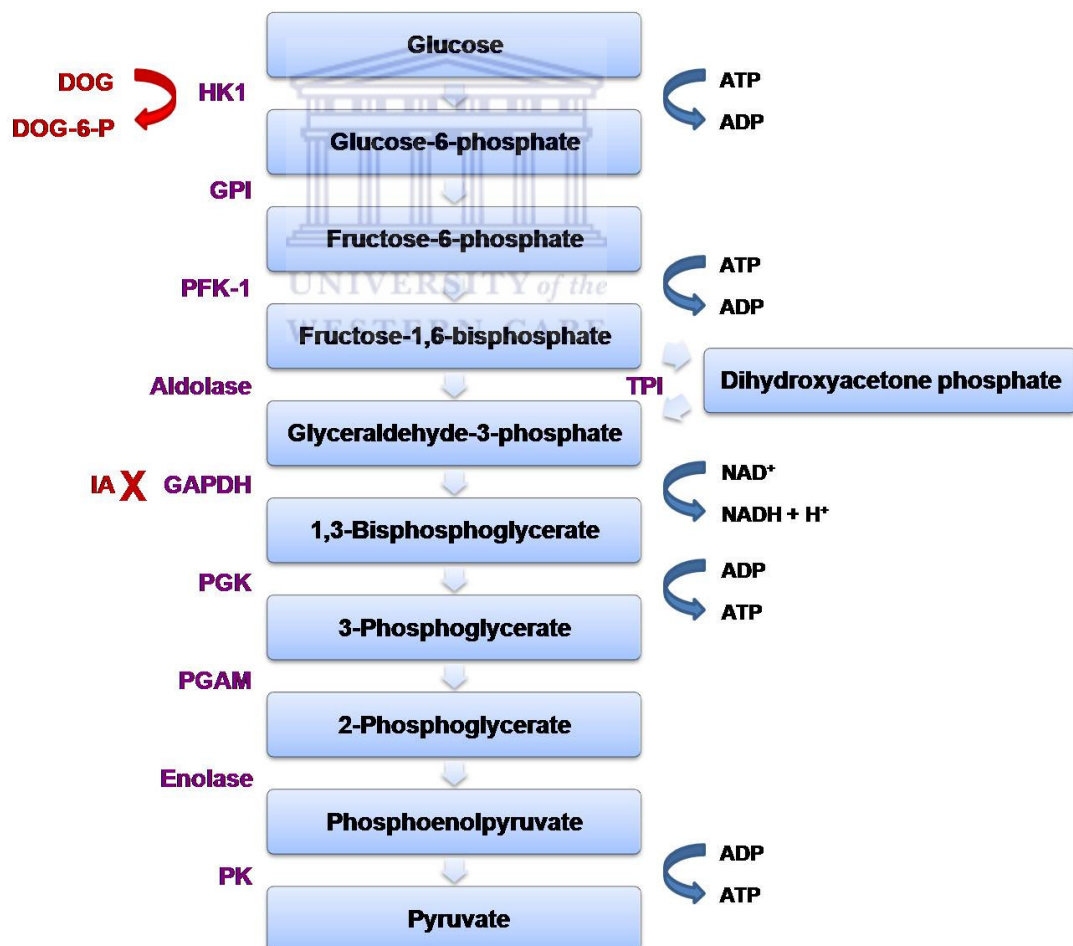
Figure 6.1. Schematic representation of the glycolytic pathway during which glucose is metabolised to pyruvate in ten enzyme-mediated steps. The enzymes are indicated in purple – HK1 = hexokinase 1, GPI = glucosephosphate isomerase, PFK-1 = phosphofructokinase 1, TPI = triphosphate isomerase, GAPDH = glyceraldehyde-3-phospahte dehydrogenase, PGK = phophoglycerate kinase, PGAM = phosphoglycerate mutase, PK = pyruvate kinase. The inhibitory effects of 2-deoxyglucose (DOG) and iodoacetamide (IA) are indicated in red (see text for details).

Antimycin A and carbonyl cyanide *m*-chlorophenylhydrazone (CCCP) are both inhibitors of mitochondrial respiration as indicated in Figure 6.2. Antimycin A specifically blocks complex III of the ETC and thus inhibits the flow of electrons from cytochrome b to cytochrome c and through the remaining parts of the ETC. CCCP is a hydrophobic proton carrier and can transport protons across a proton-impermeable membrane due to its protonophoric action (Terada, 1990). As indicated in Fig. 6.2, CCCP is an uncoupler of the proton gradient across the inner mitochondrial membrane and thus lowers the mitochondrial membrane potential and the protons available for the ATP synthase complex (V).
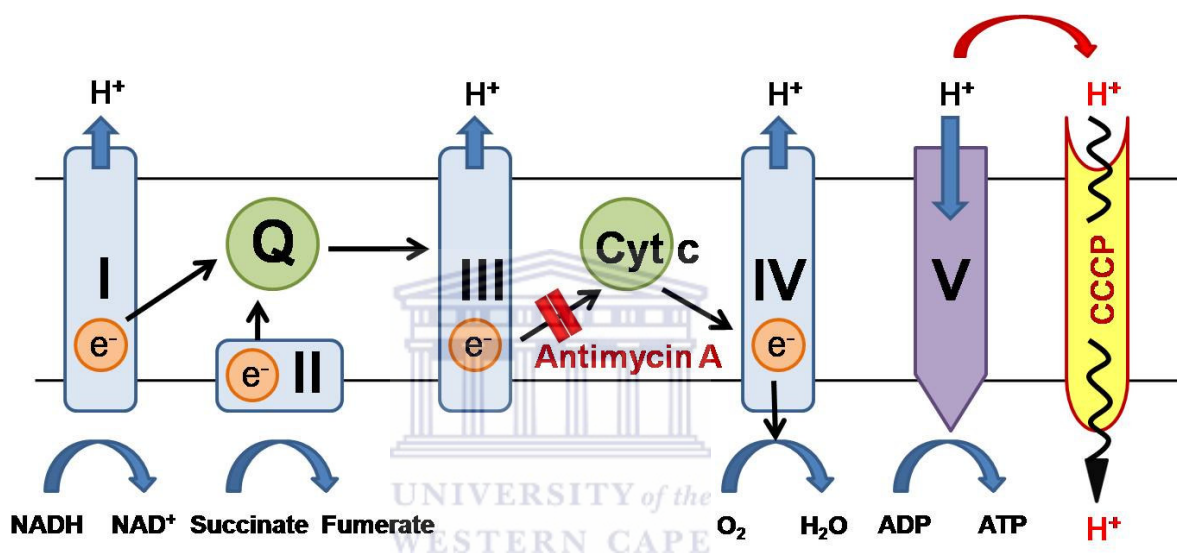
Figure 6.2. Schematic presentation of the electron transfer chain (ETC) located in the inner mitochondrial membrane. The enzyme complexes are indicated with I, II, III, IV, V and the electron carriers include ubiquinone (Q) and cytochrome c (Cyt c). The inhibitory effect of Antimycin A and carbonyl cyanide *m*-chlorophenylhydrazone (CCCP) are indicated in red (see text for details). (Modified from Ramalho-Santos *et al.*, 2009)

After several trial experiments using the four metabolic inhibitors mentioned above, IA and CCCP showed significant effects on sperm motility and was therefore selected as inhibitors for all subsequent experiments. These two inhibitors have been employed for similar sperm metabolic studies on human and animal sperm reported previously (Mukai and Okuno, 2004; Pasupuleti, 2007; Nascimento *et al.*, 2008b). CCCP was also selected as OXPHOS inhibitor due to its function as uncoupler of the proton gradient, rather than just inhibiting one of the enzyme complexes of the ETC, which could result in different effects on sperm motility (St John *et al.*, 2005). Several concentration of IA (0.05, 0.5, 1, 2, 2.5 and 5 mM) and CCCP (0.5, 5, 50 and 500 µM) were tested to determine the most effective concentration for inhibition of sperm motility. This resulted in the selection of 2 mM for IA and 5 µM for CCCP in all subsequent experiments. The effect of these metabolic inhibitors on sperm motility was

apparent after 30 minutes of exposure to the spermatozoa in most of the samples. If the percentage motility and swimming speeds were still very high and similar to the control sample (no clear indication of inhibition of motility), sampling was also done after 60 minutes of incubation. This second sampling was generally only necessary if the original semen sample had a total motility value of more than 70%.

6.2.3 Design of experiments

All possible combinations of the media, inhibitors and controls were included in the current study are displayed in Figure 6.3. The pathways expected to be active and responsible for ATP production and maintenance of sperm motility within each combination (due to substrate availability and no inhibition) is indicated in Table 6.2.
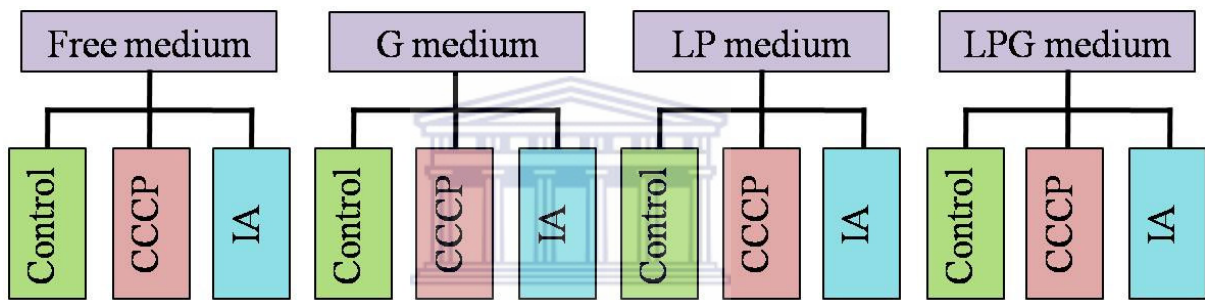
Figure 6.3. Layout of the combination of media (G = glucose, L = lactate and P = pyruvate) and treatments (control, CCCP, IA) used for metabolic experiments to determine the percentage motility and ATP production by human spermatozoa.

Table 6.2. Combinations of media, inhibitors and controls with the expected metabolic pathways responsible for ATP production and maintenance of sperm motility

	Free medium	G medium*	LP medium*	LPG medium*
Control	Only endogenous substrates	Glycolysis & OXPHOS	OXPHOS	Glycolysis & OXPHOS
CCCP	Only endogenous substrates for glycolysis	Glycolysis	None	Glycolysis
IA	Only endogenous substrates for OXPHOS	None	OXPHOS	OXPHOS

* = glucose (G) medium, lactate-pyruvate (LP) medium, lactate-pyruvate-glucose (LPG) medium

Previous studies included only some of these combinations in their experimental protocols and subsequently based their conclusions on the data thus generated. However, it was decided to include all possible combinations in the present study and thereby not leaving any results to assumptions. In the trial experiments reported in section 6.2.3 to test the inhibitory effect of IA and CCCP on sperm motility, a combination of these two inhibitors was also evaluated. Since this combination of IA and CCCP resulted in a significant decrease in the percentage motile spermatozoa as well as the sperm kinematic parameters in all four media (similar to the results obtained with IA alone), this combination was not included in the subsequent experiments.

6.2.4   Sperm washing, motile sperm selection and inhibition

Human semen samples were collected and evaluated according to the procedures reported in Chapter 3. After the determination of the most effective concentration of the metabolic inhibitors (6.2.2), spermatozoa from three donors were used in the metabolic experiments. The spermatozoa were prepared and selected according to a combination of the simple washing procedure recommended by the WHO (WHO, 2010) and the swim-up technique described in section 3.2.4.2. This modified technique involved several washing, incubation and centrifugation steps and is described below.

After mixing the semen sample, 150-250 µl semen was placed in twelve separate 2 ml microcentrifuge tubes (according to the lay-out depicted in Fig. 6.3). The exact volume of semen used in each of the twelve aliquots depended on the sperm concentration and the volume of the whole semen sample. Medium was added to the semen aliquots at a ratio of 1.5-2.0:1 (e.g. 400 µl medium to 200 µl semen) and carefully mixed by gentle pipetting. The sperm suspension was washed by centrifugation at 300-400 g for 10 minutes (the same protocol was followed in all the subsequent centrifugation steps). Hereafter the supernatant was removed using a pipette and care was taken not to disturb the pellet. A volume of 100-200 µl medium was slowly layered onto the pellet (without disturbing it) and the sample was incubated for 30 minutes at 37 ℃. This incubation time was sufficient to allow motile spermatozoa to swim into the overlaying medium (similar to the swim-up technique). Motile spermatozoa were extracted using a pipette by removing most of the media layered onto the pellet (100-200 µl) and placing it into a clean microcentrifuge tube. The selected spermatozoa were centrifuged and the supernatant was removed using a pipette (without disturbing the

pellet). A final volume of 100 µl of medium containing the inhibitor (except for control) was layered onto the pellet, allowing some mixing of the medium and the pellet. The spermatozoa were incubated for 30 minutes before the sampling for motility analysis started.

The medium referred to in the above described technique was the free medium, the glucose medium, the lactate-pyruvate medium or the glucose-lactate-pyruvate medium (see Table 6.1). Depending on the experiment (see Fig. 6.3), the same medium was used throughout, e.g. if the experiment included the glucose medium, this medium was used for the sperm washing, sperm selection and inhibition steps.

6.2.5 Assessment of sperm motility using CASA

Motility parameters were assessed by using the same equipment and basic procedures described in Chapter 5. All motility measurements were done using the Nikon Eclipse 50i microscope with phase negative settings and at 50 frames/second. A 5 µl sample of the treated spermatozoa was selected for assessment after 30 minutes of incubation. The same motility parameters were measured as described in Chapter 5, namely the total percentage motile spermatozoa, curvilinear velocity (VCL), straight line velocity (VSL), average path velocity (VAP), linearity (LIN), straightness (STR), wobble (WOB), amplitude of lateral head displacement (ALH) and beat cross frequency (BCF).

After the percentage rapid, medium and slow swimming sperm were analysed according to the selected default values for humans (20 > slow > 30 > medium > 50 > rapid) (Table 5.1) the VCL settings were adjusted as described in Chapter 5 and indicated in Table 5.6 (22 > slow > 48 > medium > 83 > rapid). Subsequently all these percentages were recalculated. With these recalculated values it will be possible to determine whether it would be sufficient to only evaluate the percentage total motility of a sample or whether it would be more accurate to evaluate the effect of a treatment on the percentage rapid, medium and slow swimming spermatozoa.

6.2.6 ATP analysis

The ATP levels of three samples of human spermatozoa were determined using the ENLITEN® ATP Assay System Bioluminescence Detection Kit (Promega, Cape Town, South Africa). This assay uses recombinant luciferase to catalyze the following reaction:

$$\text{ATP} + \text{D-Luciferin} + O_2 \rightarrow \text{Oxyluciferin} + \text{AMP} + \text{PPi} + CO_2 + \text{Light (560 nm)}$$
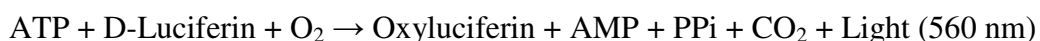
Since ATP is the limiting component in the luciferase reaction, the emitted light is proportional to the ATP concentration of the sample.

The ATP analysis was done on the same sperm samples prepared for motility analysis and after 30 minutes of incubation with the inhibitors. After the motility parameters were evaluated, the samples were centrifuged at 500 *g* for 10 minutes and the supernatant was removed. The spermatozoa were then washed by adding 100 µl PBS (4 ^{o}C) and centrifugation at 10 000 rpm, for 10 minutes at 4 ^{o}C. The supernatant was subsequently removed. The pellet was resuspended in 50 µl ice-cold lysis buffer (100 mM Tris-HCl and 4 mM EDTA, pH 7.75), followed by 150 µl boiling (100 ^{o}C) lysis buffer (Essmann *et al.*, 2003). Samples were incubated for 2 minutes at 99 ^{o}C. Lysates were centrifuged at 10 000 rpm, for 1 minute at 4 ^{o}C. The supernatant was collected in two aliquots of 50 µl each (duplicate samples) and the sperm concentration in the supernatant was determined for each of the samples. After the three sperm samples were processed according to the method described above, ATP levels of the duplicate samples were measured by adding 50 µl reconstituted luciferase reagent (rL/L Reagent) to the 50 µl supernatant (thawed at room temperature). The ATP assay was performed by acquiring the chemiluminescence in a Glomax-96 luminometer (Promega, Cape Town, South Africa). The ATP concentration was determined in relative light units (RLU) and was subsequently re-calculated as RLU/million spermatozoa to take the sperm concentration of the samples into account. Two additional ATP parameters were determined, namely the ATP of the treatment as a percentage of the ATP of the treatment's control and the ATP of the treatment as a percentage of the ATP of the LPG-medium's control.

6.2.7 Statistical analysis

The statistical software and statistical tests utilized were identical to those described in Chapter 3.

6.3 Results

Effect of metabolic inhibitors in different media

The effect of both inhibitors on the total percentage motile spermatozoa, the kinematic parameters of the spermatozoa and the production of ATP in the four different media are presented in Table 6.3. For each medium used, the effect of CCCP and IA were compared to the control of that specific medium to indicate any changes in the measured parameters due to

144

Table 6.3. Sperm motility, kinematic parameter and ATP production measurements (mean ± SD) of human spermatozoa (n = 3) to indicate the effect of the two metabolic inhibitors (CCCP and IA) in the four different media (free medium, glucose (G) medium, lactate-pyruvate (LP) medium and lactate-pyruvate-glucose (LPG) medium)

Free medium	Control	CCCP	IA
Motility (%)	83.8 ± 14.7[a]	20.2 ± 19.2[b]	28.3 ± 14.5[b]
VCL (µm/s)	76.9 ± 4.6[a]	36.5 ± 19.0[b]	39.9 ± 13.2[b]
VSL (µm/s)	34.5 ± 6.7[a]	9.7 ± 9.3[b]	7.0 ± 3.6[b]
VAP (µm/s)	44.2 ± 6.3[a]	20.3 ± 10.9[b]	18.0 ± 5.9[b]
LIN (%)	44.6 ± 6.3[a]	23.2 ± 11.2[b]	16.5 ± 4.2[b]
STR (%)	77.6 ± 4.4[a]	41.4 ± 19.0[b]	36.6 ± 9.3[b]
WOB (%)	57.2 ± 5.1[a]	55.5 ± 4.3[b]	45.2 ± 0.1[b]
ALH (µm)	2.5 ± 0.3[a]	0.7 ± 1.0[b]	0.1 ± 0.2[b]
BCF (Hz)	14.5 ± 0.6[a]	3.0 ± 4.7[b]	0.3 ± 0.6[b]
ATP RLU/10⁶ sperm	0.6 ± 0.2[a]	0.2 ± 0.1[b]	0.1 ± 0.1[b]
ATP % Own Control	100.0 ± 0.0[a]	26.9 ± 14.1[b]	13.9 ± 5.5[b]
ATP % LPG Control	43.8 ± 13.2[a]	10.9 ± 5.6[b]	5.8 ± 2.3[b]

G medium	Control	CCCP	IA
Motility (%)	90.7 ± 3.1[a]	80.8 ± 8.3[a]	17.8 ± 6.3[b]
VCL (µm/s)	103.7 ± 8.5[a]	88.5 ± 11.4[a]	29.8 ± 6.9[b]
VSL (µm/s)	48.3 ± 1.8[a]	36.9 ± 10.9[a]	3.8 ± 1.9[b]
VAP (µm/s)	60.0 ± 3.4[a]	48.9 ± 10.4[a]	12.6 ± 4.9[b]
LIN (%)	46.7 ± 3.5[a]	41.1 ± 7.1[a]	12.3 ± 4.2[b]
STR (%)	80.5 ± 3.5[a]	74.6 ± 7.0[a]	29.5 ± 8.7[b]
WOB (%)	57.9 ± 1.8[a]	54.8 ± 4.6[a]	41.3 ± 7.5[b]
ALH (µm)	2.9 ± 0.5[a]	2.8 ± 0.4[a]	0.1 ± 0.2[b]
BCF (Hz)	16.4 ± 1.4[a]	14.3 ± 2.6[a]	0.3 ± 0.6[b]
ATP RLU/10⁶ sperm	1.1 ± 0.8[a]	2.3 ± 1.0[a]	0.9 ± 0.7[a]
ATP % Own Control	100.0 ± 0.0[a]	234.2 ± 91.5[b]	36.9 ± 15.7[c]
ATP % LPG Control	73.7 ± 45.9[a]	145.8 ± 26.4[b]	55.7 ± 28.7[a]

LP medium	Control	CCCP	IA
Motility (%)	91.8 ± 5.6[a]	11.8 ± 11.0[b]	23.2 ± 11.2[b]
VCL (µm/s)	88.5 ± 3.4[a]	30.9 ± 8.0[b]	28.1 ± 4.2[b]
VSL (µm/s)	38.7 ± 1.5[a]	5.0 ± 4.2[b]	4.1 ± 2.2[b]
VAP (µm/s)	49.6 ± 1.4[a]	15.0 ± 7.7[b]	11.6 ± 4.6[b]
LIN (%)	43.8 ± 3.5[a]	14.6 ± 8.7[b]	14.7 ± 7.9[b]
STR (%)	78.0 ± 3.4[a]	32.3 ± 14.9[b]	34.0 ± 7.6[b]
WOB (%)	56.1 ± 2.7[a]	47.1 ± 18.8[b]	41.2 ± 15.1[b]
ALH (µm)	2.9 ± 0.5[a]	0.0 ± 0.0[b]	0.2 ± 0.2[b]
BCF (Hz)	14.5 ± 0.8[a]	0.0 ± 0.0[b]	0.1 ± 0.2[b]
ATP RLU/10⁶ sperm	1.2 ± 0.8[a]	0.3 ± 0.2[a]	0.3 ± 0.2[a]
ATP % Own Control	100.0 ± 0.0[a]	26.5 ± 6.7[b]	24.0 ± 5.8[b]
ATP % LPG Control	73.3 ± 34.5[a]	18.0 ± 6.4[b]	17.8 ± 10.1[b]

LPG medium	Control	CCCP	IA
Motility (%)	94.6 ± 2.3[a]	89.6 ± 7.8[a]	30.7 ± 24.1[b]
VCL (µm/s)	106.0 ± 8.5[a]	82.5 ± 7.1[b]	38.2 ± 12.2[c]
VSL (µm/s)	49.3 ± 6.9[a]	32.3 ± 4.4[b]	7.8 ± 4.2[c]
VAP (µm/s)	61.6 ± 5.2[a]	44.4 ± 3.4[b]	17.3 ± 6.6[c]
LIN (%)	46.5 ± 4.8[a]	39.0 ± 2.4[a]	19.6 ± 4.7[b]
STR (%)	79.8 ± 5.1[a]	72.4 ± 4.8[a]	44.0 ± 7.9[b]
WOB (%)	58.1 ± 2.6[a]	54.0 ± 2.0[a]	44.7 ± 9.3[a]
ALH (µm)	3.2 ± 0.6[a]	3.0 ± 0.3[a]	0.5 ± 0.5[b]
BCF (Hz)	15.7 ± 2.2[a]	11.9 ± 1.3[b]	1.4 ± 1.5[c]
ATP RLU/10⁶ sperm	1.5 ± 0.5[a]	2.7 ± 1.4[a]	0.7 ± 0.5[a]
ATP % Own Control	100.0 ± 0.0[a]	173.8 ± 37.6[b]	45.8 ± 19.2[c]
ATP % LPG Control	100.0 ± 0.0[a]	173.8 ± 37.6[b]	45.8 ± 19.2[c]

VCL = curvilinear velocity, VSL = straight-line velocity, VAP = average path velocity, LIN = linearity, STR = straightness, WOB = wobble, ALH = amplitude of lateral head displacement, BCF = beat cross frequency, ATP = adenosine triphosphate, RLU = relative light units
a, b, c = values labelled with different superscript letters in the same row were significantly different (P < 0.05)

the inhibition of a specific pathway.

In the free medium, the total percentage motile spermatozoa in the control sample was more than 80%, as was consistently found and reported in the previous chapters when selecting highly motile spermatozoa. The sperm kinematic parameters in the control sample were still reasonably high and ATP was produced. In both the CCCP and IA inhibited samples, all the parameters measured were significantly lower than the control sample, with no difference between the two inhibited samples.

In the glucose medium, there was no significant difference in the total percentage motile spermatozoa or any of the sperm kinematic parameters evaluated between the control and CCCP inhibited samples. The ATP production in the CCCP inhibited sample was, however, extremely high compared to the control sample when it was expressed as a percentage of the ATP production in the control sample (% ATP Own Control) or the control sample of the LPG medium (% ATP LPG Control). All the motility parameters and one of the ATP measurements were significantly lower in the IA inhibited sample. An example of the difference in the sperm motility tracks for the control, CCCP and IA inhibited samples in the glucose medium are presented in Figure 6.4.

Almost all the measured parameters had significantly lower values in both the CCCP and IA inhibited samples compared to the control in the lactate-pyruvate medium. An example of the difference in the sperm motility tracks for the control, CCCP and IA inhibited samples in this medium are presented in Figure 6.5.

In the lactate-pyruvate-glucose medium, the CCCP inhibited sample had a similar total percentage motile spermatozoa than the control sample, but significantly lower values were recorded for some of the kinematic parameters. The ATP produced in the CCCP inhibited sample was, however, significantly higher than that of the control sample, as was reported for the glucose-medium above. Once again almost all the parameters measured were significantly lower in the IA inhibited sample.

Effect of the same treatment in different media
The data presented in Table 6.3 can be re-grouped and presented in terms of the treatments to compare their effect in the four different media, as indicated in Table 6.4. This comparison

146
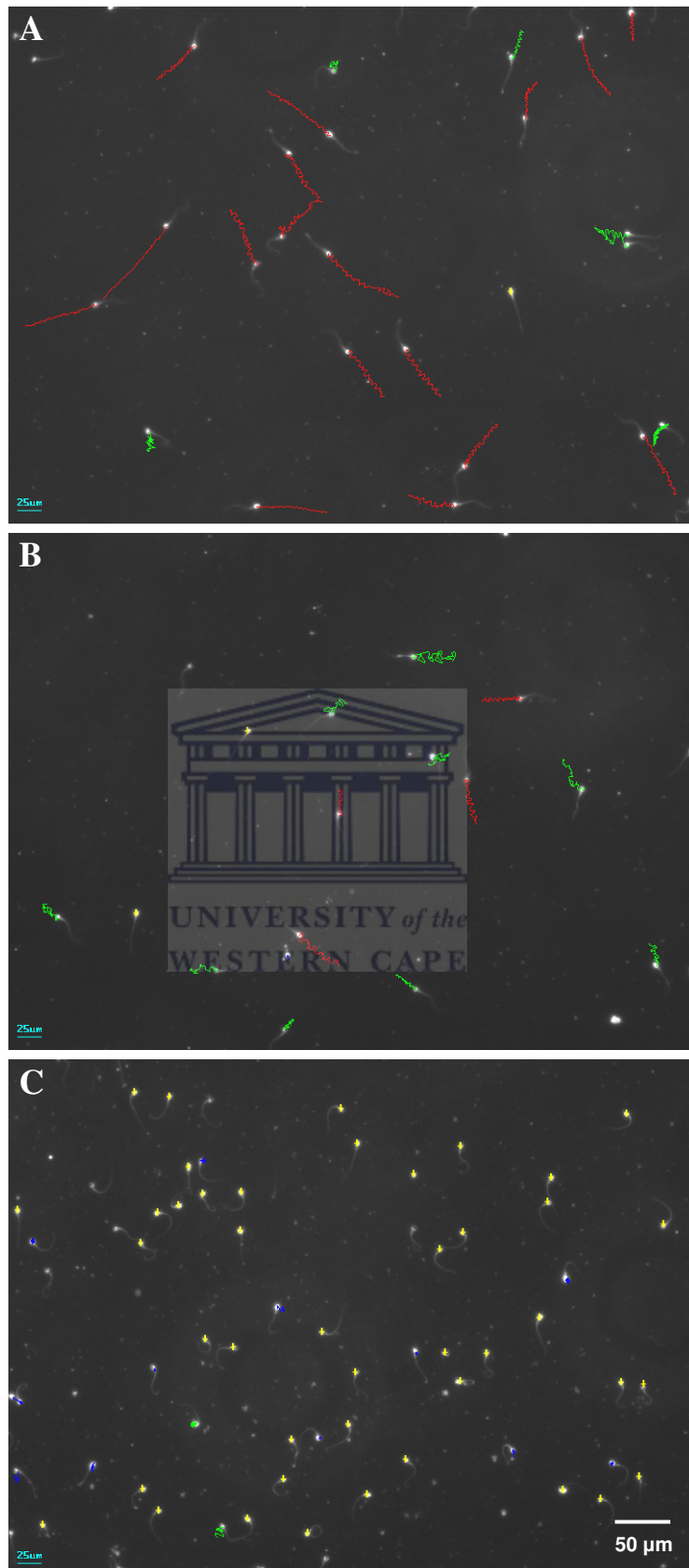
Figure 6.4. Sperm motility tracks of human spermatozoa captured by the SCA® system to illustrate the difference in the kinematic parameters with different treatments in glucose medium. **A**) Control, **B**) CCCP inhibited and **C**) IA inhibited. The actual sperm kinematic parameters are presented in Table 6.3. Red tracks = rapid progressive swimming spermatozoa, green tracks = rapid swimming spermatozoa, blue tracks = medium progressive swimming spermatozoa, yellow crosses = static spermatozoa.
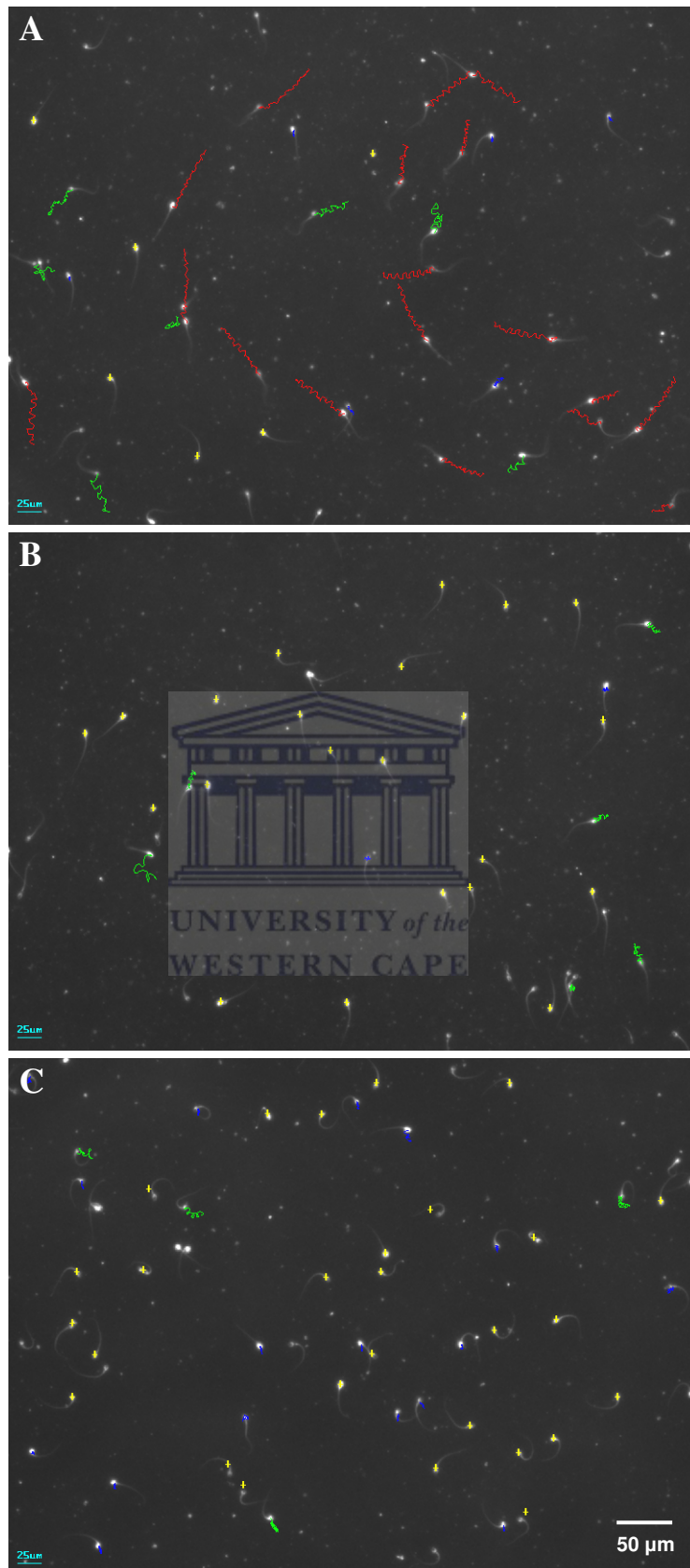
Figure 6.5. Sperm motility tracks of human spermatozoa captured by the SCA® system to illustrate the difference in the kinematic parameters with different treatments in lactate-pyruvate medium. **A**) Control, **B**) CCCP inhibited and **C**) IA inhibited. The actual sperm kinematic parameters are presented in Table 6.3. Red tracks = rapid progressive swimming spermatozoa, green tracks = rapid swimming spermatozoa, blue tracks = medium progressive swimming spermatozoa, yellow crosses = static spermatozoa.

Table 6.4. Sperm motility, kinematic parameter and ATP production measurements (mean ± SD) of human spermatozoa (n = 3) to indicate the effect of the same treatment (control, CCCP or IA) in the four different media (free medium, glucose (G) medium, lactate-pyruvate (LP) medium and lactate-pyruvate-glucose (LPG) medium)

CONTROL	Free medium	G medium	LP medium	LPG medium
Motility (%)	83.8 ± 14.7	90.7 ± 3.1	91.8 ± 5.6	94.6 ± 2.3
VCL (µm/s)	76.9 ± 4.6[a]	103.7 ± 8.5[b]	88.5 ± 3.4[a]	106.0 ± 8.5[b]
VSL (µm/s)	34.5 ± 6.7[a]	48.3 ± 1.8[b]	38.7 ± 1.5[a]	49.3 ± 6.9[b]
VAP (µm/s)	44.2 ± 6.3[a]	60.0 ± 3.4[b]	49.6 ± 1.4[a]	61.6 ± 5.2[b]
LIN (%)	44.6 ± 6.3	46.7 ± 3.5	43.8 ± 3.5	46.5 ± 4.8
STR (%)	77.6 ± 4.4	80.5 ± 3.5	78.0 ± 3.4	79.8 ± 5.1
WOB (%)	57.2 ± 5.1	57.9 ± 1.8	56.1 ± 2.7	58.1 ± 2.6
ALH (µm)	2.5 ± 0.3	2.9 ± 0.5	2.9 ± 0.5	3.2 ± 0.6
BCF (Hz)	14.5 ± 0.6	16.4 ± 1.4	14.5 ± 0.8	15.7 ± 2.2
ATP RLU/10⁶ sperm	0.6 ± 0.2	1.1 ± 0.8	1.2 ± 0.8	1.5 ± 0.5
ATP % Own Control	100.0 ± 0.0	100.0 ± 0.0	100.0 ± 0.0	100.0 ± 0.0
ATP % LPG Control	43.8 ± 13.2[a]	73.7 ± 45.9[ab]	73.3 ± 34.5[ab]	100.0 ± 0.0[b]

CCCP	Free medium	G medium	LP medium	LPG medium
Motility (%)	20.2 ± 19.2[a]	80.8 ± 8.3[b]	11.8 ± 11.0[a]	89.6 ± 7.8[b]
VCL (µm/s)	36.5 ± 19.0[a]	88.5 ± 11.4[b]	30.9 ± 8.0[a]	82.5 ± 7.1[b]
VSL (µm/s)	9.7 ± 9.3[a]	36.9 ± 10.9[b]	5.0 ± 4.2[a]	32.3 ± 4.4[b]
VAP (µm/s)	20.3 ± 10.9[a]	48.9 ± 10.4[b]	15.0 ± 7.7[a]	44.4 ± 3.4[b]
LIN (%)	23.2 ± 11.2[ab]	41.1 ± 7.1[ac]	14.6 ± 8.7[b]	39.0 ± 2.4[c]
STR (%)	41.4 ± 19.0[a]	74.6 ± 7.0[b]	32.3 ± 14.9[a]	72.4 ± 4.8[b]
WOB (%)	55.5 ± 4.3	54.8 ± 4.6	47.1 ± 18.8	54.0 ± 2.0
ALH (µm)	0.7 ± 1.0[a]	2.8 ± 0.4[b]	0.0 ± 0.0[a]	3.0 ± 0.3[b]
BCF (Hz)	3.0 ± 4.7[a]	14.3 ± 2.6[b]	0.0 ± 0.0[a]	11.9 ± 1.3[b]
ATP RLU/10⁶ sperm	0.2 ± 0.1[a]	2.3 ± 1.0[b]	0.3 ± 0.2[a]	2.7 ± 1.4[b]
ATP % Own Control	26.9 ± 14.1[a]	234.2 ± 91.5[b]	26.5 ± 6.7[a]	173.8 ± 37.6[b]
ATP % LPG Control	10.9 ± 5.6[a]	145.8 ± 26.4[b]	18.0 ± 6.4[a]	173.8 ± 37.6[b]

IA	Free medium	G medium	LP medium	LPG medium
Motility (%)	28.3 ± 14.5	17.8 ± 6.3	23.2 ± 11.2	30.7 ± 24.1
VCL (µm/s)	39.9 ± 13.2	29.8 ± 6.9	28.1 ± 4.2	38.2 ± 12.2
VSL (µm/s)	7.0 ± 3.6	3.8 ± 1.9	4.1 ± 2.2	7.8 ± 4.2
VAP (µm/s)	18.0 ± 5.9	12.6 ± 4.9	11.6 ± 4.6	17.3 ± 6.6
LIN (%)	16.5 ± 4.2	12.3 ± 4.2	14.7 ± 7.9	19.6 ± 4.7
STR (%)	36.6 ± 9.3	29.5 ± 8.7	34.0 ± 7.6	44.0 ± 7.9
WOB (%)	45.2 ± 0.1	41.3 ± 7.5	41.2 ± 15.1	44.7 ± 9.3
ALH (µm)	0.1 ± 0.2	0.1 ± 0.2	0.2 ± 0.2	0.5 ± 0.5
BCF (Hz)	0.3 ± 0.6	0.3 ± 0.6	0.1 ± 0.2	1.4 ± 1.5
ATP RLU/10⁶ sperm	0.1 ± 0.1	0.9 ± 0.7	0.3 ± 0.2	0.7 ± 0.5
ATP % Own Control	13.9 ± 5.5	36.9 ± 15.7	24.0 ± 5.8	45.8 ± 19.2
ATP % LPG Control	5.8 ± 2.3[ac]	55.7 ± 28.7[b]	17.8 ± 10.1[c]	45.8 ± 19.2[bc]

VCL = curvilinear velocity, VSL = straight-line velocity, VAP = average path velocity, LIN = linearity, STR = straightness, WOB = wobble, ALH = amplitude of lateral head displacement, BCF = beat cross frequency, ATP = adenosine triphosphate, RLU = relative light units

a, b, c = values labelled with different superscript letters in the same row were significantly different ($P < 0.05$)

was possible since all these measurements were done with the same original human semen samples which were divided into twelve aliquots to include all the combinations as indicated in Figure 6.3.

In all four control samples, the total percentage motile spermatozoa were similar in the different media ($P > 0.05$). In terms of the sperm kinematic parameters, it was only the swimming speed parameters (VCL, VSL and VAP) that were significantly higher in the glucose-containing media compared to the free and lactate-pyruvate media. A significantly lower ATP production was recorded in the free media, but the lower ATP production in the glucose and lactate-pyruvate media relative to the lactate-pyruvate-glucose medium (ATP % LPG Control) was not significant.

In the CCCP inhibited samples, most of the sperm motility and kinematic parameters in the free and lactate-pyruvate media were similar and significantly lower than the values in the other two media. In the IA inhibited samples, all four media revealed equally low values for almost all the parameters. It was only for the number of ATP molecules produced relative to the lactate-pyruvate-glucose medium (ATP % LPG Control) that significant differences were found between the four media.
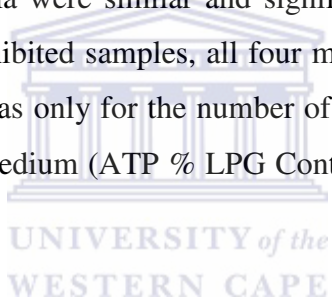
To summarize the effect of the metabolic inhibitors on the production of ATP indicated in Table 6.3 and 6.4, it seems as if the medium played an important role in the number of ATP molecules produced. If either glycolysis (with IA) or OXPHOS (with CCCP) were inhibited, a significantly higher production of ATP was always found in the glucose-containing media.

Evaluation of the effect on sperm motility according to different motility parameters
The effect of the two metabolic inhibitors in the four different media on sperm motility was only presented in terms of the total percentage motile spermatozoa in Table 6.3 and Table 6.4. The percentage rapid, medium and slow swimming sperm were, however, also determined according to the selected default VCL intervals for humans (similar to Chapter 5). Hereafter the VCL settings were adjusted as recommended in Chapter 5 and all the motility percentages and sperm kinematic parameters for the three swimming speed classes were recalculated (data not shown here). The total percentage motile spermatozoa and the various percentages of rapid swimming spermatozoa for all the combinations of media and inhibitors are presented in Table 6.5.

150

Table 6.5. The percentage motile human spermatozoa (n = 3) (mean ± SD) for the different treatments (control, CCCP or IA) in the four media (free medium, glucose (G) medium, lactate-pyruvate (LP) medium and lactate-pyruvate-glucose (LPG) medium) to indicate the effect of evaluating different motility parameters

Media	Treatment	Total AVE (%)[1]	Rapid DEF (%)[2]	Rapid ADJ (%) (expected)[3]	Rapid ADJ (%) (measured)[4]
Free medium	**Control**	83.8 ± 14.7	70.4 ± 19.3	67.0	34.0 ± 6.9*
	CCCP	20.2 ± 19.2	8.7 ± 14.4	16.2	2.9 ± 5.0*
	IA	28.3 ± 14.5	7.2 ± 6.1	22.6	2.5 ± 3.1*
G medium	**Control**	90.7 ± 3.1[a]	83.1 ± 2.4[b]	72.6	69.7 ± 5.2
	CCCP	80.8 ± 8.3[a]	70.5 ± 9.3[b]	64.6	45.7 ± 9.4*
	IA	17.8 ± 6.3[a]	1.1 ± 1.1[b]	14.2	0.1 ± 0.2*
LP medium	**Control**	91.8 ± 5.6	82.4 ± 10.9	73.4	52.7 ± 5.3*
	CCCP	11.8 ± 11.0[a]	2.5 ± 4.3[b]	9.4	0.1 ± 0.2*
	IA	23.2 ± 11.2[a]	1.3 ± 2.2[b]	18.6	0.0 ± 0.0*
LPG medium	**Control**	94.6 ± 2.3	90.1 ± 2.8	75.7	74.4 ± 3.5
	CCCP	89.6 ± 7.8	80.3 ± 10.3	71.7	42.2 ± 12.5*
	IA	30.7 ± 24.1	7.9 ± 12.0	24.6	3.0 ± 5.2*

[1]Total AVE (%) = total percentage motile spermatozoa (as indicated in Table 6.3 and Table 6.4)
[2]Rapid DEF (%) = percentage rapid swimming spermatozoa calculated according to the selected default VCL intervals
[3]Rapid ADJ (%) (expected) = recalculated percentage rapid swimming spermatozoa according to the adjusted VCL intervals as expected in a good quality sperm sample (80% of total motile spermatozoa)
[4]Rapid ADJ (%) (measured) = recalculated percentage rapid swimming spermatozoa according to the adjusted VCL intervals as measured in the metabolic experiments
a, b = values labelled with different superscript letters in the same row were significantly different (P < 0.05)
*The measured percentage rapid swimming spermatozoa was lower than the expected percentage rapid swimming spermatozoa in all three repeats of the experiment

If the total percentage motile spermatozoa (Total AVE) was compared to the percentage rapid swimming spermatozoa according to the selected default VCL intervals (Rapid DEF), significant lower values were found among most of the treatments in the glucose and lactate-pyruvate media. On the other hand, when the expected percentage rapid swimming spermatozoa after adjustment of the VCL intervals (Rapid ADJ) were compared to the actual measured values for the same parameters, lower values were recorded for almost all the experimental combinations. The combinations indicated with a red background in the glucose and lactate-pyruvate-glucose media were reported as not having a significantly different total percentage motile spermatozoa compared to the control samples (P > 0.05) in Table 6.3. Similarly, the values indicated with a red background in the free and lactate-pyruvate media were originally reported as not having significantly different total percentage motile spermatozoa when the control samples for all four media were compared in Table 6.4.

Two examples of how the adjusted VCL intervals influenced the percentage rapid, medium and slow swimming spermatozoa and their sperm kinematic parameters relative to the Total AVE values are presented in Table 6.6 for the lactate-pyruvate-glucose medium.

Table 6.6. Sperm motility and kinematic parameter measurements (mean ± SD) of human spermatozoa (n = 3) in the lactate-pyruvate-glucose medium to indicate the effect of determining different motility parameters in the control and CCCP inhibited samples

LPG CONTROL	Total AVE	Rapid ADJ	Medium ADJ	Slow ADJ
Motility (%)	94.6 ± 2.3	74.4 ± 3.5	16.2 ± 3.1	4.0 ± 1.3
VCL (μm/s)	106.0 ± 8.5	118.2 ± 10.0	68.1 ± 1.0	25.2 ± 9.0
VSL (μm/s)	49.3 ± 6.9	55.9 ± 8.2	28.0 ± 3.3	6.8 ± 4.5
VAP (μm/s)	61.6 ± 5.2	68.7 ± 6.2	39.4 ± 0.9	12.0 ± 4.4
LIN (%)	46.5 ± 4.8	47.3 ± 5.0	41.2 ± 5.5	25.0 ± 7.6
STR (%)	79.8 ± 5.1	81.1 ± 5.2	71.0 ± 6.8	52.4 ± 15.5
WOB (%)	58.1 ± 2.6	58.2 ± 2.9	57.8 ± 2.1	47.7 ± 0.5
ALH (μm)	3.2 ± 0.6	3.3 ± 0.6	1.7 ± 0.6	
BCF (Hz)	15.7 ± 2.2	16.1 ± 2.2	10.7 ± 4.5	

| LPG CCCP	Total AVE	Rapid ADJ	Medium ADJ	Slow ADJ
Motility (%)	89.6 ± 7.8	42.2 ± 12.5	39.1 ± 11.7	8.2 ± 4.3
VCL (μm/s)	82.5 ± 7.1	104.5 ± 1.5	68.8 ± 2.0	35.5 ± 4.0
VSL (μm/s)	32.3 ± 4.4	40.5 ± 4.7	27.4 ± 2.7	8.2 ± 2.9
VAP (μm/s)	44.4 ± 3.4	54.7 ± 3.3	38.5 ± 0.7	18.7 ± 3.3
LIN (%)	39.0 ± 2.4	38.8 ± 4.2	39.7 ± 2.8	23.2 ± 7.2
STR (%)	72.4 ± 4.8	74.0 ± 5.6	71.0 ± 5.5	43.5 ± 7.7
WOB (%)	54.0 ± 2.0	52.3 ± 2.5	56.0 ± 0.7	52.5 ± 7.1
ALH (μm)	3.0 ± 0.3	3.2 ± 0.3	2.4 ± 0.1	
BCF (Hz)	11.9 ± 1.3	12.5 ± 1.3	10.2 ± 1.8	

VCL = curvilinear velocity, VSL = straight-line velocity, VAP = average path velocity, LIN = linearity, STR = straightness, WOB = wobble, ALH = amplitude of lateral head displacement, BCF = beat cross frequency, AVE = average, ADJ = adjusted

Comparing the kinematic parameters of the Total AVE and the Rapid ADJ spermatozoa in both the control and CCCP inhibited samples, revealed similar values for these two groups. The unique kinematic parameters for each of the swimming speed classes (sperm subpopulations) also seem similar between the two treatments. As was noted in Table 6.5, the difference in the percentage motile spermatozoa in the Total AVE and Rapid ADJ groups can clearly be seen, e.g. 89.6% vs 42.2% in the CCCP inhibited sample. Another important factor that was revealed when the adjusted swimming speed class values were determined, was the shift in the percentage motile spermatozoa that was grouped into each class. The control samples (74% rapid, 16% medium and 4% slow) had a higher percentage rapid swimming

spermatozoa compared to the CCCP inhibited samples (42% rapid, 39% medium and 8% slow).

Summary of sperm metabolism results

Figure 6.6 summarizes the most important results reported in the previous paragraphs, tables and figures of section 6.3. The total percentage motile spermatozoa, percentage rapid swimming spermatozoa (Rapid ADJ), VCL and ATP production (% of LPG control) of all the experimental combinations are illustrated in Figure 6.6.

6.4 Discussion

Mammalian spermatozoa generate energy intracellularly and expend most of the ATP produced to sustain motility. This is not surprising, especially for internal fertilizing species, where sperm motility is an essential function of the ability of spermatozoa to transport their genetic material to the fertilization site. The generation of ATP and its effective utilization in spermatozoa therefore play an important role in male fertility.

Sperm motility and ATP production were subsequently selected as the two main parameters in this study to indicate the importance of different metabolic pathways in human sperm metabolism. Most previous studies on mammalian sperm metabolism also measured these two parameters as well as oxygen uptake or consumption as an indication of actively respiring spermatozoa (see Storey, 2008 for a review of earlier methods employed). Additionally, the current study also included the use of CASA for the objective measurement of various sperm kinematic parameters. It could therefore be determined if these sperm kinematic parameters were influenced by the inhibition of different metabolic pathways and if it correlates to changes detected in human sperm motility.

All the combinations of the metabolic inhibitors and four different media (as indicated in able 6.2) presented the possibility to test which metabolic pathway, namely glycolysis, OXPHOS, or the combination of these pathways would maintain sperm motility and ATP production. These two pathways and their combinations were evaluated at least twice during all the experiments as indicated in Table 6.2. A discussion of these expected results and the actual measurements presented in section 6.3 will follow in the next few paragraphs.
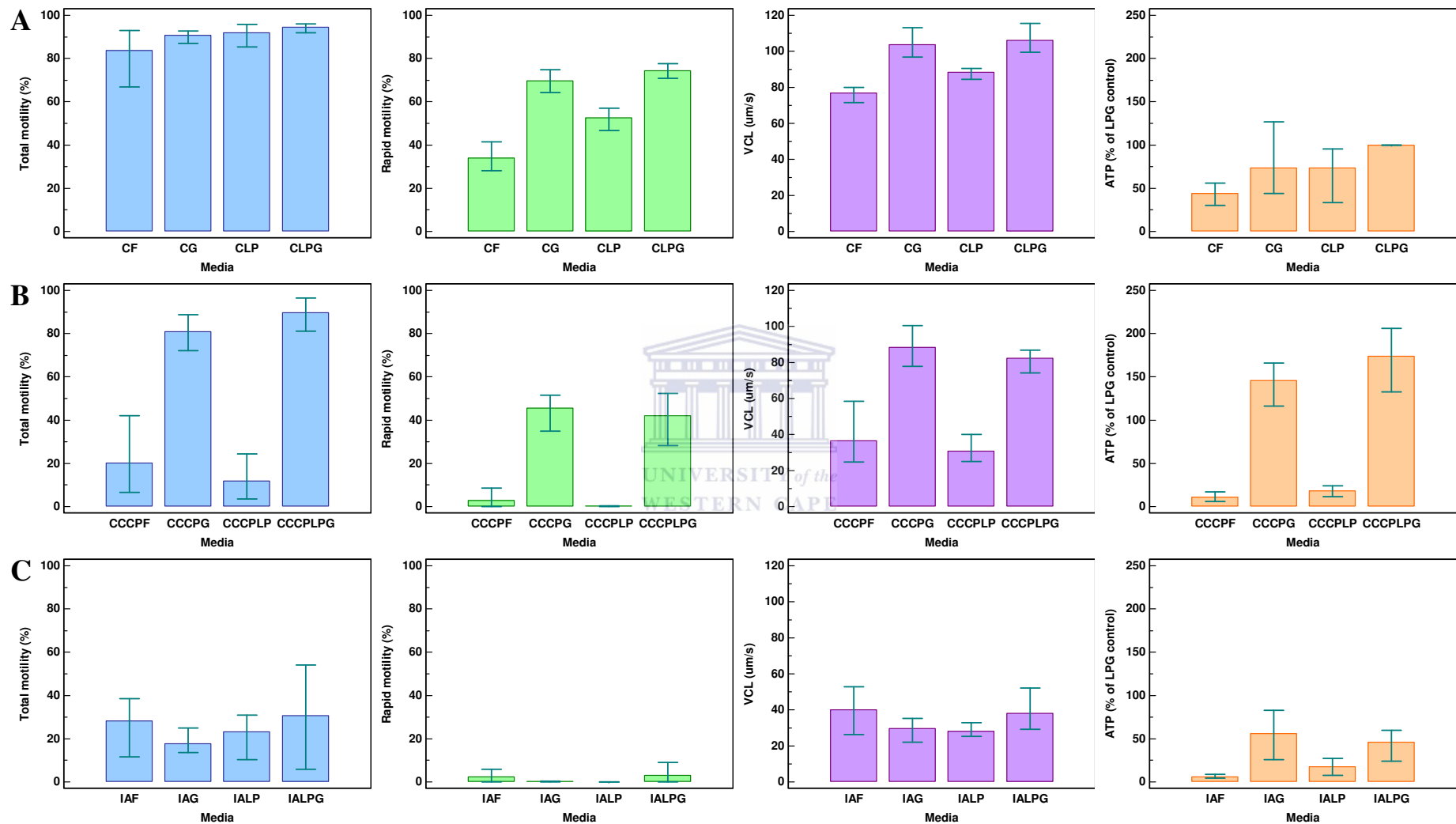
Figure 6.6. The effects of two metabolic inhibitors and four different media on various sperm parameters evaluated for human spermatozoa. **A**) Control samples, **B**) Inhibition with CCCP, **C**) Inhibition with IA. The data is presented as mean values and the bars are indicating the range of the actual values. The actual values of these parameters and the statistical significance of the data are presented in Table 6.3, 6.4 and 6.5. The Rapid motility parameter refers to the percentage rapid swimming spermatozoa after the VCL intervals were adjusted. F = free medium, G = glucose medium, LP = lactate-pyruvate medium, LPG = lactate-pyruvate-glucose medium.

Firstly, in the free medium, the absence of any metabolic substrates technically meant that there would be no activity in either the glycolytic or OXPHOS pathways, unless endogenous substrates (part of or inside the spermatozoa) could be used for metabolic reactions. The high total percentage motile spermatozoa and the moderate ATP production in the control sample compared to the inhibited samples was an indication that both glycolysis and OXPHOS were probably taking place. This maintenance of sperm motility in the absence of seminal plasma or other metabolizable substrates by "endogenous respiration" has been reported in many earlier studies on human and other mammalian spermatozoa (Nevo, 1965, 1966; Mann and Lutwak-Mann, 1981; Ford and Harrison, 1981). Ford and Harrison (1981) as well as Williams and Ford (2001), however, reported that sperm motility began to decline within the first hour in the absence of metabolic substrates. In the present study it was also found that although sperm motility seemed to be maintained, the sperm kinematic parameters and ATP production was lower when compared to the control samples of the glucose or lactate-pyruvate-glucose medium. In studies on boar and rhesus monkey spermatozoa, it was found that if spermatozoa were unable to use glucose or lactate for metabolism, the levels of carnitine and acetylcarnitine significantly increased (Jones and Bubb, 2000; Lin *et al.*, 2009). These two metabolites are associated with the mitochondrial oxidation of fatty acids. The fact that spermatozoa can metabolize lipids for energy production is well-known and some evidence exist that spermatozoa make use of phospholipids for endogenous respiration (Mann and Lutwak-Mann, 1981; Jones and Bubb, 2000).

In the control sample of the glucose medium, it was expected that both glycolysis and OXPHOS would be active since the products of the glycolytic pathway, namely pyruvate and lactate, can be metabolized in the mitochondria by OXPHOS. Thus, both these pathways were involved in the high percentage motile spermatozoa and sperm kinematic parameters measured in the control sample. The CCCP inhibited sample, however, would only be able to produce ATP for sperm motility through glycolysis, since pyruvate and probably lactate produced by glycolysis can theoretically not be utilized by the CCCP-inhibited mitochondria. Although both the total percentage motile spermatozoa and the sperm kinematic parameters were lower in the CCCP inhibited than in the control sample, this decline was not significant and therefore it can be concluded that glycolysis could maintain sperm motility. This fact was confirmed by the inhibition of the glycolytic pathway by IA that resulted in significantly lower values of almost all the parameters measured. Numerous previous studies on human and other mammalian spermatozoa reported similar results when either glycolysis or

155

OXPHOS was inhibited in media containing glucose (Suter *et al.*, 1979; Mukai and Okono, 2004; Hung *et al.*, 2008).

The lactate-pyruvate medium was included in this study to create conditions where the spermatozoa would only be able to produce ATP for sperm motility through OXPHOS. Thus, the high total percentage of motile spermatozoa in the control sample of this medium indicated that OXPHOS could maintain sperm motility. The swimming speeds (VCL, VSL, and VAP) were, however, more comparable to the control sample of the free medium and significantly lower than the controls of the two glucose-containing media. Nascimento *et al.* (2008a) also found a decrease in the VCL of human sperm when OXPHOS was inhibited by Antimycin A in media containing pyruvate and lactate compared to media containing glucose. When mitochondrial respiration was inhibited by CCCP, all the parameters measured in the current study had extremely low values, as was expected and reported previously (Mukai and Okuno, 2004). The inhibition of glycolysis by IA in this medium was not expected to have any effect since this pathway would not be able to metabolize the lactate and pyruvate available (it will only be able to metabolize an endogenous source of glucose, if present). Surprisingly, the values of all the parameters decreased significantly and were similar to the values of the CCCP inhibited sample. This effect in the absence of glucose was also reported by Nascimento *et al.* (2008a) for human spermatozoa inhibited by DOG, but not for rhesus monkey spermatozoa inhibited by α-chlorohydrin (ACH) (also an inhibitor of GAPDH) (Hung *et al.*, 2008) or mouse sperm inhibited by IA (Pasupuleti, 2007). The reason for the difference in the findings of the present study compared to that of Pasupuleti (2007) was probably that the latter study used a much lower concentration of IA (0.5 mM). This concentration was found too low to have an effect on human sperm motility in the present study. The possible reasons for this unexpected effect of IA are mentioned below in the next part of the discussion.

The control sample of the lactate-pyruvate-glucose medium was considered as another example where both glycolysis and OXPHOS would be active. As expected, the control sample had a high total percentage of motile spermatozoa and the sperm kinematic parameters were all similar to the control sample of the glucose medium. In the CCCP inhibited sample, only glycolysis could take place and the maintenance of the high percentage motile spermatozoa indicated that this pathway could maintain sperm motility. However, several of the sperm kinematic parameter values were significantly lower than that of the control

sample. A similar decrease in the sperm swimming speeds has been detected by Hung *et al.* (2008) when rhesus monkey spermatozoa were inhibited with pentachlorophenol (another inhibitor of OXPHOS) in glucose-containing media. The inhibition of glycolysis by IA in the lactate-pyruvate-glucose medium would still leave the OXPHOS pathway active, especially since both lactate and pyruvate would be available for mitochondrial respiration. The decrease in both the total percentage motile spermatozoa and almost all the sperm kinematic parameters were thus unexpected. Technically this meant that OXPHOS could not maintain sperm motility and was similar to the results reported above for the IA inhibition in the lactate-pyruvate medium. These results, however, contradicted the results reported for the control sample of the lactate-pyruvate medium.

The use of IA for inhibition of sperm metabolism has been reported as early as the 1940's (Lardy and Phillips, 1941; O'Donnell and Ellory, 1970). IA and a related molecule, iodoacetic acid, are also well-known inhibitors of glycolysis and ATP production in studies on the effect of hypoxia and ischemia in various tissues, e.g. liver, heart and nervous system (Dawson *et al.*, 1993; Webster *et al.*, 1994; Corbett and Lees, 1997). The fact that IA inhibits the GAPDH enzyme in the glycolytic pathway means that it should have the same effect on sperm metabolism as that which has been reported for ACH. The results of the IA inhibition in both glucose-containing media of the present study compared to previous studies with ACH, show that the results were indeed similar (a decrease in sperm motility was reported when inhibited by IA or ACH in glucose-containing media) (Ford and Harrison, 1981; Hung *et al.* 2008). These results have, however, been much debated in recent review articles on sperm metabolism (Ford, 2006; Ruiz-Pesini *et al.*, 2007; Storey, 2008). The main contentions about the use of inhibitors of GAPDH or sperm-specific GAPDHs knockout mice have been the effect on the ATP available for sperm motility, the availability of phosphate for OXPHOS and the build-up of glycolytic intermediates.

In Figure 6.7 the effect of ACH and IA on the glycolytic pathway is indicated. If GAPDH is inhibited, it technically means that the ATP-consuming reactions of glycolysis can still take place, but not the ATP-generating reactions. It was shown by Miki *et al.* (2004) in GAPDHs knockout mice that there was a build-up of glycolytic intermediates upstream of GAPDH in the presence of glucose, indicating that the first few steps of glycolysis was still taking place. The question is thus: what source of ATP is used for the first few steps of glycolysis? If the only other source of ATP production is OXPHOS, there is a possibility that these ATP

molecules could be used by glycolysis (Ruiz-Pesini *et al.*, 2007). The point of contention is therefore between two possibilities. On the one hand, are the decreases in sperm motility and ATP production reported when glycolysis was inhibited by ACH and IA due to glycolysis being essential to maintain sperm motility? Or on the other hand, is it due to the fact that the ATP from OXPHOS was depleted by glycolysis? Another possibility mentioned by Ford (2006) was that it might not be ATP itself that is depleted by the futile steps of glycolysis but rather that it competes with OXPHOS for the phosphate present in spermatozoa to produce more ATP molecules. The inhibition of the glycolytic pathway by DOG (see Figure 6.1) could have a similar effect on the ATP levels due to the fact that the reaction producing DOG-6-P uses ATP (Ford, 2006; Pasupuleti, 2007).
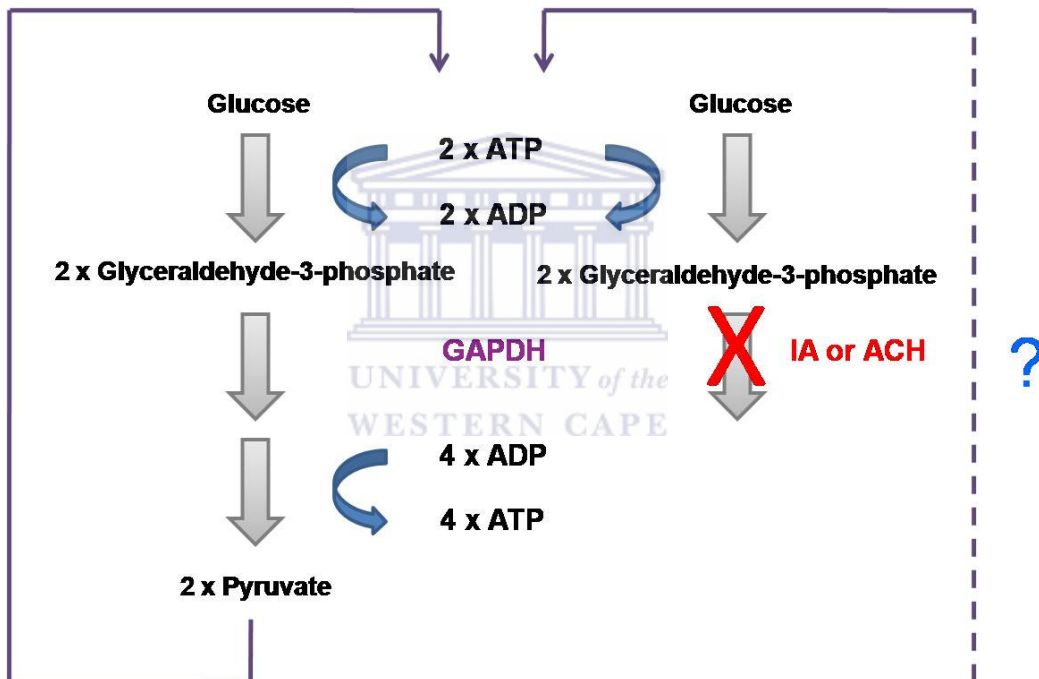
Figure 6.7. Schematic presentation of glycolysis and the effect of the inhibition of glyceraldehyde-3-phosphate dehydrogenase (GAPDH). The left side of the diagram indicates the ATP-consuming and ATP-producing phases of glycolysis. The right side of the diagram indicates that the ATP-producing phase of glycolysis is eliminated by the inhibition of GAPDH. (Modified from Ruiz-Pesini *et al.*, 2007)

The above arguments could clearly explain why IA caused a decrease in all the sperm motility parameters in the current study. The only result which could not be explained, however, was the effect of IA inhibition in the lactate-pyruvate medium where glycolysis is not supposed to be active. One possible explanation could be that the concentration of IA was too high in the present study (see above comparison with Pasupuleti, 2007) and therefore a significant effect was experienced on sperm motility in all the media. Alternatively IA might have a detrimental effect on spermatozoa that was more severe than just the inhibition of glycolysis. Due to the

158

fact that IA binds covalently with the sulfhydryl group of cysteine (Anson, 1940), it is possible that a high concentration of IA can have a detrimental effect on the disulfide bonds present in the nucleus, connecting piece, fibrous sheath and mitochondria of mammalian spermatozoa (Calvin and Bedford, 1971; Sutovsky *et al.*, 1997). Accordingly it might be problematic to find the accurate cut-off point where a specific concentration of IA will inhibit glycolysis but does not also cause damage to the cell or organelle membranes. Finally, although there is no evidence for such an effect at this point in time, the inhibition of GAPDH by IA might have an influence on the lactate-pyruvate shuttle (as discussed below and proposed in Figure 6.8) which could affect the use of lactate and pyruvate for mitochondrial respiration.

Taking all the effects of the IA inhibitions into consideration, it is evident from the present study that all possible combinations of media and inhibitors should be evaluated. If only the glucose media were used in the current study, the main conclusion would have been that glycolysis is essential for sperm motility, as was reported in previous studies (Mukai and Okuno, 2004; Miki *et al.*, 2004). With IA seemingly not being a reliable inhibitor to test whether OXPHOS could maintain sperm motility, the only evidence for this could be gathered from the control sample of the lactate-pyruvate medium.

The low levels of ATP produced in the free medium, especially with the CCCP and IA inhibition was expected and also reported in previous studies (Williams and Ford, 2001; Mukai and Okuno, 2004). Similar concentrations of ATP produced in the control samples of the glucose and lactate-pyruvate media could be another indication that OXPHOS alone can produce enough energy to sustain sperm motility. The extremely high concentration of ATP produced in the glucose-containing media relative to their control samples (ATP % Own Control) was surprising. Mukai and Okuno (2004) reported ATP levels in CCCP inhibited mouse spermatozoa in glucose-containing media to be similar to but not higher than the control samples. According to Duchen (1999), the intact ETC responds to the MMP depolarization caused by CCCP by consuming oxygen at a maximal rate, but there is no driving force for the synthesis of ATP. It can therefore only be speculated that since glycolysis was the only active pathway under these conditions, the loss of ATP produced by the mitochondria was compensated for by increasing the rate of glycolysis and thus ATP production. Although the IA inhibited samples produced lower levels of ATP than their own controls, these ATP levels were still higher than that in the free and lactate-pyruvate media.

159

This can partly be explained by previous studies which have reported that the inhibition of glycolysis with DOG or ACH resulted in a decrease in the ATP levels, but that the mitochondrial activity was still high (Mukai and Okuno, 2004; Hung *et al.*, 2008; Nascimento *et al.*, 2008a). This could possibly mean that the mitochondria were still producing ATP, but that these inhibitors (DOG, ACH and IA) had an effect on the ATP levels (as explained above and proposed in Figure 6.7).

Evaluation of sperm motility according to different motility parameters may present different conclusions when comparing the total percentage motile spermatozoa with the percentage rapid swimming spermatozoa. Firstly, in the control samples of all four media, it was found that according to the total percentage motile spermatozoa, all media and their associated active metabolic pathways (glycolysis and/or OXPHOS) could maintain sperm motility. However, in both the control samples of the free and lactate-pyruvate media the lower than expected percentage rapid swimming spermatozoa was an indication that OXPHOS alone could not maintain sperm motility for an extended period of time. The significant decreases in the swimming speed parameters reported in these control samples thus corresponded to lower percentage rapid swimming spermatozoa rather than to the total percentage motile spermatozoa. Secondly, in the CCCP inhibited samples of the two glucose-containing media, these media and their associated active metabolic pathway (glycolysis) could maintain sperm motility according to the evaluation of the total percentage motile spermatozoa. However, the lower than expected percentage rapid swimming spermatozoa in these two samples was also an indication that glycolysis alone could not maintain sperm motility for an extended period of time. Once again the decrease in the swimming speed parameters (VCL, VSL, and VAP) of the lactate-pyruvate-glucose medium corresponded to this lower percentage rapid swimming spermatozoa. A similar decrease in the percentage rapid progressive swimming spermatozoa ($\leq 50\%$) was reported by St John *et al.* (2005) when human spermatozoa were treated with rotenone, potassium cyanide and oligomycin as inhibitors of OXPHOS in a medium containing 2 mM glucose (representative of the concentration in the female reproductive tract). It is evident from the above that the percentage rapid swimming spermatozoa might be a more reliable parameter to detect changes in sperm motility than the total percentage motile spermatozoa. The example of the shift in the percentage rapid, medium and slow swimming spermatozoa of the inhibited CCCP sample compared to the control also indicated the value of rather evaluating sperm subpopulations than the total sperm population (as mentioned in Chapter 5).

Another important fact revealed by the above comparison in motility parameters was that neither glycolysis nor OXPHOS seemed to be able to maintain sperm motility when it was the only active metabolic pathway available. On the other hand, when both these metabolic pathways were active, as seen in the control samples of the glucose-containing media, both the percentage motile spermatozoa and the kinematic parameters remained high. Thus, although both glycolysis and OXPHOS can essentially produce ATP for sperm motility independent of one another, it seems that both these pathways need to work together in order to maintain sperm motility in human spermatozoa for an extended period of time. A previous study on human spermatozoa has also reported that sperm velocities were highest when both glucose and lactate were available in the media (Yeung *et al.*, 1996).

A link between glycolysis and OXPHOS as evident from the literature is the presence of a lactate-pyruvate shuttle in spermatozoa of various mammalian species, e.g. rabbit, boar, bull and rat (Storey and Kayne, 1977; Calvin and Tubbs, 1978; Gallina *et al.*, 1994). Figure 6.8 is a schematic representation of the proposed functioning of the lactate-pyruvate shuttle in human spermatozoa.
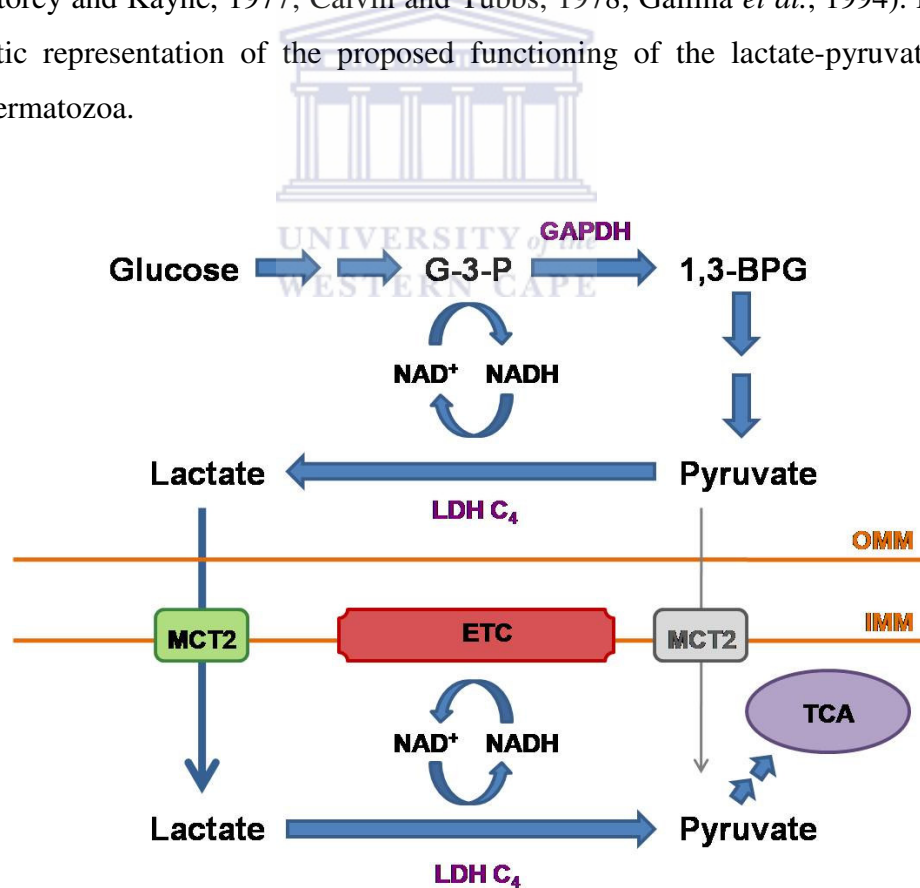
Figure 6.8. Schematic presentation of the proposed lactate shuttle in spermatozoa. The operation of this shuttle would deliver both hydrogen atoms and lactate into mitochondria for oxidation. MCT2 can transport both lactate and pyruvate across the IMM. G-3-P = glyceraldehyde-3-phosphate, 1,3-BPG = 1,3-bisphosphoglycerate, GAPDH = glyceraldehydes-3-phosphate dehydrogenase, LDH C_4 = lactate dehydrogenase C_4, MCT2 = monocarboxylate transporter 2, ETC = electron transfer chain, TCA = tricarboxylic acid cycle, OMM = outer mitochondrial membrane, IMM = inner mitochondrial membrane.

These spermatogenic lactate shuttles are, similar to lactate shuttles in other tissues, necessary to transport hydrogen atoms produced in the cytosol (present in the form of NADH), e.g. through glycolysis, into the mitochondria for utilization by the ETC. At the same time, this shuttle system assists in maintaining a constant supply of cytosolic NAD^+ to sustain oxidation of substrates in the cytosol as well as to prevent a build-up of lactate. The fact that this shuttle-system exists in mammalian spermatozoa has been supported by numerous studies that found the sperm-specific enzyme LDH C_4 to be present in both the cytosol and inside sperm mitochondria (see Fig. 6.8 and review by Gladden, 2004). It was also reported that a monocarboxylate transporter (MCT), namely MCT2, was present on sperm tails and could therefore possibly transport lactate (and pyruvate) across the inner mitochondrial membrane (Garcia *et al.*, 1995). Although no reports have been found in the literature that this lactate-pyruvate shuttle exists in human spermatozoa, the LDH C_4 enzyme is present in human spermatozoa (Burgos *et al.*, 1979).

Brooks *et al.* (1999) reported that the presence of intracellular lactate shuttles requires that glycolysis and OXPHOS be viewed as linked pathways as opposed to two alternative processes. This could possibly also be the case in human and other mammalian spermatozoa. Interestingly, the lactate-pyruvate shuttle seems to be absent in mouse spermatozoa (Gallina *et al.*, 1994) and this species uses a branched-chain 2-hydroxy acid/2-oxo acid shuttle and LDH C_4 to transport hydrogen atoms into their mitochondria (Gerez de Burgos, 1978; Coronel *et al.*, 1986). Although only speculative, this could possibly mean that glycolysis and OXPHOS are operating more independently in mouse spermatozoa and indicates why glycolysis may be the preferred pathway in the spermatozoa of this species. Another often forgotten factor that would determine the importance of these two pathways is the substrates that are available to the spermatozoa in the female reproductive system (Storey, 2008). In their review of the role of mitochondria in sperm function, Ruiz-Pesini *et al.* (2007) have mentioned that the high levels of lactate (relative to glucose and to blood plasma) in the uterus and oviducts of human, swine and mouse supports the important role of lactate and thus OXPHOS as energy source for spermatozoa.

The question which still remains is whether diffusion is sufficient enough to deliver the ATP produced by the mitochondria to the end of the principal piece for generation of the flagellar beat. Certain protein kinase (enzyme) shuttles have been proposed to transfer ATP away from and return ADP to the mitochondria (see Figure 6.9 and review by Ford, 2006). These shuttles

would eliminate the need for diffusion to deliver the ATP molecules to the distal end of the sperm flagellum. Relatively high concentrations of creatine phosphate and creatine phoshokinases have been reported in invertebrate sperm which could provide a shuttle for ATP along the sperm flagellum (Ellington and Kinsey, 1998). Although mammalian sperm only contain low concentrations of creatine phosphate, various kinase enzymes, e.g. creatine phosphokinase, adenylate kinase and 3-phosphoglycerate kinase, are present in human and other mammalian spermatozoa (Ford, 2006). Recent reports of the localization of various protein kinases and ATP carrier proteins to either the midpiece or to both the principal piece and midpiece of human and mouse spermatozoa might be indicative of the operation of such shuttle systems in mammalian spermatozoa (Reinton *et al.*, 2000; Cao *et al.*, 2006; Kamp *et al.*, 2007; Kim *et al.*, 2007; Nakamura *et al.*, 2008). Many of these proteins are also important regulators of ATP production during glycolysis or associated with glycolytic enzymes. This could possibly mean that glycolysis and OXPHOS are also linked processes on a different level, namely the machinery for the one process (glycolysis) can also be used by the other (OXPHOS) to distribute its products (ATP molecules).
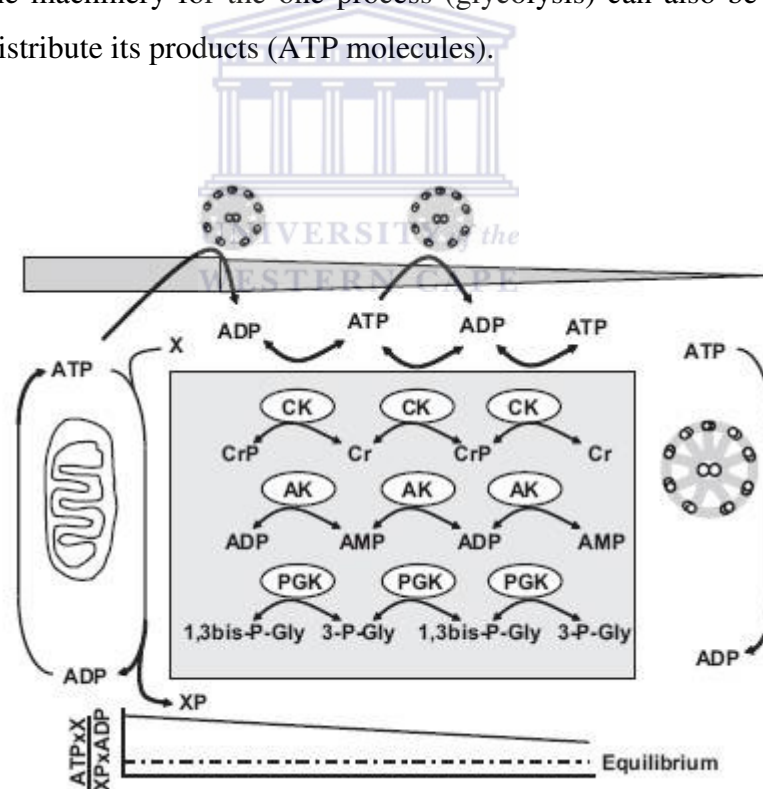
Figure 6.9. Schematic presentation of potential ATP shuttles in the sperm flagellum. ATP produced by the mitochondria is hydrolyzed to ADP along the flagellum to provide energy for flagellar bending. ADP is then re-phosphorylated to ATP by transfer of phosphate from creatine phosphate (CrP), ADP or 1,3-bisphospho-glycerate (1,3bis-P-Gly). These enzymatic reactions are catalyzed by creatine kinase (CK), adenylate kinase (AK) or 3-phosphoglycerate kinase (PGK) and the enzymes operate close to equilibrium. The ATP generated by OXPHOS in the midpiece can support motility or the phosphorylation of creatine (Cr), AMP or 3-phospho-glycerate (3-P-Gly) (indicated as X). The net effect is to establish a gradient of disequilibrium of the kinase reactions (XP + ADP ↔ ATP + X) along the flagellum in order to sustain the ATP concentration at the distal end of the flagellum. This will eliminate the need for diffusion of ATP over long distances. (From Ford, 2006)

In conclusion, it was found that neither glycolysis nor OXPHOS alone can maintain sperm motility for an extended period of time in human spermatozoa. The highest values for the percentage motile spermatozoa, sperm kinematic parameters and ATP production were found when both these pathways were active. The results of the present and numerous previous studies suggest that a link does exist between glycolysis and OXPHOS in mammalian spermatozoa. The importance of the selection of media containing various metabolic substrates and appropriate inhibitors of the different pathways for metabolic studies were highlighted. It is proposed that evaluating the total percentage motile spermatozoa in metabolic studies was not sufficient to indicate changes in sperm motility. The evaluation of different subpopulations of spermatozoa or sperm swimming parameters resulted in more reliable and comparable data. The fact that sperm mitochondria seem to play a role in sperm motility indicates the importance of these organelles as structural components of mammalian spermatozoa and it confirms that sperm mitochondria are related to sperm function in terms of sperm motility. Finally, it is suggested that both glycolysis and OXPHOS play an important role in human sperm motility and that neither of these processes are predominant or mutually exclusive.
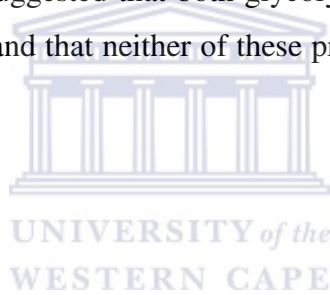
CHAPTER 7: The relationship of sperm mitochondria and the sperm midpiece to sperm form and function in selected mammalian species

7.1 Introduction

An enormous variation in sperm size and shape across all animal taxa has been reported by numerous studies. A quest for understanding the adaptive significance of these variations has resulted in more in-depth studies on the size and structure of different sperm components during the past few decades. Such comparative studies usually aim to determine how the variation in sperm structure among species contributes to the differences in sperm function (Pitnick *et al.*, 2009).

The purpose of the present study was to conduct a comparative investigation into the variation of the size of different sperm components while only including a selected group of mammalian species (Chapter 3). Furthermore, one component of the spermatozoon, namely the midpiece and its mitochondria, was studied in more detail to indicate the variation in its size and structure among the different species (Chapter 4). Sperm motility measurements were used as an assessment of sperm function (Chapter 5) and the role of sperm mitochondria in sperm motility was confirmed in Chapter 6.

However, some questions still remain to be answered and will be the focus of the current chapter. Firstly, comparing the absolute and relative sizes of the different sperm components, is the sperm midpiece related to the other sperm components? Secondly, are there relationships among the structure, arrangement and activity of the sperm mitochondria, the size of the other sperm components and the sperm swimming characteristics? Finally, given the measurements of various sperm midpiece and mitochondrial parameters, can these parameters predict the values of specific sperm morphometry or sperm motility parameters and if so, which of the midpiece and/or mitochondrial parameters play the most important part?

The main aim of the current chapter was therefore to determine the relationships among the sperm mitochondria and midpiece morphometry measurements, the dimensions of the other sperm components and the motility parameters by using various statistical exploratory graphs and statistical models.

7.2   Materials and methods

7.2.1   Comparative data included from previous chapters

The data of the seven mammalian species used in the current chapter to perform various statistical analyses was reported and discussed in Chapters 3-5. The absolute and relative values of various sperm morphometry parameters were presented in Table 3.4 and 3.5 respectively. The absolute midpiece morphometry and flow cytometry measurements were presented in Table 4.1 while Table 4.2 included the relative midpiece morphometry measurements. Only the sperm kinematic parameter values measured at 50 frames/second for the seven mammalian species (top part of Table 5.7) were included as sperm motility parameters for the statistical analyses included in the current chapter.

7.2.2   Statistical analysis

The STATISTICA data analysis software system, version 10 (StatSoft Inc.), was used for all the statistical analyses mentioned below.

Biplots

Principal component analysis (PCA) biplots were constructed for different subsets of the data mentioned above in section 7.2.1. These biplots were used to determine the distribution of the six or seven species with regards to certain sperm parameters. An indication of the correlation between various sperm parameters were also portrayed in these graphs. Biplots are a type of exploratory graph used in statistics that allows information on both the cases (e.g. seven mammalian species) and variables (e.g. sperm parameters) of a data matrix to be displayed graphically. In the biplots constructed for the current study, cases are displayed as points while variables are displayed as linear axes. The arrangement of the points in a biplot results in the recognition of groups containing similar values for the variables portrayed. The angles between the projected axes in the biplot are an indication (not an exact estimation) of the correlation between different variables, with smaller angles between axes implying higher correlations. The direction of the axes is also an indication of whether two variables are positively (axes point in same direction) or negatively (axes point in opposite directions) correlated. The relative values of the cases for a specific variable can be obtained by projecting the case onto the variable (drawing a line from the case point perpendicular to the variable).

Correlation coefficients

The correlations between sperm parameters were determined by making use of the Spearman rank correlation coefficient (r). Since the main focus of the current study was to determine the relationship between the midpiece parameters and the other sperm parameters, only the correlations between ten midpiece parameters and all the other sperm parameters mentioned in 7.2.1 were determined. The ten midpiece parameters included eight of the parameters presented in Table 4.1 (total number of gyres, mitochondrial height, radius of midpiece (r_b), thickness of the mitochondrial sheath ($r_b - r_a$), midpiece length, midpiece volume, straight-line midpiece length (SLMPL) and flow cytometry). Midpiece ellipticity was included as a ninth midpiece parameter due to the variation in this parameter reported for all seven species in Chapter 3 and because it is an indication of the two-dimensional shape of the sperm midpiece. Due to the proposed importance of using relative rather than only absolute parameters (see discussion sections of Chapters 3 and 4), the ratio of midpiece volume to head length (MPV/HL) was included as the tenth midpiece parameter.

Multiple regression analysis

A multiple regression analysis was used to determine the relationship between various dependant variables (21 selected sperm parameters) and independent or predictor variables (seven midpiece parameters). The selected sperm parameters included various sperm morphometry parameters and all the sperm motility parameters. The regression coefficient (R^2) as well as the beta coefficient (b*) was calculated. Beta coefficients are standardized coefficients that result from an analysis performed on variables that have been standardized so that they have variances of 1. This standardization assists in determining which of the independent variables have a greater effect on the dependent variable in multiple regression analysis, when the variables are measured in different units of measurement. Due to the fact that all seven midpiece parameters were not determined for the naked mole-rat spermatozoa, this species was not included in the multiple regression analysis or redundancy analysis.

Redundancy analysis

A redundancy analysis was performed to serve as a summary of all the different regression analyses performed. In this analysis, the dependent variables are plotted in a similar fashion as for the biplots, but the principal component axes were constrained to run in the direction of the predictor variables. The resulting graph depicts the predictor variable directions with the dependent variables plotted relative to the predictor variable directions.

7.3 Results

Species distributions and sperm parameter associations

The biplot of all the absolute sperm morphometry parameters is presented in Figure 7.1 with the first two principal components explaining 87% of the variance among these parameters. The arrangement of all the individuals in the biplot resulted in the formation of several groups that represented the seven species and clearly indicated the species specificity of the sperm morphometry data. A close association was, however, found for the three non-human primate species which confirmed the similarities in their sperm morphometry reported in Chapter 3.
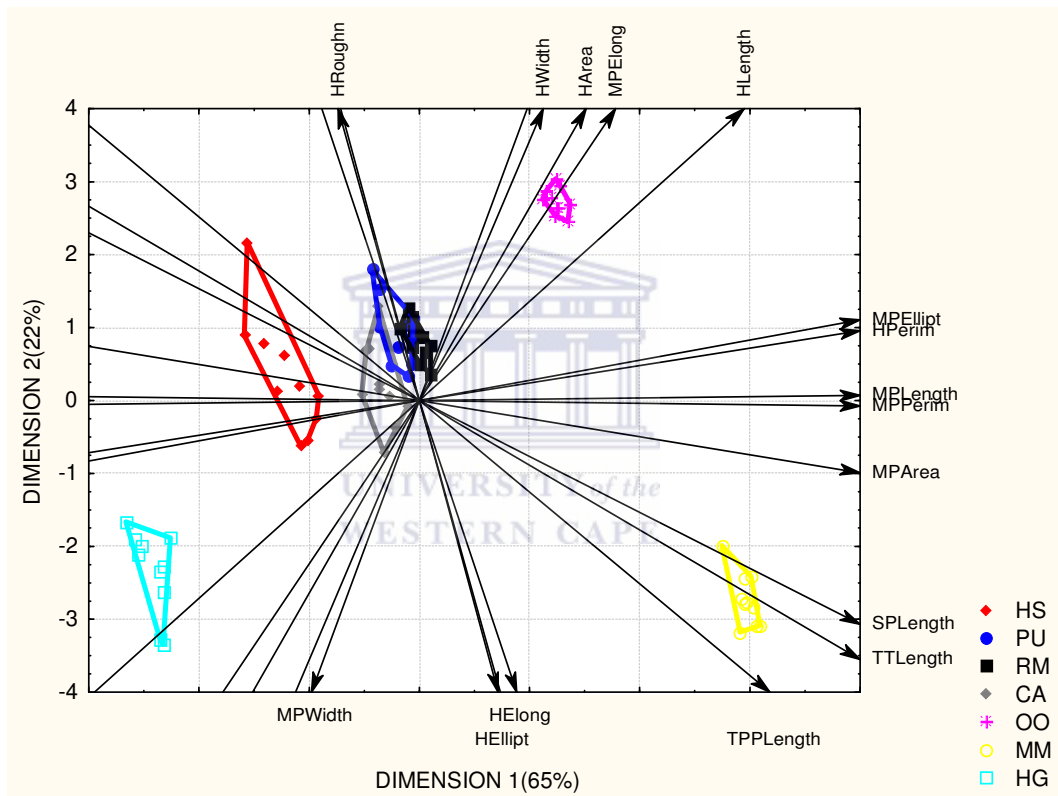
Figure 7.1. PCA biplot of absolute sperm morphometry parameters for seven mammalian species (n=10). HS = *Homo sapiens* (human), PU = *Papio ursinus* (chacma baboon), RM = *Macaca mulatta* (rhesus monkey), CA = *Chlorocebus aethiops* (vervet monkey), OO = *Ovis orientalis* (merino ram), MM = *Mus musculus* (house mouse), HG = *Heterocephalus glaber* (naked mole-rat), H = head, MP = midpiece, SP = sperm, TT = total tail, TPP = tail principal piece, Roughn = roughness, Elong = elongation, Ellipt = ellipticity, Perim = perimeter.

The distribution of the species relative to one another was due to the specific characteristics of their spermatozoa. For example, the mouse had the largest spermatozoa (highest relative value for the length of the midpiece, principal piece and total sperm), ram spermatozoa had the largest value for several sperm head parameters and the naked mole-rat spermatozoa had the lowest value for most parameters. In terms of the sperm morphometry parameters itself, the close association of most of the head and midpiece parameters respectively was probably due

to the fact that the length and width parameters were used to determine the area and perimeter parameters. Interestingly, the width of the midpiece seems to be negatively associated with head length, width and area. Furthermore, the head perimeter seemed to be associated with most of the midpiece parameters.

The biplot of the midpiece morphometry parameters is presented in Figure 7.2 with the first two principal components explaining 91% of the variance among these parameters. The naked mole-rat was not included in the construction of this biplot since the midpiece parameters were not determined for this species. Similar to Fig. 7.1, the distribution of the six species relative to each other clearly indicated the species specificity of the midpiece morphometry data for the human, ram and mouse spermatozoa. The overlap of the three non-human primate species confirmed the similarities in their midpiece parameters reported in Chapter 4.

Figure 7.2. PCA biplot of midpiece morphometry parameters for six mammalian species (n=5). HS = *Homo sapiens* (human), PU = *Papio ursinus* (chacma baboon), RM = *Macaca mulatta* (rhesus monkey), CA = *Chlorocebus aethiops* (vervet monkey), OO = *Ovis orientalis* (merino ram), MM = *Mus musculus* (house mouse), r_b = radius of the midpiece, r_a = radius of the axonemal-outer dense fiber complex, $r_b – r_a$ = thickness of the mitochondrial sheath, MPV = midpiece volume, SLMPL = straight-line midpiece length, MP = midpiece, Total # Gyres = total number of gyres, FlowCytom = flow cytometry.

Specific characteristics of the individual species' midpieces and mitochondrial sheaths were confirmed. For example, mouse spermatozoa had the longest midpiece whereas the three non-

human primate species had the thickest mitochondrial sheaths. The close association of the radius of the midpiece (r_b) and thickness of the mitochondrial sheath ($r_b - r_a$) was expected since the radius of the axoneme (r_a) was almost identical for all seven species included in the study (see Chapter 4). Furthermore, this indicated that probably only one of these parameters (r_b or $r_b - r_a$) needs to be determined in future to reveal a similar species distribution. The close association between the total number of gyres and flow cytometry and their negative association with mitochondrial height also confirmed the results of Chapter 4.

The biplot of the midpiece morphometry parameter ratios is presented in Figure 7.3 with the first two principal components explaining 95% of the variance among these parameters. Once again, the naked mole-rat was not included in the construction of this biplot. The distribution of the six species confirmed the species specificity of these parameters (as reported in Chapters 3 and 4). The close association of several related midpiece parameter ratios also indicated that only one of these ratios probably needs to be determined in future to reveal a similar species distribution.

Figure 7.3. PCA biplot of midpiece morphometry ratios for six mammalian species (n=5). HS = *Homo sapiens* (human), PU = *Papio ursinus* (chacma baboon), RM = *Macaca mulatta* (rhesus monkey), CA = *Chlorocebus aethiops* (vervet monkey), OO = *Ovis orientalis* (merino ram), MM = *Mus musculus* (house mouse), MPL = midpiece length, MPV = midpiece volume, HL = head length, HA = head area, TTL = total tail length, SPL = sperm length.

Figures 7.4 and 7.5 represent the biplots constructed for the sperm kinematic parameters of six mammalian species measured at 50 and 75 frames/second respectively. In these two figures the first two principal components explained 96-98% of the variance among these parameters. Although the arrangement of all the individuals did reveal certain groups, the boundaries of the individual species were less clear. The overlap between the baboon and vervet monkey as well as the rhesus monkey and ram confirmed the similarities in their sperm kinematic parameters as reported in Chapter 5.

The swimming speed parameters (VCL, VSL and VAP) seemed to be closely associated with each other and as a result the three derived sperm velocity parameters (LIN, STR and WOB) were also closely associated. Interestingly, the associations between the sperm kinematic parameters did not change when the measurements at 50 frames/second were compared to 75 frames/second. Thus, in all subsequent statistical analyses, only the sperm kinematic parameters measured at 50 frames/second were included. The beat cross frequency (BCF) values were not included in any of the sperm motility biplots due to the low R-squared (R^2) coefficients and thus inaccurate representation on the biplot.
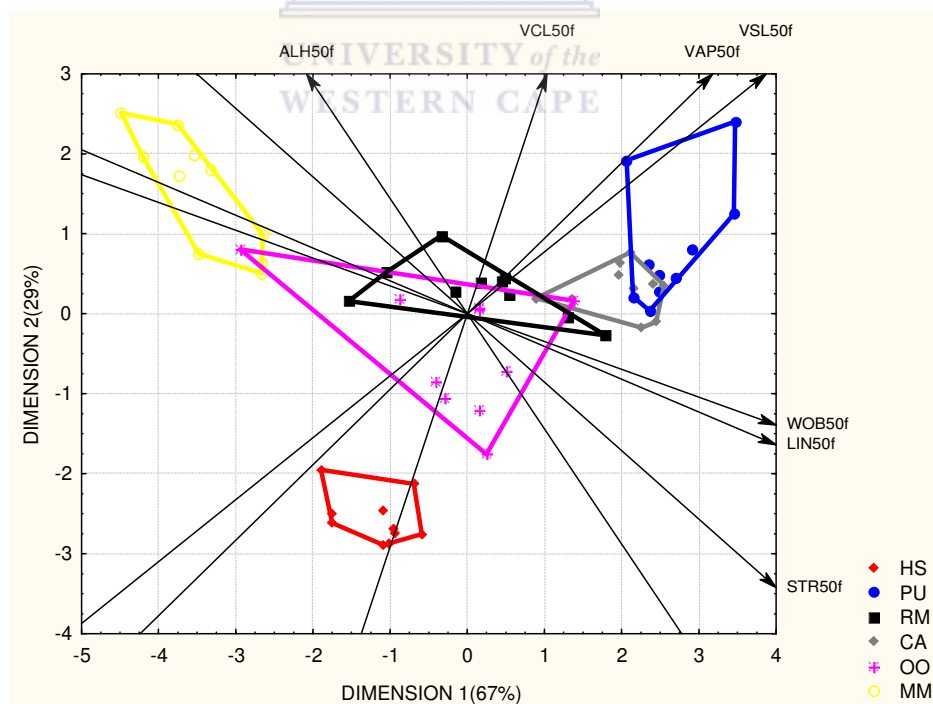
Figure 7.4. PCA biplot of sperm kinematic parameters for six mammalian species (n=10) measured at 50 frames/second. HS = *Homo sapiens* (human), PU = *Papio ursinus* (chacma baboon), RM = *Macaca mulatta* (rhesus monkey), CA = *Chlorocebus aethiops* (vervet monkey), OO = *Ovis orientalis* (merino ram), MM = *Mus musculus* (house mouse), VCL = curvilinear velocity, VSL = straight-line velocity, VAP = average path velocity, LIN = linearity, STR = straightness, WOB = wobble, ALH = amplitude of lateral head displacement, f = frames per second.

171
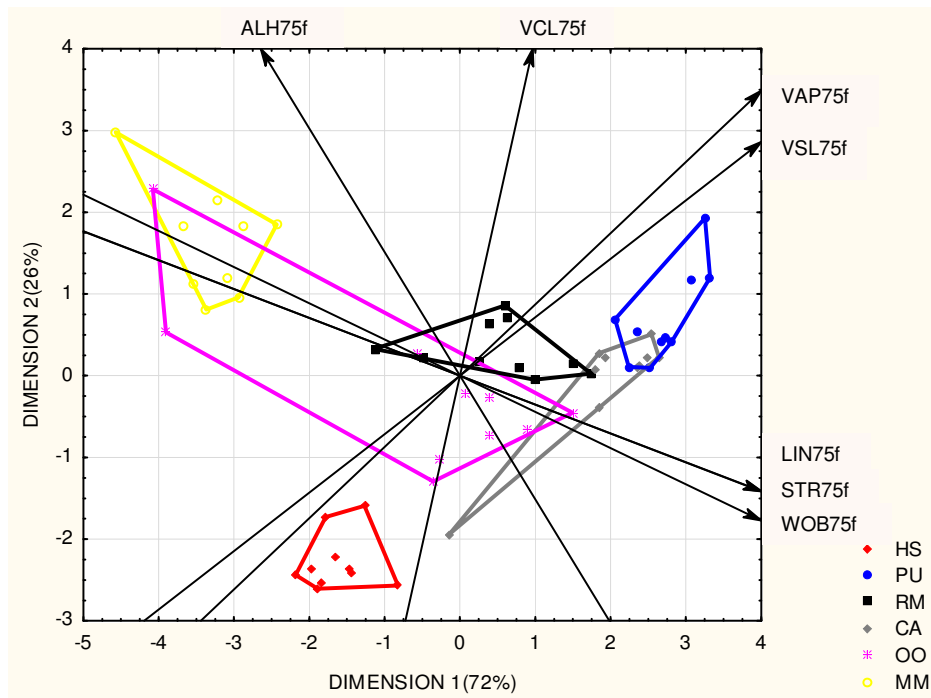
Figure 7.5. PCA biplot of sperm kinematic parameters for six mammalian species (n=10) measured at 75 frames/second. HS = *Homo sapiens* (human), PU = *Papio ursinus* (chacma baboon), RM = *Macaca mulatta* (rhesus monkey), CA = *Chlorocebus aethiops* (vervet monkey), OO = *Ovis orientalis* (merino ram), MM = *Mus musculus* (house mouse), VCL = curvilinear velocity, VSL = straight-line velocity, VAP = average path velocity, LIN = linearity, STR = straightness, WOB = wobble, ALH = amplitude of lateral head displacement, f = frames per second.

When the motility data of the naked mole-rat were also included (see Fig. 7.6), the STR became more associated with the swimming speed characteristics (VAP and VSL) than with the other derived kinematic parameters (WOB and LIN). This shift was probably due to the low straightness (STR) value (61%) of the naked mole-rat sperm swimming tracks relative to the spermatozoa of other six species (81-92%) reported in Chapter 5. The distribution of the species relative to each other was, however, similar to that in Fig. 7.4.

The fact that the biplots presented in Figs. 7.1-7.6 above confirmed the results reported in Chapters 3-5, it prompted the construction of an additional biplot that included selected sperm morphometry, midpiece morphometry and sperm kinematic parameters. The purpose of the biplot presented in Figure 7.7 was thus to determine if this statistical tool would be able to indicate relationships among the selected sperm parameters. The selection of the sperm parameters was based on the association of various sperm parameters in Figs. 7.1-7.6. For instance, if there was several sperm parameters that were closely associated, especially the related parameters (e.g. r_b and $r_b - r_a$ or MPV/HA and MPL/HA), only one of these

172

parameters were selected. The naked mole-rat was not included in this biplot due to the fact that several of the midpiece parameters were not determined for this species.

Figure 7.7 revealed similar species specificity for the sperm parameters compared to the previous biplots, due to the fact that most species could be identified as separate groups, with some overlap between the three non-human primate species. Several associations between the sperm parameters could also be identified. Examples of these include the positive and negative associations between certain morphometry and kinematic parameters, e.g. r_b and VSL, VCL and MPV/HL, ALH and midpiece length, BCF and total tail length and LIN, head length and flow cytometry. There also seemed to be an association between several of the two-dimensional head and midpiece parameters, e.g. the length and ellipticity, of both the head and midpiece.
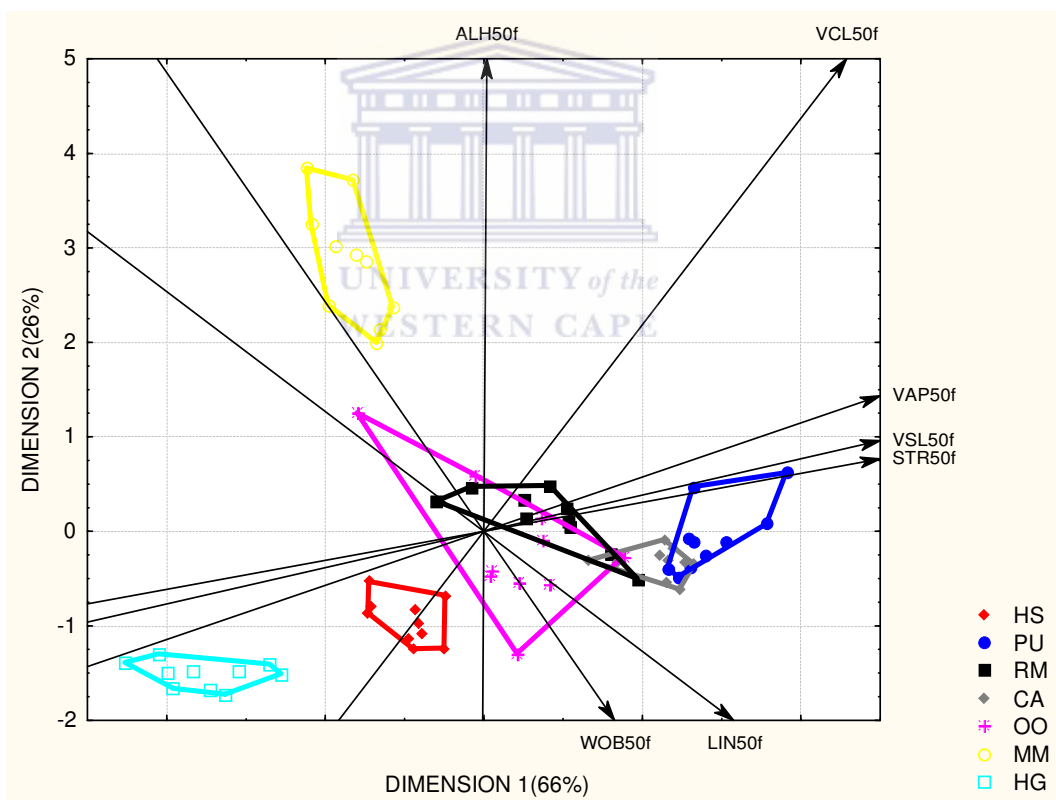
Figure 7.6. PCA biplot of sperm kinematic parameters for seven mammalian species (n=10) measured at 50 frames/second. HS = *Homo sapiens* (human), PU = *Papio ursinus* (chacma baboon), RM = *Macaca mulatta* (rhesus monkey), CA = *Chlorocebus aethiops* (vervet monkey), OO = *Ovis orientalis* (merino ram), MM = *Mus musculus* (house mouse), HG = *Heterocephalus glaber* (naked mole-rat), VCL = curvilinear velocity, VSL = straight-line velocity, VAP = average path velocity, LIN = linearity, STR = straightness, WOB = wobble, ALH = amplitude of lateral head displacement, f = frames per second.

173
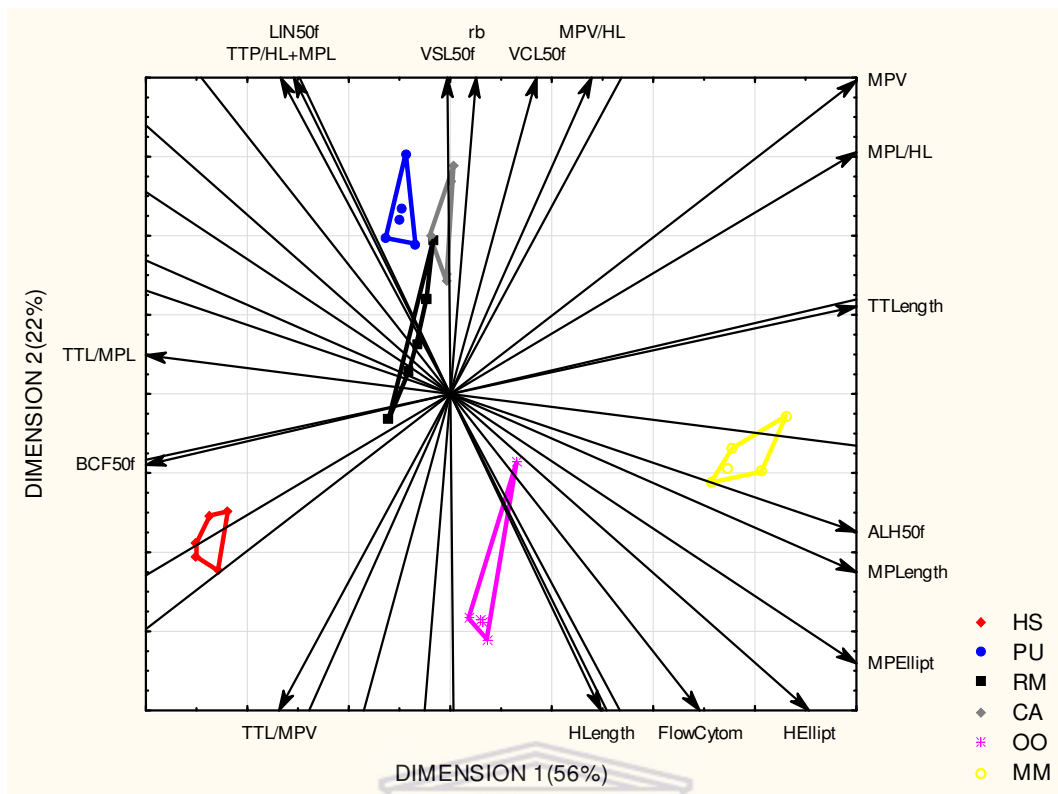
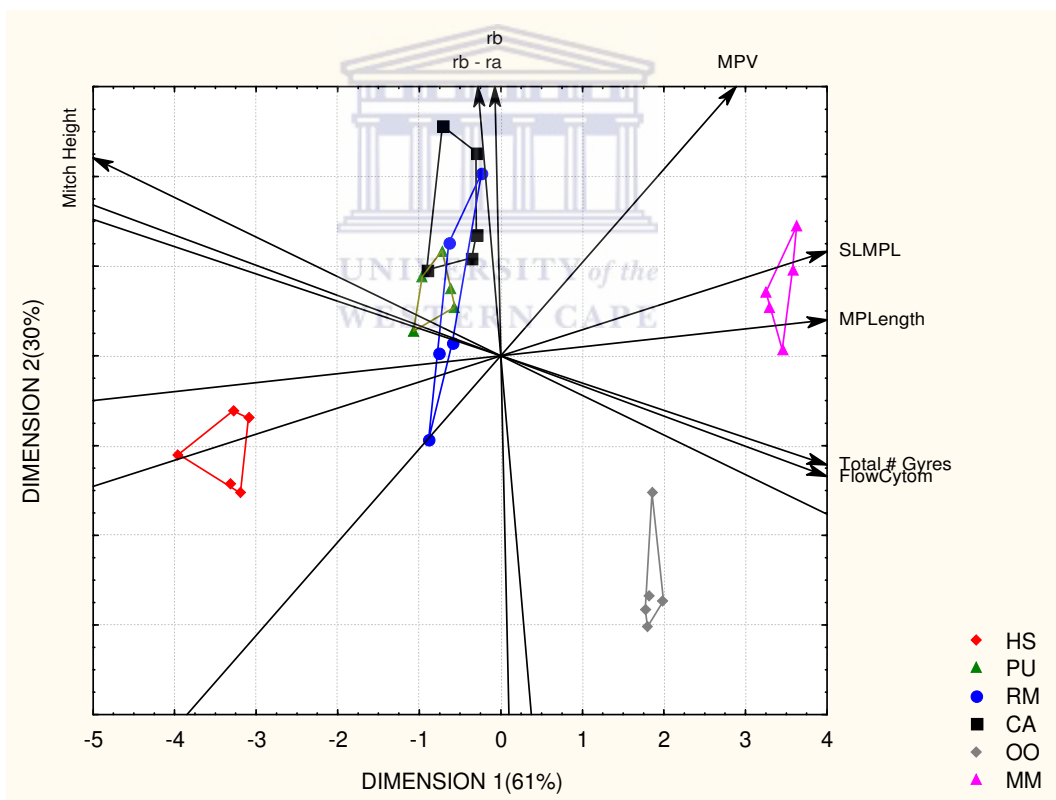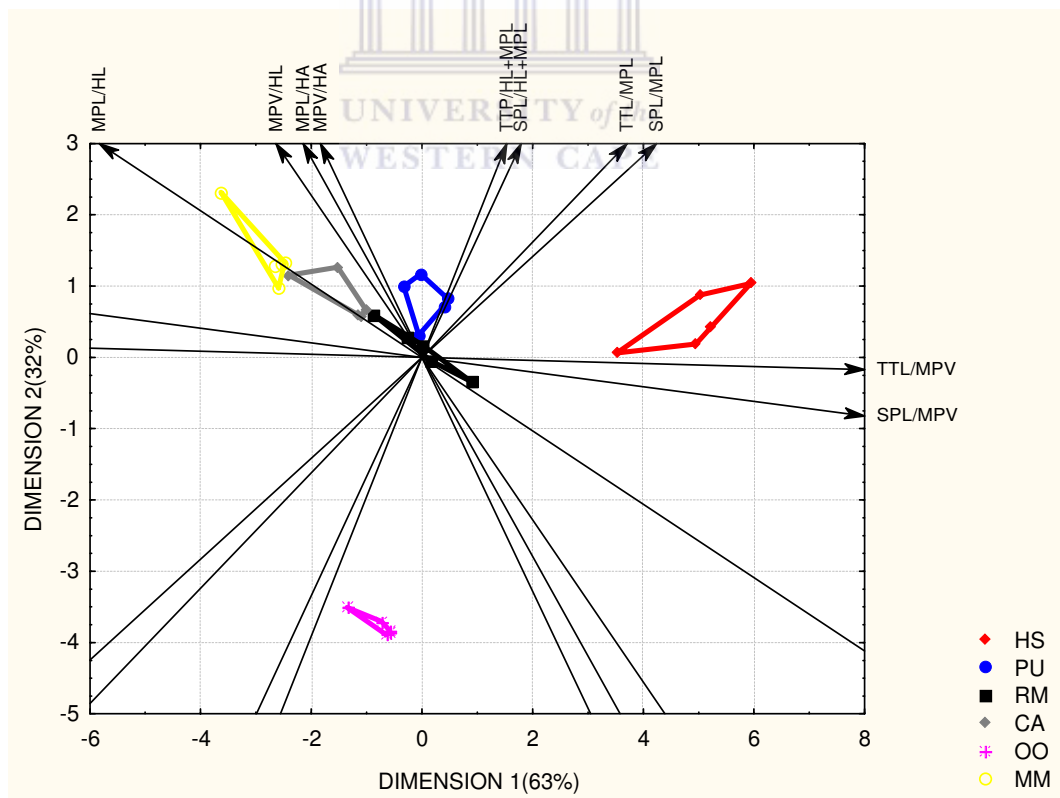**Figure 7.7.** PCA biplot of selected sperm parameters for six mammalian species (n=5). HS = *Homo sapiens* (human), PU = *Papio ursinus* (chacma baboon), RM = *Macaca mulatta* (rhesus monkey), CA = *Chlorocebus aethiops* (vervet monkey), OO = *Ovis orientalis* (merino ram), MM = *Mus musculus* (house mouse), VCL = curvilinear velocity, VSL = straight-line velocity, LIN = linearity, ALH = amplitude of lateral head displacement, BCF = beat cross frequency, f = frames per second, HL = head length, MPL = midpiece length, MPV = midpiece volume, r_b = radius of midpiece, TT = total tail, TTL = total tail length, Ellipt = ellipticity, FlowCytom = flow cytometry.

Relationships between the sperm midpiece and other sperm parameters

Although all the biplots revealed associations between certain sperm parameters, these graphical presentations are descriptive in nature and do not test any specific hypotheses of the associations between different parameters. Correlation coefficients were therefore determined as an indication of the relationships between any two sperm parameters. The correlations of ten midpiece parameters and all the sperm morphometry and sperm motility parameters are presented in Appendix 5. Although some of these parameters were significantly correlated, they had rather low correlation coefficients (r ≤ 0.50) and in these cases 50-70% of the variability was not accounted for.

After the correlations between the ten midpiece parameters and all the other sperm component parameters were determined, several of these sperm parameters and some midpiece parameters were eliminated as presented in Table 7.1. The rationale for eliminating some

sperm parameters was to include a) only those parameters which revealed some association with the midpiece parameters and b) only the parameters which will be easy to assess in future studies. Firstly, sperm parameters which did not reveal a highly significant correlation with ($P > 0.001$) any of the midpiece parameters were removed (e.g. head roughness, head regularity, midpiece regularity). Secondly, if several closely related parameters, e.g. total tail length and total sperm length or MPL/HA and MPL/HL, had similar correlations with midpiece parameters, one of these parameters was eliminated. Three midpiece parameters were also eliminated since the correlations of these parameters with the other sperm parameters did not reveal more information than a second, related midpiece parameter (e.g. r_b similar to $r_b - r_a$, midpiece ellipticity similar to midpiece length and MPV/HL similar to midpiece volume).

There seemed to be a high positive correlation ($P < 0.001$ in orange and $P < 0.05$ in pink) between most midpiece parameters and the other two main sperm components (head and tail). Interestingly the mitochondrial height was negatively correlated with all the sperm morphometry parameters. The thickness of the mitochondrial sheath ($r_b - r_a$) and the midpiece volume were less correlated with the sperm head parameters. Additionally, the size of the midpiece (midpiece length and volume) was highly correlated with the tail principal piece length and the total sperm length.

Most of the midpiece morphometry parameters were also significantly related to one another ($P < 0.001$). The thickness of the mitochondrial sheath was not highly correlated to any of the other midpiece parameters. It should, however, be taken into account that many of these parameters were probably correlated because one parameter was used to derive another, e.g. midpiece length will be related to midpiece area, perimeter, ellipticity, elongation, midpiece volume and straight-line midpiece length. To avoid these "artificially" high correlation coefficients resulting in misleading deductions, these coefficients were coloured blue in Table 7.1.

The sperm morphometry ratios showed significant relationships with most of the midpiece morphometry parameters, while mitochondrial height was only truly related to one of the ratios (TTL/TPPL+TEPL). It was interesting to find that several of the ratios without a midpiece parameter were highly correlated with certain midpiece morphometry parameters, e.g. TTL/HL and MPV, TTL/TPPL+TEPL and MPL and flow cytometry. Moreover, a

175

Table 7.1. Correlation coefficients (r) between seven midpiece morphometry parameters (n=5) and selected sperm morphometry (n=10) and motility parameters (n=10) for seven mammalian species

	# Gyres	Mitch Ht	$r_b - r_a$	MPL	MPV	SLMPL	FlowCyt
HLength (µm)	0.89	-0.84	-0.35	0.88	0.31	0.79	0.67
HWidth (µm)	0.81	-0.82	-0.39	0.78	0.18	0.69	0.51
HArea (µm²)	0.90	-0.83	-0.35	0.89	0.30	0.80	0.71
HPerimeter (µm)	0.94	-0.74	-0.22	0.91	0.50	0.86	0.70
HEllipticity	0.57	-0.33	-0.22	0.18	0.39	0.56	0.52
HElongation	0.61	-0.35	-0.16	0.28	0.45	0.58	0.52
MPLength (µm)	0.88	-0.61	-0.12	X	0.58	0.86	0.84
MPWidth (µm)	0.11	0.03	0.59	0.34	0.51	0.09	0.01
MPArea (µm²)	0.92	-0.67	-0.15	0.97	0.55	0.88	0.85
MPPerimeter (µm)	0.89	-0.62	-0.13	1.00	0.58	0.86	0.84
MPEllipticity	0.83	-0.60	-0.09	0.97	0.60	0.86	0.82
MPElongation	0.85	-0.63	-0.11	0.97	0.60	0.87	0.83
MPRoughness	-0.83	-0.62	0.09	-0.96	-0.61	-0.87	-0.83
Total # Gyres	X	-0.79	-0.19	0.88	0.50	0.91	0.79
Mitch Height (µm)	-0.79	X	0.29	-0.61	-0.18	-0.67	-0.59
$r_b - r_a$ (µm)	-0.19	0.29	X	-0.12	0.65	0.01	-0.04
MPVolume (µm³)	0.50	-0.18	0.65	0.58	X	0.69	0.61
SLMPL (µm)	0.91	-0.67	0.01	0.86	0.69	X	0.88
Flow cytometry	0.79	-0.59	-0.04	0.84	0.61	0.88	X
TPPLength (µm)	0.53	-0.26	0.42	0.69	0.73	0.48	0.29
SPLength (µm)	0.58	-0.31	0.36	0.73	0.71	0.50	0.35
MPL/HL	0.43	-0.10	0.63	0.76	0.91	0.55	0.58
TTL/HL	0.20	0.12	0.61	0.41	0.74	0.28	0.25
TTL/HL+MPL	-0.81	0.69	0.15	-0.87	-0.44	-0.86	-0.86
TTL/TPPL+TEPL	0.80	-0.71	-0.28	0.91	0.36	0.78	0.88
SPL/HL	0.20	0.12	0.61	0.41	0.74	0.28	0.25
SPL/HL+MPL	-0.82	0.69	0.15	-0.91	-0.45	-0.86	-0.87
SPL/TTL	-0.22	-0.08	-0.59	-0.43	-0.74	-0.27	-0.22
MPV/HL	0.38	-0.07	0.75	0.45	0.96	0.57	0.50
MPV/HA	0.17	0.18	0.80	0.26	0.89	0.37	0.30
SPL/MPV	-0.37	0.13	-0.75	-0.45	-0.94	-0.61	-0.53
VCL (µm/s)	0.11	-0.14	0.65	0.39	0.55	0.16	0.08
VSL (µm/s)	-0.05	-0.23	0.60	0.29	0.29	0.01	-0.03
VAP (µm/s)	-0.05	-0.22	0.60	0.29	0.28	0.00	-0.02
LIN (%)	-0.42	0.04	0.46	-0.09	-0.02	-0.29	-0.29
STR (%)	-0.69	0.38	0.29	-0.08	-0.26	-0.56	-0.48
WOB (%)	-0.31	-0.09	0.45	-0.14	0.02	-0.21	-0.23
ALH (µm)	0.73	-0.45	0.07	0.86	0.55	0.61	0.53
BCF (Hz)	-0.52	0.31	-0.16	0.00	-0.65	-0.65	-0.55

▢ : P < 0.001, ▢ : P < 0.05, ▢ : P > 0.05, ▢ : P < 0.001 but the one parameters was derived from the other
Gyres = total number of gyres, Mitch Ht = mitochondrial height, $r_b - r_a$ = mitochondrial sheath thickness, MPL = midpiece length, MPV = midpiece volume, SLMPL = straight-line midpiece length, FlowCyt = flow cytometry, H = head, M = midpiece, L = length, TPP = tail principal piece, TT = total tail, SP = sperm, TEP = tail end piece, VCL = curvilinear velocity, VSL = straight-line velocity, VAP = average path velocity, LIN = linearity, STR = straightness, WOB = wobble, ALH = amplitude of lateral head displacement, BCF = beat cross frequency

number of the sperm components were only significantly correlated or revealed a higher correlation with the midpiece morphometry parameters when its relative measurement (ratio) was used rather than its absolute measurement. Examples of such sperm parameters include the correlation between MPL/HL or TTL/HL and the thickness of the mitochondrial sheath (rather than HL, MPL and TTL alone) and between the TTL/TPPL+TEPL and most of the midpiece morphometry parameters (rather than these three tail parameters on their own).

In general, the midpiece morphometry parameters seemed to be less correlated with the sperm kinematic parameters than with the other sperm components. A few significantly correlated ($P < 0.001$) parameters will, however, be highlighted. The thickness of the mitochondrial sheath was the only midpiece parameter to be correlated to the swimming speed parameters (VCL, VSL and VAP). The straightness (STR) and beat cross frequency (BCF) were similarly correlated (negatively) to the number of gyres, the straight-line midpiece length and the flow cytometry. The amplitude of lateral head displacement (ALH) was the only sperm kinematic parameter that was significantly correlated with most of the midpiece morphometry parameters.

It is also important to mention that all the proposed associations between specific sperm parameters mentioned above for the biplots, were confirmed by the correlation analysis. All these proposed associations revealed significant relationships (see Table 7.1) and mostly high correlation coefficients ($r > 0.6$).

Midpiece morphometry parameters as predictor variables
Table 7.2 is an abbreviation of Table 7.1 to indicate the seven midpiece morphometry parameters that was used for multiple regression analyses in order to determine the relationship between these predictor variables and the selected sperm parameters (dependent variables).

The R-squared coefficients (R^2) and beta coefficients (b*) which were determined in the multiple regression analyses, are presented in Table 7.3. The R-squared coefficients for most sperm parameters were high (> 0.70) and thus indicated that the midpiece morphometry parameters could explain the variation in these sperm morphometry and sperm motility parameters. The beta coefficients presented in the same row as each sperm parameter were an indication of which midpiece morphometry parameter(s) had the most effect on that particular

177

sperm parameter. It is clear from Table 7.3 that midpiece volume, total number of gyres and mitochondrial sheath thickness had the most effect on the sperm morphometry and sperm motility parameters. Interestingly the mitochondrial height rather than the total number of gyres had an important effect on the sperm kinematic parameters.

Table 7.2. Correlation coefficients (r) between seven midpiece morphometry parameters (n=5) and 21 sperm morphometry (n=10) and motility parameters (n=10) used in the multiple regression analysis

	# Gyres	Mitch Ht	$r_b - r_a$	MPL	MPV	SLMPL	FlowCyt
HLength (µm)	0.89	-0.84	-0.35	0.88	0.31	0.79	0.67
HWidth (µm)	0.81	-0.82	-0.39	0.78	0.18	0.69	0.51
HArea (µm²)	0.90	-0.83	-0.35	0.89	0.30	0.80	0.71
HPerimeter (µm)	0.94	-0.74	-0.22	0.91	0.50	0.86	0.70
HEllipticity	0.57	-0.33	-0.22	0.18	0.39	0.56	0.52
HElongation	0.61	-0.35	-0.16	0.28	0.45	0.58	0.52
TPPLength (µm)	0.53	-0.26	0.42	0.69	0.73	0.48	0.29
SPLength (µm)	0.58	-0.31	0.36	0.73	0.71	0.50	0.35
TTL/HL	0.20	0.12	0.61	0.41	0.74	0.28	0.25
TTL/HL+MPL	-0.81	0.69	0.15	-0.87	-0.44	-0.86	-0.86
TTL/TPPL+TEPL	0.80	-0.71	-0.28	0.91	0.36	0.78	0.88
SPL/HL	0.20	0.12	0.61	0.41	0.74	0.28	0.25
SPL/TTL	-0.22	-0.08	-0.59	-0.43	-0.74	-0.27	-0.22
VCL (µm/s)	0.11	-0.14	0.65	0.39	0.55	0.16	0.08
VSL (µm/s)	-0.05	-0.23	0.60	0.29	0.29	0.01	-0.03
VAP (µm/s)	-0.05	-0.22	0.60	0.29	0.28	0.00	-0.02
LIN (%)	-0.42	0.04	0.46	-0.09	-0.02	-0.29	-0.29
STR (%)	-0.69	0.38	0.29	-0.08	-0.26	-0.56	-0.48
WOB (%)	-0.31	-0.09	0.45	-0.14	0.02	-0.21	-0.23
ALH (µm)	0.73	-0.45	0.07	0.86	0.55	0.61	0.53
BCF (Hz)	-0.52	0.31	-0.16	0.00	-0.65	-0.65	-0.55

☐ : P < 0.001, ☐ : P < 0.05, ☐ : P > 0.05, ☐ : P < 0.001 but the one parameters was derived from the other
Gyres = total number of gyres, Mitch Ht = mitochondrial height, $r_b - r_a$ = mitochondrial sheath thickness, MPL = midpiece length, MPV = midpiece volume, SLMPL = straight-line midpiece length, FlowCyt = flow cytometry, H = head, M = midpiece, L = length, TPP = tail principal piece, TT = total tail, SP = sperm, TEP = tail end piece, VCL = curvilinear velocity, VSL = straight-line velocity, VAP = average path velocity, LIN = linearity, STR = straightness, WOB = wobble, ALH = amplitude of lateral head displacement, BCF = beat cross frequency

Table 7.3. Coefficients of determination (R^2) and beta coefficients (b*) for seven midpiece morphometry parameters (predictor variables) and 21 sperm morphometry and motility parameters (dependent variables)

	R^2	b*						
		# Gyres	Mitch Ht	$r_b - r_a$	MPL	MPV	SLMPL	FlowCyt
HLength (µm)	0.95	1.19**				-0.41**		
HWidth (µm)	0.89	1.23**				-0.77**		
HArea (µm^2)	0.94	1.25**				-0.68**		
HPerimeter (µm)	0.94	0.97**						
HEllipticity	0.77	-0.60*		-0.89**		1.52**		
HElongation	0.73	-0.45^{ns}		-0.77*		1.36**		
TPPLength (µm)	0.92	-0.72**		-0.63**		1.65**		
SPLength (µm)	0.94	-0.54**		-0.67**		1.55**		
TTL/HL	0.85	-1.23**		-0.47*		1.69**		
TTL/HL+MPL	0.91	-1.95**		-0.80**		1.40**		
TTL/TPPL+TEPL	0.89	1.19**				-0.53**		
SPL/HL	0.85	-1.23**		-0.47**		1.69**		
SPL/TTL	0.83	0.98**				-1.14**		
VCL (µm/s)	0.75		-0.66**	0.38*		0.48*		-0.44*
VSL (µm/s)	0.71		-0.76**	0.98**		-0.57**		
VAP (µm/s)	0.72		-0.78**	0.97**		-0.52**		
LIN (%)	0.75		-0.56**	0.84**		-1.08**		
STR (%)	0.61		-0.26^{ns}	0.19^{ns}	-0.88**			
WOB (%)	0.78		-0.64**	0.84**		-1.10**		
ALH (µm)	0.90	-0.79**		-0.97**		1.77**		
BCF (Hz)	0.74		-0.19^{ns}			-0.59**		-0.46*

** = $P < 0.001$, * = $P < 0.05$, ^{ns} = $P > 0.05$

Gyres = total number of gyres, Mitch Ht = mitochondrial height, $r_b - r_a$ = mitochondrial sheath thickness, MPL = midpiece length, MPV = midpiece volume, SLMPL = straight-line midpiece length, FlowCyt = flow cytometry, H = head, TPP = tail principal piece, TT = total tail, SP = sperm, TEP = tail end piece, VCL = curvilinear velocity, VSL = straight-line velocity, VAP = average path velocity, LIN = linearity, STR = straightness, WOB = wobble, ALH = amplitude of lateral head displacement, BCF = beat cross frequency

Redundancy analysis

The redundancy analysis of the seven midpiece morphometry parameters and the sperm parameters are presented in Fig. 7.8. The midpiece morphometry parameters are indicated with arrows and the distribution of the other sperm parameters relative to these midpiece parameters are shown. Most of the sperm head and sperm kinematic parameters were grouped together. These sperm head parameters had a positive relationship with total number of gyres and flow cytometry. The swimming speed parameters had a positive relationship with the mitochondrial height and thickness of the mitochondrial sheath. The midpiece volume had a positive relationship with several of the other sperm component parameters and a negative relationship with most of the sperm kinematic parameters, except for ALH.
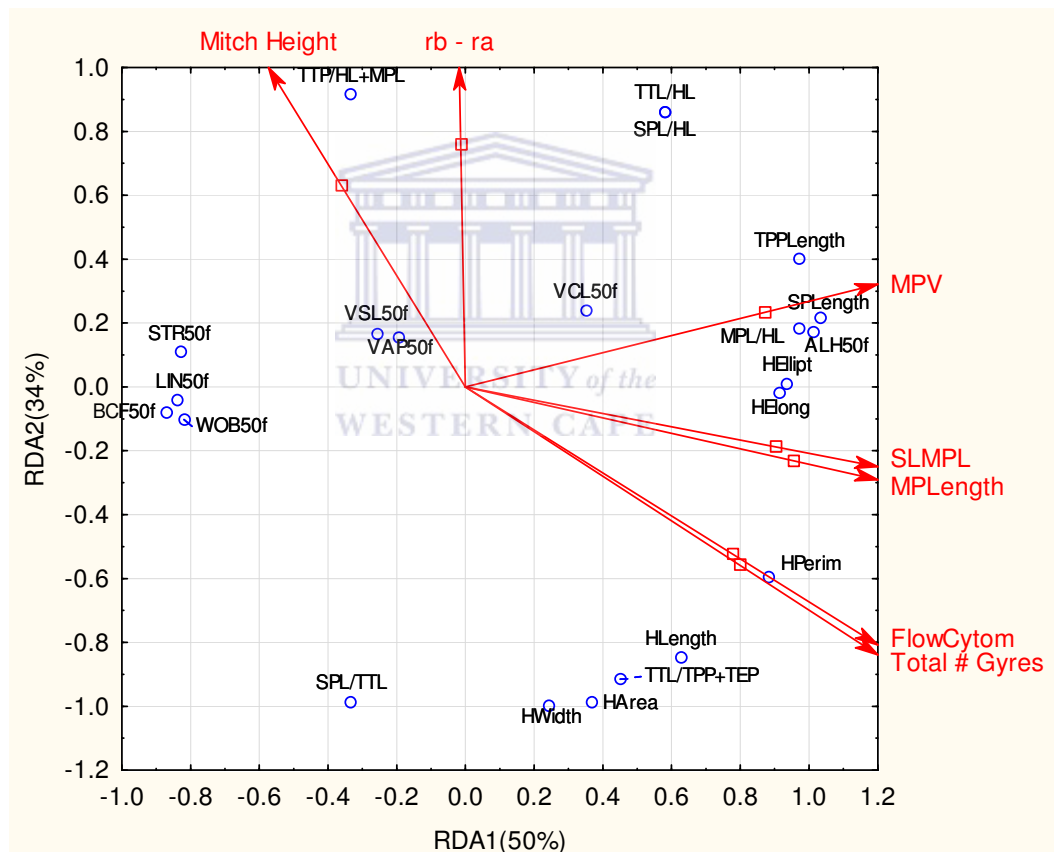
Figure 7.8. Redundancy analysis of seven midpiece morphometry parameters (predictor variables) and selected sperm morphometry and motility parameters (dependent variables). Total # Gyres = total number of gyres, Mitch Height = mitochondrial height, $r_b - r_a$ = mitochondrial sheath thickness, MP = midpiece, MPL = midpiece length, MPV = midpiece volume, SLMPL = straight-line midpiece length, FlowCytom = flow cytometry, HL = head length, TTL = total tail length, SPL = sperm length, TPP = tail principal piece, TEP = tail end piece, HEllipt = head ellipticity, HElong = head elongation, HPerim = head perimeter, VCL = curvilinear velocity, VSL = straight-line velocity, VAP = average path velocity, LIN = linearity, STR = straightness, WOB = wobble, ALH = amplitude of lateral head displacement, BCF = beat cross frequency.

7.4   Discussion

In species comparative studies, the first aim is to identify differences or variations in specific characteristics. Subsequently, attempts are usually made to establish why variations exist by postulating the significance of such supposed adaptations. However, for a characteristic to be considered as an adaptation, it must be a derived characteristic that evolved in response to certain selection pressures (Harvey and Pagel, 1991). In mammalian spermatozoa, several of its characteristics have been proposed as being derived from the "primitive" spermatozoon and are believed to be adaptations for its function in the internal environment of the female reproductive tract. Furthermore, the variation in some of these derived characteristics, namely the dimensions of several sperm components, is probably due to two selective forces, namely sperm competition and female selection (Gomendio and Roldan, 1993).

The variation in the size and shape of mammalian spermatozoa has been studied and confirmed in the present study. Moreover, the variation in the structure and dimensions of the sperm midpiece was of particular interest and its relationship with several other sperm parameters was revealed in this chapter. The various statistical tests employed have been successful in determining both the variations and species specificity of several sperm parameters as well as their correlations with each other.

The cluster analyses employed in Chapters 3-5 as well as the biplots constructed in this chapter revealed that, although there were many variations in the size and shape of the sperm components, most of the sperm parameters evaluated in the present study were species specific. An additional benefit of the biplots was that it indicated the associations between several sperm parameters, which were subsequently confirmed as significant correlations between these sperm parameters. These two statistical tests can therefore be regarded as valuable exploratory data analysis tools and should be employed in similar comparative studies to identify associations among species and sperm parameters.

The significant positive correlations reported between the length of the midpiece and that of the sperm head and sperm tail confirmed the relationship among these three sperm components. Thus the selective pressures responsible for variations in the size of the spermatozoa probably had an influence on all these sperm components collectively rather than just selecting for a change in the size of one specific sperm component. Moreover, it should

181

be noted that several of the midpiece morphometry parameters were correlated to the size of the sperm head and sperm tail as well as to one another (e.g. midpiece length, midpiece volume, total number of gyres and flow cytometry). This indicated that not only the size but also the internal structure of the sperm midpiece (sperm mitochondria) is probably an adaptation to similar selective pressures. The relatedness among the sperm midpiece and the other sperm components was also confirmed by the fact that certain sperm parameters were only significantly correlated to the midpiece morphometry parameters when their relative rather than their absolute measurements were used to determine these relationships. Similar relationships between the length of the sperm head, midpiece and flagellum have been reported by previous studies on mammalian sperm morphometry (Cardullo and Baltz, 1991; Gage, 1998; Anderson *et al.*, 2005). Gage (1998), who also measured the midpiece volume, reported no significant relationships between midpiece length and head area or between midpiece volume and head length, head area or flagellum length. In contrast, the current study found significant correlations between most of these sperm parameters, but also not between midpiece volume and head area.

The significant relationships found between the midpiece morphometry parameters and the sperm kinematic parameters can be speculated upon as being structural and/or functional adaptations for efficient sperm motility. Firstly, the positive correlations between the thickness of the mitochondrial sheath and the sperm swimming speed parameters can be due to the fact that a thicker mitochondrial sheath provides the spermatozoa with more structural support needed for generating higher speeds. Functionally, the thicker mitochondrial sheath might be the most efficient structural arrangement of sperm mitochondria (e.g. to allow a maximum number of cristae and respiratory enzymes) in order to maximize mitochondrial respiration. This mitochondrial arrangement could result in the generation of a high amount of ATP molecules for greater motility (Anderson and Dixson, 2002). Secondly, the positive relationships found between the midpiece length, total number of gyres and ALH could be an indication of how the midpiece morphometry influences the sperm swimming characteristics of each species. Taking the aforementioned correlations into consideration, it is proposed that the longer the sperm midpiece, the more gyres it contains and these two factors jointly cause the midpiece to offer less resistance to bending and therefore results in greater displacement of the sperm head (increase in ALH). Further possible reasons for the associations between

182

midpiece morphometry and sperm kinematic parameters are given in Chapter 8 after the influence of the other sperm components (head and tail) was also considered.

Previous studies have indicated that the relationships between the lengths of the sperm head, midpiece and flagellum suggests co-evolution between these three sperm components (Gage, 1998; Anderson *et al.*, 2005). In the present study, the high correlations found in the regression analysis between the midpiece morphometry parameters and the sperm morphometry components confirms the possibility that such co-evolution has taken place. These results are also an indication of the fact that not only the lengths of the three main sperm components co-evolved but that numerous other structural aspects of the sperm components were also involved in such a process. Furthermore, the midpiece morphometry parameters that have probably played the most important part in such co-evolutionary processes between the sperm components was identified as the midpiece volume, total number of gyres, thickness of the mitochondrial sheath and mitochondrial height. It is therefore suggested that the association between and a combination of these midpiece morphometry parameters rather than the individual parameters might be more important to identify relationships with other sperm parameters. This might also be the reason why many significant correlations between the midpiece morphometry parameters and the sperm morphometry and sperm kinematic parameters portrayed rather low correlation coefficients (r ≤ 0.50) (accounting only for 50% or less of the variability) in the current study or the lack of relationships reported in previous studies (Gage, 1998).

An aspect of comparative analysis that has been recognized but not controlled for in the current study is the phylogenetic relationship among species. According to Harvey and Pagel (1991), the fact that closely related species typically have characteristics that are more similar to each other than to more distantly related species, means that species cannot be treated as independent units of information when used in statistical testing. Various statistical techniques have been designed to take the degree of shared ancestry among a group of species into account and to produce a set of statistically independent data points. In terms of sperm morphometry comparisons, a number of studies investigating the relationship between sperm morphometry and sperm competition have controlled for phylogenetic effects (Gage and Freckleton, 2003; Anderson *et al.*, 2005; Immler *et al.*, 2008; Lüpold *et al.*, 2009). Gage and Freckleton (2003) in particular showed that, after controlling for phylogenetic association,

many previously reported relationships between sperm morphometry parameters and sperm competition in mammals were lost. However, Gomendio and Roldan (2008) commented that Gage and Freckleton (2003) used a poorly resolved phylogeny and that this could influence the identification of significant relationships.

None of the comparative analyses presented in the current study have included similar corrections for species relatedness. This was not done due to the fact that the current study only included seven mammalian species and such phylogenetic corrections could decrease the number of species. Another study by Gomendio and Roldan (1993) mentioned the reduction of sample size resulting from the techniques employed to control for phylogeny. However, since three of the species included in the current study were primate species and due to the fact that numerous similarities were found in their sperm morphometry, midpiece morphometry and sperm kinematic parameters, their phylogenetic relatedness could not be ignored. There was a possibility that the significant relationships reported for various sperm parameters among all seven species were due to the influence of the phylogenetic relatedness between these three primate species. Subsequently the correlation coefficients and multiple regression analysis of selected sperm parameters with the midpiece morphometry parameters were recalculated after the rhesus monkey and/or baboon data were excluded (data not shown). The removal of these two species did not result in changes to any of the relationships between the sperm parameters reported in this chapter. Interestingly, many of the correlation coefficients between the sperm parameters improved after the removal of these two species as well as the relationships determined in the multiple regression analysis.

In conclusion, the present study has confirmed that the various midpiece morphometry parameters are related to the remaining sperm morphometry parameters as well as the sperm kinematic parameters. Moreover, it was indicated that the midpiece morphometry parameters which are most likely selected for in mammalian spermatozoa are the midpiece volume, the total number of gyres, thickness of the mitochondrial sheath and the mitochondrial height. Due to the numerous relationships found between the various sperm parameters mentioned above, the results of the current study supports the idea of co-evolution between sperm components in mammalian spermatozoa.

CHAPTER 8: Final discussion

8.1   Proposed relationship between sperm morphometry and sperm kinematics

While the variations in the sperm morphometry characteristics and the relationship among them have been confirmed in the present study, the possible reasons for these phenomena have not been investigated. As mentioned previously, the variation among these sperm characteristics are probably due to two selective forces, namely sperm competition and female cryptic choice (Gomendio and Roldan, 1993). In terms of sperm competition, it has been reported by studies across various animal taxa that sperm competition has favoured the production of a large number of spermatozoa, an increase in sperm size and an increase in sperm swimming speed (Gomendio and Roldan, 1991; Byrne *et al.*, 2003; Lüpold *et al.*, 2009; Ramm and Stockley, 2010), but this proposed pattern has been challenged (Gage and Freckleton, 2003; Snook, 2005; Immler and Birkhead, 2007). On the other hand, the two female factors that seem to have the most important influence on the selection and survival of spermatozoa are the position of semen deposition (vagina, cervix or uterus) and the length of the oviducts (Gomendio and Roldan, 1993; Gomendio *et al.*, 1998). Interestingly, two studies by Anderson *et al.* (2005; 2006) have reported that sperm midpiece volume was positively correlated to both sperm competition and female oviduct length, highlighting the importance and possible adaptation of this sperm component.

One of the proposed results of sperm competition, namely an increase in sperm velocity is, however, still debated in the literature. In general it has been proposed that if sperm competition does give rise to an increase sperm size (increased midpiece and flagellum length), it would also result in greater sperm velocity due to the availability of more energy (longer midpiece) and greater propulsive forces (longer flagellum) (Cadullo and Baltz, 1991; reviewed by Lüpold *et al.*, 2009). Although, such a relationship between sperm morphometry and sperm velocity were reported in a few studies (Gomendio and Roldan, 1991; Lüpold *et al.*, 2009), other investigations did not find such a relationship between sperm size or sperm component size and sperm swimming speed (Snook, 2005, Malo *et al.*, 2006). Many studies have, however, mentioned that sperm swimming speed is probably dependant on the balance between the thrust or force generated by flagellar bending and the drag or resistance caused by the sperm head as it is driven forward in a viscous medium (Gomendio and Roldan, 2008; Humphries *et al.*, 2008; Lüpold *et al.*, 2008). Humphries *et al.* (2008) has proposed that, due

to the microscopic level at which spermatozoa operate, the assumption of a direct relationship between sperm length and sperm velocity cannot be made. It was also mentioned that since the relationship between sperm morphology and sperm velocity is not completely understood, the sperm kinematic characteristics should rather be determined and related to sperm morphology (Humphries *et al.*, 2008).

Although none of these aforementioned correlations between sperm competition and sperm component size or sperm swimming speed have been determined in the present study, the relationships between the measured sperm and midpiece morphometry parameters and the sperm kinematic parameters are discussed in the following section. The two schematic presentations included in Fig. 8.1 depict the structure of two generalized spermatozoa (A and B) and their related swimming characteristics. Spermatozoon A has features typical of the baboon and vervet monkey spermatozoa, while Spermatozoon B resembles a combination of the features of the ram and mouse spermatozoa investigated in the current study.

According to the relationships between the sperm components reported in this study, Spermatozoon A had lower values for head length, head width, midpiece length, midpiece volume, tail principal piece length, sperm length, total number of gyres and florescence staining intensity than Spermatozoon B. On the other hand, Spermatozoon A had larger values for mitochondrial sheath thickness and mitochondrial height than Spermatozoon B. In terms of the sperm kinematic parameters (see Fig. 8.1), Spermatozoon A portrayed higher swimming speeds (VCL, VSL and VAP), linearity (LIN) and beat cross frequency (BCF) than Spermatozoon B. The amplitude of lateral head displacement (ALH) was, however, larger in Spermatozoon B than in A. For the discussion in the next two paragraphs it was assumed that all these mentioned parameters of Spermatozoon A and B have co-evolved to result in structurally "balanced" spermatozoa that will be highly motile and able to reach the ovum.

It is proposed that the larger head of Spermatozoon B will need more force or power to be driven forward. According to theory, the propulsive forces of the flagellum increases with its length (Katz *et al.*, 1989) and therefore the longer flagellum of Spermatozoon B will be able to generate the increased thrust required. However, the heavier the sperm head, the more likely it is to counteract the thrust of the flagellum (Humphries *et al.*, 2008) and this would probably be the reason for the larger amplitude of lateral head displacement and the decreased

186
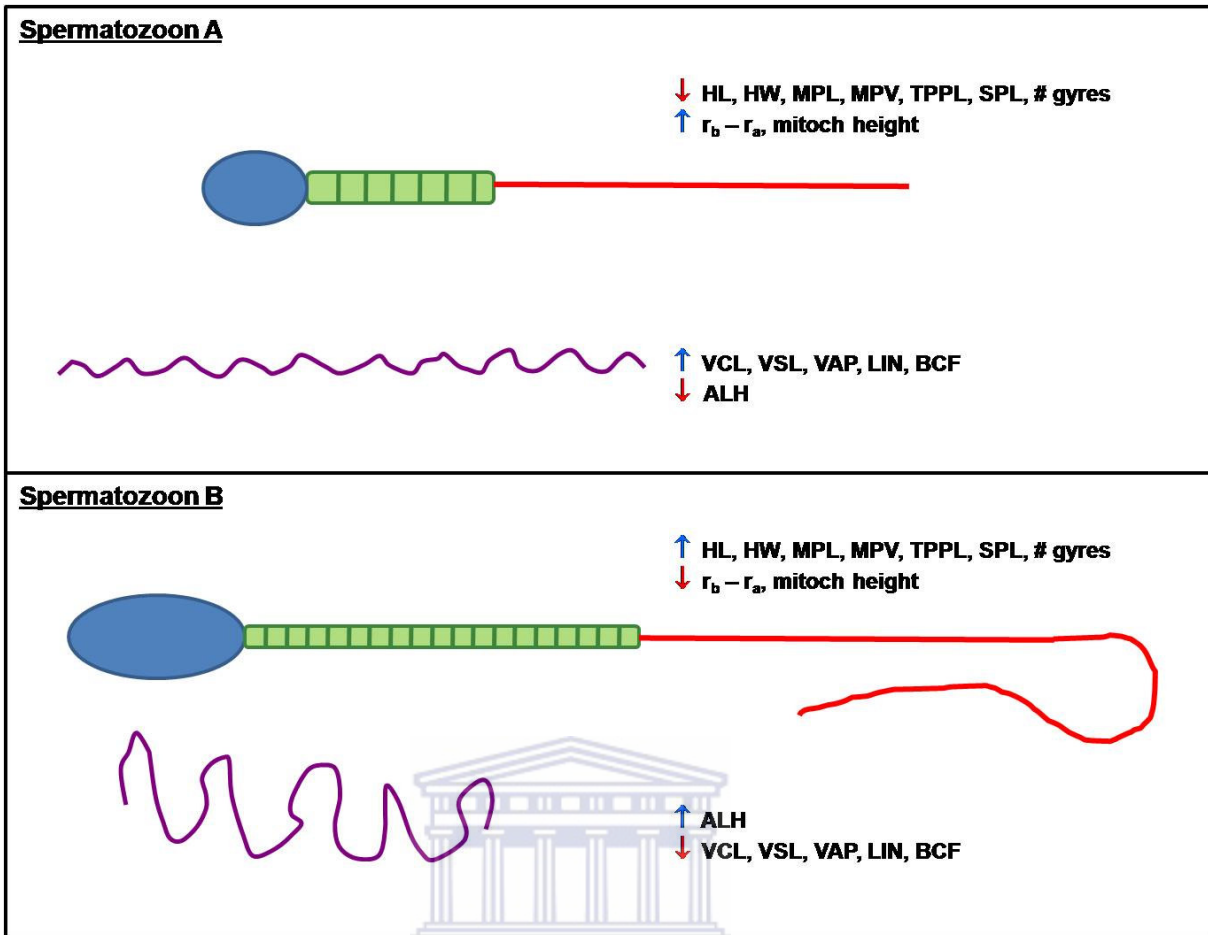
Figure 8.1. Schematic presentation of the structural features and swimming characteristics of two generalized spermatozoa. HL = head length, HW = head width, MPL = midpiece length, MPV = midpiece volume, TTPL = tail principal piece length, SPL = sperm length, # gyres = total number of gyres, $r_b - r_a$ = mitochondrial sheath thickness, mitoch height = mitochondrial height, VCL = curvilinear velocity, VSL = straight-line velocity, VAP = average path velocity, LIN = linearity, ALH = amplitude of lateral head displacement, BCF = beat cross frequency.

linearity reported for this type of spermatozoon. In turn, the increased thrust that needs to be generated would probably require more extensive sideways bending of the flagellum, which can only be achieved if the long midpiece is thinner (relative to the head size) and the mitochondrial height is smaller (less resistance to bending). This would explain the negative correlation between the midpiece width and sperm head parameters as well as between the mitochondrial height and absolute values for sperm head, midpiece and tail reported in the current study. Phillips (1977) mentioned that the helical arrangement of sperm mitochondria might be most favourable for strength and flexibility during motility by allowing a degree of sliding of the mitochondria when the flagellum bends during activated motility.

The above mentioned characteristics of Spermatozoon B might also explain the slower swimming speeds reported for the mouse and ram spermatozoa. It is proposed that the increased bending of the flagellum and the counteraction of the heavy head would slow down the spermatozoa and decrease the beat cross frequency. Thus in principle, the present study agrees with the findings of Malo *et al.* (2006) who indicated that spermatozoa with longer midpieces have slower swimming speeds and with Cardullo and Baltz (1991) who found a negative relationship between the midpiece volume and the flagellar beat frequency. Interestingly, the swimming characteristics of mouse spermatozoa may be improved if several spermatozoa cooperate by attaching to each other with the apical hook on their heads. A number of recent studies have reported that these groups or "trains" of spermatozoa portrayed an increased swimming velocity and thrusting force compared to individual spermatozoa, which might be favourable for sperm competition (Moore *et al.*, 2002; Immler *et al.*, 2007; Firman and Simmons, 2009; Fisher and Hoekstra, 2010).

Spermatozoon A with its smaller head and shorter flagellum will not be required to generate as much force as Spermatozoon B to drive itself forward. Less flagellar bending and displacement of the head would therefore be detected in Spermatozoon A. This would also explain the decreased flagellar length and increased mitochondrial height and mitochondrial sheath thickness (relative to the size of the sperm head) reported for the baboon and vervet monkey spermatozoa. All these factors will probably result in an increase in the sperm swimming speed as found in the current study. As mentioned before, it could also be argued that the thicker mitochondrial sheath either render structural support to the flagellum during increased swimming speed or it could be a functional adaptation for an increase in swimming speed. These relationships do, however, not explain the slow swimming speeds reported for the human and naked mole-rat spermatozoa (both having smaller sized sperm components) and also needs to be tested for other mammalian spermatozoa. The slow swimming velocities of the human and naked mole-rat spermatozoa could possibly be related to the proposed lack of sperm competition in these two species and the fact that the size of their components is too compromised to produce high swimming speeds.

The proposed relationships between the sperm kinematic parameters and the midpiece morphometry parameters of Spermatozoon A and B confirms the positive and negative associations between these parameters reported throughout this chapter (biplots, correlation

coefficients, multiple regression analysis and redundancy analysis) as well as the interactions between specific midpiece parameters highlighted by the beta coefficients. From the above it is clear that the possible reason why many previous studies did not find a direct relationship between sperm morphology and sperm velocity was due to the fact that these studies only took one or two sperm component measurements (midpiece and flagellum length) into consideration. The current study suggests that more detailed sperm kinematic parameters as well as the midpiece morphometry and the interactions between these parameters should be taken into account when investigating the association between sperm morphometry and sperm motility. However, the most reliable relationship between sperm morphology and sperm velocity will probably only be found when the possible effect of the female reproductive tract is also considered (Gomendio and Roldan, 2008; Humphries *et al.*, 2008).

8.2   General conclusion

Mammalian spermatozoa are believed to be adapted for the environment in which they perform their function, namely the female reproductive tract (internal fertilization). Several modifications to the "primitive" spermatozoon have been identified in "modified" mammalian spermatozoa that were proposed to be adaptations for finding and fertilizing the ovum. Two examples of these modifications are the structural complexity of the "motor apparatus" in mammalian spermatozoa needed for locomotion and the enlarged acrosome containing a high concentration of enzymes to assist in the penetration of the cells and layers surrounding the ovum. However, these modifications or adaptations to the structure of mammalian spermatozoa do not reveal conformity to a standard shape and size. Studies on the variations in sperm dimensions have intensified during the last few years and resulted in numerous hypotheses regarding the adaptive significance of these variations. In the present study, the variation in the dimensions of different sperm components of several mammalian species' spermatozoa was investigated, with emphasis on the sperm midpiece.

This comparative study assured the need for optimization and employment of standardized experimental procedures and analysis techniques to reveal the possible relationships among the numerous sperm parameters evaluated. Consequently, this study confirmed the variations in the sperm morphometry of selected mammalian species. A comprehensive study of the sperm midpiece and sperm mitochondria revealed the unique features of these sperm components among the spermatozoa of the seven mammalian species. The evaluation of

several sperm kinematic parameters disclosed the sperm swimming characteristics of the different spermatozoa and the importance of using standardized motility parameters was highlighted. Investigating the role of sperm mitochondria in human sperm metabolism indicated that these organelles are related to sperm function in terms of sperm motility. Moreover, it was suggested that both glycolysis and mitochondrial respiration are important processes for the maintenance of human sperm motility. Comparing all the above data of the seven mammalian species confirmed the species specificity of almost all the sperm parameters evaluated. Furthermore, the phylogenetic relatedness of the non-human primate species was elucidated by several similarities reported for the sperm parameters of these three species. Finally, this study revealed the relationship of the sperm midpiece morphometry and sperm mitochondria with the remaining sperm morphometry parameters as well as the sperm swimming characteristics. The proposed associations between these parameters could explain the sperm velocity of two generalized sperm structures, but not for human or naked mole-rat spermatozoa.

8.3 Future studies

Many of the sperm parameter values determined in the current study was reported here for the first time for some of the mammalian species included, e.g. the midpiece morphometry and sperm kinematic parameters. Therefore, the measurements of these sperm parameters can be used as reference values in future studies. The fact that the experimental protocols could be performed for all three non-human primate species creates the opportunity to use any one of these species as a primate model for future reproductive studies.

The data presented in the current investigation on the spermatozoa of seven mammalian species forms the basis of what could become a much larger comparative study. The optimized experimental protocols should be used in prospective studies to evaluate similar sperm morphometry and sperm motility parameters of other mammalian species. Such an increased data set can then be used to test the strength of the relationships reported here between the dimensions of the different sperm components. Furthermore, it will also be possible to test the validity of the proposed influence of sperm morphometry on sperm kinematic parameters.

Additional studies on sperm metabolism are also required to confirm the results of the present study and to compare different mammalian species. First, a reliable inhibitor of the glycolytic pathway should be identified which will not have a possible influence on the ATP production by mitochondrial respiration. Such a glycolytic inhibitor will assist in resolving the contention in the literature on whether or not glycolysis is the most important pathway to maintain sperm motility (Ford, 2006; Ruiz-Pesini *et al.*, 2007). Secondly, sperm metabolic experiments on spermatozoa from other mammalian species should be performed with as much detail as reported in the present study in order to reveal the role of glycolysis and OXPHOS in the maintenance of sperm motility. Subsequently, the results of such studies can be compared to the results reported here for human spermatozoa and the relationship of sperm metabolism to the structure of the sperm midpiece and sperm mitochondria could be determined.

As was mentioned in the previous chapters, this study only evaluated the sperm parameters of highly motile spermatozoa. An application of this study would be to compare these results to similar sperm parameters of suspected subfertile or infertile males and thereby assist in the identification of the possible causes of infertility. Several techniques used in the current study to accurately measure the midpiece and sperm mitochondrial parameters, e.g. transmission electron microscopy and flow cytometry, should be used in infertility studies to identify any midpiece abnormalities. Specific focus should be placed on abnormalities in the four midpiece morphometry parameters that are probably selected for in mammalian spermatozoa (midpiece volume, total number of gyres, thickness of the mitochondrial sheath and mitochondrial height), as was reported in the current study. If sperm motility is used as an indication of a male's fertility status, care should be taken to rather determine the percentage rapid swimming spermatozoa and their swimming characteristics than only assessing the total percentage of motile spermatozoa.

REFERENCES

Agarwal A, Makker K, Sharma R (2008). Clinical relevance of oxidative stress in male factor infertility: an update. *Am J Reprod Immunol*, 59: 2-11.

Agarwal A, Sharma RK, Nelson DR (2003). New semen quality scores developed by principal component analysis of semen characteristics. *J Androl*, 24: 343-352.

Aitken RJ (2010). Wither must spermatozoa wander? The future of laboratory seminology. *Asian J Androl*, 12: 99-103.

Aitken RJ, de Iuliis GN (2010). On the possible origins of DNA damage in human spermatozoa. *Mol Hum Reprod*, 16: 3-13.

Allen JF (1996). Separate sexes and the mitochondrial theory of ageing. *J Theor Biol,* 180: 135-140.

Amaral A, Ramalho-Santos J, St John JC (2007). The expression of polymerase gamma and mitochondrial transcription factor A and the regulation of mitochondrial DNA content in mature human sperm. *Hum Reprod*, 22: 1585-1596.

Anderson MJ, Dixson AF (2002). Motility and the midpiece in primates. *Nature*, 416: 496.

Anderson MJ, Dixson AS, Dixson AF (2006). Mammalian sperm and oviducts are sexually selected: evidence for co-evolution. *J Zool Lond*, 270: 682-686.

Anderson MJ, Nyholt J, Dixson AF (2005). Sperm competition and the evolution of sperm midpiece volume in mammals. *J Zool Lond*, 267: 135-142.

Anderson S, Bankier AT, Barrell BG, de Bruijn MHL, Coulson AR, Drouin J, Eperon IC, Nierlich DP, Roe BA, Sanger F, Schreier PH, Smith AJH, Staden R, Young IG (1981). Sequence and organization of the mitochondrial genome. *Nature*, 290: 457-464.

Ankel-Simons F, Cummins JM (1996). Misconceptions about mitochondria and mammalian fertilization: implications for theories on human evolution. *Proc Natl Acad Sci*, 93: 13859-13863.

Anson ML (1940). The reactions of iodine and iodoacetamide with native egg albumin. *J Gen Physiol,* 23: 321-331.

Auclair D, Sowerbutts SF, Setchell BP (1995). Effect of active immunization against testosterone on plasma gonadotropin concentrations, spermatogenic function, testicular blood flow, epididymis mass and mating behaviour in adult rams. *J Reprod Fertil*, 104: 17-26.

Auger J, Leonce S, Jouannet P, Ronot X (1993). Flow cytometric sorting of living, highly motile human spermatozoa based on evaluation of their mitochondrial activity. *J Histochem Cytochem*, 41: 1247-1251.

Austin CR (1976). Specialization in gametes. In *Reproduction in mammals. Book 6: The evolution of reproduction* (Austin CR, Short RV, eds.), pp. 149-183. Cambridge University Press, Cambridge.

Baccetti B, Afzelius BA (1976). *Monographs in developmental biology, Vol. 10 - The biology of the sperm cell* (Wolsky A, ed.). Karger, New York.

Ball MA, Parker GA (2003). Sperm competition games: sperm selection by females. *J Theor Biol*, 224: 27-42.

Balter M (2008). Why we're different: probing the gap between apes and humans. *Science*, 319: 404-405.

Barratt C (1995). On the accuracy and clinical value of semen laboratory tests. *Hum Reprod*, 10: 250-252.

Barroso G, Mercan R, Ozgur K, Morshedi M, Kolm P, Coetzee K, Kruger T, Oehninger S (1999). Intra- and inter-laboratory variability in the assessment of sperm morphology by strict criteria: impact of semen preparation, staining techniques and manual versus computerized analysis. *Hum Reprod*, 14: 2036-2040.

Barton NH, Charlesworth B (1998). Why sex and recombination? *Science,* 281: 1986-1990.

Bartoov B, Messer GY (1976). Isolation of mitochondria from ejaculated ram spermatozoa. *J Ultrastr Res*, 57: 68-76.

Baumber J, Ball BA, Gravance CG, Medina V, Davies-Morel MCG (2000). The effect of reactive oxygen species on equine sperm motility, viability, acrosomal integrity, mitochondrial membrane potential, and membrane lipid peroxidation. *J Androl*, 21: 895-902.

Bedford JM (1974). Biology of primate spermatozoa. In *Contributions to primatology, Vol. 3. Reproductive biology of the primates* (Luckett WP, ed.), pp. 97-139. Karger, Basel.

Bennett NC, Faulkes CG (2000). *African mole-rats: ecology and eusociality*. Cambridge University Press, Cambridge.

Bielert C, Vandenbergh JG (1981). Seasonal influences on births and male sex skin coloration in rhesus monkeys (*Macaca mulatta*) in the southern hemisphere. *J Reprod Fertil*, 62: 229-233.

Birkhead TR, Pellatt EJ, Brekke P, Yeates R, Castillo-Juarez H (2005). Genetic effects on sperm design in the zebra finch. *Nature*, 434: 383-387.

Bornman MS, van Vuuren M, Meltzer DGA, van der Merwe CA, van Rensburg SJ (1988). Quality of semen obtained by electroejaculation from chacma baboons (*Papio ursinus*). *J Med Primatol*, 17: 57-61.

Breed WG (2004). The spermatozoon of Eurasian murine rodents: its morphological diversity and evolution. *J Morphol*, 261: 52-69.

Brewer L, Corzett M, Lau EY, Balhorn R (2003). Dynamics of protamine 1 binding to single DNA molecules. *J Biol Chem*, 278: 42403-42408.

Brinders J (1994). The effects of different media and gamma irradiation on quantitative sperm motility in the wistar rat. Unpublished MSc thesis, Department of Physiological Sciences, University of the Western Cape.

Brooks GA, Brown MA, Butz CE, Sicurello JP, Dubouchaud H (1999). Cardiac and skeletal muscle mitochondria have a monocarboxylate transporter MCT1. *J Appl Physiol*, 87: 1713-1718.

Burgos C, Gerez de Burgos NM, Coronel CE, Blanco A (1979). Substrate specificity of the lactate dehydrogenase isoenzyme C_4 from human spermatozoa and a possible selective assay. *J Reprod Fertil*, 55: 101-106.

Burgos C, Maldonado C, Gerez de Burgos NM, Aoki A, Blanco A (1995). Intracellular location of the testicular and sperm-specific lactate-dehydrogenase isozyme C_4 in mice. *Biol Reprod*, 53: 84-92.

Bussalleu E, Pinart E, Yeste M, Briz M, Sancho S, Garcia-Gil N, Badia E, Bassols J, Pruneda A, Casas I, Bonet S (2005). Development of a protocol for multiple staining with fluorochromes to assess the functional status of boar spermatozoa. *Microsc Res Techn*, 68: 227-283.

Byrne PG, Simmons LW, Roberts JD (2003). Sperm competition and the evolution of gamete morphology in frogs. *Proc R Soc Lond B*, 270: 2079-2086.

Calvin HI, Bedford JM (1971). Formation of disulfide bonds in the nucleus and accessory structures of mammalian spermatozoa during maturation in the epididymis. *J Reprod Fertil Suppl*, 13: 65-75.

Calvin J, Tubbs PK (1978). Mitochondrial transport processes and oxidation of NADH by hypotonically-treated boar spermatozoa. *Eur J Biochem*, 89: 315-320.

Cannon B, Nedergaard J (2004). Brown adipose tissue: function and physiological significance. *Physiol Rev*, 84: 277-359.

Cao W, Haig-Ladewig L, Gerton GL, Moss SB (2006). Adenylate kinases 1 and 2 are part of the accessory structures in the mouse sperm flagellum. *Biol Reprod*, 75: 492-500.

Cardullo RA, Baltz JM (1991). Metabolic regulation in mammalian sperm: mitochondrial volume determines sperm length and flagellar beat frequency. *Cell Motil Cytoskel*, 19: 180-181.

Cawthon Lang KA (2005). Primate Factsheets: Rhesus macaque (*Macaca mulatta*). Taxonomy, Morphology, & Ecology. *http://pin.primate.wisc.edu/factsheets/entry/ rhesus_macaque* (available online).

Chemes HE, Olmedo SB, Carrere C, Oses R, Carizza C, Leisner M, Blaquier J (1998). Ultrastructural pathology of the sperm flagellum: association between flagellar pathology and fertility prognosis in severely asthenozoospermic men. *Hum Reprod*, 13: 2521-2526.

Choudhry TM, Berger T, Dally M (1995). In vitro fertility evaluation of cryopreserved ram semen and its correlation with relative in vivo fertility. *Theriogenology*, 43: 1195-1200.

Christensen P, Stryhn H, Hansen C (2005). Discrepancies in the determination of sperm concentration using Burker-Turk, Thoma and Makler counting chambers. *Theriogenology*, 63: 992-1003.

Christie B (2000). Doctors revise Declaration of Helsinki. *BMJ*, 321: 913.

Clausen J (1969). Lactate dehydrogenase isoenzymes of sperm cells and testes. *Biochem J*, 111: 207-218.

Cloete SWP, Gilmour AR, Olivier JJ, van Wyk JB (2004). Genetic and phenotypic trends and parameters in reproduction, greasy fleece weight and liveweight in Merino lines divergently selected for multiple rearing ability. *Aus J Exp Agric*, 44: 745-754.

Cloete SWP, Olivier JJ (2010). South African industry. In *International sheep and wool handbook* (Cottle DJ, ed.), pp. 95-112. Nottingham University Press, Nottingham.

Coetzee K, Kruger TF, Lombard CJ (1998). Predictive value of normal sperm morphology: a structured literature review. *Hum Reprod Update*, 4: 73-82.

Collins JA, van Steirteghem A (2004). Overall prognosis with current treatment of infertility. *Hum Reprod Update*, 10: 309-316.

Comhaire FH, Huysse S, Hinting A, Vermeulen L, Schoonjans F (1992). Objective semen analysis: has the target been reached? *Hum Reprod*, 7: 237-241.

Cooper TG (1984). The onset and maintenance of hyperactivated motility of spermatozoa from the mouse. *Gam Res*, 9: 55-74.

Cooper TG, Noonan E, von Ecjardstein S, Auger J, Baker HWG, Behre HM, Haugen TB, Kruger T, Wang C, Mbizvo MT, Vogelsong KM (2010). World Organization reference values for human semen characteristics. *Hum Reprod Update*, 16: 231-245.

Corbett AD, Lees GM (1997). Depressant effects of hypoxia and hypoglycaemia on neuro-effector transmission of guinea-pig intestine studied *in vitro* with a pharmacological model. *Br J Pharmacol*, 120: 107-111.

Coronel CE, Gallina FG, Gerez de Burgos NM, Burgos C, Blanco A (1986). Properties of the branched-chain 2-hydroxy acid/2-oxo acid shuttle in mouse spermatozoa. *Biochem J*, 235: 853-858.

Costello S, Michelangeli F, Nash K, Lefievre L, Morris J, Machado-Oliveira G, Barratt C, Kirkman-Brown J, Publicover J (2009). Ca^{2+} stores in sperm: their identities and functions. *Reproduction*, 138: 425-437.

Cseh S, Chan PJ, Corselli J, Bailey LL (2000). Electroejaculated baboon (*Papio anubis*) sperm requires a higher dosage of pentoxifylline to enhance motility. *J Ass Reprod Gen*, 17: 449-453.

Cummins JM (1990). Evolution of sperm form: levels of control and competition. In *Fertilization in mammals* (Bavister BD, Cummins JM, Roldan ERS, eds.), pp. 51-64. Serono Symposia, USA.

Cummins JM (1998). Mitochondrial DNA in mammalian reproduction. *Rev Reprod*, 3: 172-182.

Cummins JM (2009). Sperm motility and energetics. In *Sperm Biology: An evolutionary perspective* (Birkhead TR, Hosken DJ, Pitnick S, eds.), pp. 69-149. Academic Press, New York.

Cummins JM, Woodall PF (1985). On mammalian sperm dimensions. *J Reprod Fert*, 75: 153-175.

Darwin CR (1862). On the two forms, or dimorphic condition, in the species *Primula*, and on their remarkable sexual relations. *J Proc Linn Soc (Bot)*, 6: 77–96.

Davis RO, Gravance CG (1993). Standardization of specimen preparation, staining, and sampling methods improves automated sperm-head morphometry analysis. *Fertil Steril*, 59: 412-417.

Davis RO, Gravance CG (1994). Consistency of sperm morphology classification methods. *J Androl*, 15: 83-91.

Dawson TL, Gores GJ, Nieminen AL, Herman B, Lemasters JJ (1993). Mitochondria as a source of reactive oxygen species during reductive stress in rat hepatocytes. *Am J Physiol Cell Physiol*, 264: 961-967.

Denil J, Ohl DA, Menge AC, Keller LM, McCabe M (1992). Functional characteristics of sperm obtained by electro-ejaculation. *J Urol*, 147: 69-72.

de Graaf SP, Evans G, Maxwell WM, Downing JA, O'Brien JK (2007). Successful low dose insemination of flow cytometrically sorted ram spermatozoa in sheep. *Reprod Domest Anim*, 42: 648-653.

de Martino C, Floridi A, Marcante ML, Malorni W, Scorza-Barcellona P, Belloci M, Silvestrini B (1979). Morphological, histochemical and biochemical studies on germ cell mitochondria of normal rats. *Cell Tissue Res*, 196: 1-22.

de Villiers C, Seier JV (2010). Sudden death in chacma baboons (*Papio ursinus*). *LabAnimal Europe*, 10: 10-12.

de Visser JAGM, Elena SF (2007). The evolution of sex: empirical insights into the roles of epistasis and drift. *Nat Rev Genet*, 8: 139-149.

Downing Meisner A, Klaus AV, O'Leary MA (2005). Sperm head morphology in 36 species of artiodactylans, perissodactylans and cetaceans (mammalian). *J Morphol*, 263: 179-202.

Duchen MR (1999). Contributions of mitochondria to animal physiology: from homeostatic sensor to calcium signalling and cell death. *J Physiol*, 516: 1-17.

Dufour E, Larsson NG (2004). Understanding ageing: revealing order out of chaos. *Biochim Biophys Acta*, 1658: 122-132.

Ellington WR, Kinsey ST (1998). Functional and evolutionary implications of the distribution of phosphagens in primitive-type spermatozoa. *Biol Bull*, 195: 264-272.

Escalier D (2006). Knockout mouse models of sperm flagellum anomalies. *Hum Reprod Update*, 12: 449-461.

Essmann F, Bantel H, Totzke G, Engels IH, Sinha B, Schulze-Osthoff K, Jänicke RU (2003). *Staphylococcus aureus* a-toxin-induced cell death: predominant necrosis despite apoptotic caspase activation. *Cell Death Differ*, 10: 1260-1272.

Faulkes CG, Abbott DH, Jarvis JUM (1990). Social suppression of ovarian cyclicity in captive and wild colonies of naked mole-rats, *Heterocephalus glaber*. *J Reprod Fertil*, 88: 559-568.

Faulkes CG, Abbott DH, Jarvis JUM (1991). Social suppression of reproduction in male naked mole-rats, *Heterocephalus glaber*. *J Reprod Fertil*, 91: 593-604.

Faulkes CG, Trowell SN, Jarvis JUM, Bennett NC (1994). Investigation of numbers and motility of spermatozoa in reproductively active and socially suppressed males of two eusocial African mole-rats, the naked mole-rat (*Heterocephalus glaber*) and the Damaraland mole-rat (*Cryptomys damarensis*). *J Reprod Fertil*, 100: 411-416.

Fawcett DW (1970). A comparative view of sperm ultrastructure. *Biol Reprod Suppl*, 2: 90-127.

Fawcett DW (1975). The mammalian spermatozoon. *Dev Biol*, 44: 394-436.

Fawcett DW (1981). *The cell* (2nd Ed.). WB Saunders Company, Philadelphia.

Firman RC, Simmons LW (2009). Sperm competition and the evolution of the sperm hook in house mice. *J Evol Biol*, 22: 2505-2511.

Firman RC, Simmons LW (2010). Sperm midpiece length predicts sperm swimming velocity in house mice. *Biol Lett*, 6: 513-516.

Fisher HS, Hoekstra HE (2010). Competition drives cooperation among closely related sperm of deer mice. *Nature*, 463: 801-803.

Folgero T, Bertheussen K, Lindal S, Torbergsen T, Oian P (1993). Mitochondrial disease and reduced motility. *Hum Reprod*, 8: 1863-1868.

Ford WCL (2006). Glycolysis and sperm motility: does a spoonful of sugar help the flagellum go round? *Hum Reprod Update*, 12: 269-274.

Ford WCL, Harrison A (1981). The role of oxidative phosphorylation in the generation of ATP in human spermatozoa. *J Reprod Fertil*, 63: 271-278.

Ford WCL, Rees JM (1990). The bioenergetics of mammalian sperm motility. In *Controls of sperm motility: biological and clinical aspects*. (Gagnon C, ed.), pp. 175-202. CRC Press, Boca Raton.

Gadea J, Selles E, Marca MA (2004). The predictive value of porcine seminal parameters on fertility outcome under commercial conditions. *Reprod Dom Anim*, 39: 303-308.

Gage MJG (1998). Mammalian sperm morphometry. *Proc R Soc Lond B*, 265: 97-103.

Gage MJG, Freckleton RP (2003). Relative testis size and sperm morphometry across mammals: no evidence for an association between sperm competition and sperm length. *Proc R Soc Lond B*, 270: 625-632.

Gago C, Pérez-Sánchez F, Yeung CH, Tablado L, Cooper TG, Soler C (1998). Standardization of sampling and staining methods for the morphometric evaluation of sperm heads in the cynomolgus monkey (*Macaca fascicularis*) using computer-assisted image analysis. *Int J Androl*, 21: 169-176.

Galantino-Homer HL, Florman HM, Storey BT, Dobrinski I, Kopf GS (2004). Bovine sperm capacitation: assessment of phosphodiesterase activity and intracellular alkalinisation on capacitation-associated protein tyrosine phosphorylation. *Mol Reprod Dev*, 67: 487-500.

Gallina FG, Gerez de Burgos N, Burgos C, Coronel CE, Blanco A (1994). The lactate/pyruvate shuttle in spermatozoa: operation *in vitro*. *Arch Biochem Biophys*, 308: 515-519.

Gallon F, Marchetti C, Jouy N, Marchetti P (2006). The functionality of mitochondria differentiates human spermatozoa with high and low fertilizing capacity. *Fertil Steril*, 86: 1526-1530.

Garcia CK, Brown MS, Pathak RK, Goldstein JL (1995). cDNA cloning of MCT2, a second monocarboxylate transporter, expressed in different cells than MCT1. *J Biol Chem*, 270: 1843-1849.

Garrett C, Baker HW (1995). A new fully automated system for the morphometric analysis of human sperm heads. *Fertil Steril*, 63: 1306-1317.

Garrett C, Liu DY, Clarke GN, Rushford DD, Baker HWG (2003). Automated semen analysis: 'zona pellucida preferred' sperm morphometry and straight-line velocity are related to pregnancy rate in subfertile couples. *Hum Reprod*, 18: 1643-1649.

Gerez de Burgos NM, Burgos C, Montamat EE, Moreno J, Blanco A (1978). A shuttle system for the transfer of reducing equivalents in mouse sperm mitochondria. *Biochem Biophys Res Comm*, 81: 644-649.

Gerez de Burgos NM, Gallina F, Burgos C, Blanco A (1994). Effect of L-malate on pyruvate dehydrogenase activity of spermatozoa. *Arch Biochem Biophys*, 308: 520-524.

Gilkerson RW, Selker JML, Capaldi RA (2003). The cristal membranes of mitochondria is the principal site of oxidative phosphorylation. *FEBS Letters*, 546: 355-358.

Gladden, LB (2004). Lactate metabolism: a new paradigm for the third millennium. *J Physiol*, 558: 5-30.

Gomendio M, Harcourt AH, Roldan ERS (1998). Sperm competition in mammals. In *Sperm competition and sexual selection* (Birkhead TR, Moller AP, eds.), pp. 667-751. Academic Press, San Diego.

Gomendio M, Malo AF, Garde J, Roldan ERS (2007). Sperm traits and male fertility in natural populations. *Reproduction*, 134: 19-29.

Gomendio M, Roldan ERS (1991). Sperm competition influences sperm size in mammals. *Proc R Soc Lond B*, 243: 181-185.

Gomendio M, Roldan ERS (1993). Coevolution between male ejaculates and female reproductive biology in eutherian mammals. *Proc R Soc Lond B*, 252: 7-12.

Gomendio M, Roldan ERS (2008). Implications of diversity in sperm size and function for sperm competition and fertility. *Int J Dev Biol*, 52: 439-447.

Gopalkrishnan K, Hinduja IN, Kumar A (1991). Assessment of mitochondrial activity of human spermatozoa: motility/viability in fertile/infertile men. *Mol Androl*, 3: 243-250.

Gopalkrishnan K, Padwal V, D'Souza S, Shah R (1995). Severe asthenozoospermia: a structural and functional study. *Int J Androl*, 18(Suppl): 67-74.

Graham JK, Kunze E, Hammerstedt RH (1990). Analysis of sperm cell viability, acrosomal integrity, and mitochondrial function using flow cytometry. *Biol Reprod*, 43: 55-64.

Grasa P, Pérez-Pé R, Báguena O, Forcada F, Abecia A, Cebrián-Pérez JA, Muiño-Blanco T (2004). Ram sperm selection by a Dextran/swim-up procedure increases fertilization rates flowing intrauterine insemination in superovulated ewes. *J Androl*, 25: 982-990.

Gravance CG, Vishwanath R, Pitt C, Casey PJ (1996). Computer automated morphometric analysis of bull sperm heads. *Theriogenology*, 46: 1205-1215.

Gray MW, Burger G, Lang BF (1999). Mitochondrial evolution. *Science*, 283: 1476-1481.

Grootegoed JA, Jansen R, Van der Molen HJ (1984). The role of glucose, pyruvate and lactate in ATP production by rat spermatocytes and spermatids. *Biochim Biophys Acta*, 767: 248-256.

Groves C (2005). The taxonomy of primates in the laboratory context. In *The laboratory primate* (Wolfe-Coote, ed.), pp. 3-15. Elsevier Academic Press, London.

Gur Y, Breitbart H (2006). Mammalian sperm translate nuclear-encoded proteins by mitochondrial-type ribosomes. *Genes Dev*, 20: 411-416.

Hackenbrock CR (1968). Ultrastructural bases for metabolically linked mechanical activity in mitochondria. II. Electron transport-linked ultrastructural transformations in mitochondria. *J Cell Biol*, 37: 345-369.

Harris T, Marquez B, Suarez S, Schimenti J (2007). Sperm motility defects and infertility in male mice with a mutation in *Nsun7*, a member of the sun domain-containing family of putative RNA methyltransferases. *Biol Reprod*, 77: 376-382.

Harrison RM, Kubisch HM (2005). Male reproduction and fertilization. In *The laboratory primate* (Wolfe-Coote, ed.), pp. 119-132. Elsevier Academic Press, London.

Harvey PH, Pagel MD (1991). *The comparative method in evolutionary biology.* Oxford University Press, New York.

Henkel R, Hajimohammad M, Stalf T, Hoogendijk C, Mehnert C, Menkveld R, Gips H, Schill WB, Kruger TF (2004). Influence of deoxyribonucleic acid damage on fertilization and pregnancy. *Fertil Steril*, 81: 965-972.

Henkel R, Maas G, Bödeker RH, Scheibelhut C, Stalf T, Mehnert C, Schuppe HC, Jung A, Schill WB (2005). Sperm function and assisted reproduction technology. *Reprod Med Biol*, 4: 7-30.

Hewitson L, Takahashi D, Dominko T, Simerly C, Schatten G (1998). Fertilization and embryo development to blastocysts after intracytoplasmic sperm injection in the rhesus monkey. *Hum Reprod*, 13: 3449-3455.

Hirai M, Boersma A, Hoeflich A, Wolf E, Föll J, Aumüller R, Braun J (2001). Objectively measured sperm motility and sperm head morphometry in boars (*Sus scrofa*): relation to fertility and seminal growth factors. *J Androl*, 22: 104-110.

Ho HC, Suarez SS (2001). Hyperactivation of mammalian spermatozoa: function and regulation. *Reproduction*, 22: 519-526.

Ho HC, Wey S (2007). Three dimensional rendering of the mitochondrial sheath morphogenesis during mouse spermiogenesis. *Microsc Res Techn*, 70: 719-723.

Holt WV (2005). Is quality assurance in semen analysis still really necessary? A spermatologist's viewpoint. *Hum Reprod*, 20: 2983-2986.

Holt WV, van Look KJW (2004). Concepts in sperm heterogeneity, sperm selection and sperm competition as biological foundations for laboratory tests of semen quality. *Reproduction*, 127: 527-535.

Hosken DJ (1997). Sperm competition in bats. *Proc R Soc Lond B*, 264: 385-392.

Humphries S, Evans JP, Simmons LW (2008). Sperm competition: linking form to function. *BMC Evol Biol*, 8: 319.

Hung PH, Miller MG, Meyers SA, VandeVoort CA (2008). Sperm mitochondrial integrity is not required for hyperactivated motility, zona binding or acrosome reaction in the rhesus macaque. *Biol Reprod*, 79: 367-375.

Immler S (2008). Sperm competition and sperm cooperation: the potential role of diploid and haploid expression. *Reproduction*, 135: 275-283.

Immler S, Birkhead TR (2007). Sperm competition and sperm midpiece size: no consistent pattern in passerine birds. *Proc R Soc Lond B*, 274: 561-568.

Immler S, Calhim S, Birkhead TR (2008). Increased postcopulatory sexual selection reduces the intramale variation in sperm design. *Evolution*, 62: 1538-1543.

Immler S, Moore HDM, Breed WG, Birkhead TR (2007). By hook or by crook? Morphometry, competition and cooperation in rodent sperm. *PLoS ONE*, 2: e170.

Jansen RPS, Burton GJ (2004). Mitochondrial dysfunction in reproduction. *Mitochondrion*, 4: 577-600.

Jarvis JUM (1981). Eusociality in a mammal: cooperative breeding in naked mole-rat colonies. *Science*, 212: 571-573.

Jarvis JUM (1985). Ecological studies on *Heterocephalus glaber*, the naked mole-rat, in Kenya. *Nat Geogr Soc Res Rep*, 20: 429-437.

Jasko DJ, Lein DH, Foote RH (1990). Determination of the relationship between sperm morphologic classifications and fertility in stallions: 66 cases (1987-1988). *JAVMA*, 197: 389-394.

Jeremias J, Witkin SS (1996). Molecular approaches to the diagnosis of male fertility. *Mol Hum Reprod*, 2: 195-202.

Jones AR (1997). Metabolism of lactate by mature boar spermatozoa. *Reprod Fertil Dev*, 9: 227-232.

Jones AR, Bubb WA (2000). Substrates for endogenous metabolism by mature boar spermatozoa. *J Reprod Fertil*, 119: 129-135.

Kamp G, Schmidt H, Stypa H, Freiden S, Mahling C, Wegener G (2007). Regulatory properties of 6-phosphofructokinase and control of glycolysis in boar spermatozoa. *Reproduction*, 133: 29-40.

Kao SH, Chao HT, Wei YH (1998). Multiple deletions of mitochondrial DNA are associated with the decline of motility and fertility of human spermatozoa. *Mol Hum Reprod*, 4: 657-666.

Kasai T, Ogawa K, Mizuno K, Nagai S, Uchida Y, Ohta S, Fujie M, Suzuki K, Hirata S, Hoshi K (2002). Relationship between sperm mitochondrial membrane potential, sperm motility, and fertility potential. *Asian J Androl*, 4: 97-103.

Katz DF, Diel L, Overstreet JW (1982). Differences in the movement of morphologically normal and abnormal human seminal spermatozoa. *Biol Reprod*, 26: 566-570.

Katz DF, Drobnis EZ, Overstreet JW (1989). Factors regulating mammalian sperm migration through the female reproductive tract and oocyte vestments. *Gamete Res*, 22: 443-469.

Katz DF, Yanagimachi R (1980). Movement characteristics of hamster spermatozoa within the oviduct. *Biol Reprod*, 22: 759-764.

Kim YH, Haidl G, Schaefer M, Egner U, Mandal A, Herr JC (2007). Compartmentalization of a unique ADP/ATP carrier protein SFEC (Sperm Flagellar Energy Carrier, AAC4) with glycolytic enzymes in the fibrous sheath of human sperm flagellum principal piece. *Dev Biol*, 302: 463-476.

King FA, Yarbrough CJ, Anderson DC, Gordon TP, Gould KG (1988). Primates. *Science*, 240: 1475-1482.

Kinukawa M, Nagata M, Aoki F (2003). Changes in flagellar bending during the course of hyperactivation in hamster spermatozoa. *Reproduction*, 125: 43-51.

Kondrashov AS (1988). Deleterious mutations and the evolution of sexual reproduction. *Nature*, 336: 435-440.

Kraemer M, Fillion C, Martin-Pont B, Auger J (1998). Factors influencing human sperm kinematic measurements by the Celltrak computer-assisted sperm analysis system. *Hum Reprod*, 13: 611-619.

Krisfalusi M, Miki K, Magyar PL, O'Brien DO (2006). Multiple glycolytic enzymes are tightly bound to the fibrous sheath of mouse spermtatozoa. *Biol Reprod*, 75: 270-278.

Kushner H, Kraft-Schreyer N, Angelakos ET, Wudarski EM (1982). Analysis of reproductive data in a breeding colony of African Green Monkeys. *J Med Primatol*, 11: 77-84.

Lambrechts H, van Niekerk FE, Cloete SWP, Coetzer WA, van der Horst G (2000). Sperm viability and morphology of two genetically diverse Merino lines. *Reprod Fertil Dev*, 12: 337-344.

Lardy HA, Phillips PH (1941). The effects of certain inhibitors and activators on sperm metabolism. *J Biol Chem*, 138: 195-202.

Lhuillier P, Rode B, Escalier D, Lorès P, Dirami T, Bienvenu T, Gacon G, Dulioust E, Touré A (2009). Absence of annulus in human asthenozoospermia: Case Report. *Hum Reprod*, 24: 1296-1303.

Lightfoot J, Salamon S (1970). Fertility of ram spermatozoa frozen by the pellet method. *J Reprod Fertil*, 22: 385-398.

Lin CY, Hung PH, VandeVoort CA, Miller MG (2009). ^{1}H NMR to investigate metabolism and energy supply in rhesus macaque sperm. *Reprod Toxicol*, 28: 75-80.

Liu FGR, Miyamoto MM, Freire NP, Ong PQ, Tennant MR, Young TS, Gugel KF (2001). Molecular and morphological supertrees for eutherian (placental) mammals. *Science*, 291: 1786-1789.

Lodish H, Balitimore D, Blerk A, Zipursky SL, Matsudaria P, Darnell J (1995). *Molecular Cell Biology* (3rd Ed.). WH Freeman and Company, New York.

Logan DC (2006). The mitochondrial compartment. *J Exp Bot*, 57: 1225-1243.

Lüpold S, Calhim S, Immler S, Birkhead TR (2009). Sperm morphology and sperm velocity in birds. *Proc R Soc Lond B*, 276: 1175-1181.

Mahadevan MM, Miller MM, Moutos DM (1997). Absence of glucose decreases human fertilization and sperm movement characteristics *in vitro*. *Hum Reprod*, 12: 119-123.

Malo AF, Garde JJ, Soler AJ, García AJ, Gomendio M, Roldan ERS (2005). Male fertility in natural populations of red deer is determined by sperm velocity and the proportion of normal spermatozoa. *Biol Reprod*, 72: 822-829.

Malo AF, Gomendio M, Garde J, Lang-Lenton B, Soler AJ, Roldan ERS (2006). Sperm design and sperm function. *Biol Lett*, 2: 246-249.

207

Mannella CA (2006a). The relevance of mitochondrial membrane topology to mitochondrial function. *Biochim Biophys Acta*, 1762: 140-147.

Mannella CA (2006b). Structure and dynamicas of the mitochondrial inner membrane cristae. *Biochim Biophys Acta*, 1763: 542-548.

Mann T, Lutwak-Mann C (1981). Biochemistry of spermatozoa: chemical and functional correlations in ejaculated semen – andrological aspects. In *Male reproductive function and semen* (Mann T, Lutwak-Mann C, eds.), pp. 195-268. Springer-Verlag, Berlin.

Marchetti C, Gallego MA, Defossez A, Formstecher P, Marchetti P (2004b). Staining of human sperm with fluorochrome-labeled inhibitor of caspases to detect activated caspases: correlation with apoptosis and sperm parameters. *Hum Reprod*, 19: 1127-1134.

Marchetti C, Jouy N, Leroy-Matin B, Defossez A, Formstecher P, Marchetti P (2004a). Comparison of four fluorochromes for the detection of the inner mitochondrial membrane potential in human spermatozoa and their correlation with sperm motility. *Hum Reprod*, 19: 2267-2276.

Marchetti C, Obert G, Deffosez A, Formstecher P, Marchetti P (2002). Study of mitochondrial membrane potential, reactive oxygen species, DNA fragmentation and cell viability by flow cytometry in humans. *Hum Reprod*, 17: 1257-1265.

Marco-Jiménez F, Puchades S, Gadea J, Vicente JS, Viudes-de-Castro MP (2005). Effect of semen collection method on pre- and post-thaw Guirra ram spermatozoa. *Theriogenology*, 64: 1756-1765.

Maree L, du Plessis SS, Menkveld R, van der Horst G (2010). Morphometric dimensions of the human sperm head depend on the staining method used. *Hum Reprod*, 25: 1369-1382.

Margulis L (1996). Archaeal-eubacterial merges in the origin of Eukarya: phylogenetic classification of life. *Proc Natl Acad Sci*, 93: 1071-1076.

Martin RD (2003). Human reproduction: a comparative background for medical hypotheses. *J Reprod Immunol*, 59: 111-135.

Martin RD (2007). The evolution of human reproduction: a primatological perspective. *Yearbook Physc Antropol*, 50: 59-84.

Martínez-Heredia J, de Mateo S, Vidal-Taboada JM, Ballescà, Oliva R (2008). Identification of proteomic differences in asthenozoospermic sperm samples. *Hum Reprod*, 23: 783-791.

Matthiesson KL, McLachlan RI (2006). Male hormonal contraception: concept proven, product in sight? *Hum Reprod Update*, 12: 463-482.

Mattner PE, Voglmayr RI (1962). A comparison of ram semen collection by the artificial vagina and by electro-ejaculation. *Aust J Exp Agric Anim Husb*, 2: 78-81.

Maynard Smith J (1978). *The evolution of sex*. Cambridge University Press, Cambridge.

Mdhluli MC, Seier JV, van der Horst G (2004). The male vervet monkey: sperm characteristics and use in reproductive research. *Gynaecol Obst Invest*, 57: 17-18.

Meinhardt A, Beate W, Seitz J (1999). Expression of mitochondrial markers during spermatogenesis. *Hum Reprod Update*, 5: 108-119.

Menkveld R, Stander FSH, Kotze TJ, Kruger TF, van Zyl JA (1990). The evaluation of morphological characteristics of human spermatozoa according to stricter criteria. *Hum Reprod*, 5: 586-592.

Meschede D, Keck C, Zander M, Cooper TG, Yeung CH, Nieschlag E (1993). Influence of three different preparation techniques on the results of human sperm morphology analysis. *Int J Androl*, 16: 362-369.

Miki K (2007). Energy metabolism and sperm function. *Soc Reprod Fertil Suppl*, 65: 309-325.

Miki K, Qu W, Goulding EH, Willis WD, Bunch DO, Strader LF, Perreault SD, Eddy EM, O'Brien DO (2004). Glyceraldehyde 3-phosphate dehydrogenase-S, a sperm-specific glycolytic enzyme, is required for sperm motility and male fertility. *PNAS*, 101: 16501-16506.

Miller D, Ostermeier GC (2006). Towards a better understanding of RNA carriage by ejaculate spermatozoa. *Hum Reprod Update*, 12: 757-767.

Mocé E, Graham JK (2008). *In vitro* evaluation of sperm quality. *Anim Reprod Sci*, 105: 104-118.

Molecular Probes (2006). MitoTracker® and MitoFluor mitochondrion-selective probes. Invirogen: Manuals and Protocols.

Moller AP (1988). Ejaculate quality, testis size and sperm competition in primates. *J Hum Evol*, 17: 479-488.

Moore H, Dvoráková K, Jenkins N, Breed W (2002). Exceptional sperm cooperation in the wood mouse. *Nature*, 418: 174-177.

Morrow EH, Gage MJG (2001). Consistent significant variation between individual males in spermatozoal morphometry. *J Zool Lond*, 254: 147-153.

Mortimer D (1994). *Practical laboratory andrology*. Oxford University Press, New York.

Mortimer D, Serres C, Mortimer ST, Jouannet P (1988). Influence of image sampling frequency on the perceived movement characteristics of progressively motile human spermatozoa. *Gam Res*, 20: 313-327.

Mortimer ST (1997). A critical review of the physiological importance and analysis of sperm movement in mammals. *Hum Reprod Update*, 3: 403-439.

Mortimer ST, Maxwell WMC (1999). Kinematic definition of ram sperm hyperactivation. *Reprod Fertil Dev*, 11: 25-30.

Mortimer ST, Mortimer D (1990). Kinematics of human spermatozoa incubated under capacitating conditions. *J Androl*, 11: 195-203.

Mukai C, Okuno M (2004). Glycolysis plays a major role for adenosine triphospate supplementation in mouse sperm flagellar movement. *Biol Reprod*, 71: 540-547.

Mundy AJ, Ryder TA, Edmonds DK (1995). Asthenozoospermia and the human sperm mid-piece. *Hum Reprod* 10: 166-119.

Nakada K, Sato A, Yoshida K, Morita T, Tanaka H, Inoue S, Yonekawa H, Hayashi J (2006). Mitochondria-related male infertility. *PNAS*, 103: 15148-15153.

Nakamura M, Okinaga S, Arai K (1984). Metabolism of pachytene primary spermatocytes from rat testes: pyruvate maintenance of adenosine triphosphate level. *Biol Reprod*, 30: 1118-1197.

Nakamura N, Shibata H, O'Brien D, Mori C, Eddy EM (2008). Spermatogenic cell-specific Type I Hexokinase is the predominant hexokinase in sperm. *Mol Reprod Dev*, 75: 632-640.

Nascimento JM, Shi LZ, Chandsawangbhuwana C, Tam J, Durrant B, Botvinick EL, Berns MW (2008b). Use of laser tweezers to analyze sperm motility and mitochondrial membrane potential. *J Biomed Opt*, 13: 014002.

Nascimento JM, Shi LZ, Tam J, Chandsawangbhuwana C, Durrant B, Botvinick EL, Berns MW (2008a). Comparison of glycolysis and oxidative phosphorylation as energy sources for mammalian sperm motility, using the combination of fluorescence imaging, laser tweezers, and real-time automated tracking and trapping. *J Cell Physiol*, 217: 745-751.

Nevo AC (1965). Dependence of sperm motility and respiration on oxygen concentration. *J Reprod Fertil*, 9: 103-107.

Nevo AC (1966). Relation between motility and respiration in human spermatozoa. *J Reprod Fertil*, 11: 19-26.

Nichols SM, Bavister BD (2006). Comparison of protocols for cryopreservation of rhesus monkey spermatozoa by post-thaw motility recovery and hyperactivation. *Reprod Fertil Dev*, 18: 777-780.

O'Donnell JM, Ellory JC (1970). The binding of ouabain to spermatozoa of boar and ram. *J Reprod Fertil*, 23: 181-184.

Oliva R (2006). Protamines and male infertility. *Hum Reprod Update*, 12: 417-435.

Oliva R, Martínez-Heredia J (2008). Proteomics in the study of sperm cell composition, differentiation and function. *Syst Biol Reprod Med*, 54: 23-36.

Olson GE, Winfrey VP (1990). Mitochondria-cytoskeleton interactions in the sperm midpiece. *J Struct Biol*, 103: 13-22.

Olson GE, Winfrey VP (1992). Structural organization of surface domains of sperm mitochondria. *J Reprod Dev*, 33: 89-98.

Ott M, Gogvadez V, Orrenius S, Zhivotovsky B (2007). Mitochondria, oxidative stress and cell death. *Apoptosis*, 12: 913-922.

Paasch U, Grunewald S, Agarwal A, Glandera HJ (2004). Activation pattern of caspases in human spermatozoa. *Fertil Steril*, 81: 802-809.

Page ST, Amory JK, Bremner WJ (2008). Advances in male contraception. *Endocr Rev*, 29: 465-493.

Parker GA (1970). Sperm competition and its evolutionary consequences in the insects. *Biol Rev*, 45: 525-567.

Pasupuleti V (2007). *Role of glycolysis and respiration in sperm metabolism and motility*. Unpublished MSc thesis, Kent State University.

Paulenz H, Adnoy T, Fossen OH, Söderquist L, Andersen Berg K (2002). Effect of deposition site and sperm number on the fertility of sheep inseminated with liquid semen. *Vet Rec*, 150: 299-302.

Petrunkina AM, Waberski D, Günzel-Apel AR, Töpfer-Petersen E (2007). Determinants of sperm quality and fertility in domestic species. *Reproduction*, 134: 3-17.

Phillips, DM (1977). Mitochondrial disposition in mammalian spermatozoa. *J Ultrastr Res*, 58: 144-154.

Piasecka M, Kawiak J (2003). Sperm mitochondria of patients with normal sperm motility and with asthenozoospermia: morphological ans functional study. *Folia Histochem Cytobiol*, 41: 125-139.

Piasecka M, Gaczarzewicz D, Laszczynska M, Starczewski A, Brodowska A (2007). Flow cytometry application in the assessment of sperm DNA integrity of men with astenozoospermia. *Folia Histochem Cytobiol*, 45(Supp. 1): 127-136.

Pitnick S, Hosken DJ, Birkhead TR (2009). Sperm morphological diversity. In *Sperm Biology: An evolutionary perspective* (Birkhead TR, Hosken DJ, Pitnick S, eds.), pp. 69-149. NY: Academic Press, New York.

Poot M, Zhang YZ, Krämer JA, Wells KS, Jones LJ, Hanzel DK, Lugade AG, Singer VL, Haugland RP (1996). Analysis of mitochondrial morphology and function with novel fixable fluorescent stains. *J Hitochem Cytochem*, 44: 1363-1372.

Publicover S, Harper CV, Barratt C (2007). $[Ca^{2+}]_i$ signalling in sperm – making the most of what you've got. *Nat Cell Biol*, 9: 235-242.

Ramalho-Santos J, Varum S, Amaral S, Mota PC, Sousa AP, Amaral A (2009). Mitochondrial functionality in reproduction: from gonads and gametes to embryos and embryonic stem cells. *Hum Reprod Update*, 15: 553-572.

Ramm SA, Stockley P (2010). Sperm competition and sperm length influence the rate of mammalian spermatogenesis. *Biol Lett*, 6: 219-221.

Reinton N, Ostravik S, Haugen TB, Jahnsen T, Taskén K, Skalhegg BS (2000). A novel isoform of human cyclic 3',5'-adenosine monophosphate-dependant protein kinase, Cα-s, localizes to sperm midpiece. *Biol Reprod*, 63: 607-611.

Ren D, Navarro B, Perez G, Jackson AC, Hsu S, Shi Q, Tilly JL, Clapham DE (2001). A sperm ion channel required for sperm motility and male fertility. *Nature*, 413: 603-609.

Ridley M (1996). *Evolution*. Blackwell Science, Massachusetts, 2nd Ed.

Rijsselaere T, van Soom A, Tanghe S, Coryn M, Maes D, de Kruif A (2005). New techniques for the assessment of canine semen quality: a review. *Theriogenology*, 64: 706-719.

Ruiz-Pesini E, Diez C, Lapeña CA, Pérez-Martos A, Montoya J, Alvarez E, Arenas J, López-Pérez MJ (1998). Correlation of sperm motility with mitochondria activities. *Clin Chem* 44: 1616-1620.

Ruiz-Pesini E, Díez-Sánchez C, López-Pérez MJ, Enríquez JA (2007). The role of the mitochondrion in sperm function: is there a place for oxidative phosphorylation or is it purely a glycolytic process? *Cur Top Dev Biol*, 77: 3-19.

Ruiz-Pesini E, Lapeña CA, Díez-Sánchez C, Pérez-Martos A, Montoya J, Alvarez E, Díaz M, Urriés A , Montoro L, López-Pérez MJ, Enríquez JA (2000). Human mtDNA haplogroups associated with high or reduced spermatozoa motility. *Am J Hum Gen*, 67: 682-696.

Ruwanpura SM, McLachlan RI, Meachem SJ (2010). Hormonal regulation of male germ cell development. *J Endocrinol*, 205: 117-131.

Sathananthan AH, Ng SC, Edirisinghe R, Ratnam SS, Wong PC (1986). Human sperm-egg interaction in vitro. *Gam Res*, 15: 317-326.

Schaffer NE, McCarthy TJ, Fazleabas AT, Jeyendran RS (1992). Assessment of semen quality in a baboon (*Papio anubis*) breeding colony. *J Med Primatol*, 21: 47-48.

Schneider M, Förster H, Boersma A, Seiler A, Wehnes H, Sinowatz F, Neumüller C, Deutsch MJ, Walch A, Hrabé de Angelis M, Wurst W, Ursini F, Roveri A, Maleszewski M, Maiorino M, Conrad M (2009). Mitochondrial glutathione peroxidise 4 disruption causes male infertility. *FASEB J*, 23: 3233-3242.

Schurko AM, Neiman M, Logsdon JM Jr (2009). Signs of sex: what we know and how we know it. *Trend Ecol Evol*, 24: 208-217.

Schwartz M, Vissing J (2002). Paternal inheritance of mitochondrial DNA. *N Eng J Med*, 347: 576-580.

Seier JV (1986). Breeding vervet monkeys in a closed environment. *J Med Primatol*, 15: 339-349.

Seier JV, Conradie E, Oettle EE, Fincham JE (1993). Cryopreservation of vervet monkey semen and recovery of progressively motile spermatozoa. *J Med Primatol*, 22: 355-599.

Seier JV, Fincham JE, Menkveld R, Venter FS (1989). Semen characteristics of vervet monkeys. *Lab Anim*, 23: 43-47.

Seitz J, Möbius J, Bergmann M, Meinhardt A (1995). Mitochondrial differentiation during meiosis of male germ cells. *Int J Androl*, 18(Suppl 2): 7-11.

Serres C, Feneux D, Jouannet P, David G (1984). Influence of the flagellar wave development and propagation on the human sperm movement in seminal plasma. *Gam Res*, 9: 183-195.

Shibahara H, Obara H, Ayustawati, Hirano Y, Suzuki T, Ohno A, Takamizawa S, Suzuki M (2004). Prediction of pregnancy by intrauterine insemination using CASA estimates and strict criteria in patients with male factor infertility. *Int J Androl*, 27: 63-8.

Sibley CG, Ahlquist JE (1987). DNA hybridization evidence of hominoid phylogeny: results from an expanded data set. *J Mol Evol*, 26: 99-121.

Sifer C, Sasportes T, Barraud V, Poncelet C, Rudant J, Porcher R, Cedrin-Durnerin I, Martin-Pont B, Hugues JN, Wolf JP (2005). World Health Organization grade 'a' motility and zona-binding test accurately predict IVF outcome for mild male factor and unexplained infertilities. *Hum Reprod*, 20: 2769-2775.

Skinner JD, Smithers RHN (1990). *The mammals of the Southern African Subregion* (2nd Ed). University of Pretoria, Pretoria.

Snook RR (2005). Sperm in competition: not playing by the numbers. *Trends Ecol Evol*, 20: 46-53.

Soler C, Gadea B, Soler AJ, Fernández-Santos MR, Esteso MC, Núñez J, Moreira PN, Núñez M, Gutiérrez R, Sancho M, Garde JJ (2005). Comparison of three different staining

methods for the assessment of epididymal red deer sperm morphometry by computerized analysis with ISAS®. *Theriogenology*, 64: 1236-1243.

Sparman ML, Ramsey CM, Thomas CM, Mitalipov SM, Fanton JW, Maginnis GM, Stouffer RL, Wolf DP (2007). Evaluation of the vervet (*Chlorocebus aethiops*) as a model for assisted reproductive technologies. *Am J Primatol*, 69: 917-929.

Spinks AC, van der Horst G, Bennett NC (1997). Influence of breeding season and reproductive status on male reproductive characteristics in the common mole-rat, *Cryptomys hottentotus hottentotus*. *J Reprod Fertil*, 109: 79-86.

Spiropoulos J, Turnbull DM, Chinnery PF (2002). Can mitochondrial DNA mutations cause sperm dysfunction? *Mol Hum Reprod*, 8: 719-722.

St John JC, Jokhi RP, Barratt CLR (2005). The impact of mitochondrial genetics on male infertility. *Int J Androl*, 28: 65-73.

St John JC, Sakkas D, Barratt CLR (2000). A role for mitochondrial DNA and sperm survival. *J Androl*, 21: 189-199.

St John JC, Schatten G (2004). Paternal mitochondrial DNA transmission during nonhuman primate nuclear transfer. *Genetics*, 167: 897-905.

Storey BT (2008). Mammalian sperm metabolism: oxygen and sugar, friend and foe. *Int J Dev Biol*, 52: 427-437.

Storey BT, Kayne FJ (1977). Energy metabolism of spermatozoa. VI. Direct intramitochondrial lactate oxidation by rabbit sperm mitochondria. *Biol Reprod*, 16: 549-556.

Stouffs K, Tournaye H, Liebaers I, Lissens W (2009). Male fertility and the involvement of the X chromosome. *Hum Reprod Update*, 15: 623-637.

Suarez SS, Pacey AA (2006). Sperm transport in the female reproductive tract. *Hum Reprod Update*, 12: 23-37.

Suarez S (1996). Hyperactivated motility in sperm. *J Androl*, 17: 331-335.

216

Suarez SS (2008). Control of hyperactivation in sperm. *Hum Reprod Update*, 14: 647-657.

Suter D, Chow PYW, Martin ICA (1979). Maintenance of motility in human spermatozoa by energy derived through oxidative phosphorylation and addition of albumin. *Biol Reprod*, 20: 505-510.

Sutovsky P, Moreno RD, Ramalho-Santos J, Dominko T, Simerly C, Schatten G (1999). Ubiquitin tag for sperm mitochondria. *Nature*, 402: 371.

Sutovsky P, Moreno RD, Ramalho-Santos J, Dominko T, Simerly C, Schatten G (2000). Ubiquitinated sperm mitochondria, selective proteolysis, and the regulation of mitochondrial inheritance in mammalian embryos. *Biol Reprod*, 63: 582-590.

Sutovsky P, Navara CS, Schatten G (1996). Fate of sperm mitochondria, and the incorporation, conversion, and disassembly of the sperm tail structures during bovine fertilization. *Biol Reprod*, 55: 1195-1205.

Sutovsky P, Tengowski MW, Navara CS, Zoran SS, Schatten G (1997). Mitochondrial sheath movement and detachment in mammalian, but not nonmammalian, sperm induced by disulfide bond reduction. Mol Reprod Dev, 47: 79-86.

Szabadkai G and Duchen MR (2007). Mitochondria: the hub of cellular Ca^{2+} signalling. *Physiology*, 23: 84-94.

Tanaka H, Kohroki J, Iguchi N, Onishi M, Nishimune Y (2001). Cloning and characterization of a human ortholoque of testis-specific succinyl CoA: 3-oxo acid CoA transferase (*Scot-t*) cDNA. *Mol Hum Reprod*, 8: 16-23.

Tayama K, Fujita H, Takahashi H, Nagasawa A, Yano N, Yuzawa K, Ogata A (2006). Measuring mouse sperm parameters using a particle counter and sperm quality analyzer: a simple and inexpensive method. *Reprod Toxicol*, 22: 92-101.

Terada H (1990). Uncouplers of oxidative phosphorylation. *Environ Health Perspect*, 87: 213-218.

Thompson WE, Ramalho-Santos J, Sutovsky P (2003). Ubiquitination of prohibitin in mammalian sperm mitochondria: possible roles in the regulation of mitochondrial inheritance and sperm quality control. *Biol Reprod*, 69: 254-260.

Tremellen K (2008). Oxidative stress and male infertility – a clinical perspective. *Hum Reprod Update,* 14: 243-258.

Troiano L, Granata ARM, Cossarizza A, Kalashnikova G, Bianchi R, Pini G, Tropea F, Carani C, Franceschi C (1998). Mitochondrial membrane potential and DNA stability in human sperm cells: a flow cytometry analysis with implications for male infertility. *Exp Cell Res*, 241: 384-393.

Turner RM (2003). Tales from the tail: what do we really know about sperm motility? *J Androl*, 24: 790-803.

Turner RM (2006). Moving to the beat: a review of mammalian sperm motility regulation. *Reprod Fertil Dev*, 18: 25-38.

Urner F, Sakkas D (1996). Glucose participates in sperm-oocyte fusion in the mouse. *Biol Reprod*, 55: 917-922.

van der Horst G (2005). Reproduction: male. In *The laboratory primate* (Wolfe-Coote, ed.), pp. 527-536. Elsevier Academic Press, London.

van der Horst G, Maree L (2009). SpermBlue®: a new universal stain for human and animal sperm which is also amenable to sperm morphology analysis. *Biotechn Histochem*, 84: 299-308.

van der Horst G, Maree L, Kotzé S, Brooks N (2006). Number of sperm mitochondria and sperm velocity: species specificity and relationships in selected mammals. *Proc Microsc Soc S Afr*, 36: 52.

van der Horst G, Maree L, Kotze SH, O'Riain J (2011). Sperm structure and sperm motility in the eusocial naked mole rat, *Heterocephalus glaber*: a case of degenerative orthogenesis the absence of sperm competition? (in preparation).

van der Horst G, Seier JV, Spinks AC, Hendricks S (1999). The maturation of sperm motility in the epididymis and vas deferens of the vervet monkey, *Cercopithecus aethiops*. *Int J Androl*, 22: 197-207.

Voglmayr JK (1975). Metabolic changes in spermatozoa during epididymal transit. In *Handbook of Physiology. Section VII. Endocrinology. Volume V. Male Reproductive System* (Hamilton DW, Greep RO, eds.), pp. 437-451. American Physiology Society, Washington, DC.

Vorup-Jensen T, Hjort T, Abraham-Peskir JV, Guttmannn P, Jensenius JC, Uggerhoj E, Medenwaldt R (1999). X-ray microscopy of human spermatozoa shows a change of mitochondrial morphology after capacitiation. *Hum Reprod*, 14: 880-884.

Wang RS, Yeh S, Tzeng CR, Chang C (2009). Androgen receptor roles in spermatogenesis and fertility: lessons from testicular cell-specific androgen receptor knockout mice. *Endocr Rev*, 30: 119-132.

Wang X, Sharma RK, Gupta A, George V, Thomas AJ, Falcone T, Agarwal A (2003). Alterations in mitochondria membrane potential and oxidative stress in infertile men: a prospective observational study. *Fertil Steril*, 80 (Suppl 2): 844-850.

Webster KA, Discher DJ, Bishopric NH (1994). Regulation of *fos* and *jun* immediate-early genes by redox or metabolic stress in cardiac myocytes. *Circ Res*, 74: 679-686.

Weng SL, Taylor SL, Morshedi M, Schuffner A, Duran EH, Beebe S, Oehninger S (2002). Caspase activity and apoptotic markers in ejaculated human sperm. *Mol Hum Reprod*, 8: 984-991.

White-Cooper H, Bausek N (2010). Evolution and spermatogenesis. *Phil Trans R Soc B*, 365: 1465-1480.

Wilkins AS, Holliday R (2009). The evolution of meiosis from mitosis. *Genetics* 181: 3-12.

Williams AC, Ford WC (2001). The role of glucose in supporting motility and capacitation in human spermatozoa. *J Androl*, 22: 680-695.

Windsor DP (1997). Mitochondrial function and ram sperm fertility. *Reprod Fertil Dev*, 9: 279-284.

Windsor DP, White IG (1993). Assessment of ram sperm mitochondrial function by quantitative determination of sperm rhodamine 123 accumulation. *Mol Reprod Develop*, 36: 354-360.

Wiseman H, Halliwell B (1996). Damage to DNA by reactive oxygen and nitrogen species: role in inflammatory disease and progression to cancer. *Bioch J*, 313: 17-29.

Wolf DP (2004). Assisted reproductive technologies in rhesus macaques. *Reprod Biol Endocr*, 37: 1-11.

World Health Organization (1999). *WHO laboratory manual for the examination of human semen and sperm-cervical mucus interaction* (4th Ed.). Cambridge University Press, Cambridge, UK.

World Health Organization (2010). *WHO laboratory manual for the examination and processing of human semen* (5th Ed.). WHO Press, Switzerland.

Yeung CH, Majumder GC, Rolf C, Behre HM, Cooper TG (1996). The role of phosphocreatine kinase in the motility of human spermatozoa supported by different metabolic substrates. *Mol Hum Reprod*, 2: 591-596.

Younglai EV, Holt D, Brown P, Jurisicova A, Casper RF (2001). Sperm swim-up techniques and DNA fragmentation. *Hum Reprod*, 16: 1950-1953.

Zeviani M, Antozzi C (1997). Mitochondrial disorders. *Hum Reprod Update*, 3: 133-148.

Zhao Y, Li Q, Yao C, Wang Z, Zhou Y, Wang Y, Liu L, Wang Y, Wang L, Qiao Z (2006). Characterization and quantification of mRNA transcripts in ejaculated spermatozoa of fertile men by serial analysis of gene expression. *Hum Reprod*, 21: 1583-1590.

Zimmer C (2009). On the origin of sexual reproduction. *Science*, 324: 1254-1256.

Zinaman MJ, Brown CC, Selevan SG, Clegg ED (2000). Semen quality and human fertility: a prospective study with healthy couples. *J Androl*, 21: 145-153.

APPENDICES

APPENDIX 1: Example of the consent form completed by each human semen donor

University of the Western Cape
Private Bag X17 Bellville 7535 South Africa
Telephone: [021] 959-2255/959 2762
Fax: [021]959 1268/2266

DEPARTMENT OF MEDICAL BIOSCIENCES

SEMEN DONATION FOR RESEARCH PURPOSES - CONSENT FORM

I hereby give my voluntary consent to donate my sperm for research projects conducted by Prof G van der Horst, Ms C de Villiers and Ms L Maree at the Department of Medical Biosciences, University of the Western Cape.

By signing this consent form, I agree as follows:

1. My semen sample(s) will be used exclusively for research purposes. The researchers will not use my semen sample(s) for in-vivo insemination, genetic manipulation, or for in vitro fertilization of human oocytes for the creation of embryos and embryonic stem cells.
2. The researchers will routinely discard any semen they do not use for their research projects in a responsible manner as medical waste.
3. My involvement in these research projects will be kept confidential and any results will be recorded by using identification codes instead of names. Any report that the researchers publish will not include any information that will make it possible for the readers to identify me as a sperm donor.
4. I will not receive any financial benefits from future commercial development and scientific patents of discoveries made through the use of my sperm cells.

Signed this day ………… of ….….……….. 20..... at ……………………………..

………………………………………   **…………………………………………..**
Signature of Sperm Donor   **Printed Name**

222

APPENDIX 2: Chemical composition of Gibco Ham's F 10 Nutrient mixture

From: Invitrogen Life Science, Technical Resources, Media formulations

COMPONENTS	Molecular Weight	Concentration (mg/L)	mM
Amino Acids			
Glycine	75	7.5	0.1
L-Alanine	89	9	0.101
L-Arginine hydrochloride	211	211	1
L-Asparagine-H2O	150	15	0.1
L-Aspartic acid	133	13	0.0977
L-Cysteine	121	25	0.207
L-Glutamic Acid	147	14.7	0.1
L-Glutamine	146	146	1
L-Histidine hydrochloride-H2O	210	23	0.11
L-Isoleucine	131	2.6	0.0198
L-Leucine	131	13	0.0992
L-Lysine hydrochloride	183	29	0.158
L-Methionine	149	4.5	0.0302
L-Phenylalanine	165	5	0.0303
L-Proline	115	11.5	0.1
L-Serine	105	10.5	0.1
L-Threonine	119	3.6	0.0303
L-Tryptophan	204	0.6	0.00294
L-Tyrosine disodium salt dihydrate	261	2.62	0.01
L-Valine	117	3.5	0.0299
Vitamins			
Biotin	244	0.024	0.0000984
Choline chloride	140	0.7	0.005
D-Calcium pantothenate	477	0.7	0.00147
Folic Acid	441	1.3	0.00295
Niacinamide	122	0.6	0.00492
Pyridoxine hydrochloride	206	0.2	0.000971
Riboflavin	376	0.4	0.00106
Thiamine hydrochloride	337	1	0.00297
Vitamin B12	1355	1.4	0.00103

i-Inositol	**180**	**0.5**	**0.00278**
Inorganic Salts			
Calcium Chloride (CaCl2) (anhyd.)	**111**	**33.3**	**0.3**
Cupric sulfate (CuSO4-5H2O)	**250**	**0.0025**	**0.00001**
Ferric sulfate (FeSO4-7H2O)	**278**	**0.834**	**0.003**
Magnesium Sulfate (MgSO4) (anhyd.)	**120**	**74.62**	**0.622**
Potassium Chloride (KCl)	**75**	**285**	**3.8**
Potassium Phosphate monobasic (KH2PO4)	**136**	**83**	**0.61**
Sodium Bicarbonate (NaHCO3)	**84**	**1200**	**14.29**
Sodium Chloride (NaCl)	**58**	**7400**	**127.59**
Sodium Phosphate dibasic (Na2HPO4) anhydrous	**142**	**153.7**	**1.08**
Zinc sulfate (ZnSO4-7H2O)	**288**	**0.03**	**0.000104**
Other Components			
D-Glucose (Dextrose)	**180**	**1100**	**6.11**
Hypoxanthine Na	**159**	**4.7**	**0.0296**
Lipoic Acid	**206**	**0.2**	**0.000971**
Phenol Red	**376.4**	**1.2**	**0.00319**
Sodium Pyruvate	**110**	**110**	**1**
Thymidine	**242**	**0.7**	**0.00289**
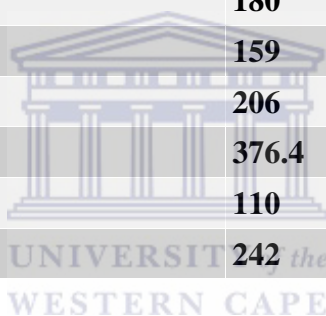
Table 5.3. (continued) Sperm motility and kinematic parameter measurements (mean ± SD) captured at 75 frames/second for six mammalian species (n = 10 individuals per species) to indicate the effect of the time of capture on these parameters

	Homo sapiens		*Papio ursinus*		*Macaca mulatta*	
	10 min	30 min	10 min	30 min	10 min	30 min
Motility (%)	94.2 ± 3.0	93.8 ± 3.6	96.8 ± 3.8	91.4 ± 6.5	95.5 ± 4.6	90.7 ± 5.8
VCL (µm/s)	134.1 ± 23.9	128.6 ± 17.8	369.4 ± 34.9	341.9 ± 43.4	325.5 ± 19.0	319.5 ± 14.5
VSL (µm/s)	85.2 ± 15.2	75.9 ± 10.6	343.7 ± 35.4	315.5 ± 47.4	239.3 ± 31.7	260.6 ± 35.0
VAP (µm/s)	96.7 ± 15.3	88.5 ± 11.5	355.7 ± 36.1	327.5 ± 45.8	262.9 ± 25.6	278.4 ± 29.4
LIN (%)	63.6 ± 4.6[a]	59.2 ± 4.7[b]	93.0 ± 2.0	90.2 ± 3.4	73.5 ± 8.7	81.5 ± 9.4
STR (%)	87.9 ± 2.4[a]	85.7 ± 2.2[b]	96.6 ± 0.9	96.2 ± 1.5	90.7 ± 4.1	93.3 ± 3.2
WOB (%)	72.4 ± 4.0	69.0 ± 4.1	96.3 ± 1.3	95.6 ± 2.2	80.7 ± 6.3	87.1 ± 7.7
ALH (µm)	2.2 ± 0.3	2.4 ± 0.3	2.4 ± 0.5	2.3 ± 0.3	3.2 ± 0.5[a]	2.7 ± 0.5[b]
BCF (Hz)	24.7 ± 2.9[a]	22.5 ± 2.0[b]	21.9 ± 2.1	22.0 ± 2.2	31.5 ± 4.8	28.5 ± 6.0
	Chlorocebus aethiops		*Ovis orientalis*		*Mus musculus*	
	10 min	30 min	10 min	30 min	10 min	30 min
Motility (%)	95.3 ± 5.4	95.7 ± 2.1	87.9 ± 4.7	83.6 ± 6.8	91.3 ± 6.2	89.2 ± 6.8
VCL (µm/s)	333.2 ± 17.8	333.5 ± 12.4	258.3 ± 40.1	248.3 ± 25.7	342.0 ± 40.7[a]	291.5 ± 89.6[b]
VSL (µm/s)	303.4 ± 20.0	302.6 ± 12.7	185.1 ± 46.6	162.5 ± 38.8	125.2 ± 16.5[a]	94.6 ± 42.1[b]
VAP (µm/s)	317.7 ± 18.6	320.0 ± 12.9	207.4 ± 44.8	186.4 ± 36.3	157.3 ± 15.9	128.0 ± 42.7
LIN (%)	91.0 ± 2.5	90.7 ± 1.6	72.2 ± 15.7	65.8 ± 15.5	36.9 ± 4.8	31.6 ± 4.0
STR (%)	95.5 ± 1.2	94.6 ± 1.0	88.4 ± 5.5	86.3 ± 6.1	79.5 ± 4.9[a]	72.2 ± 7.2[b]
WOB (%)	95.3 ± 1.6	96.0 ± 0.7	80.9 ± 14.8	75.4 ± 14.2	46.2 ± 3.5	43.7 ± 1.3
ALH (µm)	2.1 ± 0.3	2.2 ± 0.1	3.0 ± 1.0	3.0 ± 0.8	8.2 ± 1.0	8.2 ± 1.2
BCF (Hz)	18.9 ± 1.0	18.6 ± 0.7	26.1 ± 4.2	24.8 ± 5.6	11.9 ± 2.1[a]	8.6 ± 2.2[b]

VCL = curvilinear velocity, VSL = straight-line velocity, VAP = average path velocity, LIN = linearity, STR = straightness, WOB = wobble, ALH = amplitude of lateral head displacement, BCF = beat cross frequency

a, b = values labelled with different superscript letters in the same row for each individual species were significantly different (P < 0.05)

Table 5.4. (**continued**) Sperm motility and kinematic parameter measurements (mean ± SD) captured at 30 minutes after the sperm preparation was made for six mammalian species (n = 10 individuals per species) to indicate the effect of the capturing frame rate on these parameters

	Homo sapiens		*Papio ursinus*		*Macaca mulatta*	
	50 f/s	**75 f/s**	**50 f/s**	**75 f/s**	**50 f/s**	**75 f/s**
Motility (%)	93.7 ± 2.5	93.8 ± 3.6	91.9 ± 5.1	91.4 ± 6.5	91.4 ± 45.4	90.7 ± 5.8
VCL (µm/s)	115.4 ± 14.2	128.6 ± 17.8	345.7 ± 36.7	341.9 ± 43.4	289.9 ± 30.4[a]	319.5 ± 14.5[b]
VSL (µm/s)	75.4 ± 9.1	75.9 ± 10.6	313.3 ± 36.6	315.5 ± 47.4	236.6 ± 44.1	260.6 ± 35.0
VAP (µm/s)	83.9 ± 8.9	88.5 ± 11.5	333.3 ±38.3	327.5 ± 45.8	261.3 ± 37.8	278.4 ± 29.4
LIN (%)	65.6 ± 6.6[a]	59.2 ± 4.7[b]	90.6 ± 4.3	90.2 ± 3.4	81.1 ± 9.2	81.5 ± 9.4
STR (%)	89.8 ± 2.5[a]	85.7 ± 2.2[b]	94.0 ± 3.6	96.2 ± 1.5	90.0 ± 5.1	93.3 ± 3.2
WOB (%)	73.0 ± 5.5	69.0 ± 4.1	96.3 ± 1.6	95.6 ± 2.2	89.9 ± 5.9	87.1 ± 7.7
ALH (µm)	2.6 ± 0.3	2.4 ± 0.3	3.2 ± 0.3[a]	2.3 ± 0.3[b]	3.6 ± 0.4[a]	2.7 ± 0.5[b]
BCF (Hz)	18.0 ± 2.0[a]	22.5 ± 2.0[b]	15.1 ± 1.1[a]	22.0 ± 2.2[b]	17.5 ± 1.8[a]	28.5 ± 6.0[b]

	Chlorocebus aethiops		*Ovis orientalis*		*Mus musculus*	
	50 f/s	**75 f/s**	**50 f/s**	**75 f/s**	**50 f/s**	**75 f/s**
Motility (%)	92.1 ± 2.7	95.7 ± 2.1	82.2 ± 6.6	83.6 ± 6.8	87.4 ± 6.6	89.2 ± 6.8
VCL (µm/s)	322.5 ± 20.6	333.5 ± 12.4	226.9 ± 20.1	248.3 ± 25.7	256.8 ± 26.3	291.5 ± 89.6
VSL (µm/s)	287.4 ± 26.5	302.6 ± 12.7	159.9 ± 31.0	162.5 ± 38.8	91.0 ± 16.5	94.6 ± 42.1
VAP (µm/s)	309.0 ± 24.1	320.0 ± 12.9	187.6 ± 31.6	186.4 ± 36.3	115.9 ± 15.9	128.0 ± 42.7
LIN (%)	89.0 ± 3.4	90.7 ± 1.6	70.5 ± 12.5	65.8 ± 15.5	35.3 ± 3.6	31.6 ± 4.0
STR (%)	92.9 ± 1.8	94.6 ± 1.0	84.9 ± 4.5	86.3 ± 6.1	78.2 ± 4.1	72.2 ± 7.2
WOB (%)	95.7 ± 1.9	96.0 ± 0.7	82.7 ± 12.2	75.4 ± 14.2	45.0 ± 2.5	43.7 ± 1.3
ALH (µm)	3.2 ± 0.2[a]	2.2 ± 0.1[b]	3.6 ± 0.6	3.0 ± 0.8	8.7 ± 0.9	8.2 ± 1.2
BCF (Hz)	13.4 ± 1.4[a]	18.6 ± 0.7[b]	17.4 ± 3.6[a]	24.8 ± 5.6[b]	8.4 ± 1.6	8.6 ± 2.2

VCL = curvilinear velocity, VSL = straight-line velocity, VAP = average path velocity, LIN = linearity, STR = straightness, WOB = wobble, ALH = amplitude of lateral head displacement, BCF = beat cross frequency, f/s = frames per second
a, b = values labelled with different superscript letters in the same row for each individual species were significantly different (P < 0.05)

Correlation coefficients (r) between ten midpiece morphometry parameters (n=5) and all sperm morphometry and motility parameters (n=10) for seven mammalian species

	# Gyres	Mitch Ht	r_b	$r_b - r_a$	MPLength	MPEllipt	MPVolume	MPV/HL	SLMPL	FlowCytom
HLength (µm)	0.89	-0.84	-0.27	-0.35	0.88	0.86	0.31	0.04	0.79	0.67
HWidth (µm)	0.81	-0.82	-0.30	-0.39	0.78	0.76	0.18	0.09	0.69	0.51
HArea (µm^2)	0.90	-0.83	-0.27	-0.35	0.89	0.88	0.30	0.05	0.80	0.71
HPerimeter (µm)	0.94	-0.74	-0.13	-0.22	0.91	0.89	0.50	0.23	0.86	0.70
HEllipticity	0.57	-0.33	-0.17	-0.22	0.18	0.18	0.39	0.31	0.56	0.52
HElongation	0.61	-0.35	-0.11	-0.16	0.28	0.27	0.45	0.37	0.58	0.52
HW/HL ratio	-0.62	0.37	0.20	0.24	-0.23	-0.23	-0.39	-0.12	-0.59	-0.53
HRoughness	-0.44	0.11	0.33	0.38	-0.09	-0.07	-0.14	0.07	-0.33	-0.29
HRegularity	0.07	0.13	-0.44	-0.47	-0.05	-0.06	-0.30	-0.24	-0.09	-0.25
MPLength (µm)	0.88	-0.61	-0.09	-0.12	X	0.97	0.58	0.45	0.86	0.84
MPWidth (µm)	0.11	0.03	0.58	0.59	0.34	-0.45	0.51	0.62	0.09	0.01
MPArea (µm^2)	0.92	-0.67	-0.10	-0.15	0.97	0.91	0.55	0.49	0.88	0.85
MPPerimeter (µm)	0.89	-0.62	-0.10	-0.13	1.00	0.97	0.58	0.37	0.86	0.84
MPEllipticity	0.83	-0.60	-0.05	-0.09	0.97	X	0.60	0.46	0.86	0.82
MPElongation	0.85	-0.63	-0.04	-0.11	0.97	0.99	0.60	0.51	0.87	0.83
MPRoughness	-0.83	-0.62	0.03	0.09	-0.96	-0.99	-0.61	-0.34	-0.87	-0.83
MPRegularity	0.06	-0.15	0.33	0.37	-0.26	-0.27	0.29	0.36	0.13	0.24
Total # Gyres	X	-0.79	0.13	-0.19	0.88	0.83	0.50	0.31	0.91	0.79
Mitch Height (µm)	-0.79	X	0.19	0.29	-0.61	-0.60	-0.18	0.03	-0.67	-0.59
r_b (µm)	-0.13	0.19	X	0.95	-0.09	-0.05	0.69	0.79	0.07	-0.01
$r_b - r_a$ (µm)	-0.19	0.29	0.95	X	-0.12	-0.09	0.65	0.77	0.01	-0.04
MPVolume (µm^3)	0.50	-0.18	0.69	0.65	0.58	0.60	X	0.97	0.69	0.61
SLMPL (µm)	0.91	-0.67	0.07	0.01	0.86	0.86	0.69	0.48	X	0.88
Flow cytometry	0.79	-0.59	-0.01	-0.04	0.84	0.82	0.61	0.48	0.88	X
TPPLength (µm)	0.53	-0.26	0.47	0.42	0.69	0.68	0.73	0.57	0.48	0.29

TEPLength (µm)	-0.34	0.62	-0.05	-0.05	-0.36	-0.33	-0.11	0.04	-0.37	-0.39
TPP+TEP (µm)	0.39	-0.09	0.47	0.44	0.61	0.61	0.67	0.53	0.34	0.17
TTLength (µm)	0.55	-0.27	0.45	0.41	0.73	0.72	0.73	0.56	0.49	0.35
SPLength (µm)	0.58	-0.31	0.40	0.36	0.73	0.72	0.71	0.52	0.50	0.35
MPL/HL	0.43	-0.10	0.59	0.63	0.76	0.75	0.91	0.94	0.55	0.58
MPL/HA	0.19	0.17	0.65	0.68	0.63	0.63	0.82	0.89	0.32	0.38
TTL/HL	0.20	0.12	0.58	0.61	0.41	0.42	0.74	0.83	0.28	0.25
TTL/HA	-0.01	0.31	0.42	0.46	0.20	0.22	0.54	0.64	0.10	0.16
TTL/MPL	-0.81	0.68	0.16	0.17	-0.92	-0.91	-0.45	0.20	-0.85	-0.89
TTL/HL+MPL	-0.81	0.69	0.13	0.15	-0.87	-0.85	-0.44	-0.20	-0.86	-0.86
TTL/TPPL+TEPL	0.80	-0.71	-0.26	-0.28	0.91	0.90	0.36	0.27	0.78	0.88
SPL/HL	0.20	0.12	0.58	0.61	0.41	0.42	0.74	0.83	0.28	0.25
SPL/HA	-0.05	0.36	0.38	0.42	0.14	0.17	0.49	0.60	0.06	0.14
SPL/MPL	-0.81	0.69	0.16	0.18	-0.93	-0.91	-0.45	-0.20	-0.85	-0.89
SPL/HL+MPL	-0.82	0.69	0.13	0.15	-0.91	-0.89	-0.45	-0.21	-0.86	-0.87
SPL/TTL	-0.22	-0.08	-0.61	-0.59	-0.43	-0.44	-0.74	-0.62	-0.27	-0.22
SPL/TPPL+TEPL	0.80	-0.72	-0.24	-0.28	0.89	0.87	0.36	0.27	0.78	0.87
MPV/HL	0.38	-0.07	0.77	0.75	0.45	0.47	0.96	X	0.57	0.50
MPV/HA	0.17	0.18	0.79	0.80	0.26	0.27	0.89	0.95	0.37	0.30
TTL/MPV	-0.39	0.17	-0.74	-0.70	-0.46	-0.48	-0.92	-0.71	-0.63	-0.55
SPL/MPV	-0.37	0.13	-0.77	-0.75	-0.45	-0.46	-0.94	-0.74	-0.61	-0.53
VCL (µm/s)	0.11	-0.14	0.65	0.65	0.39	0.43	0.55	0.48	0.16	0.08
VSL (µm/s)	-0.05	-0.23	0.61	0.60	0.29	0.32	0.29	0.24	0.01	-0.03
VAP (µm/s)	-0.05	-0.22	0.59	0.60	0.29	0.32	0.28	0.23	0.00	-0.02
LIN (%)	-0.42	0.04	0.47	0.46	-0.09	-0.04	-0.02	0.04	-0.29	-0.29
STR (%)	-0.69	0.38	0.30	0.29	-0.08	-0.01	-0.26	-0.23	-0.56	-0.48
WOB (%)	-0.31	-0.09	0.45	0.45	-0.14	-0.10	0.02	0.53	-0.21	-0.23
ALH (µm)	0.73	-0.45	0.10	0.07	0.86	0.84	0.55	-0.43	0.61	0.53
BCF (Hz)	-0.52	0.31	-0.18	-0.16	0.00	-0.01	-0.65	-0.03	-0.65	-0.55

APPENDIX 6:
Copies of the papers published during this study
(see section 1.4.1)